A New Approach to Drug Delivery: Non-Peptidic, High Load Macrocyclic Alternatives to Cell Penetrating Peptides

Zoe Karthauser

School of Pharmacy
University of East Anglia

A thesis submitted for the degree of
Doctor of Philosophy

June 2013

Declaration

This thesis is submitted to the University of East Anglia for the Degree of Doctor of Philosophy and has not been previously submitted at this or any other university for assessment or for any other degree. Except where stated, and reference or acknowledgement is given, this work is original and has been carried out by the author alone.

Zoe Karthauser

Abstract

Calixarenes are versatile macrocycles formed from the condensation of *para-tert*-butyl-phenol and formaldehyde. *Chapter 1* describes the synthesis of these molecules and how conformational control and selective functionalisation can give an array of molecules with customised properties; this allows for various applications including those of biological relevance. The copper catalysed alkyne-azide cycloaddition (CuAAC) reaction is also introduced as a tool for functionalising calixarenes.

The phenomenon of cell penetration is of interest where a molecule has an intracellular target, for example gene therapy, delivery of cytotoxic agents or cellular imaging. *Chapter 2* introduces the mechanisms of cell uptake and the design and applications of cell penetrating peptides. Calixarenes are presented as alternatives to cell penetrating peptides and the work published to date on intracellular delivery of calixarenes is summarised. A synthetic route for calixarenes with variable fluorescent dyes and different functionalities on the upper rim *via* a common intermediate is presented. Synthesis of an analogue featuring guanidinium groups on the upper rim was achieved using carboxybenzyl (Cbz) protecting groups as a less labile alternative to butoxycarbonyl (Boc) groups. The syntheses of analogues with varied linkers for attachment of the dye are also presented. Biological evaluation revealed that the dynamics of cellular uptake and the intracellular localisation were sensitive to the upper-rim functionalisation and the dye molecule. The linker attaching the dye had less impact.

Chapter 3 describes the suitability of calixarenes as scaffolds to form glycoconjugates. These can be used to target *Pseudomonas aeruginosa*; research towards development of novel treatments of infections from this pathogen is summarised. A route that has been developed towards bifunctional calixarenes featuring a fluorescent tag and points of attachment for sugars *via* CuAAC reactions is presented. The use of alkyne protecting groups to maintain the integrity of the scaffold during transformations was found to be particularly important.

Table of Contents

List of Figures

List of Schemes

List of Tables

Abbreviations

Ac	Acetyl
ADP	Adenosine diphosphate
AFM	Atomic force microscopy
Ala	Alanine
Apaf-1	Apoptotic protease activating factor 1
APCI	Atmospheric-pressure chemical ionisation
Ar	Aromatic
ARE	Antioxidant response element
ARF6	ADP-ribosylation factor 6
Asc	Ascorbate
Asp	Aspartate
ATP	Adenosine triphosphate
ATR	Attenuated total reflectance
BAR	Bin–Amphiphysin–Rvs
BKV	BK virus
Bn	Benzyl
Boc	Butoxy carbonyl
Bz	Benzoyl
Cbz	Carboxybenzyl
CD34/69	Cluster of differentiation 34/69
cdc42	Cell division control protein 42

CHO cell	Chinese hamster ovary cell
CLIC	Clathrin-independent carriers
COSY	Correlation spectroscopy
CuAAC	Copper catalysed alkyne azide cycloaddition
DCC	Dicyclohexylcarbodiimide
DCM	Dichloromethane
DEAD	Diethyl azodicarboxylate
DIAD	Diisopropyl azodicarboxylate
DIPEA	Diisopropyl ethylamine
DMAP	Dimethylaminopyridine
DMEM	Dulbecco's modified eagle medium
DMF	Dimethylformamide
DMSO	Dimethylsulfoxide
DNA	Deoxyribonucleic acid
DOPE	1,2-Dioleoyl-sn-Glycero-3-Phosphoethanolamine
DTT	Dithiothreitol
EDCI	1-Ethyl-3-(3-dimethylaminopropyl)carbodiimide
ESI	Electrospray ionisation
FITC	Fluorescein isothiocyanate
Flk1	Fetal liver kinase 1
GDP	Guanosine diphosphate
GEEC	GPI-enriched earl endosomal compartment
GFP	Green fluorescent protein
Glc	Glucosamine
Gly	Glycine
GM1os	Monosialotetrahexosylganglioside oligosaccharide
GRAF1	GTPase regulator associated with focal adhesion kinase
GTP	Guanosine triphosphate
HA	Hemagglutinin
HCV	Hepatitis C virus
HEK-293 cell	Human embryonic kidney 293 cell
HeLa	Cervical cancer cell line from Henrietta Lacks
HIA	Hemagglutination assay
HIV	Human immunodeficiency virus
HL60 cell	Human promyelocytic leukemia cell

HMBC	Heteronuclear multiple-bond coherence spectroscopy
HOBt	Hydroxybenzotriazole
HPNP	Hydroxypropyl-p-nitrophenyl phosphate
HRMS	High resolution mass spectrometry
HSPG	Heparan sulphate proteoglycan
HSQC	Heteronuclear single-quantum coherence spectroscopy
IR	Infrared
ITC	Isothermal calorimetry
J774.A1 cell	Murine macrophage cell
Keap1	Kelch-like ECH associated protein 1
LiHMDS	Lithium hexamethyldisilazane
LPS	Lipopolysaccharide
MALDI-TOF	Matrix-assisted laser desorption ionisation time of flight
MCD	Methyl-b-cyclodextrin
MCF-7 cell	Michigan Cancer Foundation breast cancer cell
MHC	Major histocompatibility
Mp	Melting point
MRI	Magnetic resonance imaging
MS	Mass spectrometry
MTS	(3-(4,5-Dimethylthiazol-2-yl)-5-(3-carboxymethoxyphenyl)-2-(4-sulfophenyl)-2H-tetrazolium)
NAz	*N*-azido acetyl
NBD	Nitrobenzoxadiazole
Neu	Neuraminic acid
NIPAAM	N-isopropylacrylamide
NKR-P1	Natural killer receptor-p1
NMM	N-methylmorpholine
NMR	Nuclear magnetic resonance
NRD	Nile Red derivative
Nrf2	Nuclear factor erythroid 2-related factor 2
NSI	Nanospray ionisation
P3CS	Tripalmitoyl-S-glycerylcysteinylserine
p53	Tumour supressor protein
PA-IIL	Pseudomonas aeruginosa lectin II (LecB)
PA-IL	Pseudomonas aeruginosa lectin I (LecA)

PBS	Phosphate buffered saline
PC-12 cell	Rat pheochromocytoma cell
PC3 cell	Human prostate cancer cell
PCL	Polycaprolactone
PEG	Polyethyleneglycol
PI3-K	Phosphoinositide 3-kinase
PMS	Phenazine methosulfate
Rac1	Ras-related C3 botulinum toxin substrate 1
RD-4 cell	Rhabdomyosarcoma cell
RNA	Ribonucleic acid
RPMI	Roswell Park Memorial Institute medium
siRNA	Small interfering RNA
Tat	Transactivator of transcription
Tatp	Protein transduction domain of Tat
TBAF	Tetrabutylammonium fluoride
TBDMS	Tert-butyldimethylsilyl
TBTA	Tris[(1-benzyl-1H-1,2,3-triazol-4-yl)methyl]amine
TFA	Trifluoroacetic acid
THF	Tetrahydrofuran
THP-1 cell	Human leukemic monocytic cell
TLC	Thin layer chromatography
TMS	Trimethylsilyl
TPP	Triphenyl phosphine
UV	Ultraviolet
VEGF	Vascular endothelial growth factor

Acknowledgements

First and foremost, I would like to thank Susan Matthews for offering me the PhD position, for her support over the past few years, for all of her patience and for being calm and optimistic at times when I was not. Likewise I would like to thank Anja Mueller for her help and patience with the biological side of things.

Thanks go to other members of the Matthews lab, past and present, for their company, discussions about chemistry and for putting up with my taste in music. To the rest of the Medicinal Chemistry group, thank you to anyone who has been kind enough to say ‘yes’ on any occasion when I asked ‘can I pick your brain about something?’ or ‘can you help me with this?’ Thank you in particular to Zoe Waller for long chats (when you probably had much better things to be doing with your time) and for taking the time to give feedback on the thesis.

Thank you to Sebastien Vidal for looking after me during my time in Lyon, for help and advice with the sugar chemistry and for patience with the long process of refining the synthesis of the final scaffold. Thank you also to Shuai, Niko, Karine and everybody else who made my time in France pleasant.

Thank you to all of the technical and teaching lab staff for being helpful over the years.

Last but by no means least, I owe big thanks for my family for encouragement and support over the past few years and for putting up with my bad moods when I was having a bad day (or week, or month). Thank you to Sean for always being there, listening to my various rants and helping me to keep going. I could not have done this without you.

Chapter 1: Introduction

1.1 Calixarenes

Early investigation of the chemistry of phenols with formaldehyde by Baeyer found that strong-acid catalysed condensation between the two yielded a resinous, tar-like substance.[1] Later, Baekeland found that carefully controlling the reaction conditions and heating the intermediate resin yielded a more useful substance and led to the advent of the plastic Bakelite (**1**).[2]

Following on from this, Zinke and coworkers[3] investigated the base-catalysed condensation reaction using *para*-substituted phenol; this left only the *ortho*-position free to react, thus controlling the outcome of the reaction. The products obtained using various substituted phenols were proposed to be cyclic tetramers (**2**) of repeating phenol units linked by methylene bridges; although it was later shown by Cornforth *et al.* that the reaction conditions produced multiple products,[4] this led to the extensive investigation of the synthesis and properties of these molecules.

These macrocycles have come to be known as calixarenes, a term coined by Gutsche,[5] derived from the Greek *calix*, meaning 'vase', to describe their basket-like shape. The suffix 'arene' describes their component aromatic units, with the number of units indicated by the number between them; for example, the cyclic tetramer is known as calix[4]arene. The synthesis and manipulation of these macrocycles will be described in the following sections.

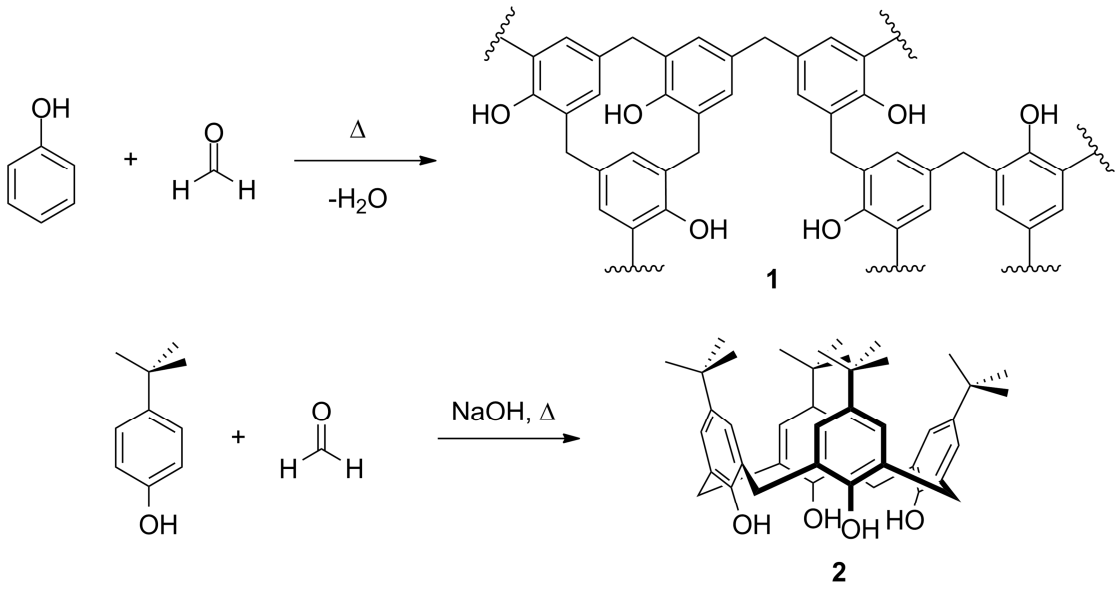

*Scheme 1.1: Condensation reactions of phenols with formaldehyde to give the cross-linked polymer Bakelite (**1**) and the cyclic tetramer calix[4]arene (**2**).*

1.1.1 Synthesis

The problem of multiple products from the procedure used by Zinke *et al.* was approached by investigating the effect of varying the reaction conditions including the temperature and the amount of base used. It was found that the latter was a critical factor, with 0.03-0.04 equivalents of sodium hydroxide base giving the optimal yield of calix[4]arene,[6] whilst 0.3 equivalents of base gave calix[6]arene as the major product.[7] This led to the modified one-pot Zinke-Cornforth procedure for the synthesis of *tert*-butyl-calix[4]arene,[8] which is commonly used for the synthesis of this derivative due to its high yield and brevity of synthesis (in comparison to multi-step procedures; see below).

Modifications of this procedure have been developed to give other macrocycle sizes. High-yielding methods for the synthesis of calix[6]-[9] and calix[8]arene[10] are available; however, the syntheses for calix[5]-[11] and calix[7]arene[12] are less efficient. Larger macrocycles, i.e. calix[9]- up to calix[12]arene have also been synthesised using a base-catalysed procedure,[13] but acid-catalysis is more effective in producing the larger calixarenes, up to calix[20]arene.[14] Modified procedures have also yielded calixarenes in which the methylene bridge has been replaced with a heteroatom, including oxa-,[15] aza-[16] and thiacalixarenes.[17]

As an alternative to the one-pot methods, calixarenes can also be synthesised in a multi-step manner *via* linear intermediates. The non-convergent stepwise synthesis of Hayes and Hunter[18] had an early role in the confirmation of the cyclic tetramer structure and was improved upon by Kammerer.[19] Convergent synthesis was later developed by Böhmer and co-workers,[20] using a fragment condensation approach. However, although stepwise synthesis offers the opportunity for diversification by using different building blocks in each step, these syntheses are longer and generally give poorer yields. The one-pot methods are therefore normally preferred.

1.1.2 Conformation

Calixarenes are conformationally mobile due to the ability of individual rings to undergo transannular rotation. Although larger calixarenes can adopt a wide range of potential conformers, calix[4]arene can adopt just four distinct conformations. These are the cone (**2**), where all of the hydroxyl groups are pointing in the same direction; partial cone (**3**), where one phenol has rotated to point one hydroxyl group towards the upper rim; 1,3-alternate (**4**), where two opposite phenols have rotated; and 1,2-alternate (**5**), where two adjacent phenols have rotated (see Figure 1.1).

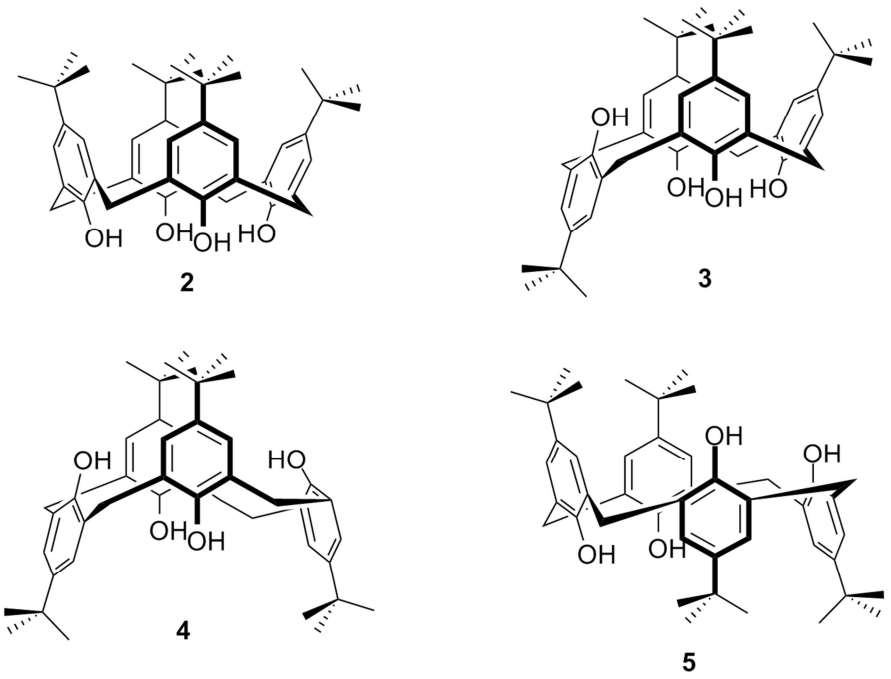

*Figure 1.1: Conformations of calix[4]arene: cone (**2**), partial cone (**3**), 1,3-alternate (**4**) and 1,2-alternate (**5**).*

These conformations are interchangeable in solution;[21] however the calixarene can be locked into a particular conformation by preventing transannular rotation. This can be accomplished by functionalisation of the lower rim, either by blocking the calixarene cavity with a bridging chain between two phenol groups, or by sterically hindering the movement of the phenol through the annulus. The latter can be achieved by forming an ether with any aliphatic chain longer than ethyl.[22,23] Calixarenes can therefore be synthesised in specific conformations by alkylating the lower rim, with the base utilised influencing the final conformation *via* metal templating effects.[24,25] However other factors such as solvent and reaction time can also have an effect.[26]

1.1.3 Functionalisation

Calixarenes can be independently functionalised at either of their rims, the side bearing the phenol groups being termed the lower, narrow or *endo* rim, whilst the opposite is referred to as either the upper, wide or *exo* rim. This, combined with the ability to control the conformation, allows for dramatic diversification of the simple core molecule.

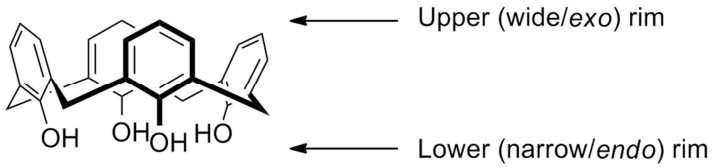

Figure 1.2: Designation of calixarene rims.

1.1.3.1 Lower-rim functionalisation

As noted previously, the lower rim can be functionalised by alkyl or aryl ether (**6**) formation. Selective partial alkylation is possible by utilising a specific base or limiting the amount of alkylating agent available.[25] Whilst alkyl chains can be used to simply lock the conformation, various functional groups can also be introduced by use of suitably functionalised alkylating agents. Furthermore, multiple alkylation events can be used to give diverse function on the lower rim.

Alternatively, the hydroxyl groups of the lower rim can be removed (i.e. replaced with H, as in **7**) *via* reductive cleavage of their phosphonate esters.[27] The hydroxyl groups can also be replaced with a thiol (**7**),[28] or, *via* a monospirodienone intermediate (**8**), be selectively replaced with amine, azide and halogen functionalities (**9**).[29,30]

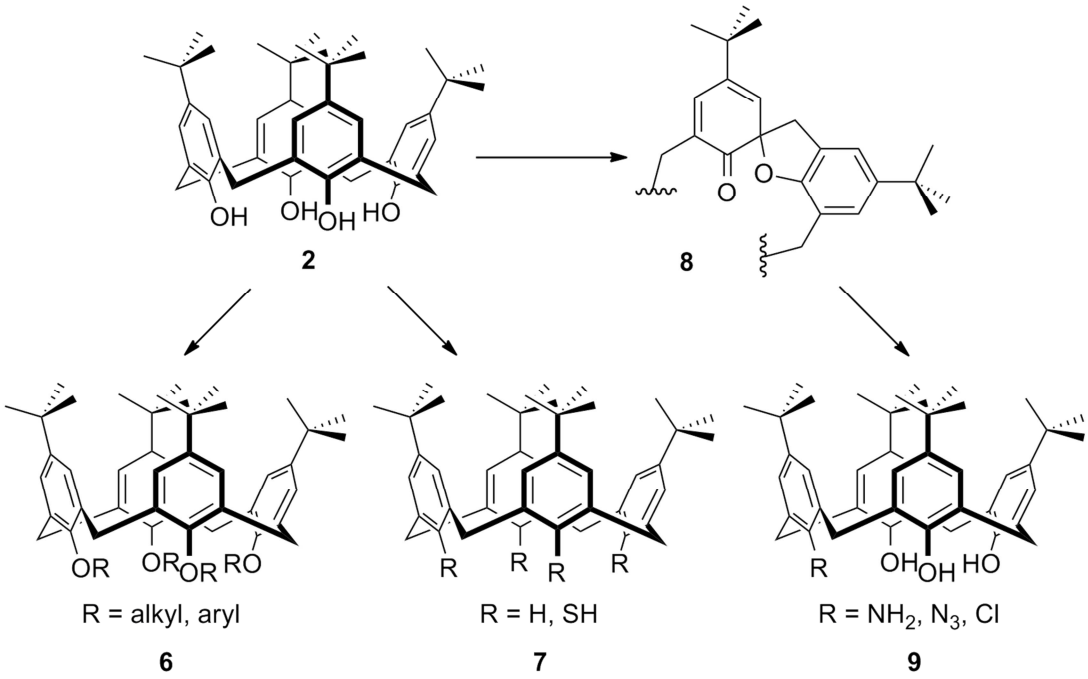

Scheme 1.2: Routes for functionalisation of lower rim.

1.1.3.2 Upper-rim functionalisation

The main method for upper-rim functionalisation involves electrophilic aromatic substitution. Nitro groups (**10**) can be introduced directly by using *ipso*-nitration to replace the *tert*-butyl groups,[31] which can easily be reduced (**11**) to give access to other functionalities, including amines, amides and guanidines (**12**). Sulphonate groups (**13**) can also be introduced in a single step.[32] Other functionalities require the prior removal of the *tert*-butyl groups using a reverse Friedel-Crafts reaction with phenol.[33] The free positions on the upper rim (**14**) can subsequently be converted to, for example, bromo, cyano and carboxyl functionalities (**15**).[34] Also, chloromethylation (**15**)[35] is possible and can be followed by nucleophilic substitution

of the chloride to give access to various functionalities with a methylene spacer to the aromatic ring of the calixarene.

Other indirect methods of upper rim functionalisation include the use of tetra-allyl ether of calix[4]arene (**16**), which undergoes heat-induced Claisen rearrangement to transfer the allyl moieties to the upper-rim (**17**) and can be reacted further to give various functionalities (**18**) *via* ozonolysis of the double bond.[36] Alternatively, the upper rim can be functionalised using an intermediate calix-quinone (**19**); an example of a product available *via* this route (**20**) is shown in Scheme 1.3.[37]

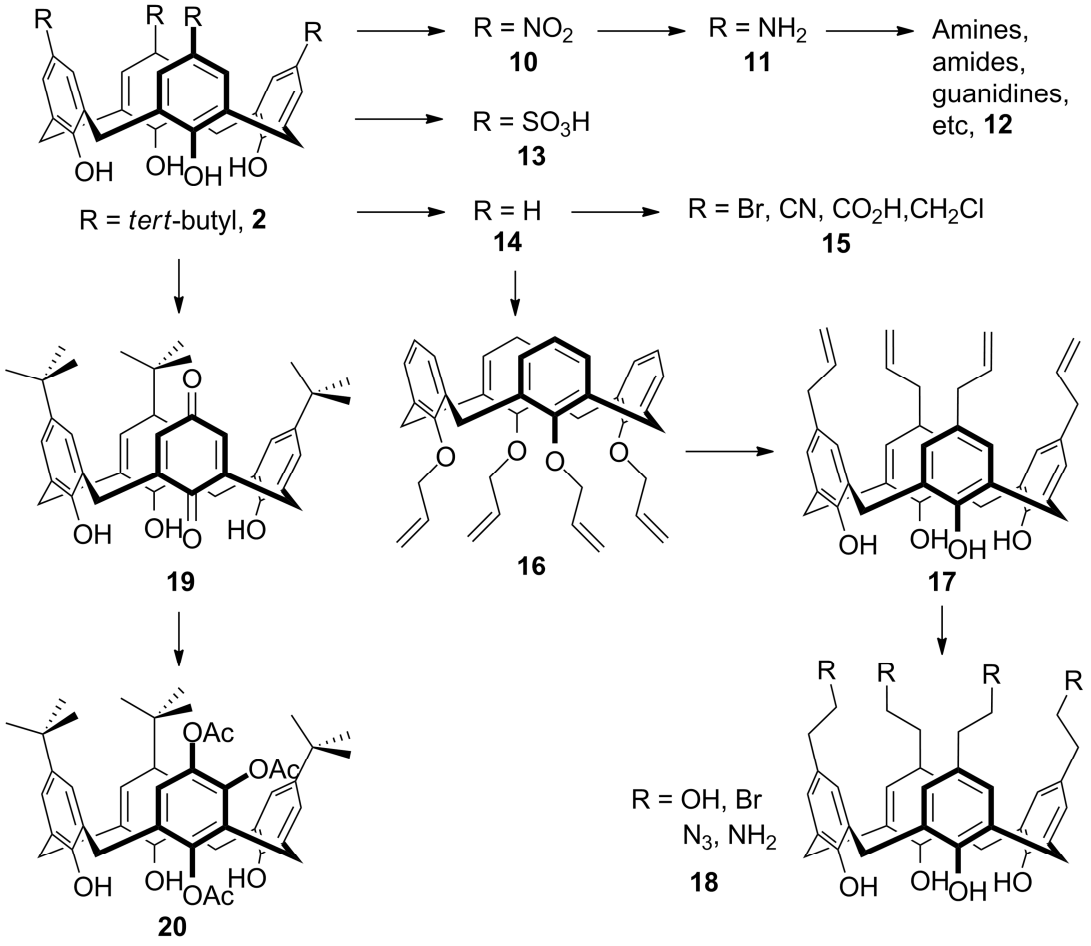

Scheme 1.3: Routes to functionalisation of the upper rim.

1.1.4 Applications in biological systems

Various potential biological applications of calixarenes have been found, either by directly exploiting the properties of functionalised calixarenes or by using them as scaffolds for controlled presentation of active groups. Some of these applications will be examined in the following sections.

1.1.4.1 Artificial Receptors

Calixarenes can be used to present a binding surface for a target molecule and so can mimic receptors. For example, a synthetic lectin (**21**) was synthesised[38] using a macrobicyclic calixarene with a peptide bridge between opposite aromatic units and a phosphate group in the middle of this bridge to cooperate with the hydrogen bonding of the peptide (see Figure 1.3). The lower rim was ester functionalised to provide a means to immobilise the scaffold or alternatively could be deprotected to reveal charged moieties to increase solubility in water.

Lipophilic sugar derivatives were tested for binding to **21** in organic media. The receptor displayed good selectivity for β-octylglucoside over its α- form and also selectivity over β-octylgalactoside. Replacing the phosphate with an acid or methyl ester reduced the association. It was concluded that the phosphate group was most important for strength of binding, with hydrogen bonding and steric factors governing the selectivity.

Hamilton and co-workers constructed synthetic receptors for proteins by targeting the protein surface to modulate protein-substrate interactions. Protein targets were selected that had active sites that were formed of a hydrophobic region surrounded by polar areas. This pattern could be matched to a calixarene with polar arms surrounding its hydrophobic cavity. These arms took the form of pseudocyclopentapeptides, which formed a stable hairpin loop structure, whose residues could be varied to give different activities.[39–41]

With an anionic GlyAspGlyAsp sequence, the calixarene (**22**) bound to Cytochrome C, complementing a hydrophobic region surrounded by cationic lysine residues. This was found to disrupt the interaction of Cytochrome C with reducing agents.[39] Further investigation found that the interaction was strong enough to compete with cytochrome C peroxidase and may be able to disrupt the interaction with Apaf-1 (apoptosis protease activating factor-1).[40]

By changing Asp to Lys, a peptidomimetic capable of binding to a patch of anionic residues in vascular endothelial growth factor (VEGF) was synthesised.[41] This prevents VEGF from binding to its receptor, Flk-1 (fetal liver kinase 1), thus halting the VEGF stimulated tyrosine phosphorylation of the receptor and subsequent activation of other protein kinases. Antiangiogenesis, antitumorigenesis and antimetastasis activities were found *in vivo*. Binding to VEGF was highly selective, with other growth factors remaining unaffected.

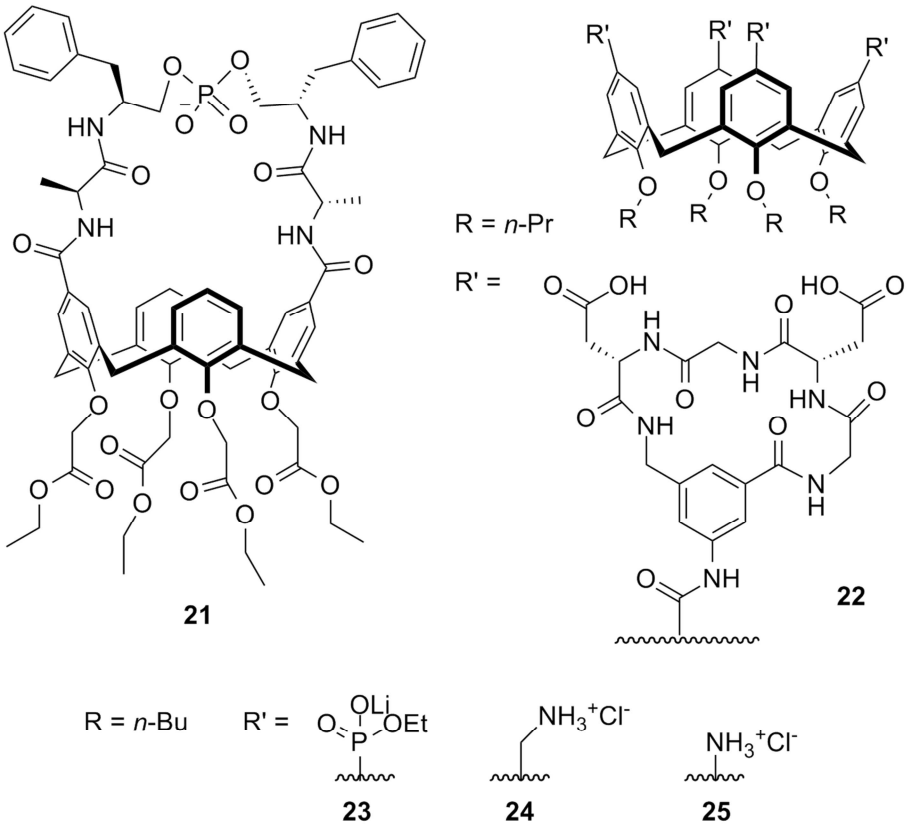

*Figure 1.3: Calixarene based lectin mimetic (**21**),*[38] *calixarene with pseudocylcopentapeptide upper rim featuring AspGlyAspGly sequence (**22**)*[39] *and amphiphilic calixarenes with anionic (**23**) and cationic (**24** and **25**) upper rims.*[42]

Synthetic receptors can also be constructed using multiple calixarenes incorporated into lipid monolayers, which can self-organise to optimise binding of a protein. An amphiphilic calixarene with butyl groups on the lower rim and charged phosphonate groups at the upper rim (**23**) was synthesised and incorporated into a lipid monolayer in a concentration dependent fashion.[43] The calixarenes were distributed evenly in the monolayer, but addition of poly-arginine or larger peptides containing arginine or lysine residues stimulated self-assembly and multi-point binding.

Similarly, by adorning the upper rim with cationic moieties (**24** and **25**), acidic proteins could be attracted to the monolayer.[42] In both cases it is proposed that binding occurs with excess calixarene in the aqueous phase, followed by embedding of the ligand-protein complex in the monolayer.

It has been shown that cationic and anionic ligands can be combined in the monolayer to give a combined response to a given protein. A fingerprint can be obtained by measuring the response to anionic, cationic, polar and mixed bilayers, allowing selective detection at nanomolar concentrations.[42] By constructing vesicles also containing polydiacetylene, a chromatic polymer, a colorimetric response was

observed on protein binding and likewise a fingerprint could be obtained for a given protein.[44]

Calixarenes can also bind to stabilise protein structures. For example, the protein p53, which protects against tumours by either inducing DNA repair or cell apoptosis, contains a tetramerisation domain which is mutated in some cancers. The R337H mutation destabilises the tetramer, but the integrity can be recovered by using a 'clip' in the form of a cone calixarene with four guanidinomethyl groups on the upper rim and hydrophobic loops on the lower rim (**26**).[45] Two of these bind per tetramer, interacting with hydrophobic pockets between monomers and with glutamate residues above the pockets (see Figure 1.4b). The loops on the lower rim help to restrict conformational freedom, strengthening the binding.

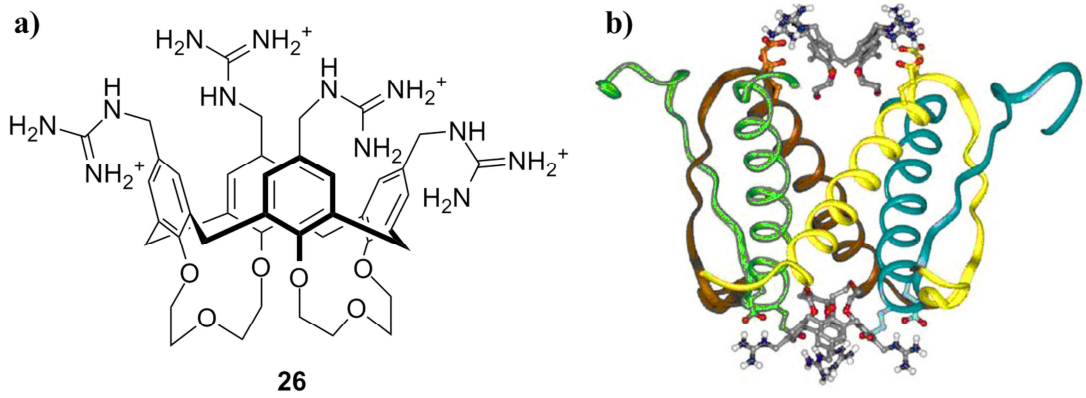

*Figure 1.4: a) Tetraguanidinomethylcalixarene ligand (**26**); b) Interaction of **26** with p53 tetramer (© 2008 by the National Academy of Sciences of the United States of America).*[45]

1.1.4.2 Artificial Transporters

Ion transporters are involved in a number of processes and their malfunction can be associated with disease states, for example cystic fibrosis. Synthesis of artificial analogues is therefore of interest.

Transport of alkali metal cations across phospholipid bilayers has been achieved using lower-rim ester-functionalised calixarenes (see Figure 1.5).[46] Selectivity and efficiency was found to be dependent on macrocycle size, with the calix[4]arene derivative (**27**) having the best selectivity and transport efficiency for Na^+, whilst calix[5]arene and calix[6]/[7]arenes were also able to transport K^+ and Cs^+, respectively.

Further work[47] led to the synthesis of cholic acid derivatives, in both cone and 1,3-alternate conformations. Though both conformations were able to mediate Na^+ and H^+ transport across a phospholipid bilayer, the latter (**28**) was found to be more active;

this, combined with the similarity in the length of the calixarene and the thickness of the vesicle, led to the conclusion that the 1,3-alternate calixarene was able to span the bilayer.

Anion transport has also been achieved. A calixarene in the 1,3-alternate conformation with a tetrabutyl amide functionalised lower rim (**29**)[48] was found to mediate Cl^- transport in liposomes, planar lipid bilayers and in HEK-293 cells, with a concomitant change in pH. This may occur by H^+/Cl^- symport or Cl^-/OH^- antiport. Though this calixarene was not large enough to span the bilayer, it may have been able to form aggregates (as observed with a tetramethyl amide derivative in HCl) to allow it to form ion channels.

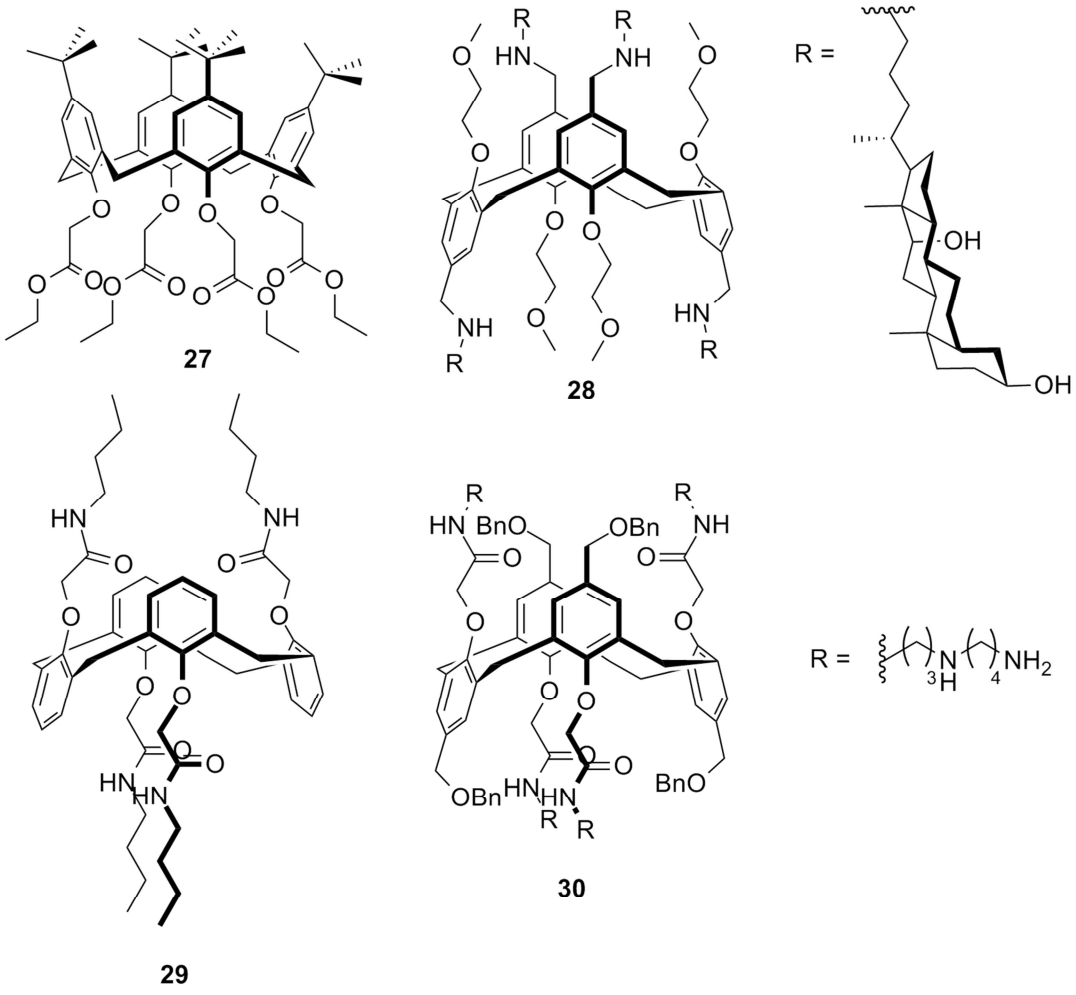

*Figure 1.5: Artificial transporters based on ester ((**27**),*[46] *cholic acid (**28**),*[47] *amide (**29**)*[48] *and spermidine (**30**)*[49] *functionalised calixarenes.*

It was also found that the activity of the corresponding partial cone derivatives of these tetra-amide calixarenes was influenced by the upper rim functionalisation.[50] The *para-tert*-butyl and unfunctionalised calixarenes had different crystal packing, which was proposed to be the reason for the inactivity of the former compared with the latter.

The non-linear concentration dependence of the transport suggested that the calixarene forms aggregates which are responsible for transport. Co-aggregates with the inactive *tert*-butyl derivative inhibited transport. Although it was determined that the single inverted amide of the partial cone was not required for transport function, it was suggested that this could be exploited for synthesis of dimers or oligomers.

Another 1,3-alternate calixarene, this time functionalised at the lower rim with spermidine (**30**) was able to span the entire bilayer without forming an aggregate.[49] It displayed some selectivity towards I^- and Br^- over Cl^-, whilst oxo-anions showed poor transport. This calixarene also showed a moderate antiproliferative effect against murine monocyte/macrophage J774.A1 cancer cells.

1.1.4.3 Artificial Enzymes

The potential for calixarenes to act as enzyme mimics by organising catalytic moieties has also been investigated. For example, artificial metallonucleases, which cleave phosphodiester bonds in DNA and RNA, can be synthesised by pre-organising catalytic Cu(II).

To investigate this, cone calixarenes with one, two or three copper centres tethered to the upper rim via [12]-ane azamacrocyles were synthesised.[51] A 10^4 fold rate enhancement was achieved for the 1,2-di- (**31**) and tri-copper derivatives and it was concluded that there was cooperativity between the metal centres in the cleavage of the phosphodiester bond; however, the third metal gave no additional rate enhancement, excluding simultaneous cooperation between all three. The 1,3-di-copper species showed no cooperativity, indicating a sensitivity to the distance between the metal centres. It was proposed that one metal centre tethers the non-reacting part of the molecule, whilst the other activates the phosphoryl group for cleavage.

For diribonucleoside monophosphates, it was found that substrates containing a uracil base gave the best activity with these catalysts.[52] It was proposed that the uracil may be deprotonated, providing an electrostatic interaction between the base and the metal centre. By contrast, for longer oligonucleoside monophosphates, greater selectivity for bonds adjacent to adenosine and cytosine was found, with the most scissile bond being 5'-pCpA. This mimics the activity of ribonuclease A. In this case the interaction with the terminal phosphate seems to dominate, resulting in the preferential cleavage of the naturally more labile CpA bond.

A metal-free artificial phosphodiesterase has also been synthesised, in this case utilising upper-rim guanidinium moieties for catalytic function.[53] In an investigation of the catalytic activity towards the transesterification of 2-hydroxypropyl *p*-nitrophenylphosphate (HPNP) it was found that a 1,3-diguanidine calixarene (**32**) gave much greater activity than the corresponding monomer, indicating a marked synergistic effect, whilst a triguanidine derivative gave no further improvement. A mechanism of action was proposed where a neutral guanidine acts as a general base catalyst, whilst the other, protonated guanidinium serves to stabilise the negatively charged transition state *via* a bidentate hydrogen bond. A third guanidine only behaves as a spectator and functionalisation with four guanidine moieties leads to steric repulsion.

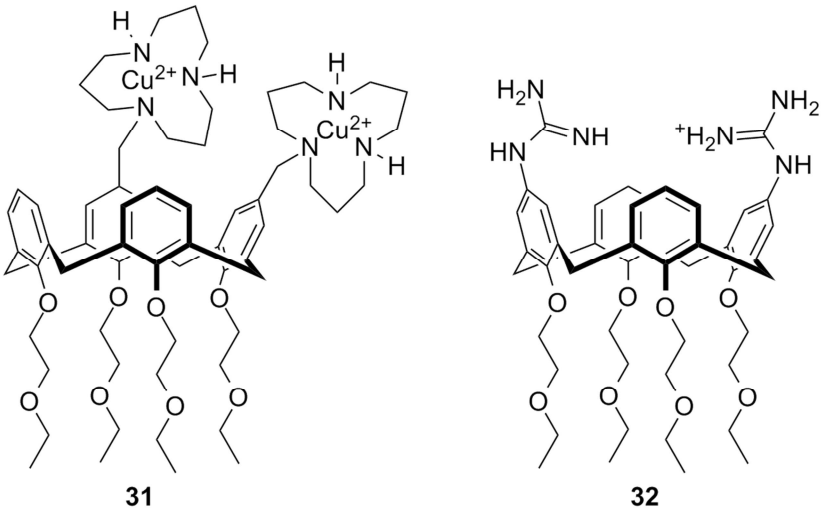

31 **32**

*Figure 1.6: 1,2-difunctionalised artificial metallonucelease (**31**)*[51] *and 1,3-diguanidine functionalised calixarene catalyst (**32**) in the catalytically active form.*[53]

1.1.4.4 Anticancer applications

In addition to the potential applications covered above, other therapeutic applications of calixarenes have been more directly investigated. This includes targeting of cancer cells and the use of calixarenes as antimicrobials (see section 1.1.4.5).

CD69 is a C-type lectin-like receptor expressed during activation of T-lymphocytes and natural killer (NK) cells. This was targeted using a carboxylated thiacalixarene (**33**) to disrupt the process of CD69-induced apoptosis that is involved in tumour immunology.[54] This calixarene was found to inhibit the binding of CD69 to a multivalent mimic of cancer cell sialomucins without affecting another C-type lectin, NKR-P1, displaying its potential as a selective ligand. Moreover, it was able to protect $CD69^{high}$ lymphocytes from apoptosis induced by the sialomucin mimic. It may

therefore be able to intervene in tumour immunology by preventing inactivation or apoptosis of CD69-bearing cells.

Calixarenes could also be utilised in cancer chemotherapy indirectly, by mediating delivery of cytotoxic agents. This could be accomplished by using bifunctional calixarenes decorated with folic acid moieties.[55] These groups bind with high affinity to folate receptor, which is a marker for cancer cells and activated macrophages. A folic acid functionalised calixarene (**34**), with triethylene glycol chains on the lower rim, was developed to mitigate the poor bioavailability of hydrophobic drug molecules and was found to solubilise the drug indomethacin by forming aggregates at physiological pH. Such a system could potentially be used to both solubilise a drug and to deliver it selectively to cancer cells.

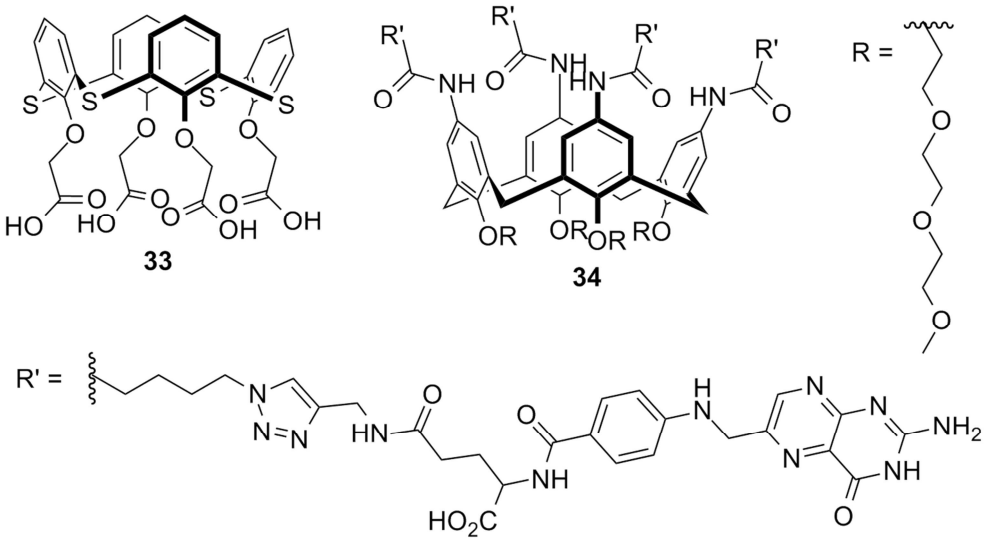

*Figure 1.7: CD69-binding carboxylated thiacalixarene (**33**)*[54] *and multivalent folic acid conjugate (**34**).*[55]

1.1.4.5 Antimicrobial activity

Calixarenes can be used as scaffolds to present antibiotic functionalities. One example of this is a mimic of the antibiotic vancomycin, synthesised using a macrobicyclic calixarene (**35**) with a bridge between opposite aromatic units.[56] The bridge was a pseudopeptide, to mimic the glycopeptide antiobiotic, formed of two amino acids linked by a 1,3,5-diethylene triamine spacer.

Vancomycin binds to mucopeptide precursors that form gram positive bacterial cell walls. The dipeptide N-Ac-Ala-Ala was used as a model of the peptidoglycan branch and binding studies were carried out with this. It was found that the scaffold containing two alanine residues bound to the target more strongly than N-acetyl alanine alone. It was concluded that the ligand was able to form both electrostatic

interactions between its carboxylate group and the ammonium group of the host and hydrogen bonds to the pseudopeptide bridge. The calixarene displayed antibacterial activity which was selective towards gram-positive bacteria.

A drug molecule can also be tethered to a calixarene using a labile linker. A *tetra-para*-aminoethylcalixarene with a tethered nalidixic acid molecule (**36**) was found to be highly stable as a solid, but released the drug molecule in biological medium.[57] Although the subsequent free alcohol of the calixarene was considerably less active as an antibiotic, a synergistic effect was found between the calixarene and nalidixic acid against both gram-positive and gram-negative bacterial strains.

Certain functionalised calixarenes have also been found to have intrinsic antimicrobial activity. For example, *para*-sulfonato and *para*-phenylazocalixarenes in particular were shown by Lamartine *et al.*[58] to have antibacterial and antifungal activities. More focussed investigation of agents against tuberculosis has also been carried out, based on early observations that macrocylcon, a *para-tert*-octylcalix[8]arene functionalised on the lower rim with polyethylene glycol chains, could be used to treat pulmonary tuberculosis.[59] A polyethylene glycol-functionalised calix[6]arene (**37**) was found to reduce viable counts of mycobacteria in lungs and spleens of infected mice by stimulating the host's antimycobacterial mechanisms. A host-mediated mechanism such as this could help to overcome multi drug resistance.

Guanidine functionalised calixarenes have also been investigated for their antimicrobial properties. A *para*-guanidinoethylcalixarene (**38**) was found to exhibit a significant effect against both gram-positive and gram-negative bacterial strains, with much greater activity than the corresponding monomer.[60] Later studies indicated that interactions of the calixarene with phospholipid bilayers were characterised by a combination of electrostatic and apolar interactions and that both are required for antibiotic activity; the monomer, lacking the apolar core of the calixarene, is thus unable to bring about the same intensity of effect.[61]

Anionic calixarenes have been investigated for their potential to treat viral infections such as HIV. A set of calixarenes, including those functionalised with sulphonate, carboxylate and phosphonate groups, with some featuring bithiazole moieties on the lower rim, were tested for their anti-HIV activity.[62] Bithiazole functionalisation was found to increase activity, with the sulphonated derivative (**39**) giving the best activity by interfering in early stages of infection. They were also found to have little or no cytotoxicity, indicating their potential applicability to anti-HIV therapy.

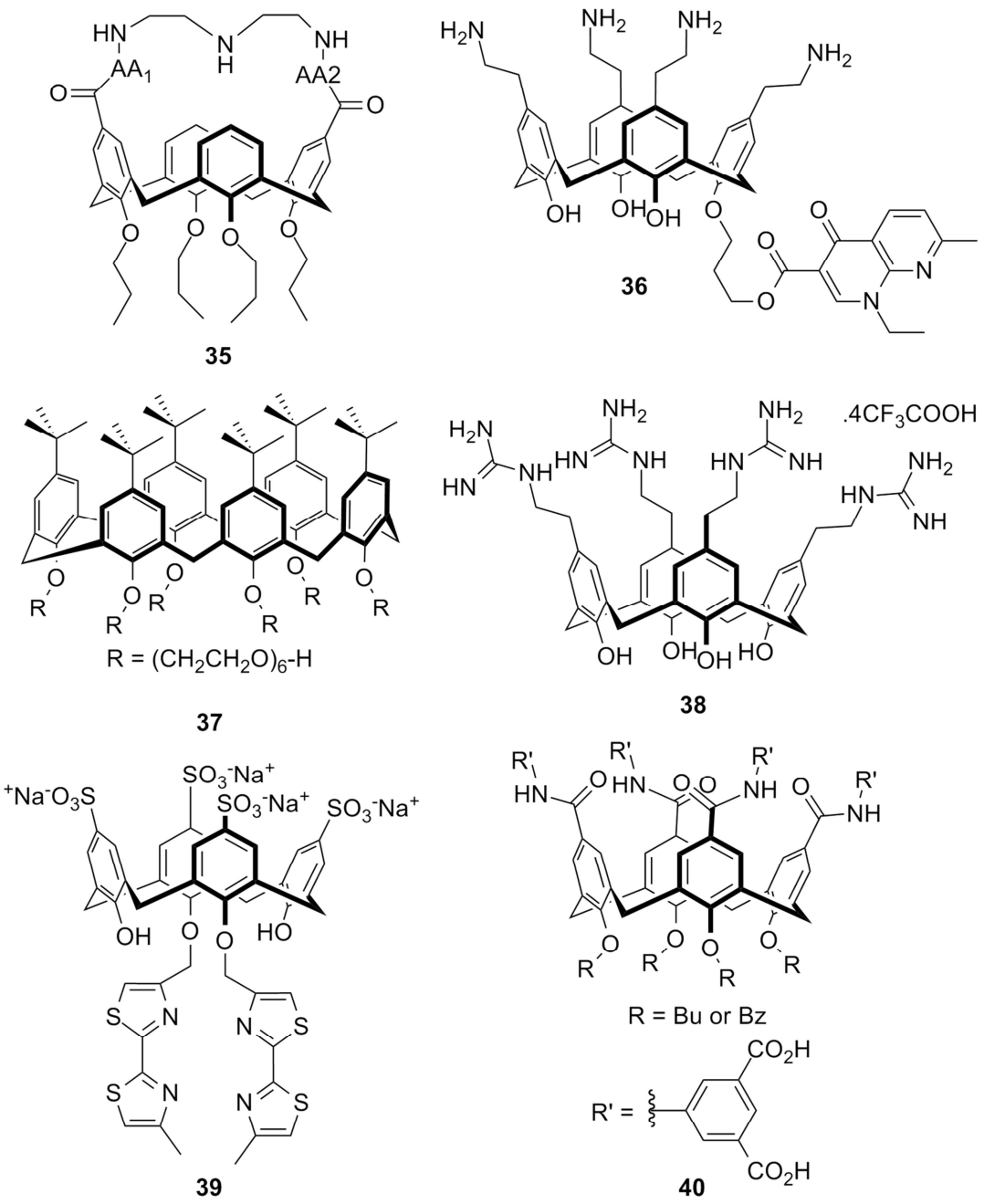

*Figure 1.8: Antimicrobial calixarenes: general structure of vancomycin mimic (**35**) where AA = amino acid,*[56] *nalidixic acid prodrug (**36**),*[57] *macrocyclon analogue (**37**),*[63] *guanidinium antibacterial agent (**38**),*[60] *anti-HIV agent (**39**),*[62] *and dual function anti-HIV and –HCV agent (**40**).*[64]

The problem of co-infection of HIV and hepatitis C virus (HCV) has led to the search for anti-virals with activity towards both of these targets. A calixarene-based antiviral agent (**40**)[64] has been found which meets this goal, displaying antiviral activity in multiple cell lines. The isophthalic acid head groups were found to be important for activity, along with the locking into the cone conformation provided by either butyl or benzyl ethers on the lower rim.

1.1.4.6 Other applications

Medical diagnostics could be aided through the use of calixarene-based DNA chips. Song *et al.* developed a DNA chip using a monolayer of calixarenes functionalised with anionic groups which were able to bind DNA appended with a repeat of 9-guanines (9G-DNA chip). The chip was shown to be able to selectively bind a Cy5 labelled DNA sequence complementary to that bound to the calixarenes.[65] They subsequently demonstrated the ability of a 9G-DNA chip to detect human papillomavirus (HPV) in clinical samples.[66]

Other applications include the use of calixarenes as cell penetration agents, for example for cellular imaging or their use in DNA transfection. This will be examined in Chapter 2. Calixarene-based glycoconjugates have also found a number of potential applications and will be examined in Chapter 3.

1.2 Click chemistry

Click chemistry is a term coined by Sharpless et al.,[67] the requirements for such a reaction being that it must be modular, wide in scope, high yielding, produce only inoffensive by-products, be stereospecific, have simple reaction conditions, use readily available materials and reagents, use benign or easily removed solvent and give a product that is stable and easily purified. Reactions that satisfy these criteria include nucleophilic ring opening reactions (for example, those of aziridenes),[68] Michael additions (such as thiol-ene coupling)[69] and cycloaddition reactions. The most well-known example of the latter is a Huisgen 1,3-dipolar cycloaddition[70] reaction between azides and terminal alkynes to give triazoles.[71] Although thermal activation gives a mixture of regioisomers, this reaction gained renewed interest on the discovery that the addition of copper(I) as a catalyst gives specifically the 1,4-regioisomer (see Scheme 1.4).[72,73] This is now known as the copper catalysed azide-alkyne click (or CuAAC) reaction.

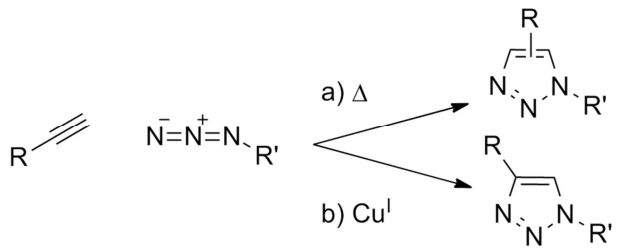

Scheme 1.4: Outcome of the 1,3-dipolar cycloaddition reaction between an azide and alkyne under a) thermal conditions, and b) copper catalysed conditions.

The copper catalyst can be added directly using a copper salt such as copper(I)iodide in combination with a base such as diisopropylethylamine (DIPEA),[73] or can be generated in situ from copper(II) sulphate by adding sodium ascorbate as a reducing agent.[72] Addition of amine ligands can accelerate the reaction by stabilising the active copper(I) species and improving its solubility in organic solvent, with tris(benzyltriazolyl)methyl amine (TBTA)[74] being particularly effective for this purpose.

Due to experimental challenges the mechanism of the CuAAC reaction has been difficult to elucidate. However, recent work[75] has provided valuable insight into the highly reactive, non-isolable reaction intermediates. Based on the observation that halo-acetylides, whilst formally internal alkynes, are still able to undergo cycloaddition, the authors tested the reactivity of preformed copper(I)-acetylide and found that without addition of exogenous copper the reaction did not proceed. This demonstrates the necessity of a second, π-bound copper centre for the reaction.

Further work using an isotopically enriched copper catalyst on the copper(I)-acetylide found that, unexpectedly, the copper(I)-triazolide formed from the cycloaddition was isotopically enriched 50% of the time. This indicated that the second copper centre was not simply acting as a π-bound ligand. After excluding the possibility of exchange occurring on the copper(I)-acetylide or after the formation of the copper(I)-triazolide, this led to a proposed cyclic intermediate after the first C-N bond formation where the two copper centres become equivalent. The subsequent oxidation step is then facilitated by the copper centres each acting as a stabilising donor ligand for the other. The full proposed mechanism is shown in Scheme 1.5.

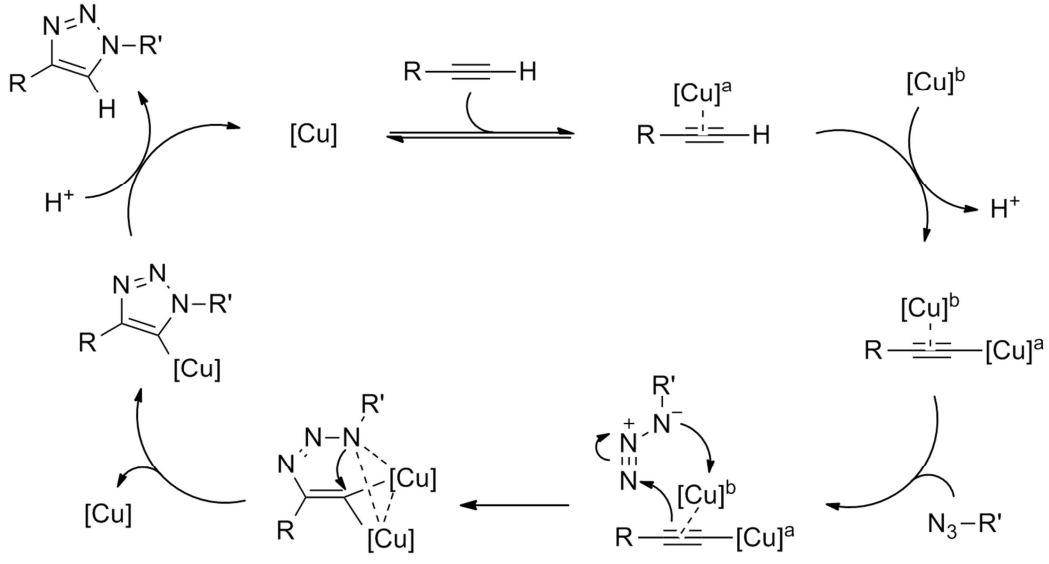

Scheme 1.5: Proposed mechanism for the CuAAC reaction.[75]

1.2.1 Click chemistry for calixarene functionalisation

The CuAAC reaction has been applied to a wide array of different molecules, including calixarenes. With their scope for selective functionalisation on both the upper and lower rims, these macrocycles lend themselves well to the modular synthesis approach provided by click chemistry. Although they can be furnished with either azide or alkyne moieties on both upper and lower rims, this section will focus on the use of lower-rim alkyne functionalised calixarenes due to their use in the syntheses presented in this thesis.

1.2.1.1 Background

Prior to the development of the copper-catalysed version of the azide-alkyne dipolar cycloaddition, this reaction was used to functionalise calixarenes under thermal conditions.[76] By combining a lower-rim 1,3-diazido calixarene (**41**) with either lower-rim mono- (**42**) or 1,3-dipropargyl (**43**) calixarenes, trimers (**44**) and doubly-bridged dimers (**45**) were synthesised, respectively. This provides an early example of the use of cycloaddition chemistry to provide access to multicalixarenes. However, without the copper catalyst, mixtures of regioisomers were obtained.

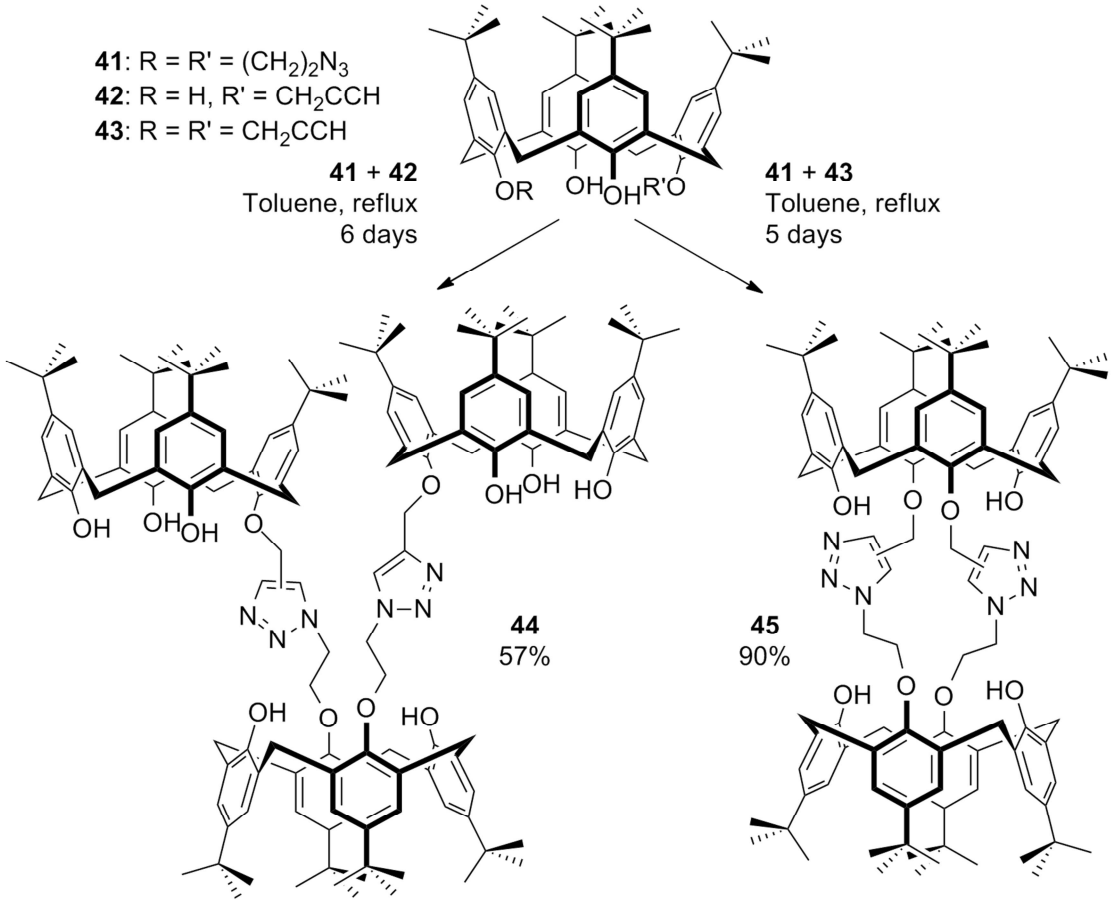

Scheme 1.6: Products of thermal cycloaddition reactions between azides and alkynes.[76]

Interestingly, although all possible isomers of **45** were synthesised, only two regiosomers of **44** were obtained. In the latter case the isomers could therefore be easily separated.

Several years later, after the advent of the CuAAC reaction, Ryu and Zhao[77] investigated the potential of this reaction. Their aim was to synthesise water-soluble calixarenes through a modular approach that would provide a route to various functionalised calixarenes without the need for protection/deprotection steps. Although they were able to introduce a variety of functionalities (including sulfonates and quaternary amines) to the lower rim *via* an azide-functionalised calixarene (**46**), attempts to furnish the lower rim with carboxylic acid moieties using tetra-propargyl calixarene (**47**) were unsuccessful (see Scheme 1.7, compounds **48** and **49**, respectively). The authors suggested that side-reactions between alkyne groups were responsible for the observed complex mixture of products and that for this reason, and due to the greater ease and safety of storing the various alkyne-based small-molecule precursors compared with azides, the azide-functionalised calixarenes were more effective precursors.

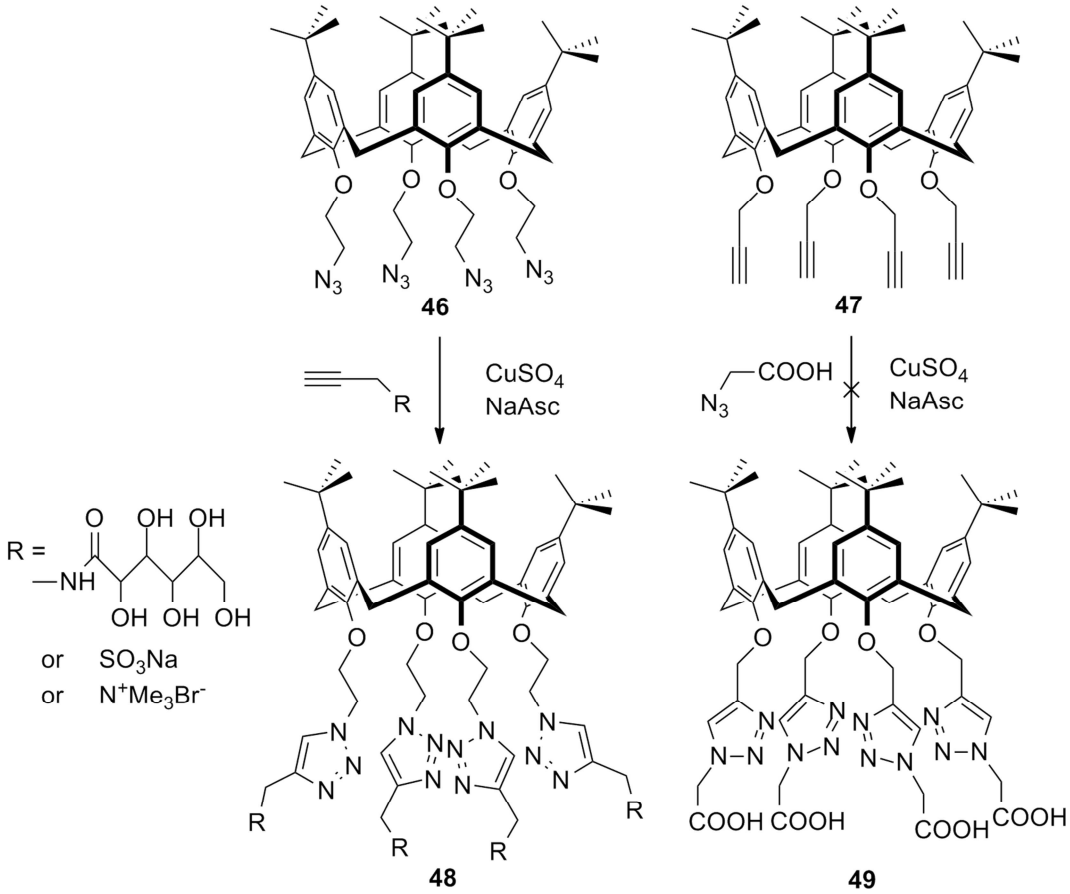

Scheme 1.7: Lower-rim alkyne vs. lower-rim azide for CuAAC mediated synthesis of water soluble calixarenes.[77]

However, in 2006 Chen *et al.*[78] demonstrated the successful use of tetra-propargyl calixarene in CuAAC chemistry by functionalising it with triazole-linked aminoethyl moieties, showing the applicability of the reaction to lower-rim alkynes. Such molecules have since been widely utilised in the CuAAC reaction.

1.2.1.2 Preparation of Lower-Rim- Alkynes

Lower-rim alkynes are easily accessible by utilising a Williamson ether formation between the phenols of the calixarene and propargyl bromide. The degree of functionalisation and the conformation of the calixarene can be controlled to give different arrangements of the functionalised scaffold.[25] The main methods of accessing partially and fully propargylated calixarenes, as described below, are summarised in Scheme 1.8.

Chetcuti *et al.*[79] synthesised several different alkyne-functionalised calixarenes, although they did not utilise them in a CuAAC reaction. Mono, 1,3-di and tetra-alkyne derivatives were synthesised by refluxing in acetone with K_2CO_3 as a base to control the conformation by forming electrostatic interactions between K^+ and the oxygens of the lower rim. The degree of functionalisation was controlled by varying the amount of alkylating agent, using 1, 3 or 6 equivalents of propargyl bromide respectively, and increasing the reaction time. The 1,3-alternate conformation of the tetra-propargyl derivative was obtained in a stepwise manner by using the 1,3-dipropargyl calixarene and treating it with excess propargyl bromide in the presence of Cs_2CO_3 as a base.

Matthews and coworkers[80] used a different approach to access partially-propargylated derivatives. Instead of leaving free phenols, the calixarenes were first partially alkylated with propyl bromide. Using a mixture of $Ba(OH)_2$ and BaO as a base afforded the tripropyl, whilst the 1,3-dipropyl was accessible using K_2CO_3. The 1,2-dipropyl was synthesised using NaH as the base with 2.2 equivalents of propyl bromide. In contrast with the method used by Chetcuti *et al.*, the mono-propyl derivative was obtained using CsF as a weak base and 1.1 equivalents of alkylating agent. All of these derivatives were subsequently treated with an excess of propargyl bromide in the presence of NaH to exhaustively alkylate the lower rim and lock the final calixarene into the cone conformation, with the desired number of alkyne groups present.

Tetra-propargylated derivatives were also synthesised.[80] The cone conformer was synthesised using the method of Ryu and Zhao,[77] utilising NaH as a base instead of the K_2CO_3 used by Chetcuti *et al.*; the calixarene is held in the cone conformation in a

similar manner. The 1,3-alternate conformer was synthesised using the same method as Chetcuti; however in this case a mixture of products was obtained, and therefore also gave access to the partial cone conformer. Similarly, Puddephatt *et al.*,[81] although using K_2CO_3 as a base, also obtained a mixture of partial cone and 1,3-alternate, in ratios of 2:1 and 4:1 after 24 and 48 hours, respectively. This suggests that the 1,3-alternate conformation can convert into the more stable partial cone with prolonged heating.

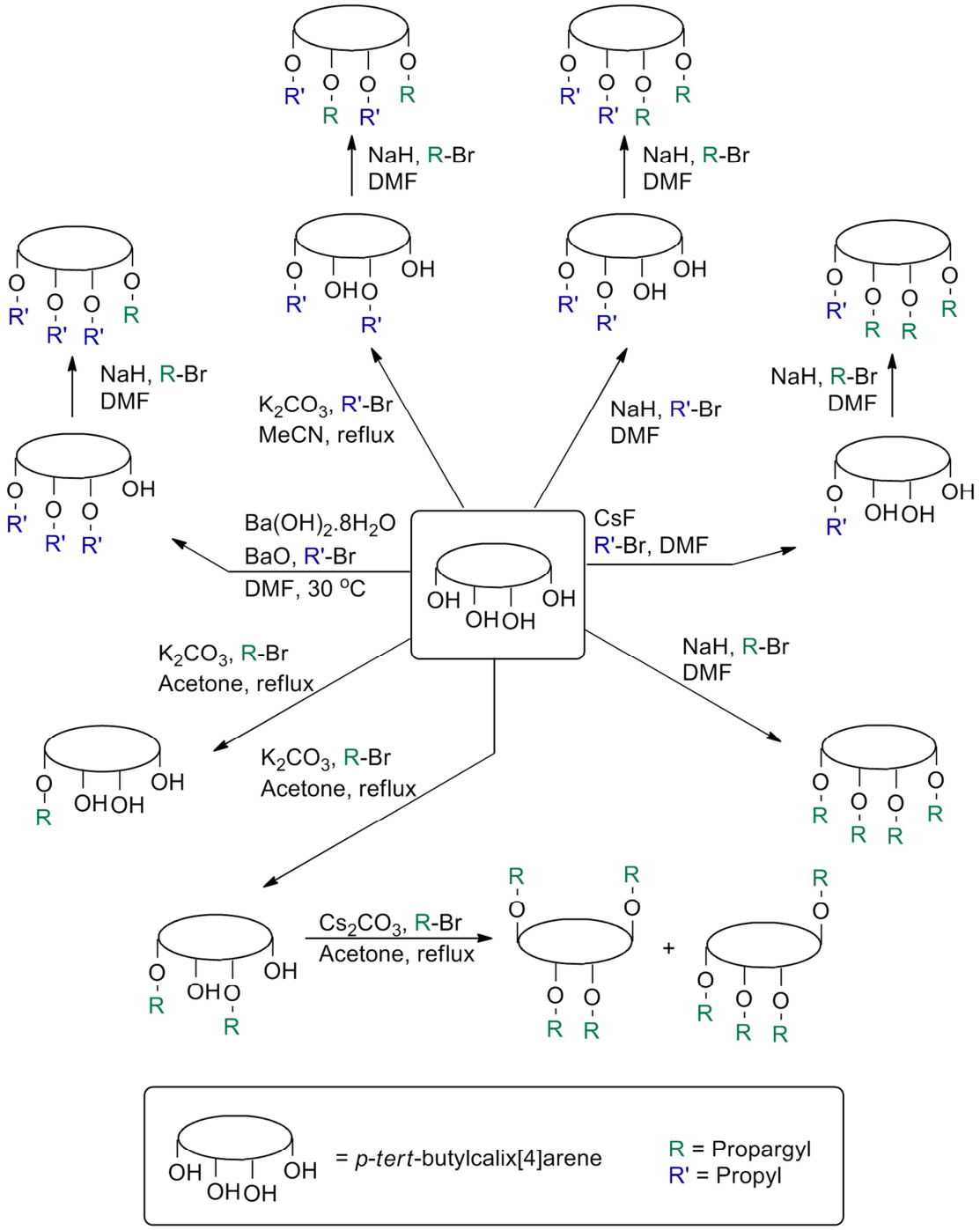

Scheme 1.8: Summary of main methods that have been used for accessing partially and fully propargylated calixarenes, with the latter in different conformations.

An alternative method for mono-alkylation was provided by Bonnamour *et al.*,[82] in which the 1,3-dialkyl derivative is treated with $TiCl_4$ to furnish the mono-alkylated calixarene. This was demonstrated for a number of different functionalities, including but-3-ynyl.

These alkyne-functionalised scaffolds have found a number of applications, which will be examined in the following section.

1.2.1.3 Applications

As noted in section 1.2.1.1, the work of Chen *et al.*[78] led to the successful functionalisation of lower-rim tetra-propargyl calixarene. The triazole-linked aminoethyl functionalised calixarene (**50**) was synthesised in cone and partial cone conformers as part of a library of molecules. This was aimed at creating topomimetics of amphiphilic α-helices and β-sheets for neutralisation of lipopolysaccharide (LPS) endotoxin from Gram negative bacteria. Administration of the cone conformer to mice given a lethal dose of LPS from *Salmonella* resulted in 100% survival, although it was less effective against LPS from other strains of bacteria.

Click chemistry has also been applied to the formation of calixarene-based cavitands and nanotubes. Morales Sanfrutos *et al.*,[83] following on from the previous work using thermal cycloaddition conditions,[76] investigated the use of the CuAAC reaction to react dipropargyl-functionalised calixarenes with diazide-functionalised calixarenes or bis-azidomethylbenzenes. In the former case only the tube-like dimer (**51**) was formed. With the latter, in addition to the desired benzene-capped calixarenes (**52**) a doubly-bridged dimer was formed. However, a preference was found for the product that formed by the second click reaction being intramolecular, such that the doubly-bridged dimer was always the minor product.

Lower-rim propargylated calixarenes have also been incorporated into co-polymers. For example, conjugation of 1,3-dipropargyl calixarene to a cyclodextrin gave a product that was able to form a complex with adamantyl units on poly-N-isopropylacrylamide (poly(NIPAAM)).[84] In another case the bifunctionality was centred on the calixarene itself (**53**) by using ring-opening polymerisation with ϵ-caprolactone to give polycaprolactone (PCL) chains followed by click chemistry to introduce polyethylene glycol (PEG) chains.[85]

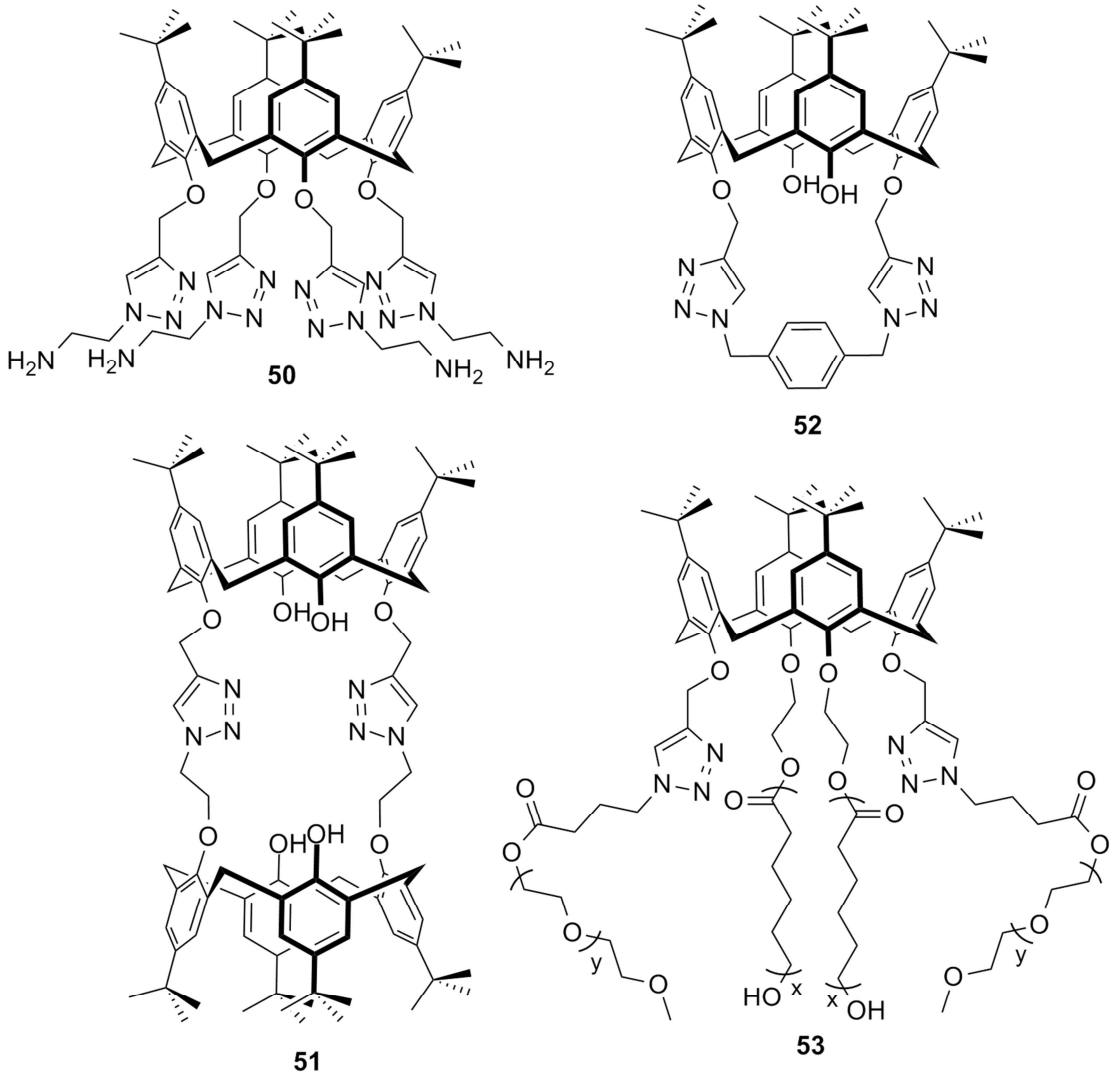

*Figure 1.9: Lower-rim triazole linked ethylamine (**50**), calixarene-based cavitand (**52**), calix-tube (**51**) and calixarene-centred copolymer (x = 25, y = 22) (**53**).*

The 1,3-dipropargyl calixarene in particular has found extensive use in the synthesis of ion sensors due to the ability of triazole rings to bind cations. These sensors commonly exploit a change in conformation of the side-chains on ion-binding to give a measureable change in fluorescence properties.

Chung and coworkers have synthesised a number of calixarene-based molecules capable of sensing cations[86–90] and anions[87] by functionalisation with triazole-linked fluorescent moieties, such as anthracene and pyrene. Several of these sensors are ditopic, utilising a second functionality to bind another ion, for example combining two triazole linked anthracenes with a calix-crown structure (**54**);[86] this example is also switchable, with a second binding event reversing the change in fluorescence. A 1,2-difunctionalised sensor utilising pyrene was also synthesised and was found to give superior binding to Ag^+ compared with the 1,3-derivative.[90]

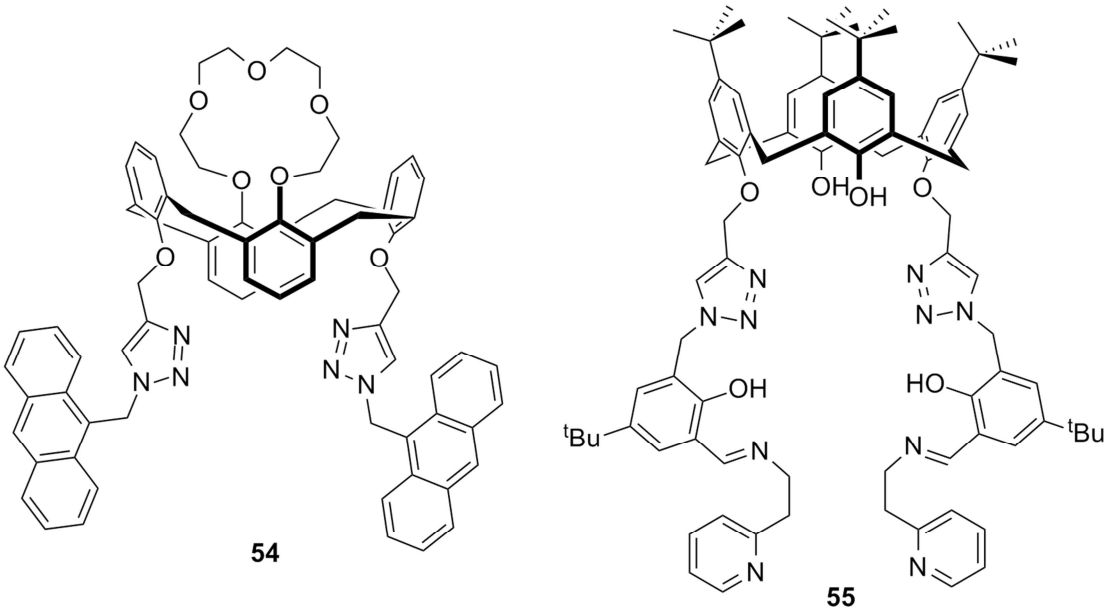

*Figure 1.10: Examples of ion sensors synthesised by Chung and coworkers (**54**)*[86] *and Pathak et al. (**55**).*[91]

Kim and coworkers have also synthesised dipyrene functionalised calixarenes, capable of binding Cd^{2+}, Zn^{2+} and I^-.[92,93] During the course of developing the latter, a mono-pyrene derivative was synthesised with a quaternary amine on the opposite calixarene ring; the amine was noted to behave as an intramolecular ligand during the CuAAC reaction, enhancing the reactivity.[93]

Other work on sensors includes that of Li and coworkers. A calixarene with a bridging anthraquinone on the lower rim, linked *via* triethyleneglycol chains and triazole rings, gave a switchable fluorescence response with selective binding of Ca^{2+} and subsequent quenching by interaction of the complex with F^-.[94] Other ion binding calixarenes have also been synthesised that have no fluorescent moiety, but have the ability to extract cations from aqueous to organic phase in a biphasic mixture.[95,96]

The work of Pathak *et al.* on calixarene-based sensors has had more of a biological focus. The sensors developed by this group are based on a common motif: the 1,3-dipropargyl calixarene is conjugated to benzaldehyde moieties, which are then used to form a Schiff-base to various molecules to diversify the scaffold (for example compound **55**).[91,97–100] This has yielded sensors which bind cations using not the triazole moieties as noted previously, but the Schiff-base groups.

A Zn^{2+} binding calixarene featuring imine-linked thiophene units has been developed[99] which gives a switchable response, with increase in fluorescence on Zn^{2+} binding being reversed by addition of cysteine or dithiothreitrol (DTT) due to ligand displacement. Release of Zn^{2+} from its complex with cysteine or DTT by addition of

Cd^{2+} or Hg^{2+} and concomitant restoration of fluorescence was also demonstrated. These two processes mimic metallothionein and metal-detoxification, respectively.

Similarly, a Zn^{2+} complex with a pyridyl-imine derivative provided the means for selective recognition of cysteine by fluorescence switching. This was shown to be applicable to both the free amino acid and protein-bound cysteine.[91] This amino-acid sensing application was extended further with a triazole-linked *o*-iminophenol functionalised calixarene.[100] The function of this molecule was diversified by forming complexes with different metal cations, which were shown to display selective sensing properties towards different amino acids depending on the incorporated metal, with similarities to amino acid-metal ion pairs found in metalloproteins.

Other work by Pathak *et al.* has demonstrated the applicability of switchable sensors inside living cells. This will be examined in Chapter 2.

Click chemistry also provides easy access to glycoconjugates. Galante *et al.*[101] synthesised lower-rim tetrapropargyl calixarene in cone and partial cone conformations as part of a larger library including upper- and lower-rim azide functionalised calixarenes, which were then used to form glycoconjugates with suitably functionalised lactose moieties for testing as trypanocidal agents. Although the partial cone showed little activity, the cone conformer (**56**) showed activity comparable to the established drug benznidazole.

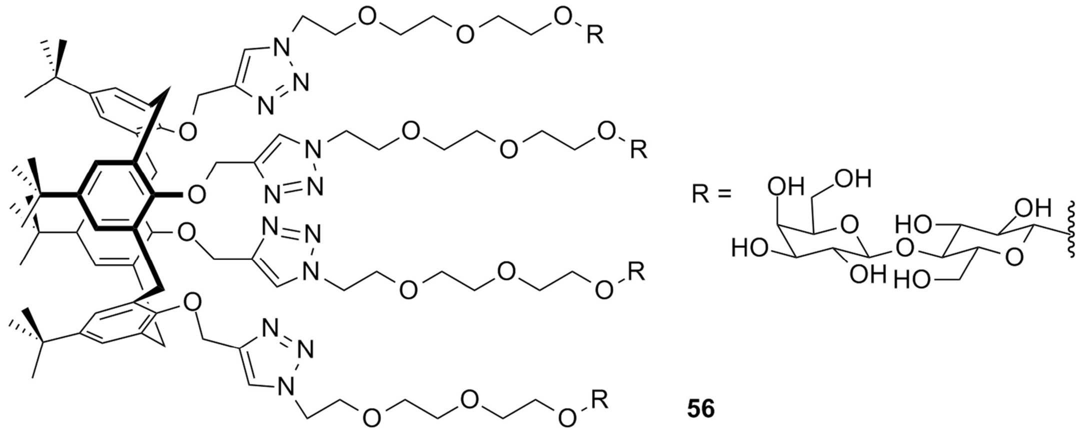

56

*Figure 1.11: Example of glycoconjugate (**56**) functionalised with lactose moieties.*[101]

Chinta and Rao[102] used 1,3-dipropargyl calixarene to synthesise galactosyl and lactosyl functionalised calixarenes. After testing binding to amino acids, which interestingly showed that the triazole ring was involved in the interaction with tryptophan, binding to the target protein, Jacilin, was confirmed.

The various propargylated calixarenes synthesised by Matthews and coworkers[80] were also conjugated to sugars. By performing a click reaction between the calixarene

scaffolds and azide-functionalised galactose, linked by triethylene glycol, water-soluble glycoconjugates were synthesised with different valencies and conformations for targeting the PA-IL lectin of *Pseudomonas aeruginosa*. These, and other glycoconjugates, will be examined in more detail in Chapter 3.

1.3 Overview of thesis

Chapter 1 has provided an overview of the key themes that are present throughout the thesis: calixarenes, their potential biological applications and the use of click chemistry in combination with these scaffolds.

Chapter 2 will examine in more detail the concept of cell penetration, cell penetration agents and the use of calixarenes in this context. The present research undertaken to add to this body of work will then be presented, including the synthesis and biological evaluation of novel calixarene-based cell penetration agents.

Chapter 3 will explain the glycoside-cluster effect and how multivalent glycocongugates can be used to exploit this. The use of calixarenes as a scaffold to this end will be examined, particularly in the context of targeting *Pseudomonas aeruginosa*. A synthetic strategy towards bi-functional fluorescent calixarene-based glycoconjugates will be presented.

1.4 References

(1) Baeyer, A. *Ber. Dtsch. Chem. Ges.* **1872**, *5*, 1094–1100.

(2) Baekeland, L. H. Method of Making Insoluble Product of Phenol and Formaldehyde. *US942699* **1908**.

(3) Zinke, A.; Kretz, R.; Leggewie, E.; Hössinger, K.; Hoffmann, G.; Ostwalden, P. W. v.; Wiesenberger, E.; Sobotka, M. *Monatshefte für Chemie* **1952**, *83*, 1213–1227.

(4) Cornforth, J. W.; D'arcy Hart, P.; Nicholls, G. A.; Rees, R. J. W.; Stock, J. A. *Br. J. Pharmacol. Chemother.* **1955**, *10*, 73–86.

(5) Gutsche, C. D.; Muthukrishnan, R. *J. Org. Chem.* **1978**, *43*, 4905–4906.

(6) Gutsche, C. D.; Iqbal, M.; Stewart, D. *J. Org. Chem.* **1986**, *51*, 742–745.

(7) Gutsche, C. D.; Dhawan, B.; No, K. H.; Muthukrishnan, R. *J. Am. Chem. Soc.* **1981**, *103*, 3782–3792.

(8) Gutsche, C. D.; Iqbal, M. *Org. Synth.* **1990**, *68*, 234–236.

(9) Gutsche, C. D.; Dhawan, B.; Leonis, M.; Stewart, D. *Org. Synth.* **1990**, *68*, 238.

(10) Munch, J. H.; Gutsche, C. D. *Org. Synth.* **1990**, *68*, 243.

(11) Stewart, D. R.; Gutsche, C. D. *Org. Prep. Proced. Int.* **1993**, *25*, 137–139.

(12) Vocanson, F.; Lamartine, R.; Lanteri, P.; Longeray, R.; Gauvrit, J. Y. *New J. Chem.* **1995**, *19*, 825–829.

(13) Dumazet, I.; Regnouf-de-Vains, J.-B.; Lamartine, R. *Synth. Commun.* **1997**, *27*, 2547–2555.

(14) Gutsche, C. D.; Rogers, J. S.; Stewart, D.; See, K.-A. *Pure Appl. Chem.* **1990**, *62*, 485–491.

(15) Gilbert, E. E. *J. Heterocycl. Chem.* **1974**, *11*, 899–904.

(16) Tsue, H.; Ono, K.; Tokita, S.; Ishibashi, K.; Matsui, K.; Takahashi, H.; Miyata, K.; Takahashi, D.; Tamura, R. *Org. Lett.* **2011**, *13*, 490–493.

(17) Kumagai, H.; Hasegawa, M.; Miyanari, S.; Sugawa, Y.; Sato, Y.; Hori, T.; Ueda, S.; Kamiyama, H.; Miyano, S. *Tetrahedron Lett.* **1997**, *38*, 3971–3972.

(18) Hayes, B. T.; Hunter, R. F. *J. Appl. Chem.* **2007**, *8*, 743–748.

(19) Kämmerer, H.; Happel, G.; Caesar, F. *Die Makromolekulare Chemie* **1972**, *162*, 179–197.

(20) Böhmer, V.; Chhim, P.; Kämmerer, H. *Die Makromolekulare Chemie* **1979**, *180*, 2503–2506.

(21) Gutsche, C. D. *Calixarenes: An Introduction, 2nd Edition*; The Royal Society of Chemistry, 2008.

(22) Groenen, L. C.; Van Loon, J. D.; Verboom, W.; Harkema, S.; Casnati, A.; Ungaro, R.; Pochini, A.; Ugozzoli, F.; Reinhoudt, D. N. *J. Am. Chem. Soc.* **1991**, *113*, 2385–2392.

(23) Iwamoto, K.; Araki, K.; Shinkai, S. *J. Org. Chem.* **1991**, *56*, 4955–4962.

(24) Iwamoto, K.; Fujimoto, K.; Matsuda, T.; Shinkai, S. *Tetrahedron Lett.* **1990**, *31*, 7169–7172.

(25) Iwamoto, K.; Araki, K.; Shinkai, S. *Tetrahedron* **1991**, *47*, 4325–4342.

(26) Iwamoto, K.; Shinkai, S. *J. Org. Chem.* **1992**, *57*, 7066–7073.

(27) Goren, Z.; Biali, S. E. *J. Chem. Soc. Perkin Trans. 1* **1990**, 1484–1487.

(28) Gibbs, C. G.; Sujeeth, P. K.; Rogers, J. S.; Stanley, G. G.; Krawiec, M.; Watson, W. H.; Gutsche, C. D. *J. Org. Chem.* **1995**, *60*, 8394–8402.

(29) Aleksiuk, O.; Cohen, S.; Biali, S. E. *J. Am. Chem. Soc.* **1995**, *117*, 9645–9652.

(30) Van Gelder, J. M.; Aleksiuk, O.; Biali, S. E. *J. Org. Chem.* **1996**, *61*, 8419–8424.

(31) Verboom, W.; Durie, A.; Egberink, R. J. M.; Asfari, Z.; Reinhoudt, D. N. *J. Org. Chem.* **1992**, *57*, 1313–1316.

(32) Kumar, S.; Chawla, H. M.; Varadarajan, R. *Indian J. Chem. Sect. B* **2003**, *42B*, 2863–2865.

(33) Gutsche, C. D.; Levine, J. A. *J. Am. Chem. Soc.* **1982**, *104*, 2652–2653.

(34) Gutsche, C. D.; Pagoria, P. F. *J. Org. Chem.* **1985**, *50*, 5795–5802.

(35) Almi, M.; Arduini, A.; Casnati, A.; Pochini, A.; Ungaro, R. *Tetrahedron* **1989**, *45*, 2177–2182.

(36) Gutsche, C. D.; Levine, J. A.; Sujeeth, P. K. *J. Org. Chem.* **1985**, *50*, 5802–5806.

(37) Reddy, P. A.; Gutsche, C. D. *J. Org. Chem.* **1993**, *58*, 3245–3251.

(38) Segura, M.; Bricoli, B.; Casnati, A.; Munoz, E. M.; Sansone, F.; Ungaro, R.; Vicent, C. *J. Org. Chem.* **2003**, *68*, 6296–6303.

(39) Hamuro, Y.; Calama, M. C.; Park, H. S.; Hamilton, A. D. *Angew. Chem., Int. Ed.* **1997**, *36*, 2680–2683.

(40) Wei, Y.; McLendon, G. L.; Hamilton, A. D.; Case, M. A.; Purring, C. B.; Lin, Q.; Park, H. S.; Lee, C. S.; Yu, T. N. *Chem. Commun.* **2001**, 1580–1581.

(41) Sun, J. Z.; Blaskovich, M. A.; Jain, R. K.; Delarue, F.; Paris, D.; Brem, S.; Wotoczek-Obadia, M.; Lin, Q.; Coppola, D.; Choi, K. H.; Mullan, M.; Hamilton, A. D.; Sebti, S. M. *Cancer Res.* **2004**, *64*, 3586–3592.

(42) Zadmard, R.; Schrader, T. *J. Am. Chem. Soc.* **2005**, *127*, 904–915.

(43) Zadmard, R.; Arendt, M.; Schrader, T. *J. Am. Chem. Soc.* **2004**, *126*, 7752–7753.

(44) Kolusheva, S.; Zadmard, R.; Schrader, T.; Jelinek, R. *J. Am. Chem. Soc.* **2006**, *128*, 13592–8.

(45) Gordo, S.; Martos, V.; Santos, E.; Menendez, M.; Bo, C.; Giralt, E.; de Mendoza, J.; Menéndez, M. *Proc. Natl. Acad. Sci. U. S. A.* **2008**, *105*, 16426–16431.

(46) Jin, T.; Kinjo, M.; Kobayashi, Y.; Hirata, H. *J. Chem. Soc. Faraday Trans.* **1998**, *94*, 3135–3140.

(47) Maulucci, N.; De Riccardis, F.; Botta, C. B.; Casapullo, A.; Cressina, E.; Fregonese, M.; Tecilla, P.; Izzo, I. *Chem. Commun.* **2005**, 1354–1356.

(48) Sidorov, V.; Kotch, F. W.; Abdrakhmanova, G.; Mizani, R.; Fettinger, J. C.; Davis, J. T. *J. Am. Chem. Soc.* **2002**, *124*, 2267–2278.

(49) Izzo, I.; Licen, S.; Maulucci, N.; Autore, G.; Marzocco, S.; Tecilla, P.; De Riccardis, F. *Chem. Commun.* **2008**, *26*, 2986–8.

(50) Seganish, J. L.; Santacroce, P. V; Salimian, K. J.; Fettinger, J. C.; Zavalij, P.; Davis, J. T. *Angew. Chem., Int. Ed.* **2006**, *45*, 3334–8.

(51) Cacciapaglia, R.; Casnati, A.; Mandolini, L.; Reinhoudt, D. N.; Salvio, R.; Sartori, A.; Ungaro, R. *J. Am. Chem. Soc.* **2006**, *128*, 12322–12330.

(52) Cacciapaglia, R.; Casnati, A.; Mandolini, L.; Peracchi, A.; Reinhoudt, D. N.; Salvio, R.; Sartori, A.; Ungaro, R. *J. Am. Chem. Soc.* **2007**, *129*, 12512–12520.

(53) Baldini, L.; Cacciapaglia, R.; Casnati, A.; Mandolini, L.; Salvio, R.; Sansone, F.; Ungaro, R. *J. Org. Chem.* **2012**, *77*, 3381–9.

(54) Bezouska, K.; Snajdrová, R.; Krenek, K.; Vancurová, M.; Kádek, A.; Adámek, D.; Lhoták, P.; Kavan, D.; Hofbauerová, K.; Man, P.; Bojarová, P.; Kren, V. *Bioorg. Med. Chem.* **2010**, *18*, 1434–40.

(55) Consoli, G. M. L.; Granata, G.; Geraci, C. *Org. Biomol. Chem.* **2011**, *9*, 6491–5.

(56) Casnati, A.; Fabbi, M.; Pelizzi, N.; Pochini, A.; Sansone, F.; Ungaro, R.; DiModugno, E.; Tarzia, G. *Bioorg. Med. Chem. Lett.* **1996**, *6*, 2699–2704.

(57) Dibama, H. M.; Clarot, I.; Fontanay, S.; Salem, A. Ben; Mourer, M.; Finance, C.; Duval, R. E.; Regnouf-de-Vains, J.-B. *Bioorg. Med. Chem. Lett.* **2009**, *19*, 2679–82.

(58) Lamartine, R.; Tsukada, M.; Wilson, D.; Shirata, A. *Comptes Rendus Chim.* **2002**, *5*, 163–169.

(59) Boyd, D. H. A.; Stewart, S. M.; Somner, A. R.; Crofton, J. W.; Rees, R. J. W. *Tubercle* **1959**, *40*, 369–376.

(60) Mourer, M.; Duval, R. E.; Finance, C.; Regnouf-de-Vains, J.-B. *Bioorg. Med. Chem. Lett.* **2006**, *16*, 2960–3.

(61) Sautrey, G.; Orlof, M.; Korchowiec, B.; Regnouf-de-Vains, J.-B.; Rogalska, E. *J. Phys. Chem. B* **2011**, *115*, 15002–12.

(62) Mourer, M.; Psychogios, N.; Laumond, G.; Aubertin, A.-M.; Regnouf-de-Vains, J.-B. *Bioorg. Med. Chem.* **2010**, *18*, 36–45.

(63) Colston, M.; Hailes, H. *Infect. Immun.* **2004**, *72*, 6318–6323.

(64) Tsou, L. K.; Dutschman, G. E.; Gullen, E. A.; Telpoukhovskaia, M.; Cheng, Y.-C.; Hamilton, A. D. *Bioorg. Med. Chem. Lett.* **2010**, *20*, 2137–9.

(65) Song, K.-S.; Nimse, S. B.; Kim, J.; Kim, J.; Nguyen, V.-T.; Ta, V.-T.; Kim, T. *Chem. Commun.* **2011**, *47*, 7101–7103.

(66) Nimse, S. B.; Song, K.-S.; Kim, J.; Ta, V.-T.; Nguyen, V.-T.; Kim, T. *Chem. Commun.* **2011**, *47*, 12444–6.

(67) Kolb, H. C.; Finn, M. G.; Sharpless, K. B. *Angew. Chem., Int. Ed.* **2001**, *40*, 2004–2021.

(68) Ferraris, D.; Drury, W. J.; Cox, C.; Lectka, T. *J. Org. Chem.* **1998**, *63*, 4568–4569.

(69) Hoyle, C. E.; Bowman, C. N. *Angew. Chem., Int. Ed.* **2010**, *49*, 1540–1573.

(70) Huisgen, R. In *1,3-Dipolar Cycloaddition Chemistry, Volume 1*; Padwa, A., Ed.; Wiley, 1984; pp. 1–176.

(71) Huisgen, R.; Szeimies, G.; Möbius, L. *Chem. Ber.* **1967**, *100*, 2494–2507.

(72) Rostovtsev, V. V; Green, L. G.; Fokin, V. V; Sharpless, K. B. *Angew. Chem., Int. Ed.* **2002**, *41*, 2596–9.

(73) Tornøe, C. W.; Christensen, C.; Meldal, M. *J. Org. Chem.* **2002**, *67*, 3057–3064.

(74) Chan, T. R.; Hilgraf, R.; Sharpless, K. B.; Fokin, V. V *Org. Lett.* **2004**, *6*, 2853–2855.

(75) Worrell, B. T.; Malik, J. A.; Fokin, V. V. *Science* **2013**, *340*, 457–460.

(76) Calvo-Flores, F. G.; Isac-García, J.; Hernández-Mateo, F.; Pérez-Balderas, F.; Calvo-Asín, J. a; Sanchéz-Vaquero, E.; Santoyo-González, F. *Org. Lett.* **2000**, *2*, 2499–2502.

(77) Ryu, E. H.; Zhao, Y. *Org. Lett.* **2005**, *7*, 1035–1037.

(78) Chen, X. M.; Dings, R. P. M.; Nesmelova, I.; Debbert, S.; Haseman, J. R.; Maxwell, J.; Hoye, T. R.; Mayo, K. H. *J. Med. Chem.* **2006**, *49*, 7754–7765.

(79) Chetcuti, M. J.; Devoille, A. M. J.; Othman, A. Ben; Souane, R.; Thuéry, P.; Vicens, J. *Dalton Trans.* **2009**, 2999–3008.

(80) Cecioni, S.; Lalor, R.; Blanchard, B.; Praly, J.-P.; Imberty, A.; Matthews, S. E.; Vidal, S. *Chem.--Eur. J.* **2009**, *15*, 13232–13240.

(81) Xu, W.; Vittal, J. J.; Puddephatt, R. J. *Can. J. Chem.* **1996**, *74*, 766–774.

(82) Bois, J.; Espinas, J.; Darbost, U.; Felix, C.; Duchamp, C.; Bouchu, D.; Taoufik, M.; Bonnamour, I. *J. Org. Chem.* **2010**, *75*, 7550–7558.

(83) Morales-Sanfrutos, J.; Ortega-Muñoz, M.; Lopez-Jaramillo, J.; Hernández-Mateo, F.; Santoyo-González, F. *J. Org. Chem.* **2008**, *73*, 7768–7771.

(84) Garska, B.; Tabatabai, M.; Ritter, H. *Beilstein J. Org. Chem.* **2010**, *6*, 784–788.

(85) Gou, P.; Zhu, W.; Shen, Z. *J. Polym. Sci., Part A: Polym. Chem.* **2010**, *48*, 5643–5651.

(86) Chang, K.-C.; Su, I.-H.; Senthilvelan, A.; Chung, W.-S. *Org. Lett.* **2007**, *9*, 3363–3366.

(87) Chang, K.-C.; Su, I.-H.; Wang, Y.-Y.; Chung, W.-S. *European J. Org. Chem.* **2010**, *2010*, 4700–4704.

(88) Ho, I.-T.; Haung, K.-C.; Chung, W.-S. *Chem. Asian J.* **2011**, *6*, 2738–2746.

(89) Wang, N.-J.; Sun, C.-M.; Chung, W.-S. *Tetrahedron* **2011**, *67*, 8131–8139.

(90) Wang, N.-J.; Sun, C.-M.; Chung, W.-S. *Sensors Actuators B Chem.* **2012**, *171-172*, 984–993.

(91) Pathak, R. K.; Tabbasum, K.; Hinge, V. K.; Rao, C. P. *Chem.--Eur. J.* **2011**, *17*, 13999–14003.

(92) Park, S. Y.; Yoon, J. H.; Hong, C. S.; Souane, R.; Kim, J. S.; Matthews, S. E.; Vicens, J. *J. Org. Chem.* **2008**, *73*, 8212–8218.

(93) Kim, J.-S.; Park, S.-Y.; Kim, S.-H.; Thuery, P.; Souane, R.; Matthews, S. E.; Vicens, J. *Bull. Korean Chem. Soc.* **2010**, *31*, 624–629.

(94) Zhan, J.; Fang, F.; Tian, D.; Li, H. *Supramol. Chem.* **2012**, *24*, 272–278.

(95) Li, H.; Zhan, J.; Chen, M.; Tian, D.; Zou, Z. *J. Incl. Phenom. Macrocycl. Chem.* **2010**, *66*, 43–47.

(96) Zhan, J.; Tian, D.; Li, H. *New J. Chem.* **2009**, *33*, 725–728.

(97) Pathak, R. K.; Ibrahim, S. M.; Rao, C. P. *Tetrahedron Lett.* **2009**, *50*, 2730–2734.

(98) Pathak, R. K.; Dikundwar, A. G.; Row, T. N. G.; Rao, C. P. *Chem. Commun.* **2010**, *46*, 4345–4347.

(99) Pathak, R. K.; Hinge, V. K.; Mondal, M.; Rao, C. P. *J. Org. Chem.* **2011**, *76*, 10039–10049.

(100) Pathak, R. K.; Dessingou, J.; Rao, C. P. *Anal. Chem.* **2012**, *84*, 8294–8300.

(101) Galante, E.; Geraci, C.; Sciuto, S.; Campo, V. L.; Carvalho, I.; Sesti-Costa, R.; Guedes, P. M. M.; Silva, J. S.; Hill, L.; Nepogodiev, S. A.; Field, R. A. *Tetrahedron* **2011**, *67*, 5902–5912.

(102) Chinta, J. P.; Rao, C. P. *Carbohydr. Res.* **2013**, *369*, 58–62.

Chapter 2: Calixarene-Based Cell-Penetration Agents

2.1 Introduction

2.1.1 Mechanisms of cell uptake

Uptake of molecules or larger structures into cells across the largely impermeable cell membrane is essential for a number of processes. Foreign bodies such as pathogens are removed and destroyed by phagocytosis,[1] whilst other endocytosis mechanisms are involved in cellular signalling by regulation of the number of receptors on a cell's surface.[2] Endocytosis can also be exploited by pathogens to gain entry to cells.[3] Endocytosis processes can be categorised into three main groups: clathrin-mediated, caveolae dependent and clathin- and caveolae-independent (see Figure 2.1). These will be examined further in the following sections.

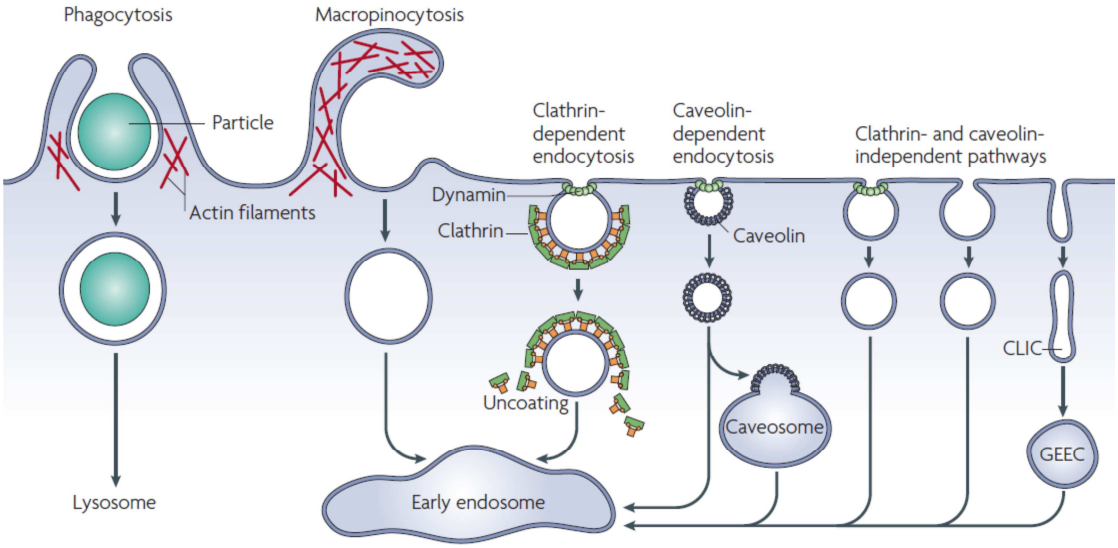

Figure 2.1: Mechanisms of endocytosis. Reprinted by permission from Macmillan Publishers Ltd: Nature Reviews Molecular Cell Biology[4] *© 2007*

2.1.1.1 Clathrin mediated endocytosis

Clathrin mediated endocytosis is involved in the internalisation of lipids and proteins, such as a transmembrane receptor and its ligand, from the cell membrane. It is utilised at nerve synapses where it has a role in the recycling of synaptic vesicles following the release of neurotransmitters and is important for proper signal transmission.[5] In the gut, it is involved in the uptake of iron (for example by transferrin), lectins and even viruses.[6] The endocytosis process is summarised in Figure 2.2.

Clathrin mediated endocytosis requires the protein clathrin to form a coat on the cytoplasmic face of the membrane. The structure is a triskelion with each of the three arms consisting of a light chain and a heavy chain of clathrin; these molecules then

form the lattice that coats the vesicle.[7] A number of accessory proteins are also required. These include adaptor proteins, such as AP2, which links the clathrin to the cell membrane. For example, AP2 recognises the cytoplasmic face of transferrin and links it to the nucleating clathrin.[8]

The membrane becomes deformed at the site of clathrin nucleation, creating a clathrin coated pit. More accessory proteins aid in this deformation of the membrane. For example, epsin type proteins partially insert an amphipathic helix into the cell membrane, displacing lipid residues in a wedge-like manner to create a curve.[9] Further polymerisation leads to constriction of the vesicle neck. Dynamin, a GTPase, forms a helical polymer around the neck, such that subsequent GTP hydrolysis results in scission of the vesicle from the cell membrane to form a clathrin coated vesicle.[10] Recruitment of dynamin is effected by amphiphysin, which also binds to clathrin and AP2.[11] The protein coat is then removed by auxilin and heat shock cognate protein 70 kD (HSC70).[12] The vesicle can then undergo intracellular trafficking followed by fusion to the target membrane.

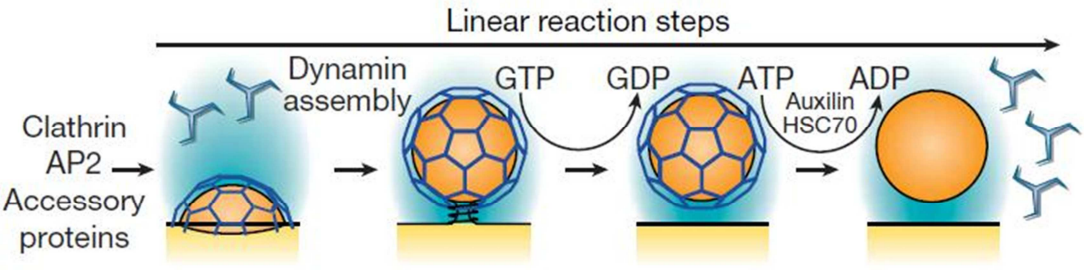

Figure 2.2: Scheme of key steps in clathrin mediated endocytosis. Reprinted by permission from Macmillan Publishers Ltd: Nature[7] *© 2007*

2.1.1.2 Caveolae

Caveolae ('little caves') are flask-shaped invaginations in the cell membrane, forming a microdomain that is a type of lipid raft. They are particularly abundant in smooth muscle, fibroblasts, adipocytes and epithelial cells[13], but some cells such as lymphocytes lack caveolae.[14] Previously associated only with non-specific bulk transfer of fluid-phase cargoes, caveolae dependent endocytosis is now implicated in a number of processes. These include a role in calcium mediated signalling in endothelial cells, both negative and positive regulation of membrane bound receptors and cholesterol homeostasis.[15]

Caveolae are enriched with caveolin type proteins. Caveolin1 (or caveolin3 in muscle cells) is crucial for their formation. Caveolin1 has an intramembrane domain that inserts into the cell membrane, forming a hairpin loop with both *N*- and *C*-

terminal domains in the cytoplasm. It is palmitoylated and can bind cholesterol and fatty acids to stabilise its oligomers.[16] It is thought that caveolin itself effects the curvature of the membrane in the formation of the caveolae. The amphipathic structure can be seen as analogous to those involved in clathrin mediated endocytosis, with the inserted loop deforming the membrane. In addition, the enrichment of cholesterol within the membrane envelope may enhance the curvature.[9]

Although dynamin is required for scission, it has been shown that not all caveolae pinch off from the membrane. Caveosomal structures have been found distant from the cell membrane that were still connected to it,[17] suggesting that some caveolae are stable structures that are not involved in endocytosis.

2.1.1.3 Clathrin- and caveolin-independent pathways

It has been found that cells in which clathrin and caveolin have been depleted can still undergo cholesterol dependent endocytosis. GPI-anchored proteins (GPI-AP) are not usually concentrated into clathrin coated pits or caveolae although the latter play a role. Instead, clathrin-independent carriers (CLICs) can form and transfer the structures to GPI-AP-enriched early endosomal compartments (GEECs), more tubular in shape than typical vesicles. This pathway is regulated by the G-protein cdc42.[18] This is a lipid raft associated process, with the clustering of the GPI-APs dependent on cholesterol.[19] This does not create sufficient membrane curvature so other proteins with Bin–Amphiphysin–Rvs (BAR)-type domains such as GRAF1 are recruited to the curved membrane and induce further curvature.[9]

Another lipid-raft associated process is macropinocytosis. This occurs when protrusions in the cell membrane fuse back to the lipid bilayer to form large, fluid-filled macropinosomes, which is associated with extensive actin rearrangement to give characteristic ruffles.[20] It has been shown to be important in class II MHC-positive cells in the uptake of antigens.[21] A number of enzymes have been shown to be important for this process, including phosphoinositide 3-kinase (PI3-K), the GTPase Rac1 and ARF6.[20,22] The localisation of Rac1 and ARF6 to the membrane seems to be cholesterol dependent and cholesterol depletion inhibits macropinocytosis.[23] However, cholesterol depletion is a non-specific inhibitor. It may be that the observed inhibition is a secondary effect, for example due to interference with the actin cytoskeleton at the cell membrane.[20]

2.1.2 Cell penetration agents

Many therapeutic targets lie within cells. As such, it is essential for drugs or other therapeutic agents to be able to cross the cell membrane. In some cases this barrier prevents the agent being available within the cell, for example in the delivery of nucleic acids in gene therapy. Therefore it is important to investigate ways to facilitate the delivery of various molecules into cells.

2.1.2.1 Cell penetrating peptides

Some naturally occurring peptides are able to cross the cell membrane. One early observation of this was the Antennapedia homeodomain, the DNA binding portion of a transcription factor from *Drosophila*, which was found to penetrate cells in culture.[24] Further examples have also been found, including the transactivator of transcription (Tat) protein from HIV, from which the protein transduction domain (Tatp) was isolated.[25]

The potential usage of such peptides as cell penetration agents to deliver cargos into cells has led to extensive investigation of the mechanisms of their uptake into cells and the essential features that allow them to do so. This has informed the design of synthetic cell penetrating peptides and the investigation of potential applications. These investigations will be examined in the following sections.

2.1.2.1.1 Cellular uptake mechanisms

In order to facilitate the design of cell penetrating peptides, their uptake mechanisms into cells have been investigated. Early work seemed to indicate an energy-independent, non-endocytotic mechanism of uptake due to the observation that at 4 °C there was no inhibition of uptake into cells.[24,25] However, subsequent work has suggested that this was an artefact of the procedures used to fix the cells.[26] Fixation using paraformaldehyde resulted in the cellular membranes becoming more leaky, leading to release of the peptides from endosomes to give the observed diffuse staining. Furthermore, excess peptide associated with the external surface of the membrane was able to leak into the cell even at low temperature.

Following this, many studies have been carried out on live cells. Nakase *et al.*[27] suggested that macropinocytosis was the dominant mechanism of uptake based on the observation that uptake of Tatp and other arginine rich peptides was associated with actin rearrangement. Also, inhibitors of macropinocytosis such as ethylisopropylamiloride inhibited their uptake. However, penetratin, a cell penetrating

peptide derived from the third helix Antennapedia homeodomain, was not affected by the same inhibitors except at high concentrations, suggesting that multiple mechanisms may be used by the same peptide.

They also suggested an important role of heparan sulphate proteoglycan (HSPG). Deficiency of this cell surface structure led to decreased uptake efficiency and was associated with a lack of induction of macropinocytosis by arginine-rich peptides, although this effect was less prominent for the 8 residue arginine oligomer, R8. They suggested that HSPG may act as a receptor for macropinocytosis by concentrating the cargo at the cell surface and stimulating the endocytosis.

However, other studies of Tatp have shown colocalisation with transferrin in HeLa cells, implicating clathrin mediated processes.[28] Consistent with this, treatment with chlorpromazine, an inhibitor of clathrin mediated endocytosis, gave 50% inhibition of uptake.[29] Other studies in the same cell line also found colocalisation with caveolin1,[30] although inhibitors of caveolae such as filipin did not have a significant impact on uptake.[29]

It has also been shown that a direct translocation mechanism may play a role, even in live cells. Fretz *et al.*[31] studied the uptake of octaarginine into cells under varying conditions in $CD34^+$ leukaemia cells. It was found that at low temperature there was diffuse staining of the cytoplasm and localisation to the nucleus, consistent with the original assumptions about endocytosis-independent uptake. At increasing temperature, localisation to endocytotic vesicles occurred, whilst at 37 °C this was the only staining present. A concentration threshold was implicated by the observation that at higher concentrations of peptide diffuse staining became evident once more. Cholesterol depletion also gave diffuse staining. This suggests that either cholesterol inhibits direct translocation, or that disruption of endocytosis necessitates an alternative mechanism.

Cumulatively, the data suggests that multiple mechanisms may be important, perhaps even operating in a concerted manner. Mechanistic studies have been complicated by the fact that a number of factors influence the mechanism that a peptide is taken up by. The type of cell, cell penetrating peptide and cargo all have an effect on the mechanism.[32] An example of the latter has been demonstrated by Tünnemann *et al.*[33] who found that varying the size of a peptide-based cargo attached to Tat from a peptide to a globular protein led to differences in uptake. The globular protein cargo was taken up only by endocytosis, whereas the peptide was also taken up by an unknown, rapid mechanism of translocation.

In summary, the dependence of uptake on a number of variables precludes the use of a single universal cell penetrating peptide. On the other hand, it may allow fine tuning for selective applications.

2.1.2.1.2 Design of cell penetrating peptides

Much work has been carried out to determine which features are essential for cellular uptake in order to design optimised cell penetrating peptides. Studies of individual segments of the Antennapedia homeodomain found that a 16 amino acid stretch corresponding to the third α-helix without its N-terminal glutamate (now known as penetratin) was the essential component for its translocation.[24] However, the α-helical structure is not essential for uptake, since introduction of 1-3 proline residues to interrupt the secondary structure did not prevent uptake.[34]

In the case of Tatp, studies to determine the key features of the peptide determined that translocation was due to a cluster of basic amino acids (six arginines and two lysines), whilst the amphipathic α-helix, initially thought to be a key determinant for uptake, was not essential.[25] It has also been found that deletion of arginine in Tatp is more detrimental to its cellular uptake efficiency than deletion of lysine.[32]

The difference in acidities between lysine and guanidinium cations has been proposed as a reason for this effect.[35] Lysine is sufficiently acidic to release a proton to water in order to reduce charge repulsion with neighbouring cationic groups; however, the guanidinium group of arginine is not sufficiently acidic to do the same. Therefore in order to stabilise the positive charge arginine may instead act as an anion scavenger. This may increase its tendency to bind to the negatively charged phosphate groups on the cell membrane.

It has also been proposed that arginine can create Gaussian negative curvature in the cell membrane, which is associated with the formation of pores, invaginations and protrusions. Arginine can form both electrostatic interactions and multiple hydrogen bonds, giving a bidentate mode of binding to multiple polar head groups of the cell membrane, whereas lysine can only form a hydrogen bond. This allows poly-arginine to give Gaussian negative curvature.[36] The ability of poly-arginine to do this would depend on the degree of intrinsic curvature in the membrane and so depend on the composition of the lipid bilayer, including the amount of cholesterol, accounting for some differences between cell types.

The length of an arginine oligomer is also important. Oligomers of 5-20 residues are taken up into cells, with maximum efficiency at 15 arginine residues. However the

R8 peptide has been most extensively studied as it gives a good compromise between uptake efficiency and ease of synthesis.[32,37]

Further studies into the effects of modifications of cell penetrating peptides found that both D- and L-isomers were efficiently taken up into cells, indicating that the backbone conformation of the peptide was not important. This suggests that enzyme interactions at the cell surface, which would depend on chirality, are not responsible for uptake. The D-isomer of an oligoarginine seemed to have superior uptake, perhaps due to its greater stability to proteolysis and longer *in vivo* lifetime.[32]

These observations led to the study of non-peptidic guanidinium-rich transporters, such as those based on peptoids and carbamates, which lack secondary structure and have greater flexibility. These will be examined further in section 2.1.2.2.

2.1.2.1.3 Applications

Cell penetrating peptides have been used to deliver a variety of cargoes into cells which would otherwise have poor uptake efficiency, or no uptake at all.

Peptide-based therapies have great potential but are hampered by the inability of most peptides to cross the cell membrane. However, peptides lend themselves to improvement with cell penetrating peptides as their incorporation can be included during the peptide synthesis. An example of this is the targeting of Nuclear factor (erythroid-derived 2)-like 2 (Nrf2).[38] This binds to the anti-oxidant response element (ARE) when not bound by its regulator Keap1 and so this interaction provides a target for treatment of inflammation. A 14-mer peptide, designed to interact with Keap1, when combined with Tatp was able to disrupt this interaction *in vivo*, giving downstream expression of heme oxygenase and supressing expression of tumor necrosis factor, a pro-inflammatory cytokine.

A further example is provided by Psorban, a cell penetrating peptide conjugate that is currently undergoing clinical trials. It is based on cyclosporine-A, a cyclic peptide with anti-inflammatory effects that is used to treat psoriasis. It was conjugated to R7, which allowed it to cross cutaneous barriers and penetrate into the target T-cells in inflamed skin, giving an anti-inflammatory response when used topically and avoiding the side-effects associated with systemic use.[39]

Nucleic acids can also be delivered, with potential applications in transfection and gene therapy. One such cargo is siRNA, small sections of double-stranded RNA that are capable of affecting the expression of target complementary genes by post-transcriptional silencing. Both covalent[40,41] and non-covalent[42] conjugates of cell

penetrating peptides with siRNA have been investigated and gave successful gene silencing, though vesicular accumulation was identified as a barrier in the latter case. This led to the development of PepFect6.[43] This transportan 10-based peptide features several trifluoromethylquinoline moieties, whose pH buffering capability leads to osmotic swelling and subsequent endosomal release. It was internalised into multiple cell lines with low toxicity and gave *in vivo* gene silencing in mouse models. However a more simple poly-arginine R15 was also able to internalise siRNA and give gene silencing, with cellular localisation suggesting endosomal escape, and gave reduction in tumor growth in a mouse model.[44]

Another example of their use is aiding in the delivery of small drug molecules by improving their properties. For example, polyarginine can be used to improve the water solubility and uptake of paclitaxel.[45] A different facet of this is improving availability of a drug by circumventing the action of efflux pumps which can give resistance. To this end a doxorubicin-Tatp conjugate was synthesised, which successfully exerted a cytotoxic effect on resistant cell lines.[46]

Cell penetrating peptides also have uses in cellular imaging. This is important therapeutically for visualising diseased tissue and also for improving understanding of biological processes. Jiang *et al.*[47] exploited the increased concentration of extracellular proteases in tumour tissue by conjugating a fluorescein peptide hairpin to a polyarginine cell penetrating peptide with an associated polyanionic segment. Proteolytic cleavage of the anionic domain was most prominent in the tumour tissue, allowing internalisation of the probe and selective visualisation of the tumour cells.

MRI can also be used to visualise cells, relying on the incorporation of MRI contrast agents which enhance the magnetic spin coupling of protons in water. Tat-iron oxide nanoparticles allow delivery of the contrast agents into cells and have been used for in vivo, real time tracking of T-cells with no effect on the normal immune function.[48]

2.1.2.2 Non-peptidic cell penetration agents

As noted in section 2.1.2.1.2, the ability of a cell penetrating peptide to resist proteolysis influences the efficacy of its uptake. The desire to find alternatives that will remain stable for longer periods in living cells has led to the investigation of non-peptidic systems.

Oligoarginine peptoids have the same 1,4-spacing for their side chains as their peptidic counterparts, but instead of the side chain being attached to carbon, it is

attached to the nitrogen (see Figure 2.3). This eliminates the secondary structure formed by N-H hydrogen bonding and increases flexibility. It was found that these structures were superior to Tatp in their uptake and that increasing the chain length between the backbone and the guanidinium moieties further increased uptake efficiency. This suggests that greater flexibility is important in uptake.[49]

Oligocarbamates have also been investigated, which are characterised by 1,6-spacing between their side chains (see Figure 2.3). Superior uptake was found relative to oligoarginine peptides. This shows that 1,4-spacing between side chains is not required for cell penetration.[50]

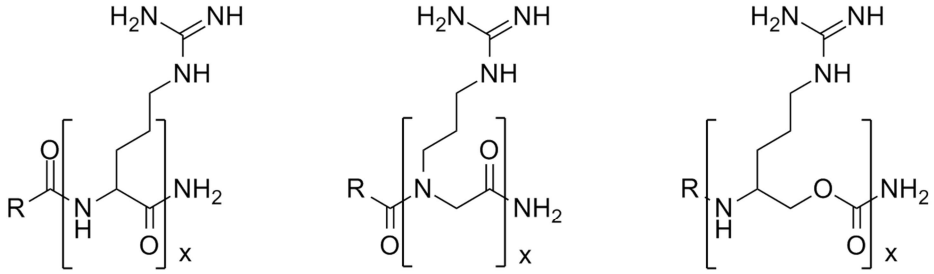

57 **58** **59**

*Figure 2.3: Oligoguanidinium compounds based on peptides (**57**), peptoids (**58**) and carbamates (**59**).*[49,50]

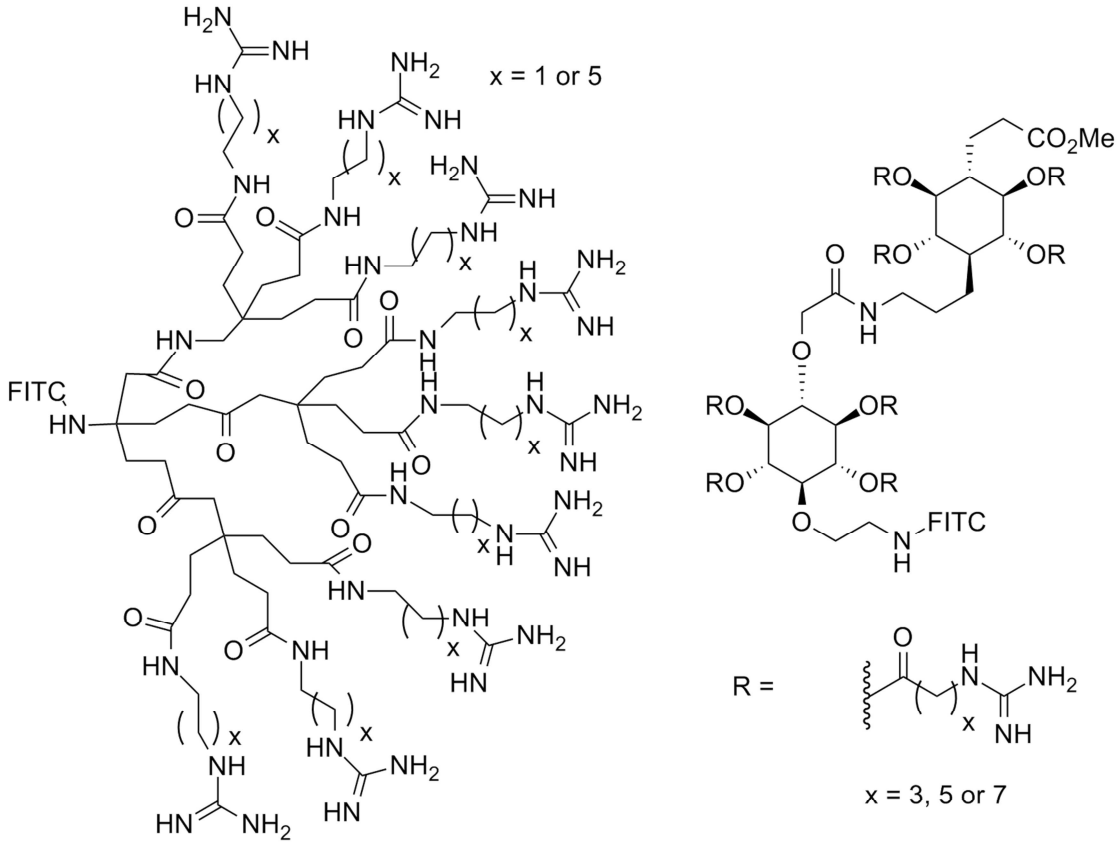

60 **61**

*Figure 2.4: Cell penetration agents based on a dendrimer (**60**)*[51] *and an inositol dimer (**61**).*[52] *FITC = fluorescein isothiocyanate.*

Other systems that have been investigated include guanidinium dendrimers[51] and carbohydrate based scaffolds[52] (see Figure 2.4). Macrocyclic scaffolds have also been investigated, including those based on calixarenes, which will be discussed in more detail in the following section.

2.1.2.2.1 Calixarenes as cell penetration agents

Depending on their functionalisation, calixarenes can have low cytotoxicity and immunogenicity;[53–55] this, combined with the ability to create a diverse range of scaffolds, makes them an attractive choice for cell penetration agents. Their properties have been exploited in a number of ways. For example, the ion sensing capabilities of appropriately functionalised calixarenes can be put to work inside of living cells. Pathak *et al.* have synthesised several calixarenes based on a common intermediate with a linker installed *via* a CuAAC reaction, diversified by adding different head groups with an imine linkage (see Figure 2.5).[56–58]

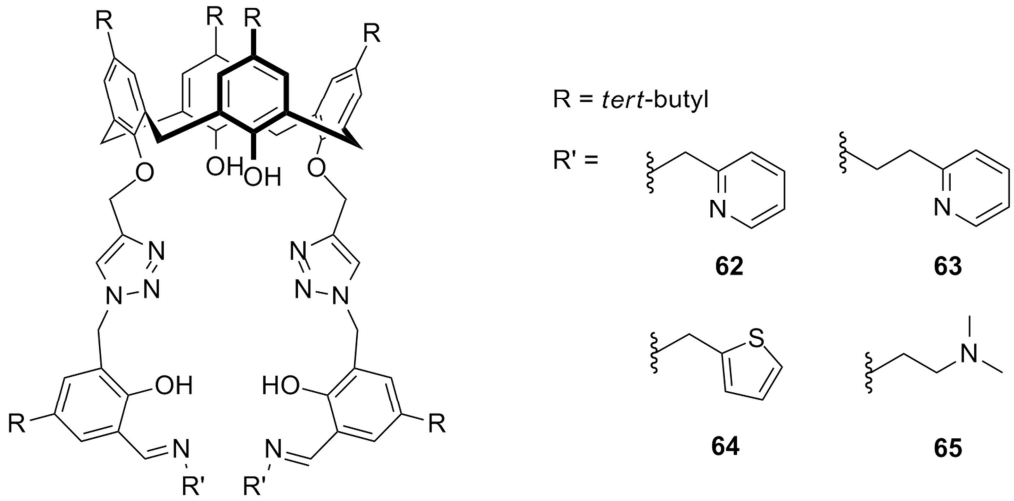

*Figure 2.5: Cell permeable cation binders based on pyridyl (**62**, **63**), thiophenyl (**64**) and dimethylamino (**65**) conjugates.*[56–58]

In all cases the fluorescence properties of the molecule were modulated by cation binding. In the absence of binding, the molecules had very weak fluorescence due to excited state proton transfer between the salicyl-OH and the imine-N. Cation binding supresses this process and results in 'switch-on' fluorescence which can then be monitored.

For the pyridyl conjugates,[56] selective binding of both compounds **62** and **63** with Zn^{2+} over a variety of other cations was found, with stronger binding of **62** attributed to a less distorted binding site. However, in a competitive binding assay the fluorescence was quenched in the presence of Cu^{2+}, precluding the use of these conjugates as Zn^{2+} sensors in the presence of Cu^{2+}. In both cases the *in vivo*

fluorescence was demonstrated by incubating HeLa cells first with the calixarene, giving only weak observable fluorescence after washing, followed by 1:1 Zn^{2+}/pyrithione, resulting in intense fluorescence. This showed that the calixarene was penetrating inside of the cells and retained its cation binding ability. It was also demonstrated that in the case of the more weakly binding compound **63**, Zn^{2+} could be removed from the complex by competitive binding to the metal by phosphate-based ligands, resulting in loss of fluorescence. However, in this case this process was not demonstrated *in vivo*.

Similar results were found for the thiophenyl conjugate **64**, with selective binding to Zn^{2+} found.[57] Fluorescence could be perturbed by addition of phosphate-based ligands to the complex, with complete quenching observed with pyrophosphate (PPi) due to its strong Zn^{2+} binding capabilities. The cell permeability was again demonstrated in HeLa cells, where fluorescence could be switched on as described before and switched off by treating the cells with PPi.

For the dimethylamino conjugate **65**,[58] the complex with Cd^{2+} was investigated to develop a sensor for cysteine by exploiting the selective soft ion binding of this amino acid with Cd^{2+}. The fluorescence of the metal complex could be switched off by adding cysteine, demonstrating binding to and removal of Cd^{2+} by the amino acid. The binding of cysteine was competitive in the presence of all other amino acids, which had no significant effect on the fluorescence properties, and the ability of reduced dithiothreitol but not its oxidised form to affect fluorescence shows that the thiol on the cysteine is used for binding. The applicability to live cells was demonstrated by the switch-on fluorescence associated with incubating MCF-7 cells first with free ligand, then with Cd^{2+}/pyrithione after washing with buffer. The fluorescence could then be switched off by further treatment of these cells with cysteine.

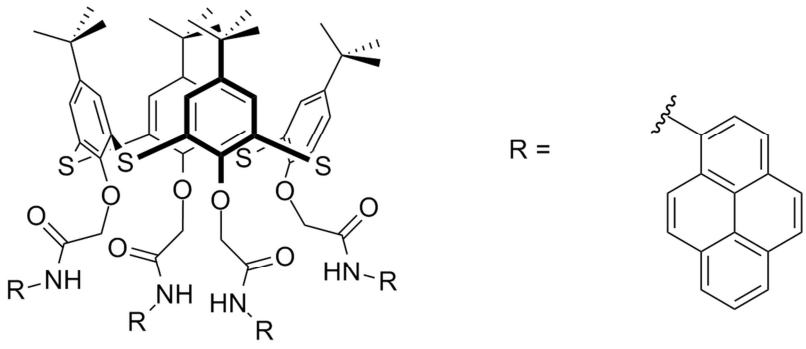

66

*Figure 2.6: Cell permeable thiacalixarene based Fe^{3+} sensor (**66**).*[59]

Similarly, a tetra-pyrene appended thiacalixarene (**66**) synthesised by Kumar *et al.*[59] was shown to selectively bind to Fe^{3+} out of a number of other metal ions

including Fe^{2+}, this time resulting in quenching of fluorescence. Incubation of PC3 cells with the ligand alone resulted in fluorescence within the cells, demonstrating the cell permeability of the thiacalixarene. This fluorescence could then be continuously quenched by treating these cells with varying concentrations of Fe^{3+}, showing potential application as an *in vivo* Fe^{3+} sensor.

The potential cell permeability of calixarenes has also been demonstrated by their ability to effect transfection. This has been accomplished with single calixarenes[54,60] and also multicalixarenes.[61]

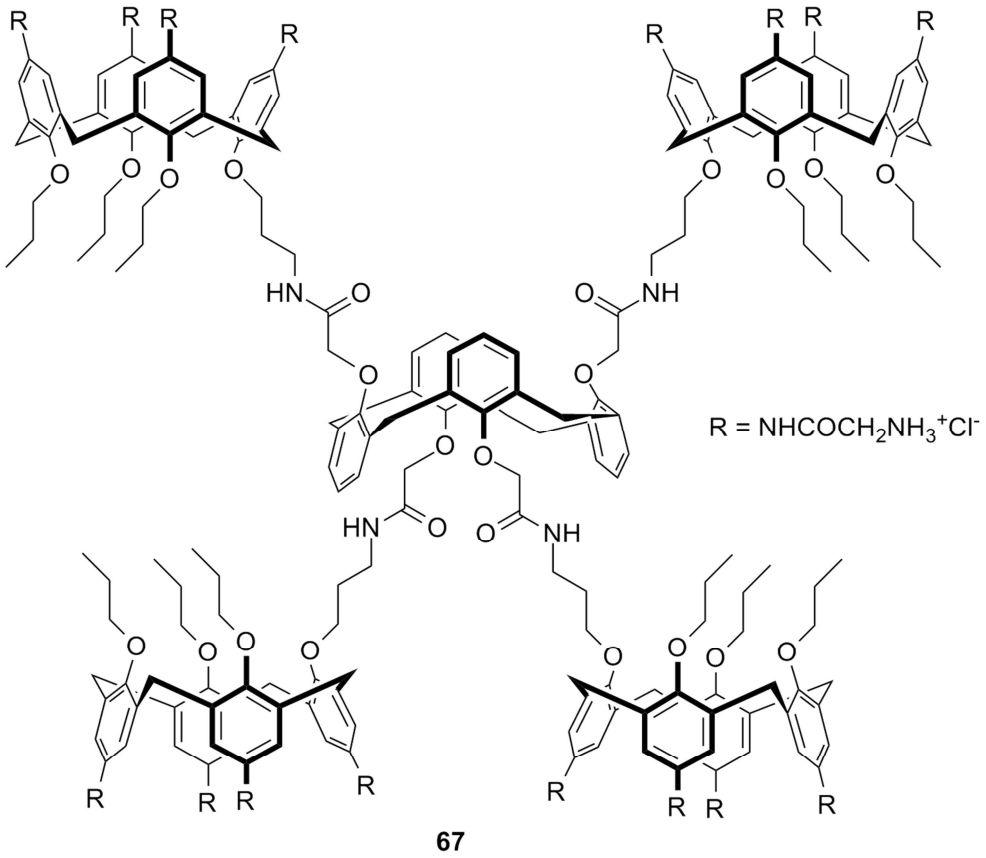

67

*Figure 2.7: Glycine functionalised multicalixarene (**67**).*[61]

In a comparison of different multicalixarenes and single calixarenes, Lalor *et al.*[61] found that a multicalixarene (**67**) with its core in the 1,3-alternate conformation and the pendent calixarenes functionalised with glycine moieties on their upper rims was able to promote transfection of the plasmid pDs2-mito, resulting in a fluorescent protein inside the mitochondria. By comparison, an analogous multicalixarene with aromatic amine functionalization and also a single calixarene appended with glycine moieties, whilst able to bind to DNA, were unable to promote transfection. However, without a fluorescent marker the uptake and cellular fate of these calixarenes was unknown.

In other work on single calixarenes, Sansone *et al.*[60] investigated the ability of calixarenes functionalised with aromatic guanidinium groups on the upper rim to effect transfection. They found that the rigid scaffold provided by calix[4]arene coupled with hexyl or octyl chains on the lower rim (**68**) gave a suitable, pre-organised amphiphilic molecule capable of driving DNA condensation by a combination of electrostatic and hydrophobic interactions, and promoting transfection. However, the transfection efficiency of pEGFP-C1, a plasmid coding for green fluorescent protein (GFP), was low and the cytotoxicity too high, with cell death occurring at a concentration of 40 μM. Further investigation of cell uptake was not carried out on this compound.

Further work[54] was carried out on calixarenes with the guanidinium moieties placed on the lower rim *via* a C3 spacer. A calixarene of this form with no upper rim functionalization (**69**) exhibited low cytotoxicity, with 70-75% viable cells at 10 μM concentration. However, the presence of *tert*-butyl or hexyl groups on the upper rim gave molecules that, despite having similarly low toxicity to **69** when simply incubated with cells, suffered increased cytotoxicity under transfection conditions.

In contrast with the poor transfection ability of **68**, when used with the helper lipid DOPE (dioleoylphosphatidylethanolamine) **69** was able to efficiently transfect pEGFP-C1 into RD-4 cells. It was rationalised that the greater flexibility of the cationic head groups when on the lower rim may improve DNA binding. Also, the hydrophobic cavity of **69** may give better interactions with DOPE than its aromatic guanidinium counterpart **68** (supported by the lack of any effect of DOPE on transfection with the latter), giving an assembly with superior transfection properties and lower toxicity.

The mechanism of uptake of the assembly was investigated by using inhibitors of different pathways of endocytosis. It was found that inhibitors of macropinocytosis (wortmannin and amiloride) and caveolae (filipin) had the most effect on supressing transfection, suggesting that these are the primary and secondary uptake mechanisms, respectively. No suppression of transfection was found with inhibitors of clathrin mediated endocytosis.

It was also found that replacing the guanidinium groups with amino moieties gave poor DNA binding properties, an inability to condense DNA and a loss of transfection capabilities. However the cellular uptake of this derivative is unknown.

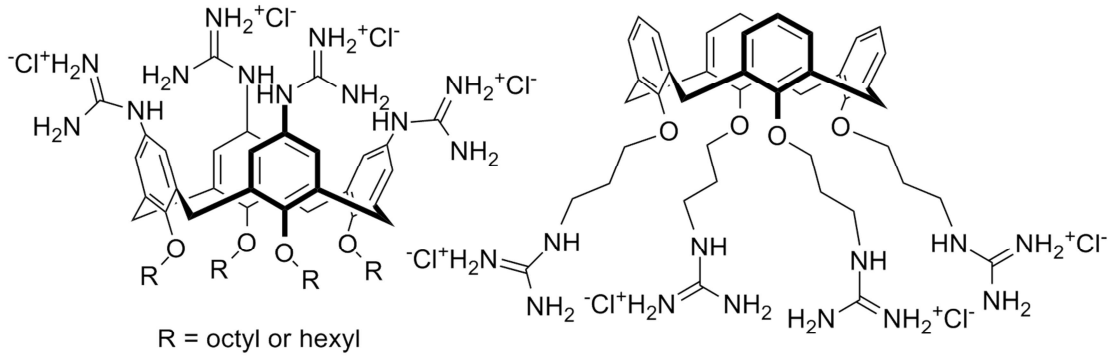

68 **69**

*Figure 2.8: Upper rim (**68**)[60] and lower rim (**69**)[54] guanidinium functionalised calixarenes.*

Recent work by Bagnacani *et al.*[62] further investigated the use of cationic calixarenes as transfection agents, this time using conjugation to amino acids to give arginine or lysine functionalisation on the upper and lower rims; the upper rim (**70**) and lower rim (**71**) arginine appended calixarenes are shown in Figure 2.9. In comparison with **68** and **69**, these derivatives bear an additional primary amino group on each side-chain.

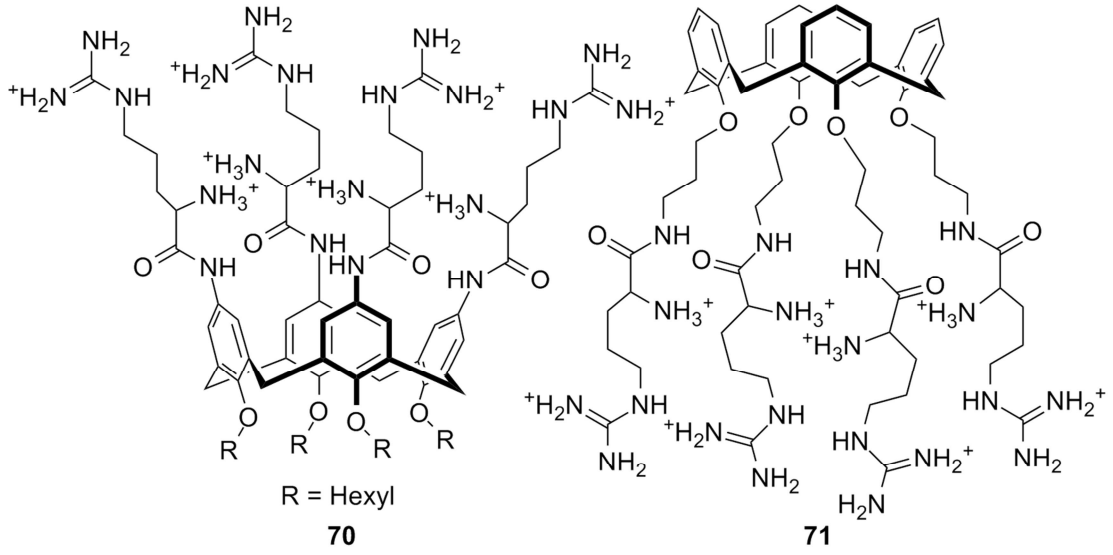

70 **71**

*Figure 2.9: Upper rim (**70**) and lower rim (**71**) arginine functionalised calixarenes.*[62]

Once again the DNA transfection ability seemed to be related to the ability to condense DNA. The lower-rim derivatives gave poor transfection due to the lack of amphiphilicity in comparison with the upper-rim derivatives, which were functionalised with hexyl groups on the lower rim. Comparison with non-cyclic derivatives showed the importance of the cyclic structure. The guanidinium function was also again shown to be important for efficient transfection: whilst the upper-rim lysine was able to give some transfection in the presence of DOPE, **70** gave superior transfection without the adjuvant, interestingly with a loss in efficiency when DOPE

was used. Remarkably, **70** was superior or at least comparable with commercially available LTX lipofectamine in most cell lines tested, with similar impact on cell viability under transfection conditions.

Another example of a cell permeable calixarene is an amphiphilic cationic calixarene that was synthesised as part of a synthetic membrane.[63] A combination of calixarenes functionalised at the upper rim with trimethylamine (cationic) or phosphate (anionic) groups, with dodecyl chains on the lower rim, were used to form vesicles that were stabilised by electrostatic interactions. Although the cationic calixarenes on their own formed only micelles, a dye appended analogue (**72**, see Figure 2.10), with one cationic group replaced with a triazole linked dye, was synthesised and the cell permeability evaluated. It was found to penetrate into PC-12 cells efficiently and localise within the cytoplasm. However, the mechanism of uptake was not investigated. The cytotoxicity of both the cationic and anionic forms of these calixarenes was relatively high. It was therefore decided that the less toxic octyl-appended derivatives would be more suitable, although the toxicity of the dodecyl derivatives could potentially be exploited if the vesicles stayed intact until reaching their target.

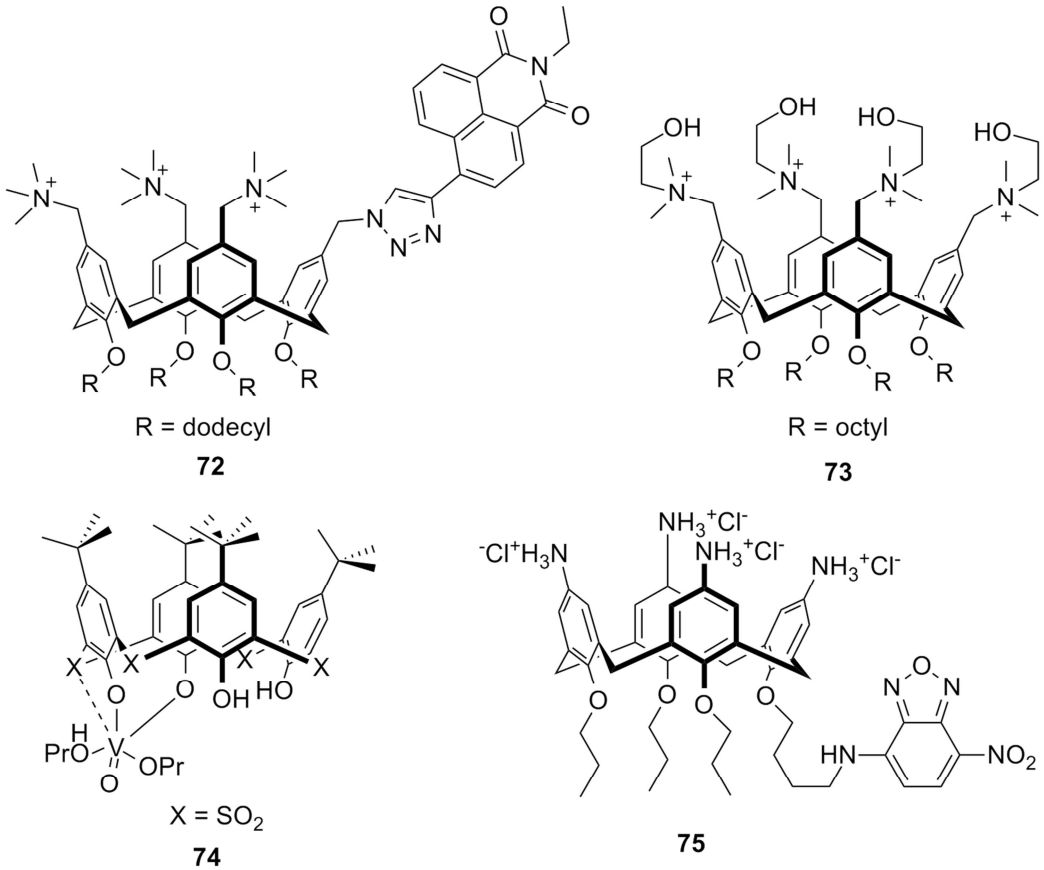

*Figure 2.10: Amphiphilic dye-appended calixarene (**72**),[63] amphiphilic micelle-forming calixarene (**73**),[64] vanadyl sulfonylcalixarene (**74**),[65] nitrobenzoxadiazole-(NBD)-appended cationic calixarene (**75**).*[55,66]

A similar calixarene was synthesised by Rodik *et al.*[64] with octyl chains on the lower rim and hydroxylethylammonium moieties on the upper rim (**73**). These, too, formed micelles, but in this case the utility of the cationic micelles as transfection agents was demonstrated. Octyl chains gave superior micelle formation as well as better DNA binding and condensation properties. When DNA was bound, the micelles were preserved, even in the presence of DOPE. It was proposed that nanoparticles are formed with the DNA molecules wrapped around and within the micelles. These nanoparticles were able to transfect DNA and the process was followed with a fluorescent DNA marker, showing slow adhesion to the cell membrane, followed by internalisation and ultimately accumulation around the nucleus. The slow uptake and relatively low transection efficiency however showed a need for optimisation of the structure in the future.

Vanadyl calixarenes have also been investigated due to the potential apoptotic and anti-tumour activities of vanadium complexes.[65] A fluorescent vanadyl sulfonylcalixarene complex (**74**) was found to penetrate into CHO cells with slow uptake over 3-4 hours. Incubation with various endocytotic inhibitors (sucrose, nystatin, monensin and methyl-β-cyclodextrin) found no inhibition of uptake, suggesting direct translocation across the cell membrane. The complex localised within the cytoplasm. This particular complex showed low toxicity in all cell types screened, but other complexes investigated displayed different cytotoxicities in different cell lines, suggesting that vanadyl calixarenes may have potential use as selective cytotoxic agents.

A more detailed analysis of cell uptake and localisation was carried out in the case of **75**, a dye-appended cationic calixarene derivative synthesised as a mimic for cell penetrating peptides with the cationic moieties clustered on a single face of a rigid scaffold. Preliminary work[55] on the this molecule, named NBDCalAm, investigated the cellular uptake of the calixarene in formaldehyde-fixed cells. It was found that cellular uptake was rapid, with images available in 10 minutes, and the fluorescence from the probe was stable, with images still available after 60 minutes. Furthermore there was no cytotoxic effect from the probe at the concentrations required for the study.

The mechanism of cellular uptake was investigated with inhibitors of caveolae-linked endocytosis and lipid raft processes (filipin, β-cyclodextrin) and clathrin mediated endocytosis (sucrose). None of these gave inhibition of uptake, indicating that the main endocytotic pathways were not responsible for uptake. Using a

counterstain against a receptor localised on the cell membrane, it was found that the probe accumulates in the cytoplasm and not in the cell membrane. It was also shown that there was no accumulation in the nucleus.

Following on from this, studies were carried out on live cells to ensure that the uptake mechanism and localisation were not artefacts of the fixing process.[66] The rapid uptake (1-3 minutes), stable fluorescence (even after 72 hours) and low cytotoxity were confirmed with live cells. Again inhibitors of clathrin mediated endocytosis (sucrose) and caveolae mediated processes (filipin, methyl-β-cyclodextrin) failed to inhibit uptake, implicating direct translocation across the cell membrane.

Co-localisation studies with Golgi apparatus and lysosome stains showed that the probe initially localised to the Golgi apparatus (after 2-3 hours) then showed localisation to the lysosomes (from 2-3 hours up to 72 hours). The route of transfer to the lysosomes via the Golgi apparatus was confirmed by the inhibition of the process by brefeldin A and its lack of effect when the probe was already localised within the lysosomes prior to brefeldin A treatment. Further studies with monensin (which affects endosomal pH), bafilomycin (an inhibitor of vacuolar ATPases) and sodium azide (which depletes the available ATP pool) both prevented localisation in the lysosomes and stimulated release of the probe from within them. This indicates that these three factors are important both for the transfer to and the retention within the lysosomes.

To further this work, the effect of using different cationic groups on the upper rim and introducing different dye molecules was investigated. This will be the subject of the remainder of Chapter 2.

2.2 Aims

Based on the previous work of our research group on NBDCalAm (as described in Section 2.2.2.1), further investigation was required as to the effects of different functionalization of the calixarene scaffold, both in the cationic groups on the upper rim and in the cargo attached to the lower rim.

To alter the properties of the upper rim, two targets were proposed in addition to the original aromatic amine: an aliphatic amine, accessible by furnishing the upper rim with glycine residues, and a guanidinium derivative as a mimic of poly-arginine cell penetrating peptides. Although the syntheses of both were previously attempted (R.

Lalor, unpublished work), problems were met, particularly with the synthesis of the guanidinium derivative.

The synthesis of NBDCalAm analogues required a masked amine on the lower rim of the calixarene in the form of propylphthalimide. For the synthesis of the guanidinium derivative, this gave the intermediate compound **76** (see Figure 2.11). The next step required removal of the phthalimide protecting group in order to react the free amine with NBD-chloride. However, reaction with hydrazine to effect this transformation also removed half of the Boc protecting groups from the upper rim.

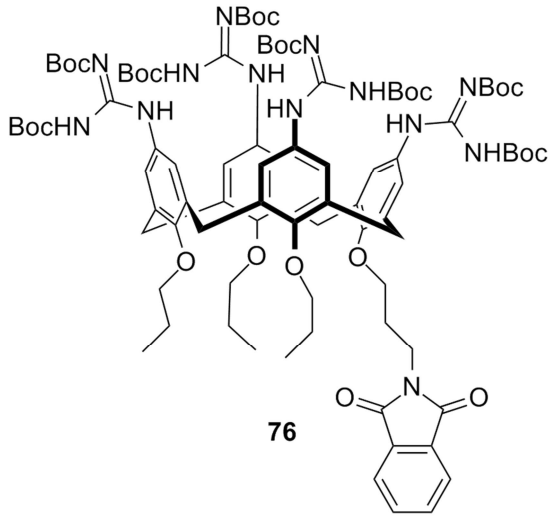

76

Figure 2.11: Intermediate in the synthesis of tetra-guanidinium calix[4]arene with NBD labelled lower rim.

In order to avoid this loss of integrity in the upper rim, it was decided to use a different method to attach the dye. The CuAAC reaction (as described in Chapter 1) was selected as a means of attachment that would require no protecting group during the functionalization of the amines on the upper rim and that would facilitate variation of the lower rim cargo. Furthermore, the use of this reaction results in 1,2,3-triazole linkers. These have topological and electronic similarities with amide bonds and can therefore be potentially used as bioisosteres of this functionality, but with greater chemical stability.[67] For example, they have been shown to be an effective replacement for the amide bond in amprenavir, an HIV-1 protease inhibitor.[68]

Since use of the CuAAC reaction would give a different linker to the dye compared with the original NBDCalAm, a pair of analogues with identical upper rims and linkers but with two different dye molecules would also be required. This would allow the effect of changing the linker to be evaluated.

In summary, the aims for this project were as follows:

- To synthesise three analogues with variation in the upper rim, i.e. aromatic amine, aliphatic amine and guanidine functionalization, with a dye molecule added to the lower rim by click chemistry;
- To synthesise analogues of the aromatic amine with different dye molecules added to the lower rim by click chemistry;
- To synthesise a pair of analogues with aromatic amine functionalised upper rims, with an identical linker on the lower rim but with two different dye molecules, one of which would preferably be the original NBD dye to allow for comparison with NBDCalAm.

2.3 Results and Discussion

2.3.1 Synthesis of water soluble click conjugates

In order to add a dye molecule by the CuAAC reaction, either an alkyne or an azide was required on the calixarene to react with either an azide or alkyne functionalised dye. Since an alkyne could be easily added to the calixarene in a single step using readily available propargyl bromide and azide derivatives of several dye molecules could be synthesised,[69–71] this is the route that was taken.

2.3.1.1 Synthesis of common intermediate

To introduce the required single propargyl group to the lower rim of calix[4]arene, two routes could have been followed. The first is to mono-propargylate the lower rim, then add the three propyl chains to lock the conformation. However, this method is not ideal as some of the 1,3-dialkyl species can be formed.[72] Therefore it was decided to use a selective tri-alkylation method, followed by introduction of the propargyl group.[73] For both alkylations, the Williamson ether synthesis can be used. This involves treating an alcohol with a base to produce an alkoxide anion, then addition of an alkyl halide, which reacts *via* an S_N2 type reaction.

The first step was to form the calix[4]arene starting material using the method of Gutsche *et al.*[74] A mixture of *para-tert*-butyl-phenol, formaldehyde solution in water and sodium hydroxide were heated to 120 °C and mechanically stirred until the intermediate polymer was formed. This was dissolved in diphenyl ether, the water of condensation driven off and the mixture heated to reflux to form the cracked product. Precipitation with ethyl acetate gave **2** as off-white crystals in 67% yield, which was used without further purification.

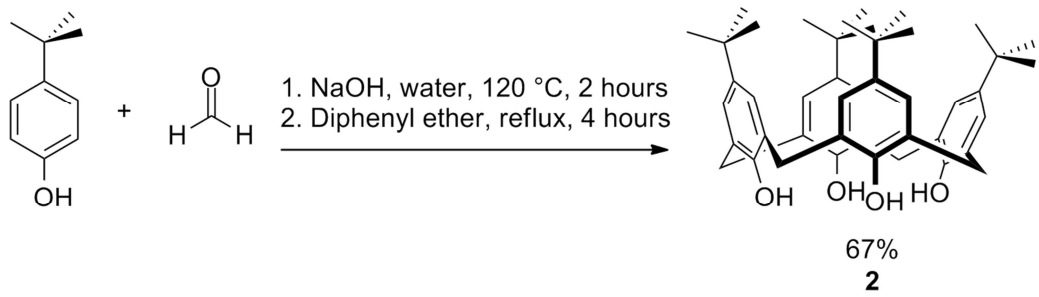

*Scheme 2.1: Synthesis of tert-butyl-calix[4]arene (**2**).*

In order to tripropylate **2**, a mixture of barium hydroxide with barium oxide was used as a base. The phenoxide anions that are formed on the calixarene interact with Ba^{2+} and in order to optimise these interactions the calixarene is held in the cone conformation. Subsequent addition of *n*-propyl bromide resulted in alkylation. The formation of the tetrapropyl product was suppressed as the final phenoxide is too strongly coordinated to react.[73] Aqueous workup and precipition from DCM with methanol gave **77** as white crystals in 79% yield.

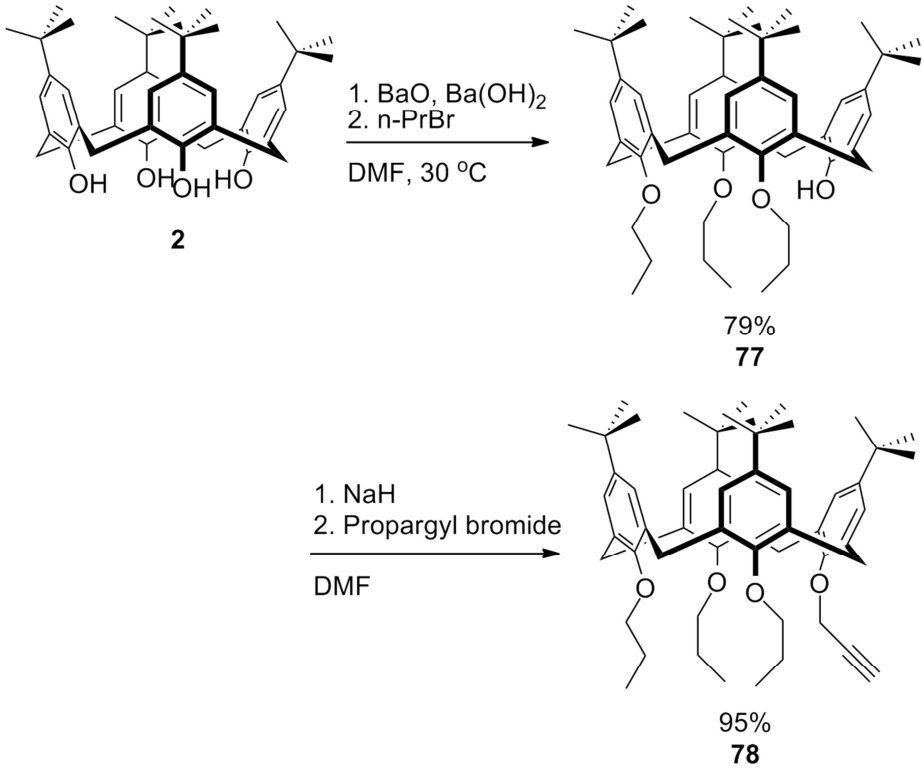

*Scheme 2.2: Selective tripropylation (**77**) and subsequent alkylation (**78**) of tert-butyl-calix[4]arene (**2**).*

To introduce the propargyl group to **77**, sodium hydride was used as a base. The Na^+ coordinates the phenoxide anions and holds the calixarene in the cone conformation as before; however, the coordination to Na^+ is weaker than Ba^{2+} allowing the final phenoxide to react. Propargyl bromide was added as the alkylating agent. With the four alkyl chains in place, the steric bulk prevents transannular

rotation, locking the conformation. Aqueous workup and column chromatography over silica gel (eluting with 2:1 DCM/hexane) gave **78** as off-white crystals in 95% yield.

The ^{1}H-NMR spectrum of compound **78** (see Figure 2.12) confirms that the product is in the cone conformation. Two pairs of doublets for the methylene bridge protons are characteristic of this conformation and symmetry and can be seen at 4.4 and 3.1 ppm; the latter pair is overlapping to give a single doublet. These peaks arise from the axial and equatorial hydrogens on the methylene bridges being in different environments (see Figure 2.12b), resulting in geminal coupling in the NMR with a splitting of 13 Hz. Taking into account the symmetry of the molecule (see Figure 2.12a), this gives the observed four doublets.

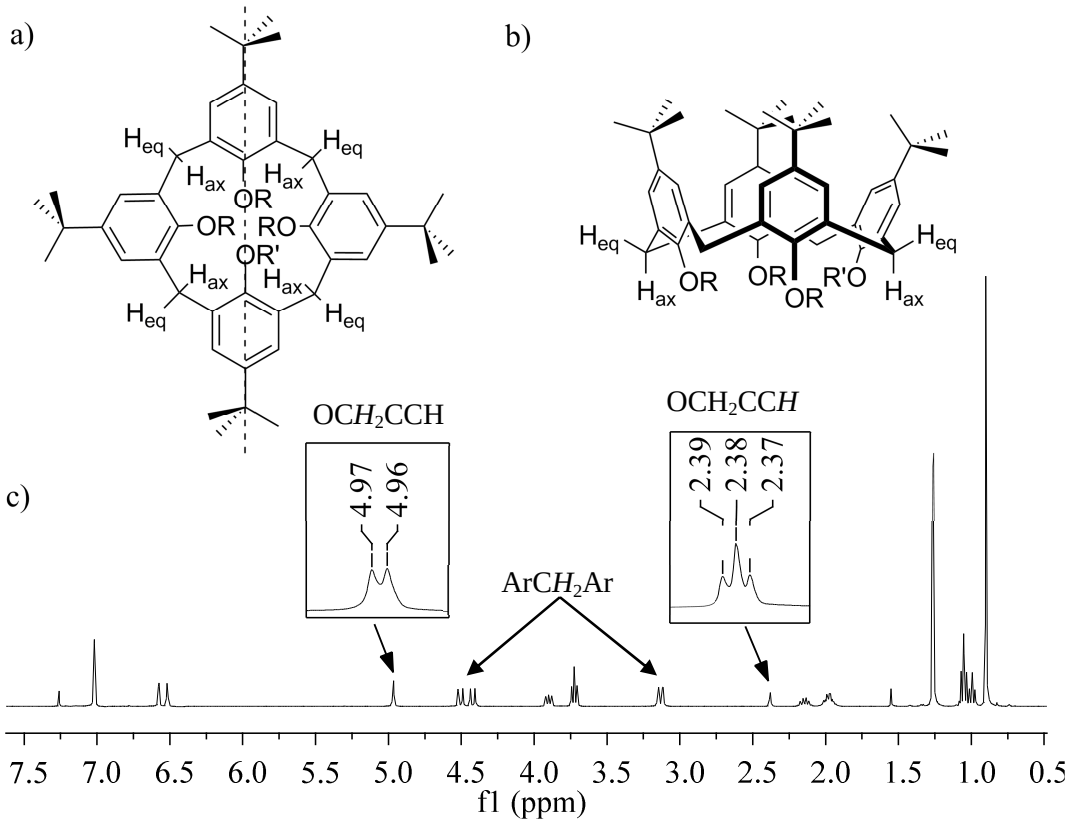

*Figure 2.12: a) Two dimensional model of compound **78**, showing rotational symmetry plane, b) Positions of axial and equatorial methylene bridge hydrogens, c) ^{1}H-NMR spectrum of **78** ($CDCl_3$).*

The presence of three propyl groups is confirmed by the presence of two peaks for each position on the C_3 chain as there are two environments for each: the two chains adjacent to the propargyl group and the one opposite (see Figure 2.12a). These peaks lie around 3.9-3.7 ppm, 2.2-1.9 ppm and 1.0 ppm. The propargyl peaks are at 5.0 and 2.4 ppm, corresponding to the CH_2 and terminal carbons, respectively. Long range coupling over the triple bond results in a doublet and a triplet with a *J* value of 2 Hz.

With the conformation of the calixarene now locked and the propargyl chain introduced, the upper rim was next modified to install the amine groups that would be required to confer water solubility or be available for further functionalisation. To this end, nitro groups were first introduced to the upper rim, which could subsequently be reduced to give the desired amino derivative.

To carry out the *ipso* nitration which would replace the *tert*-butyl groups *para* to the alkyl ethers with nitro groups, a number of methods for exhaustive nitration were available. Kumar *et al*.[75] evaluated a number of different nitrating mixtures, including HNO_3/Ac_2O, $KNO_3/AlCl_3$ and HNO_3/CH_3COOH for the exhaustive *ipso*-nitration of calixarenes and found HNO_3/CH_3COOH to give the best yields. This method and a variation using TFA instead of acetic acid were attempted. Although TFA gave a reasonable yield of 61%, the reaction was slower than with acetic acid. It was therefore decided to use the HNO_3/CH_3COOH method.

Compound **78** was stirred with excess glacial acetic acid and 100% nitric acid, giving a characteristic colour change first to blue-black, then over time to bright orange. Aqueous work up and precipitation from DCM with methanol gave **79** as light yellow crystals in yields up to 85%, sometimes with the need to purify by column chromatography over silica gel (eluting with DCM).

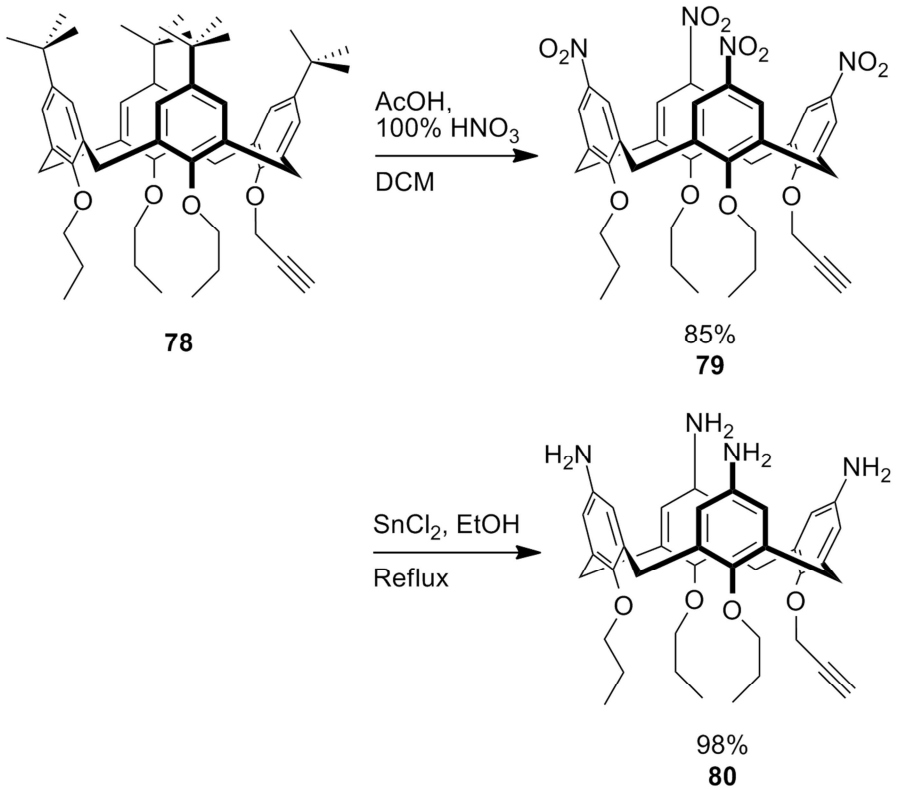

78 → 85% **79** → 98% **80**

Scheme 2.3: Ipso-*nitration of **78** and reduction to **80**.*

A number of methods were available for reduction of the nitro groups on the upper rim. Methods previously used on calixarenes include the use of hydrazine with Raney nickel,[76] palladium with either hydrazine or hydrogen[77] or heating at reflux with tin (II) chloride in ethanol.[78] The latter, being the favoured method of the group, was the first method that was attempted and gave good results.

Reduction of **79** was carried out by heating at reflux with tin chloride in ethanol for 24 hours, followed by aqueous work up with sodium hydroxide. Compound **80** was obtained as orange-brown glass in 98% yield, which was used with no further purification.

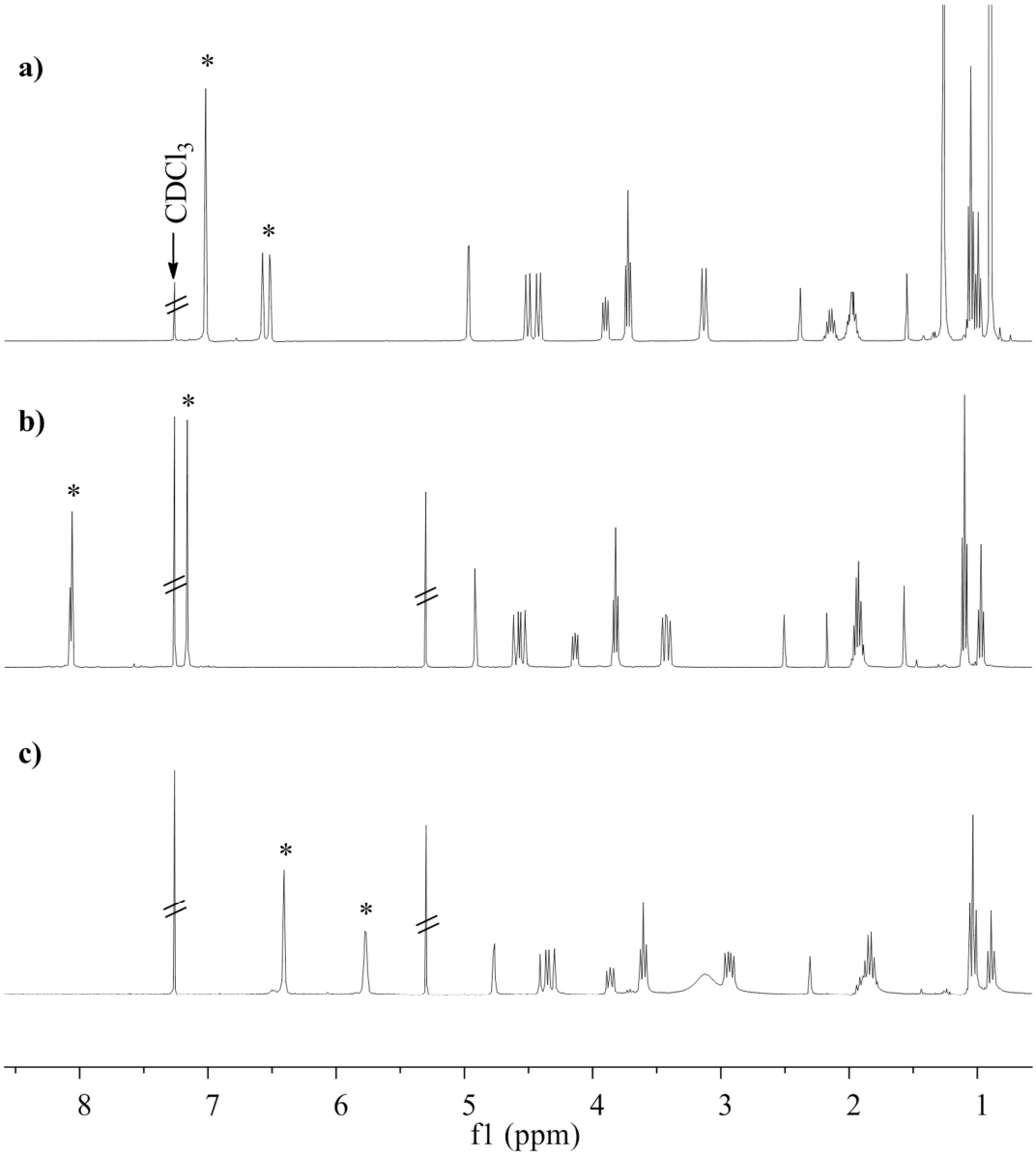

*Figure 2.13: ^{1}H-NMR spectra of a) ^{t}Bu (**78**), b) nitro (**79**) and c) amino (**80**) functionalised calixarenes in $CDCl_3$. Peaks corresponding to aromatic protons are marked with an asterisk.*

The ^{1}H-NMR spectra of **78**, **79**, and **80** are shown in Figure 2.13. The peaks corresponding to the aromatic protons (marked with an asterisk) clearly show the effect of the changing environment on the upper rim, with the electron-withdrawing nitro groups of **79** resulting in deshielding and a downfield shift in ppm relative to the *tert*-butyl groups and the amino groups of **80** giving the opposite effect.

This amine was the common intermediate from which the syntheses of the dye-conjugates diverged. It was either furnished with amine protecting groups for the aromatic amine derivatives or functionalised further for variation of the upper rim.

2.3.1.2 Synthesis of dye molecules

3-Azido-7-hydroxycoumarin

In order to add the dye molecules to the calixarene scaffold by click chemistry, it was necessary to synthesise azido derivatives of the selected dyes. The first was an azido derivative of 7-hydroxy-coumarin, which does not exhibit fluorescence until the click reaction has taken place, giving a dye-conjugate with an emission wavelength of around 500 nm.[69]

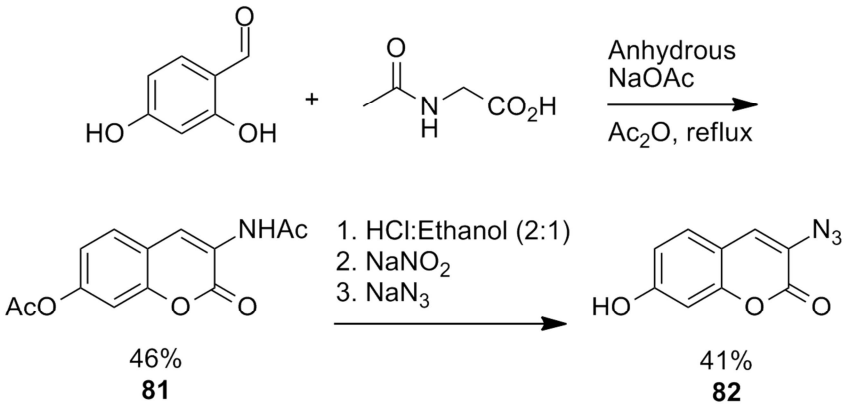

*Scheme 2.4: Synthesis of 3-acetamido7-acetoxy-coumarin (**81**) and 3-azido-7-hydroxy coumarin (**82**).*

The 3-azido-7-hydroxycoumarin (**82**) was synthesised in two stages, via 3-acetamido-7-acetoxycoumarin (**81**). The intermediate was synthesised according to Kudale *et al.*[79] from 2,4-dihydroxy benzaldehyde, *N*-acetyl glycine and sodium acetate by heating at reflux in acetic anhydride. Using the proportions directed, the mixture turned solid and the colour changed from salmon pink to orange-brown over the course of 3.5 hours. Slightly increasing the volume of acetic anhydride used relative to the published procedure prevented solidification and facilitated stirring.

Water was added, the solid was filtered and washed with water, then triturated with ethyl acetate and filtered, giving **81** as a yellow powder in 46% yield. The synthesis of **82** was then completed according to Sivakumar *et al.*[69] After heating **81** at reflux in

2:1 concentrated HCl/ethanol for 1 hour, water was added to the now red mixture, which was cooled then treated with sodium nitrite. At this stage it was important to keep the temperature below 5 °C as the diazonium intermediate could react with water to form the undesired phenol.

After 10 minutes sodium azide was added, then stirred for 15 minutes. Subsequent filtration and washing with water gave **82** as a brown amorphous solid. Purification by column chromatography over silica gel (eluting with 3:2 hexane/ethyl acetate) was sometimes necessary, giving light-brown needles, which darkened over time. Yields of up to 41% were obtained.

1-Azidomethylpyrene

The second dye that was synthesised was an azido methyl pyrene, which has an emission wavelength of around 400 nm.[70] It is also bulkier and less polar, allowing for the comparison of potentially different dynamics within cells.

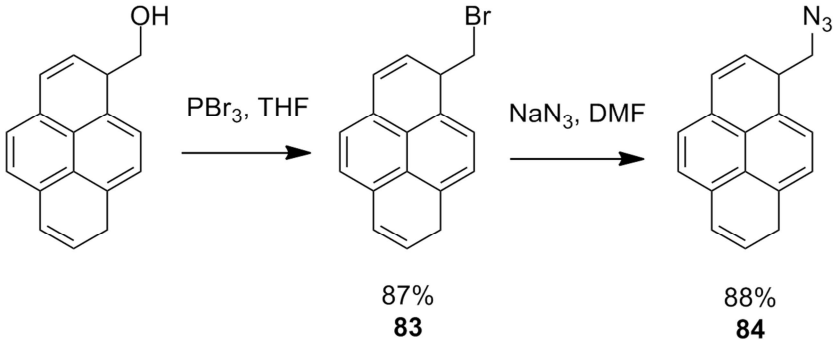

*Scheme 2.5: Synthesis of 1-bromomethyl-pyrene (**83**) and 1-azidomethyl-pyrene (**84**)*

The required 1-azido methyl pyrene (**84**) was synthesised from 1-pyrene methanol[70] by treating it with phosphorous tribromide. The resulting solid was filtered and washed with diethyl ether to afford the intermediate 1-bromo methyl pyrene (**83)** as light yellow crystals in 87% yield. This was then treated with sodium azide at 60 °C for 12 hours. Aqueous work up gave **84** as a waxy yellow solid in 88% yield.

9-Azidomethyl-10-bromoanthracene

Informed by results later obtained from the pyrene conjugate (See section 2.5.5) a second non-polar dye was synthesised. An anthracene derivative was selected to provide a dye with slightly less steric bulk that could be compared with pyrene. The starting material, 9-bromo-10-bromomethyl-anthracene (**85**) was kindly provided by the research group of Professor Ganesan.

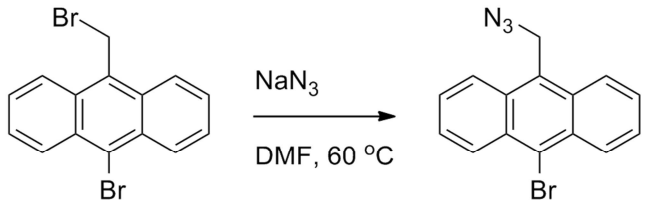

85 70% **86**

*Scheme 2.6: Synthesis of 9-azidomethyl-10-bromo-anthracene (**86**).*

The aliphatic halogen was displaced by an S_N2 reaction with sodium azide in the same way as in the synthesis of **84**. Compound **85** was heated with sodium azide at 60 °C for 18 hours, followed by aqueous workup to give **86** as a yellow solid in 70% yield. This was used directly in the subsequent CuAAC reaction.

Following the synthesis of the various dye molecules, the different dye-appended aromatic amine calixarene derivatives were synthesised, as well as a non-cationic control.

2.3.1.3 Coumarin-appended neutral calixarene

To provide a non-cationic control, the coumarin dye was first added to compound **78**. In order to carry out the CuAAC reaction, copper (I) is required as the catalyst. This can be provided directly as a copper (I) salt such as copper iodide (which also requires a base such as DIPEA), or generated *in situ* from copper (II) sulphate by maintaining reducing conditions with sodium ascorbate.[80] The latter method was selected as it is easier to maintain the copper in the catalytic form in the presence of a reducing agent.

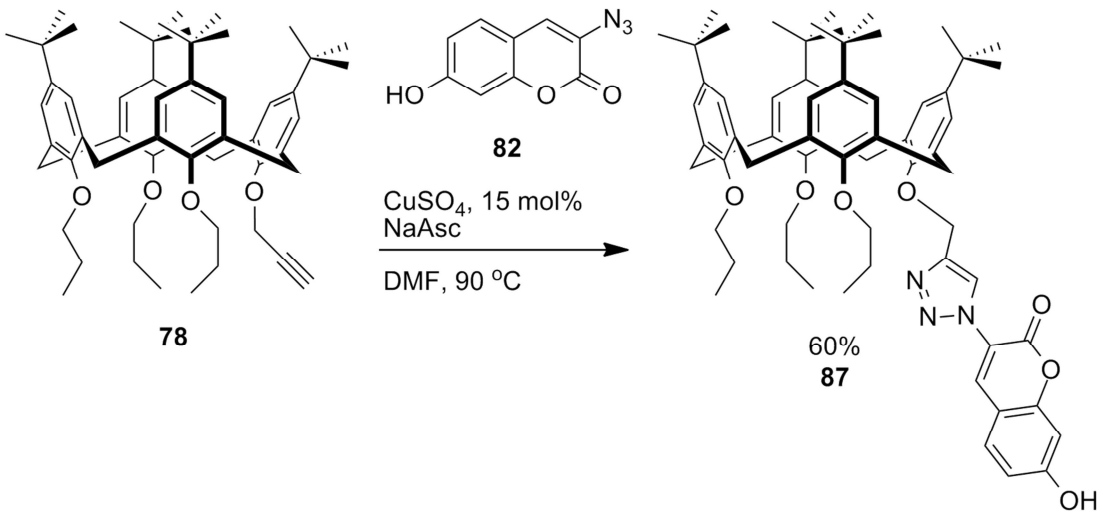

78 60% **87**

*Scheme 2.7: Click reaction of **78** with **82** to give conjugate **87**.*

A solution of **78** and **82** in DMF was treated with catalytic copper (II) sulphate with one equivalent of sodium ascorbate. The mixture was heated for 3 hours at 90 °C. Aqueous work up followed by purification by column chromatography over silica gel (eluting with 49:1 DCM/methanol) gave **87** as yellow glass in 60% yield.

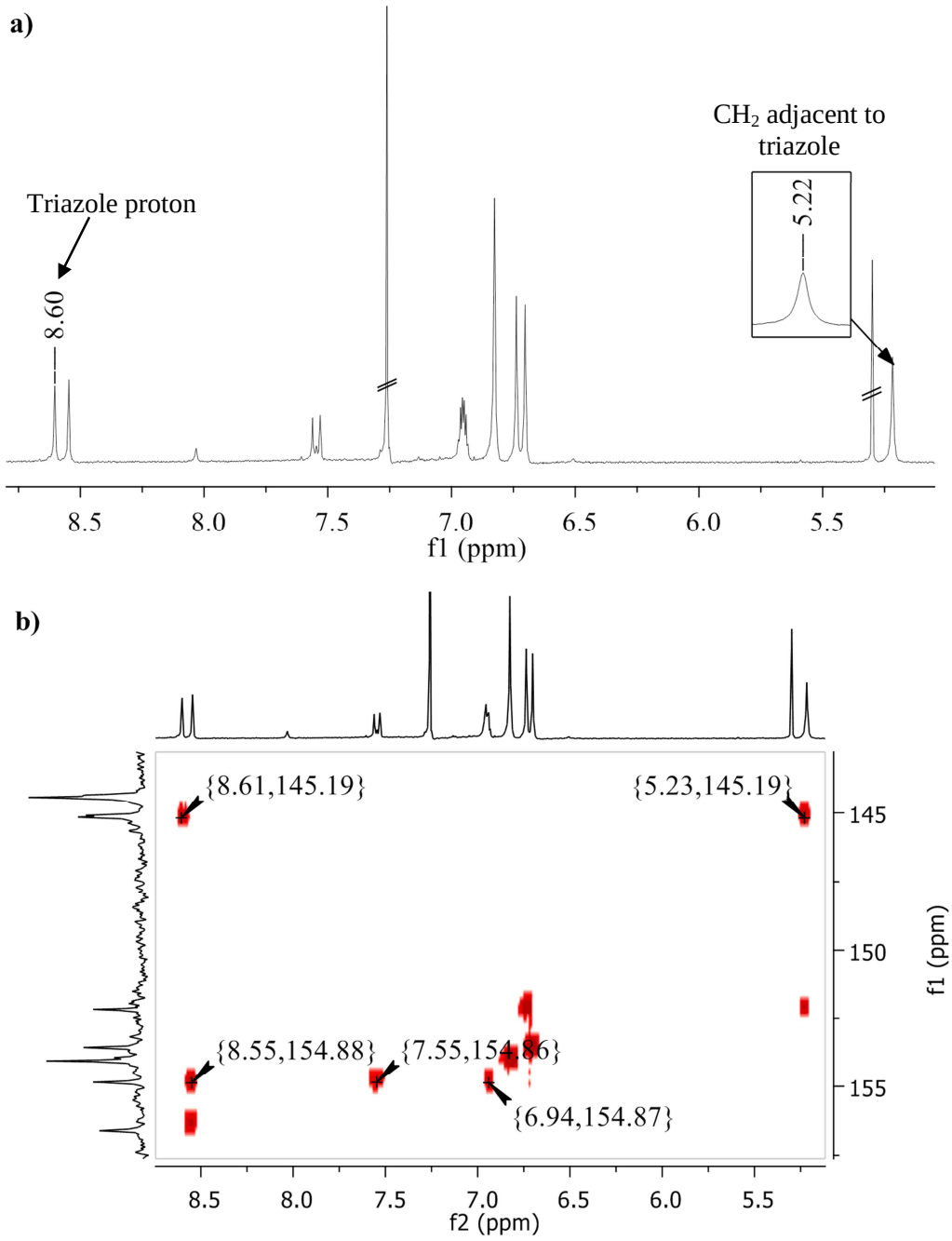

*Figure 2.14: a ^{1}H-NMR spectrum and b) 2D-HMBC of **87** ($CDCl_3$).*

The ^{1}H-NMR spectrum of **87** (see Figure 2.14a) confirms the successful click reaction between **78** and **82**. The peak that corresponds to the methylene group that was previously part of the alkyne is now a singlet at 5.2 ppm, indicating the loss of the long range coupling. This is consistent with the conversion from a triple bond to the double bond that is now part of the triazole ring.

In addition the peak arising from the proton on the triazole ring can be identified. There are two peaks downfield at 8.60 and 8.55 ppm, one of which is the proton on the triazole ring, whilst the other corresponds to the uncoupled proton on the coumarin dye. They can be differentiated by examining the 2D-HMBC spectrum (see Figure 2.14b). The proton peak at 8.60 ppm has a long-range interaction with a carbon peak at 145.19 ppm, which in turn interacts with the proton peak at 5.22 ppm that corresponds to the methylene adjacent to the triazole ring. This confirms that the peak at 8.60 ppm is the proton on the triazole ring. By contrast, the proton peak at 8.55 ppm has a long range interaction to a carbon peak at 155 ppm, which shares long range interactions with proton peaks corresponding to protons on the coumarin around 7.5 and 7.0 ppm. This confirms that the peak at 8.55 ppm is an aromatic proton on the coumarin dye.

2.3.1.4 Coumarin-appended tetra-amino calixarene

With the structure of the non-cationic control confirmed, the water-soluble derivatives were now synthesised. In preparation for the addition of the dye and to protect it from degradation over time, for example by reaction with atmospheric CO_2,[81] the amino groups of **80** were protected by introducing Boc groups. Methodology based on work by Saadioui *et al.*[82] was used, using 10 equivalents of Boc anhydride with the addition of a non-nucleophilic base to improve the yield.

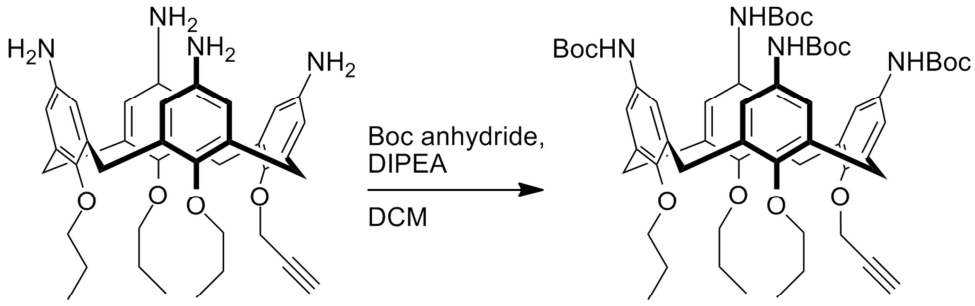

*Scheme 2.8: Protection of tetra amino calixarene (**80**).*

Tetra amino calixarene (**80**) was protected by stirring in DCM with Boc anhydride in the presence of DIPEA. The crude mixture was purified by column chromatography over silica gel (eluting with 15:1 DCM/ethyl acetate), giving **88** as off-white glass in 83% yield.

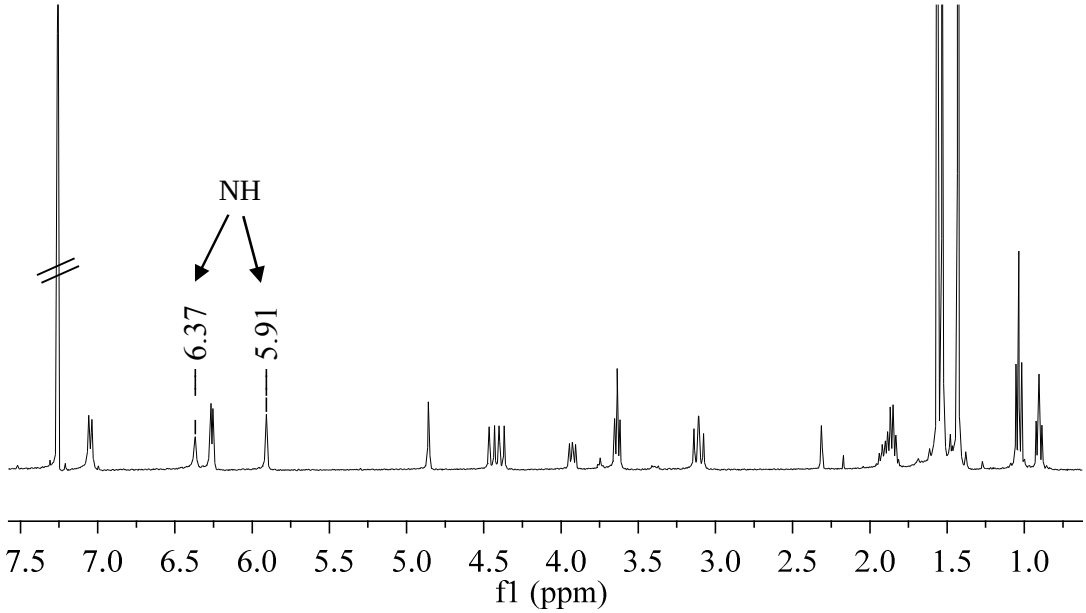

*Figure 2.15: ^{1}H-NMR spectrum of **88** ($CDCl_3$).*

The ^{1}H-NMR spectrum of **88** (see Figure 2.15) confirms the successful Boc protection. *Tert*-butyl peaks, absent after the *ipso*-nitration, are present once more with the correct integration heights for tetra functionalisation. However, the Boc *tert*-butyl peaks are at slightly higher chemical shift (around 1.5 ppm) compared with the original *tert*-butyl peaks (1.2 and 0.9 ppm) indicating proximity to the electron withdrawing carbamate group. The four singlets corresponding to the aromatic hydrogens (around 7.0 and 6.25 ppm) are slightly deshielded relative to the amino derivative. The slightly broadened peaks corresponding to N-H (6.4 and 5.9 ppm) are also visible.

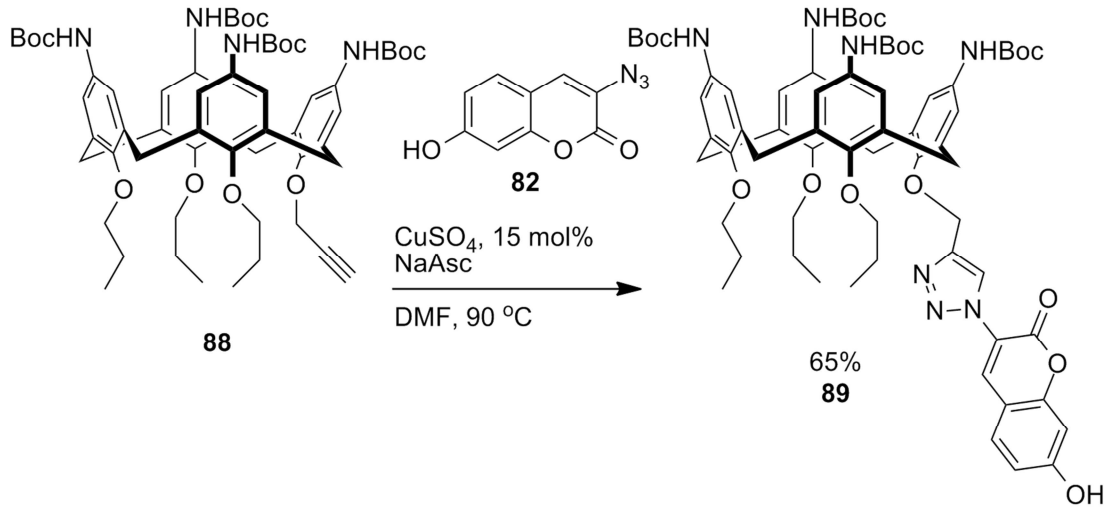

*Scheme 2.9: Click reaction of **88** with **82**.*

In order to add the dye to the Boc protected tetra amino calixarene, the same method as in section 2.3.1.3 was used. A solution of **88** and **82** in DMF was treated with catalytic $CuSO_4$ and one equivalent of sodium ascorbate. The mixture was heated

for 20 hours at 90 °C. Aqueous work up followed by purification by column chromatography over silica gel (eluting with 49:1 DCM/methanol) gave **89** as light yellow glass in 65% yield.

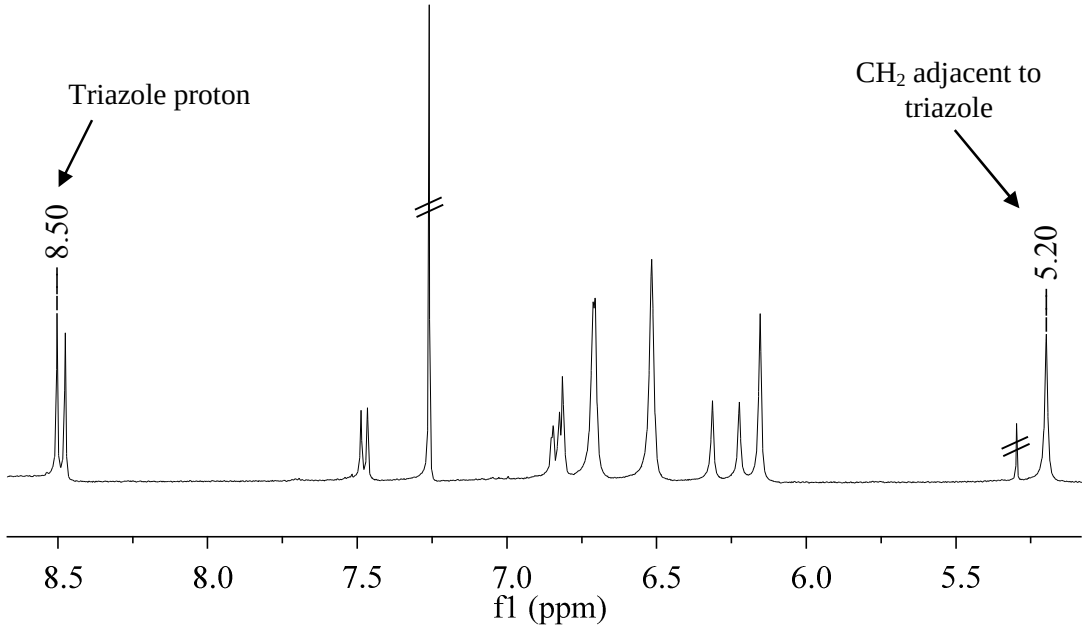

*Figure 2.16: ^{1}H-NMR spectrum of **89** ($CDCl_3$).*

The ^{1}H-NMR spectrum of **89** (see Figure 2.16) confirms the successful click reaction between **88** and **82**. The peak that corresponds to the methylene group that was previously part of the alkyne is now a singlet at 5.2 ppm and the peak arising from the proton on the triazole ring can be seen at 8.50 ppm, whilst the dye peaks lie at 8.48, 7.5 and 6.8 ppm.

2.3.1.5 Pyrene-appended tetra-amino calixarene

For the CuAAC reaction to add the pyrene dye to **88**, the same conditions as in section 2.3.1.3 were used. A solution of **88** and **84** in DMF was treated with catalytic $CuSO_4$ and one equivalent of sodium ascorbate. The mixture was heated for 3 hours at 90 °C. Aqueous work up followed by purification by column chromatography over silica gel (eluting with 97:3 DCM/acetone) gave **90** as light yellow glass in 32% yield. Some of the starting materials were also recovered, with approximately 20% of the yield lost due to incomplete reaction.

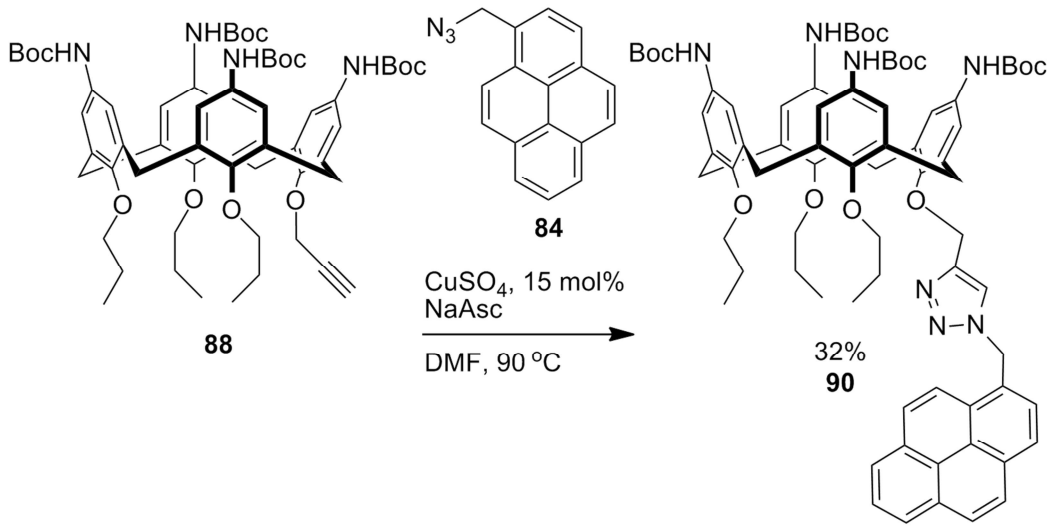

*Scheme 2.10: Click reaction of **88** with **84**.*

The ^{1}H-NMR spectrum of **90** is shown in Figure 2.17. It is worthy of note that in this case the pairs of doublets corresponding to the methylene bridges (4.28 and 3.86 ppm, 3.00 and 2.41 ppm) have greater spacing between them compared with, for example, compound **78** (see Figure 2.12). This suggests a more dramatic difference between the environments of the methylene bridges proximal to the pyrene and those distant from it.

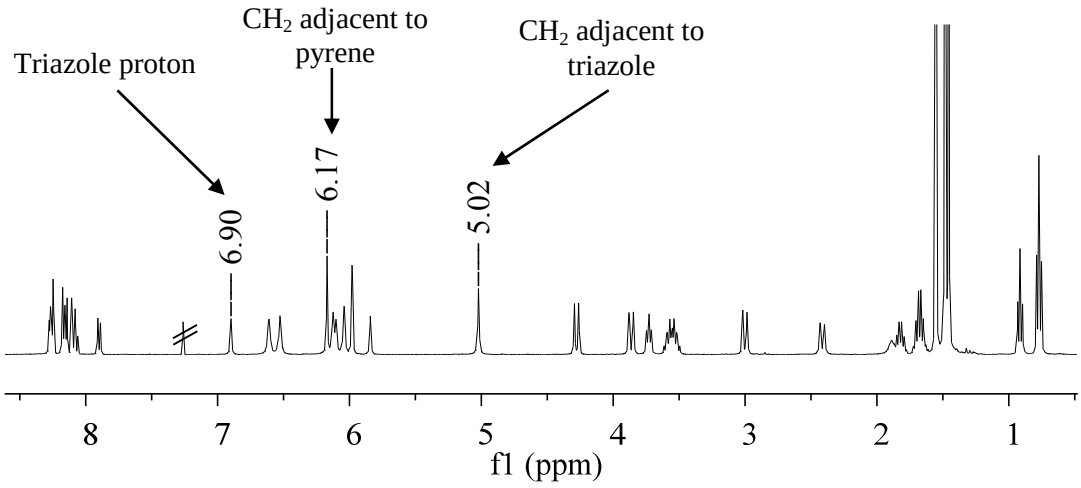

*Figure 2.17: ^{1}H-NMR spectrum of **90** ($CDCl_3$).*

Identification of the methylene that was previously part of the alkyne was less straightforward in this case compared with **87** and **89** since in this case there is an additional methylene group on the other side of the triazole ring, linking it to the pyrene. Additional information from 2D-NMR spectra was required to differentiate the two methylene groups.

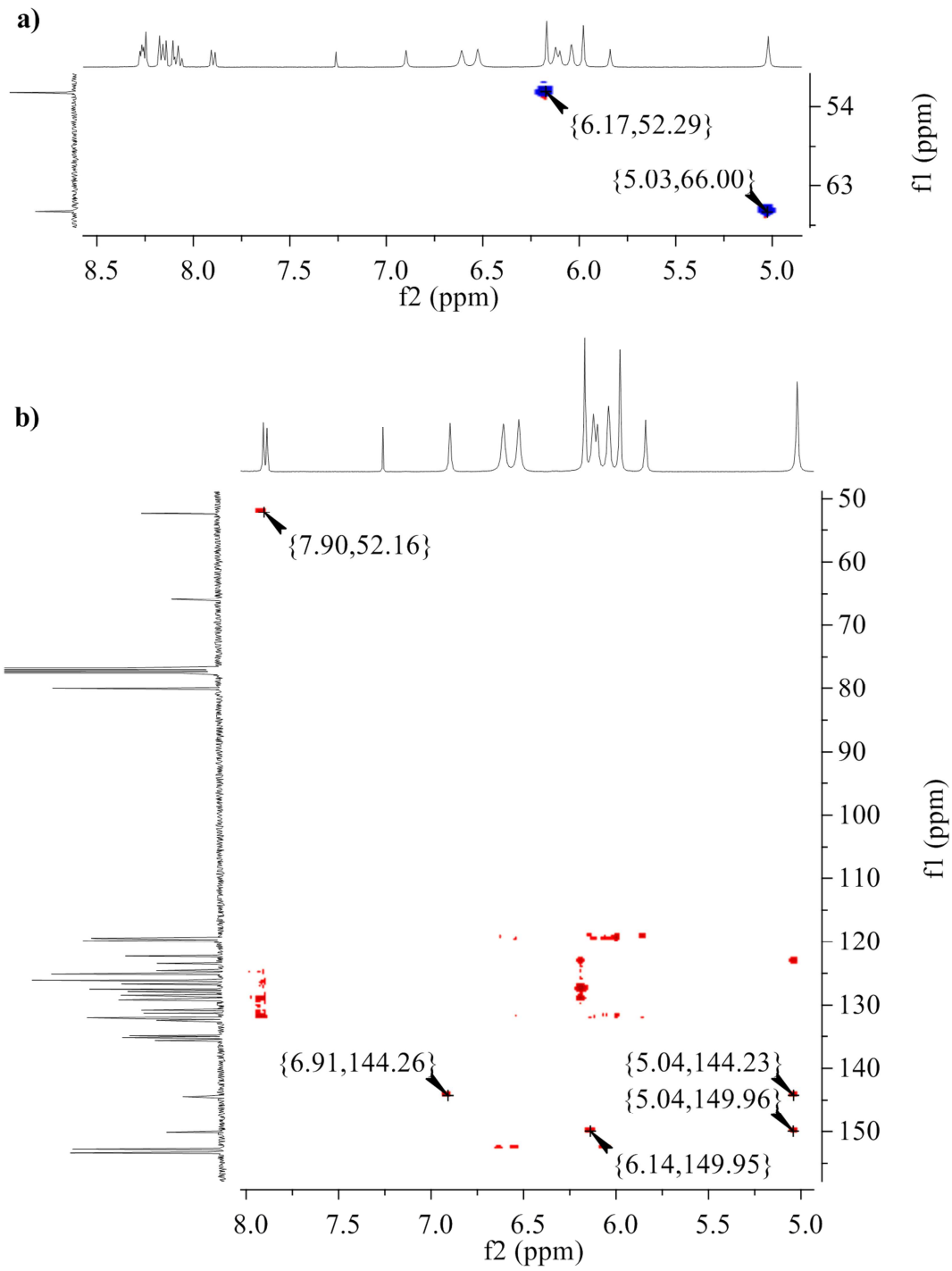

*Figure 2.18: a) 2D-HSQC and b) 2D-HMBC of **90** ($CDCl_3$).*

A 2D-HSQC spectrum identified two secondary carbon environments, at 52.29 and 66.00 ppm, that correlated to peaks in the aromatic region (6.17 and 5.02 ppm, respectively) in the ^{1}H-NMR spectrum (see Figure 2.18a). These are likely to be the two methylene groups in question. These carbon peaks were then examined in the 2D-HMBC spectrum (see Figure 2.18b). The carbon peak at 52.29 ppm has a long range coupling to a proton peak at 7.9 ppm which corresponds to a proton on the pyrene dye. This suggests that the carbon peak at 52.29 ppm, and so the proton peak at 6.17 ppm, corresponds to the methylene group adjacent to the pyrene ring.

The proton peak at 5.02 ppm should, by elimination, be the methylene group between the calixarene core and the triazole ring. Further information from the 2D-HMBC shows a long range interaction between this proton environment and a carbon at 149.96 ppm, which in turn has an interaction with a proton peak at 6.14, which corresponds to an aromatic proton on the calixarene. This mutual interaction supports this assignment of the peak at 5.02 ppm.

Finally, the 2D-HMBC also allows the peak corresponding to the proton on the triazole ring to be confirmed. The proton peak at 6.90 ppm which corresponds to a single proton is a likely candidate. This peak has a long range interaction to the carbon peak at 144.26 ppm. Since the proton peak at 5.02 ppm also has an interaction with this carbon, the peak at 6.90 ppm must correspond to the triazole proton.

2.3.1.6 Anthracene-appended tetra-amino calixarene

For the CuAAC reaction to add the anthracene dye to **88**, the same conditions as in section 2.3.1.3 were used. A solution of **88** and **86** in DMF was treated with sodium ascorbate and catalytic $CuSO_4$. The mixture was heated for 3 hours at 90 °C. Aqueous work up followed by purification by column chromatography over silica gel (eluting with 2:1 hexane/ethyl acetate) gave **91** as yellow glass in 36% yield.

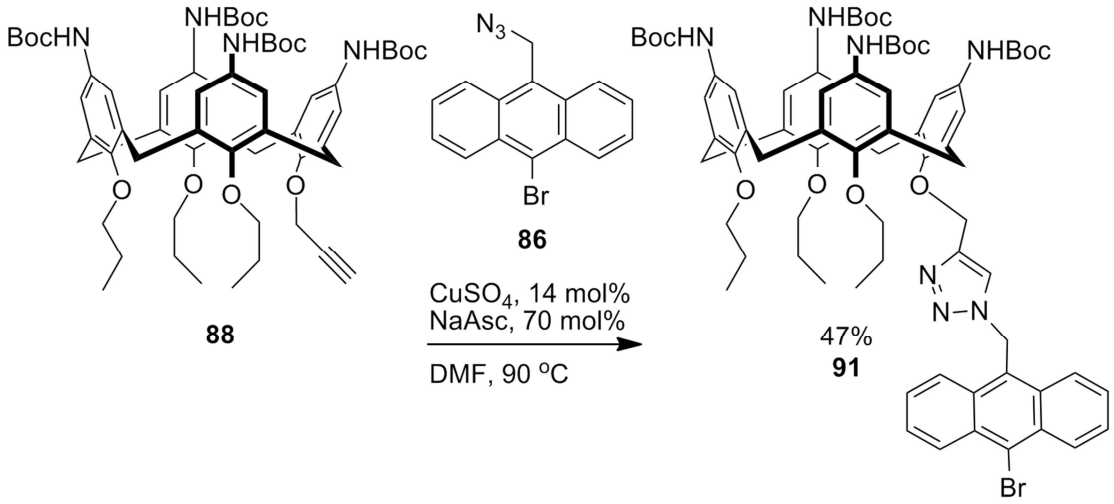

*Scheme 2.11: Click reaction of **88** with **86**.*

The ^{1}H-NMR spectrum of **91** (see Figure 2.19) shows that, as with the pyrene derivative (**90**), the methylene bridges of the calixarene core give pairs of doublets that are relatively widely spaced (4.3 and 3.7 ppm, 3.0 and 2.5 ppm). This suggests that this feature arises from having a non-polar aromatic moiety on the lower rim, perhaps resulting from π-stacking interactions between the dye and the calixarene core.

Using 2D-NMR, the success of the click reaction was confirmed by identifying the methylene bridge that was previously part of the alkyne as a singlet at 4.99 ppm, whilst the methylene bridge connecting the triazole ring to the anthracene was found at 6.32 ppm. The proton on the triazole ring itself was found at 6.60 ppm. The level of deshielding experienced by the latter proton in **90** and **91** is relatively low compared with the coumarin derivative (**89**), where the triazole ring forms part of the conjugated system of the dye.

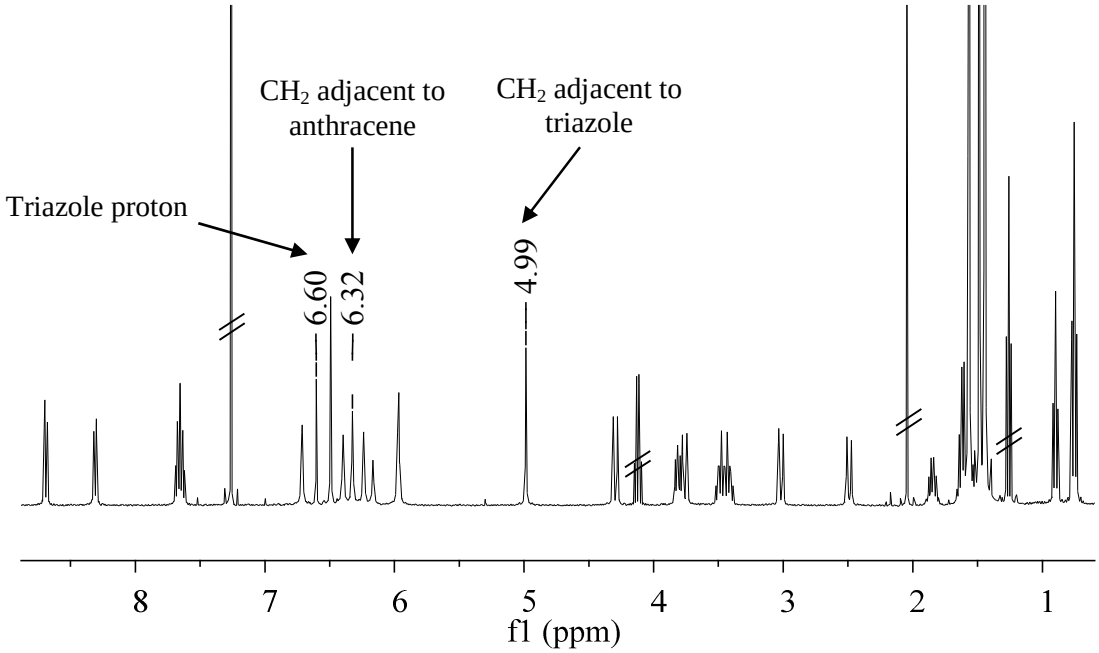

*Figure 2.19: ^{1}H-NMR spectrum of **91** ($CDCl_3$).*

2.3.1.7 Coumarin appended tetra-glycine calixarene

With the Boc-protected aromatic amine derivatives in hand, attention was turned towards modification of the upper rim. In order to synthesise an aliphatic amine derivative, it was decided to use glycine as a simple spacer that is easy to introduce *via* an amide bond.

Multiple methods are available for amide bond formation that can be applied to calixarenes, including converting the acid to an acid chloride[83] or an activated ester,[84] or using a coupling reagent.[85] The latter was selected as a simple, one pot method with good tolerance to water and no requirement for isolation of the activated intermediate. Dicyclohexylcarbodiimide (DCC) was tried first as it is a relatively cheap coupling reagent, the by-product of which can be removed by simple filtration.

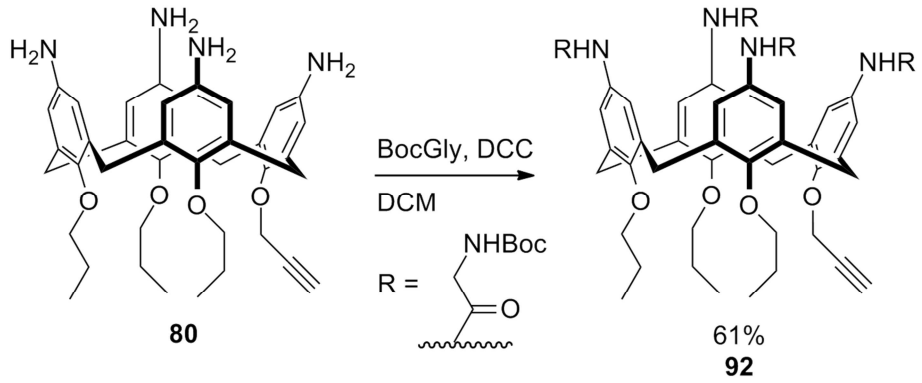

*Scheme 2.12: Coupling reaction of **80** with Boc glycine.*

Compound **80** was coupled to commercial Boc-glycine using DCC by stirring them together in DCM, with concomitant production of insoluble dicyclohexylurea as the side product. The latter was removed by filtration and the crude product purified by column chromatography over silica gel (eluting with 19:1 DCM/methanol), giving **92** as a light yellow glass in 61% yield.

The ^{1}H-NMR spectrum of **92** (see Figure 2.20) shows that the upper rim has successfully been functionalised with Boc-glycine. The methylene groups of the glycine moieties are visible at 3.85 and 3.64 ppm. The amide and carbamate protons are involved in hydrogen bonding interactions with the deuterated methanol and so cannot be seen in the NMR; this also eliminates any possibility of seeing splitting arising from coupling between the amide proton and the adjacent methylene group. The singlets from the *tert*-butyl groups can be seen around 1.5 ppm.

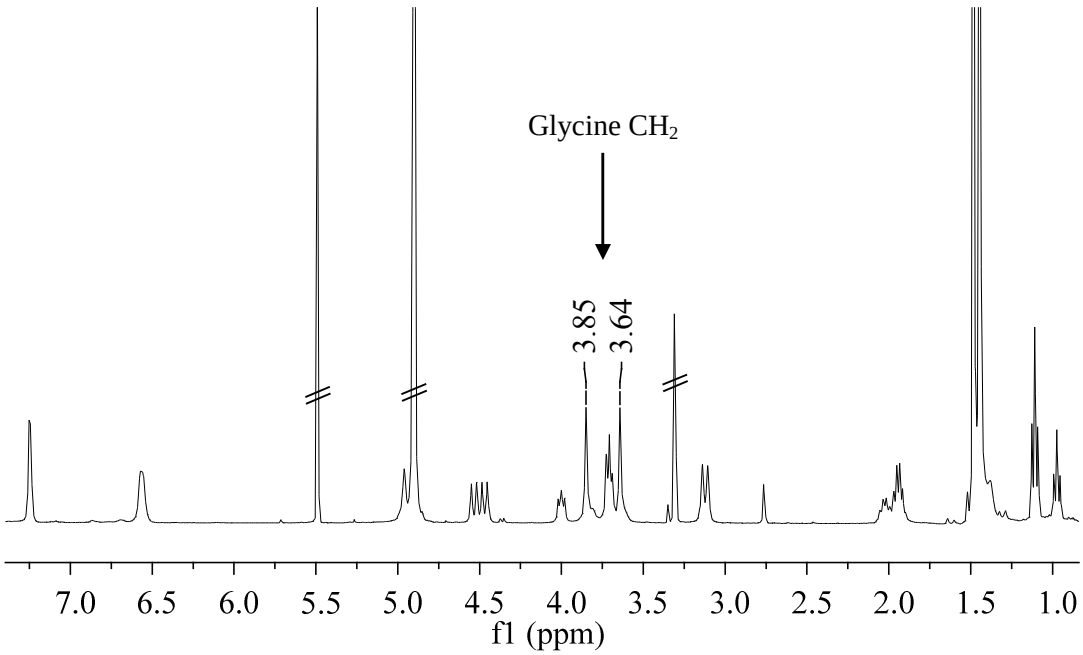

*Figure 2.20: ^{1}H-NMR spectrum of **92** (CD_3OD).*

In order to add the dye to **92**, the same method as in section 2.3.1.3 was used. A solution of **92** and **82** in DMF was treated with catalytic $CuSO_4$ and one equivalent of sodium ascorbate, heating to 90 °C for 18 hours. Aqueous work up in DCM/methanol followed by purification by column chromatography over silica gel (eluting with 97:3 DCM/methanol) gave **93** as light yellow glass in 33% yield.

The ^{1}H-NMR of **93** (see Figure 2.21) confirms the successful click reaction. The peak that corresponds to the methylene group that was previously part of the alkyne is now a singlet around 5.2 ppm. In this spectrum, the peaks corresponding to the dye are more clearly resolved. The spectrum of the dye features, starting from high ppm, a singlet, a doublet, a doublet of doublets and another doublet. These can be seen at 8.54, 7.67, 6.87 and 6.79 ppm, respectively. The singlet at 8.55 ppm corresponds to the triazole proton. The relatively broad peaks that overlap with the dye peaks correspond to the aromatic protons on the calixarene itself.

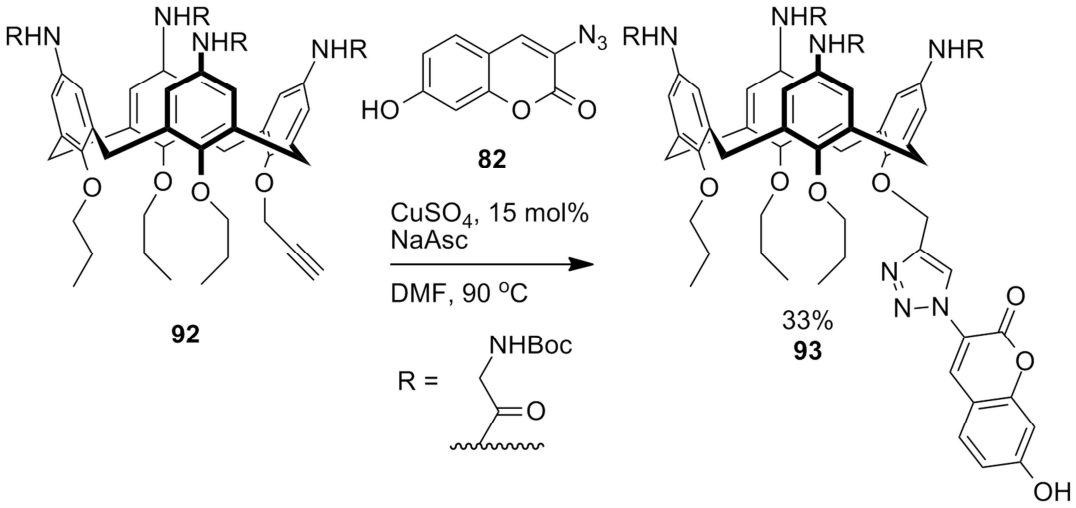

*Scheme 2.13: Click reaction of **92** with **82**.*

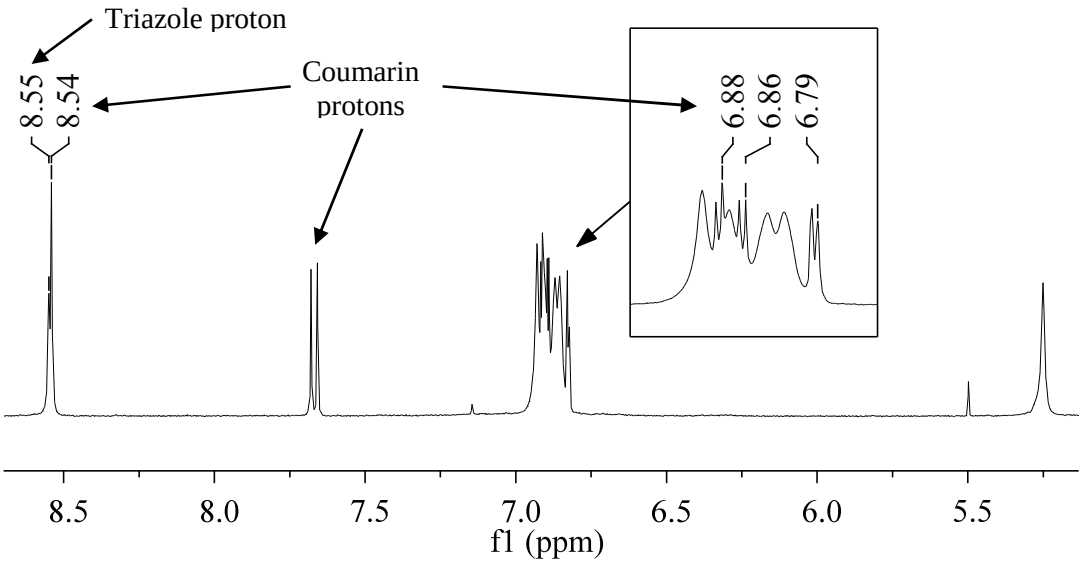

*Figure 2.21: ^{1}H-NMR spectrum of **93** (CD_3OD).*

2.3.1.8 Removal of Boc protecting groups

To remove the acid-labile Boc protecting group, the same method as employed in the synthesis of NBDCalAm was used.[55] Instead of stirring directly in a mixture of solvent and acid, such as aqueous HCl and dioxane,[60] gaseous HCl can be bubbled through a solution of the compound to rapidly remove the Boc groups from the compound. The solvent can be very easily removed once the reaction is complete.

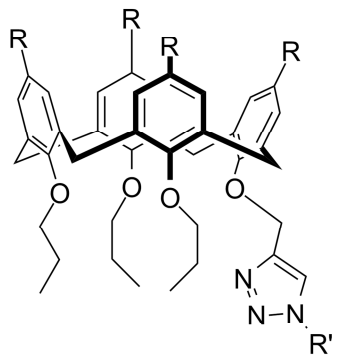

$HCl_{(g)}$, DCM/MeOH

R = NHBoc → R = $NH_3^+Cl^-$

R' = 7-hydroxycoumarin — **89** to **94**, 99%
R' = 1-methylpyrene — **90** to **95**, 99%
R' = 9-methyl-10-bromoanthracene — **91** to **96** 99%

$HCl_{(g)}$, DCM/MeOH

R = $NHCOCH_2NHBoc$ → R = $NHCOCH_2NH_3^+Cl^-$

R' = 7-hydroxycoumarin — **93** to **97**, 99%

*Scheme 2.14: Deprotection reactions on **89**, **90**, **91** and **93** to give **94**, **95**, **96** and **97**.*

Gaseous HCl, generated by dropwise addition of concentrated sulphuric acid to solid sodium chloride, was bubbled through solutions of the compounds in DCM, with the exception of **93**, which required some methanol to dissolve. After approximately 10 minutes, the hydrochloride salts of the free amines began to precipitate from solution; at this stage, methanol was added to redissolve the compounds, and the reaction continued for a further 5 minutes.

Solvent was removed under reduced pressure to give the hydrochloride salts of the compounds in quantitative yields. Compounds **94** and **97** were isolated as amorphous solids that were light orange-brown and beige in colour, respectively. Both **95** and **96** were isolated as brown amorphous solids.

2.3.2 Synthesis of the guanidinium click conjugate

The next target to be synthesised was the guanidinium derivative. This was an important target since, as described previously, poly-arginine-type cell penetration agents have been shown to be superior to poly-amines in their ability to cross the cell membrane. However, the synthesis posed various challenges. These will be examined in this section.

2.3.2.1 Synthesis of common intermediate – TBDMS route

The first issue to be addressed was a problem that was found in the synthesis of the tetra-amine intermediate. At the *ipso*-nitration stage, although the desired product could normally be isolated in reasonable yields, there was sporadically an impurity present that was very difficult to separate by column chromatography. This reduced the yield and was costly in terms of time spent on this step. In addition, the purity of the product obtained in the reduction step was inconsistent.

Other work within the group on tetra-alkyne derivatives turned up similar issues with the *ipso*-nitration, although in this case the efficiency of the transformation was even lower. The problem was addressed by use of alkyne protecting groups. It was therefore decided to apply this to the current synthesis.

The mono-alkyne (**78**) was synthesised as before. At this stage, the protecting group was installed to improve the efficiency of the following steps. *Tert*-butyl-dimethylsilane (TBDMS) was selected for its resistance to hydrolysis. It can be put in place using TBDMS-chloride *via* an S_N2 reaction by removing the mildly acidic terminal proton on the alkyne with a strong base. Compound **78** was stirred with lithium hexamethyldisilazane (LiHMDS) in THF at -70 °C to remove the terminal proton. TBDMSCl was added and the reaction continued at room temperature for 18 hours. Aqueous work-up followed by trituration of the residue with methanol to remove excess reagent gave the protected form **98** as white crystals in 93% yield.

Successful protection of the alkyne was confirmed by the ^{1}H-NMR spectrum (see Figure 2.22). The doublet that was previously generated by the methylene group of the alkyne has changed to a singlet with the loss of the long-range coupling, whilst the triplet from the terminal proton is absent. In addition, the integrals of the TBDMS peaks (not shown) are of the correct proportion for a single protecting group.

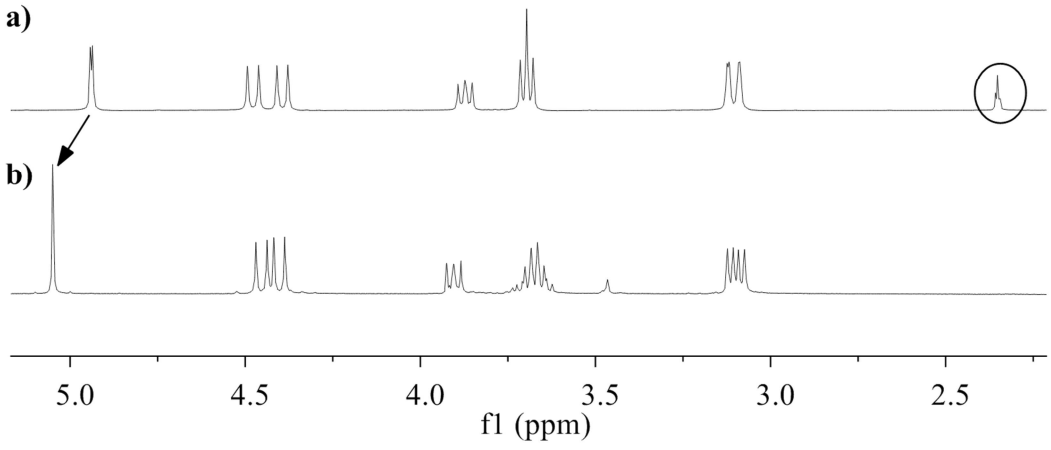

*Figure 2.22: ^{1}H-NMR spectrum of a) **78** and b) **98** ($CDCl_3$) showing loss of terminal alkyne triplet (circled) and conversion of methylene doublet to singlet.*

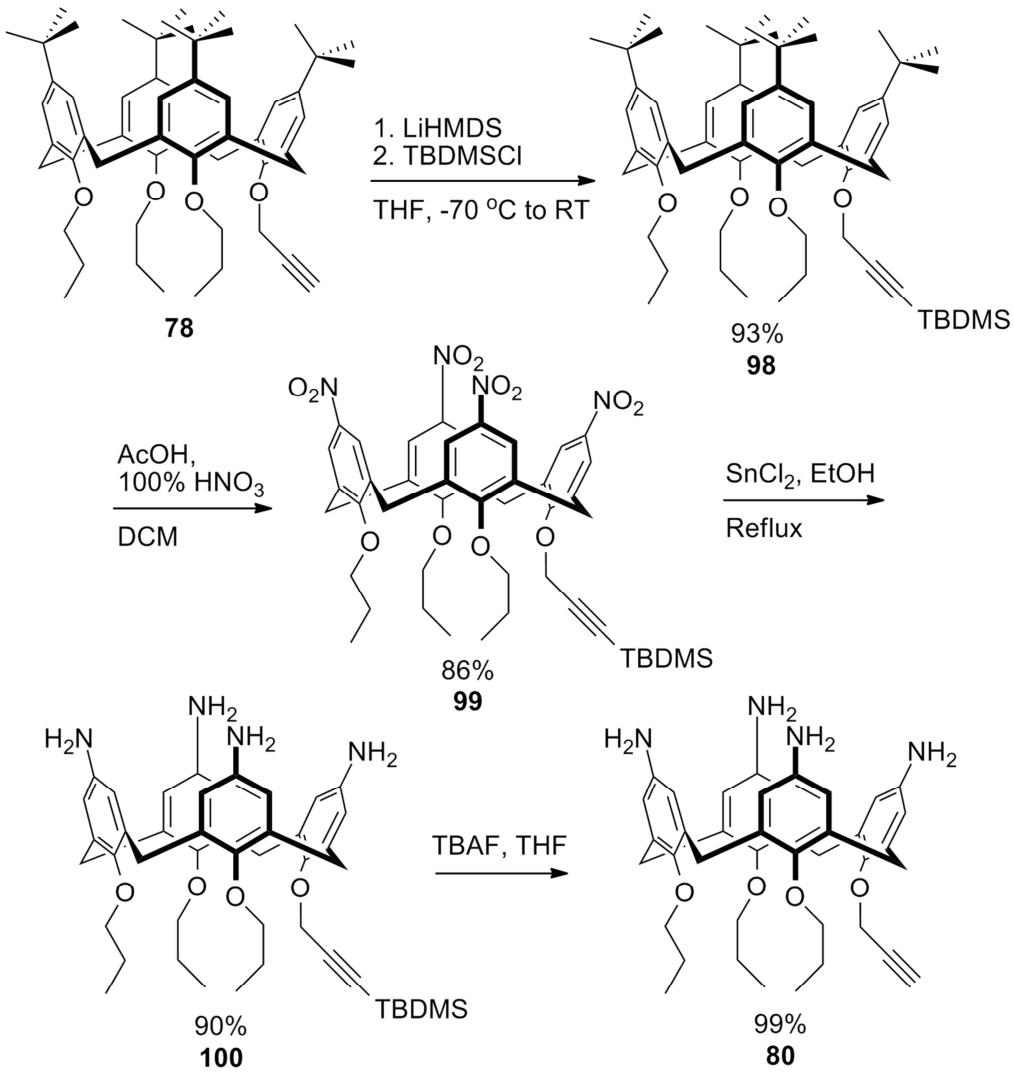

*Scheme 2.15: Synthesis of **80** from **78** via TBDMS protected route.*

The nitration was carried out the same as before. Compound **98** was stirred with excess glacial acetic acid and 100% nitric acid, giving a characteristic colour change first to blue-black, then over time to bright orange. Aqueous work up and trituration of the residue with methanol gave the tetra-nitrated product **99** as light yellow crystals in 86% yield. No further purification was necessary.

For the reduction, **99** was heated to reflux with tin (II) chloride in ethanol for 24 hours, followed by aqueous work up with sodium hydroxide. Tetra-amino compound **100** was obtained as orange-brown glass in 90% yield, which was used with no further purification.

To carry out the desilylation of **100**, a source of fluoride is needed. Tetrabutylammonium fluoride (TBAF) was selected as a mild fluoride source that does not preclude the use of glass reaction vessels. The compound was stirred with a solution of TBAF in THF for 18 hours, followed by aqueous work-up. In this case the cleaved TBDMS cannot be separated from the deprotected compound using methanol,

since both are soluble in this solvent. The broad solubility of TBDMS was exploited instead. By triturating with hexane, the TBDMS was separated from the amine. The deprotected compound, now identical to **80**, was isolated as light brown powder in quantitative yield.

2.3.2.2 Guanidinylation – Boc protection route

A number of methods for guanidinylation of amines are available which have been utilised in synthesis of guanidinium calixarenes. These include: the use of Boc-protected triflyl guanidine on its own,[86] relying on a good leaving group to drive the reaction; Boc-protected thiourea with an activating reagent such as Mukaiyama reagent (2-chloro-1-methylpyridinium iodide) or mercury chloride;[60] or the use of a Boc-protected isothiourea with mercury chloride.[87] The latter method was selected for the commercial availability and relatively low cost of the reagents.

Compound **80** was stirred with a mixture of N,N'-di-Boc-S-methylisothiourea, $HgCl_2$ and triethylamine in dry DMF for 48 hours. The byproduct, HgSMe, appeared as a white precipitate over this time and was subsequently removed by filtration. Recrystallisation from hexane allowed the majority of the excess reagent to be removed prior to purification by column chromatography over silica gel.

However, the purification of this compound revealed a problem: the Boc protecting groups were surprisingly labile, leading to degradation on the mildly acidic silica. This could be mitigated by use of triethylamine in the eluent (8:1:1 hexane/diethyl ether/triethylamine), allowing **101** to be isolated as white solid, but in poor yield (13%).

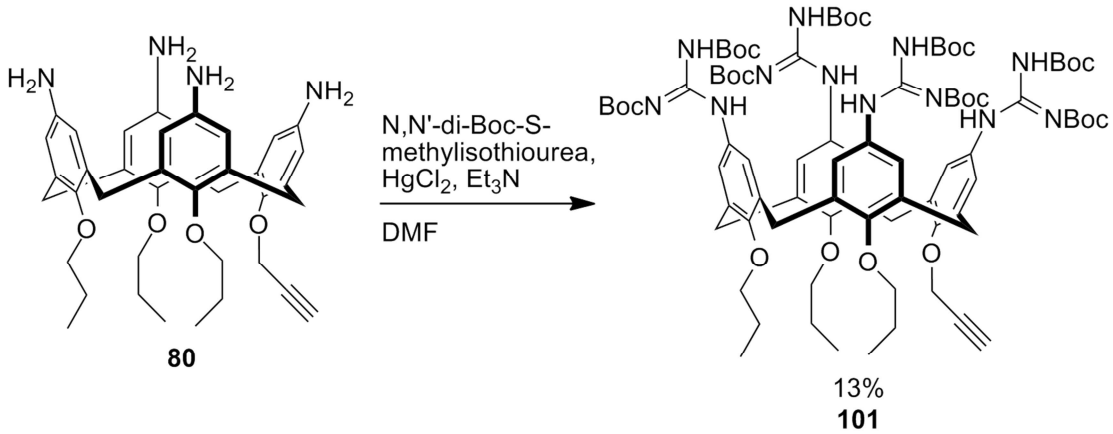

*Scheme 2.16: Synthesis of **101** from **80**.*

With the addition of the coumarin dye, an acidic phenolic proton is introduced into the molecule. Triethylamine would therefore not be suitable as a component of the eluent for purification of the dye conjugate as it would form a salt with the dye and

cause the compound to stick to the silica. Neutral alumina was another option for column chromatography; however, TLC with this matrix for compound **101** also showed degradation.

An alternative approach was therefore investigated. Removal of the Boc groups after guanidinylation would yield a stable compound and prevent loss of product due to degradation. The CuAAC reaction could then be performed in aqueous medium. With this in mind, it was decided to use the TBDMS protected tetra amine (**100**) instead, since this could improve the integrity of the molecule during the guanidinylation reaction. The synthesis could therefore take two routes:

1. Guanidinylation, followed by removal of the TBDMS group then the Boc groups;
2. Guanidinylation, followed by removal of the Boc groups then the TBDMS group.

Both of these routes were attempted.

Route 1:

Compound **100** was stirred with a mixture of N,N'-di-Boc-S-methylisothiourea, $HgCl_2$ and triethylamine in dry DMF for 48 hours. The byproduct was removed by filtration. At this stage the correct product was confirmed by NMR spectroscopy.

The ^{1}H-NMR spectrum is shown in Figure 2.23. The methylene bridges of the calixarene around 4.5 and 3.2 ppm show that the major product is a single calixarene, rather than a mixture with different symmetries. Both the guanidinium N-H peaks (around 11.6 ppm) and the aryl N-H peaks (around 10.2 and 9.5 ppm) can be seen, with the peak pattern showing correct symmetry and the integrals showing the correct number of protons for tetra-functionalisation, confirming that the tetra-guanidinium derivative (**102**) has been synthesised.

Although excess reagent can be seen in the NMR, the crude compound was of high purity compared with the crude compound **101**. This displays the utility of keeping the TBDMS group in place during guanidinylation. This crude material was carried through to the next step with a view to removing the excess reagent at a later stage, rather than losing material due to degradation during purification at this stage.

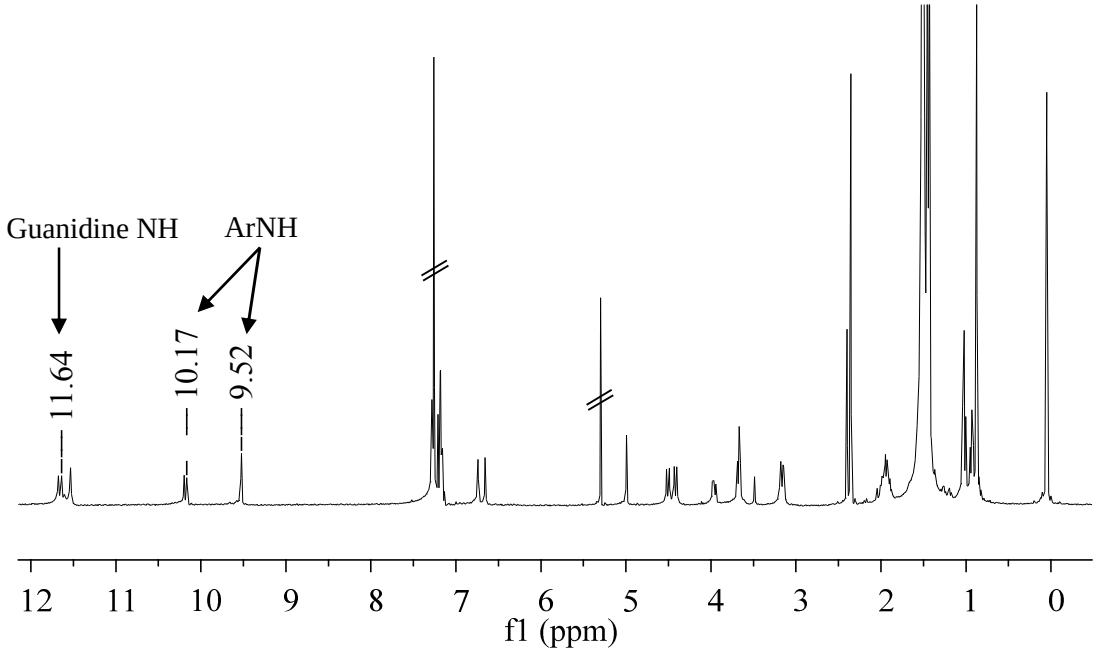

*Figure 2.23: ^{1}H-NMR spectrum of crude **102** ($CDCl_3$).*

The TBDMS group was removed from **102** by stirring it with TBAF in THF for 18 hours. Aqueous work-up grave the crude desilylated product **103**. The cleaved TBDMS group could not be separated from the product by trituration with either methanol or hexane, since the product was soluble in both of these solvents. After confirming that the free alkyne was present by ^{1}H-NMR spectroscopy, the crude product was taken through to the next reaction, once again avoiding subjecting it to column chromatography over silica gel.

Finally, gaseous HCl was bubbled through a solution of **103** in DCM, adding minimal methanol when the product began to precipitate. In contrast with the previous Boc-deprotection reactions carried out in this way, a much longer reaction time was needed; it took around 2 hours before there were no more *tert*-butyl peaks present in the ^{1}H-NMR spectrum. This was unexpected from the apparent lability of the Boc-protecting groups in previous steps. It could be that the second Boc protecting group on each guanidinium group is more difficult to remove than the first, which is supported by finding of R. Lalor that treatment of the guanidinium intermediate **76** with hydrazine removed half of the Boc-protecting groups from the molecule in a symmetrical fashion, i.e. one from each position.

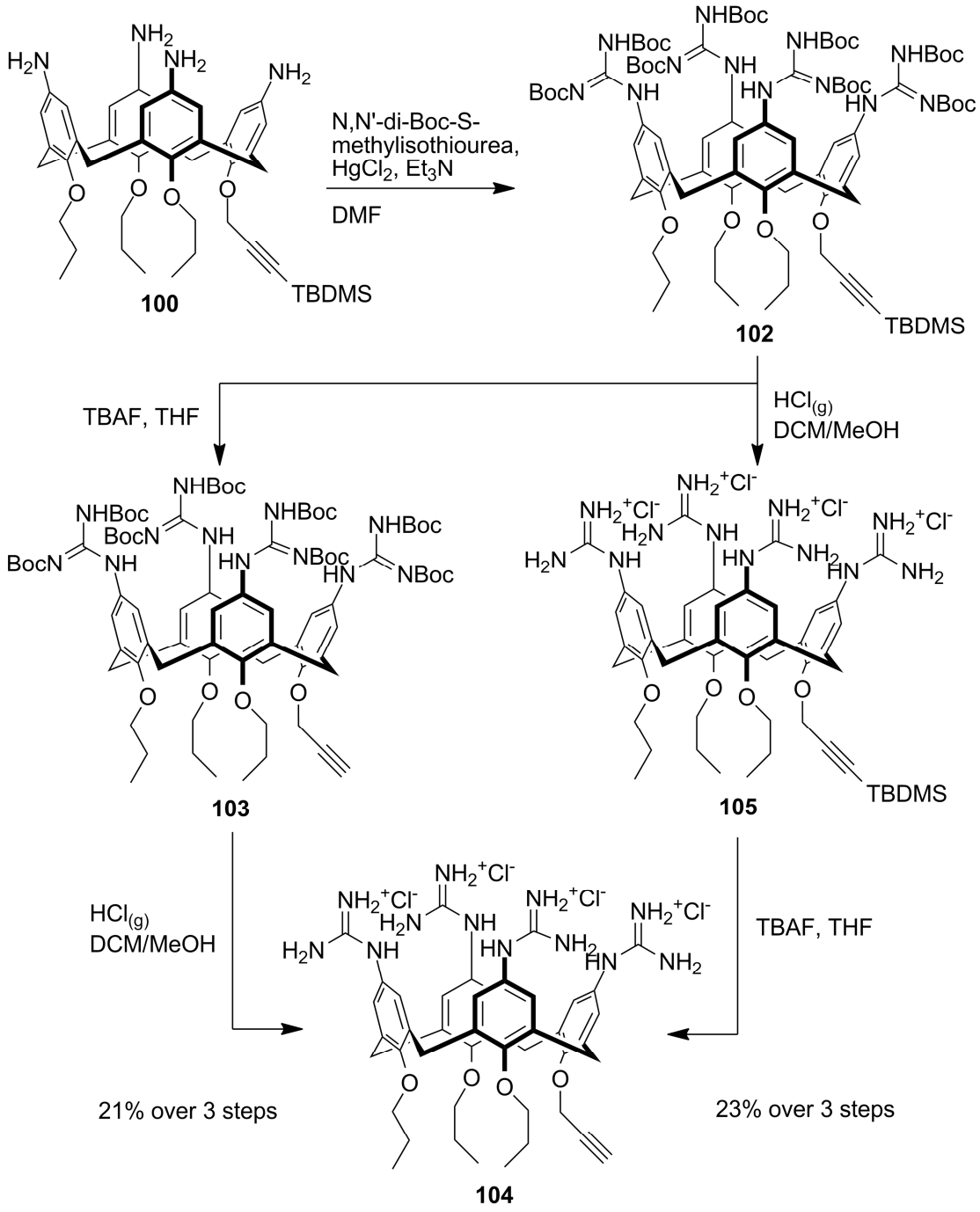

*Scheme 2.17: Two possible routes for the synthesis of **104**, via **102** followed by **103** or **105**.*

Due to the high polarity of this compound, even in neutral form, it is unsuitable for purification by column chromatography over silica gel. Therefore to remove the excess thiourea reagent (now also deprotected) and the cleaved TBDMS, reverse-phase column chromatography was used, eluting with a gradient of methanol in water. Pure fully deprotected compound **104** was obtained as off-white solid in 21% yield over 3 steps. This is favourable when compared with the synthesis of compound **101**, which was isolated pure in only 13% yield in a single step.

Route 2:

The first step in this route required removal of the Boc groups. Gaseous HCl was bubbled through a solution of compound **102** in DCM, with methanol added to redissolve any precipitate that was formed. As with the Boc-deprotection of intermediate **103**, complete removal of all Boc groups to give **105** took around 2 hours. Although the compound could be subjected to reverse-phase chromatography at this stage to remove the deprotected reagent, the compound was otherwise pure, with only a single calixarene species apparent. It was decided therefore to limit the purification to a single step to maximise the efficiency of the process.

Crude **105** was stirred with TBAF in THF for 18 hours. After quenching the reaction with saturated ammonium chloride, some of the ammonium chloride precipitated and could be removed by filtration. However, at this stage the presence of the water-soluble guanidinium compound precluded the use of aqueous work-up to remove excess reagent. The crude residue was therefore subjected to reverse-phase column chromatography to purify the product and remove all excess reagents and cleaved TBDMS, eluting with a gradient of methanol in water. Pure fully deprotected compound **104** was obtained as off-white solid in 23% yield over 3 steps.

Although this is a higher yield than obtained from route 1, such a small difference in yield may not be significant. Route 2 posed more problems, particularly with not being able to remove the excess tetrabutylammonium except by reverse phase column chromatography. However, the crude final product by this route was more pure than that of route 1. Therefore both routes have both problems and merits, but fundamentally both gave the desired product pure and in better yield than could be obtained by attempting to manipulate the Boc-protected form.

2.3.2.3 Attempted CuAAC reaction with deprotected guanidinium derivative

In order to add the dye to **104**, it was hoped to use a similar strategy to the previous CuAAC reactions. A mixture of **104** and **82** was stirred with sodium ascorbate and catalytic copper sulphate at 90 °C in several different solvent systems to test which was most effective. Ethanol, DMF, *tert*-butanol and 1:1 ethanol/water were tested; the latter gave the best conversion to product **106** according to the crude NMR (see Figure 2.24). Confirmation of the reaction was given by the loss of the alkyne triplet around 3 ppm and the conversion of the alkyne doublet around 5 ppm to the singlet of the methylene adjacent to the triazole ring. Dye peaks can also be seen downfield.

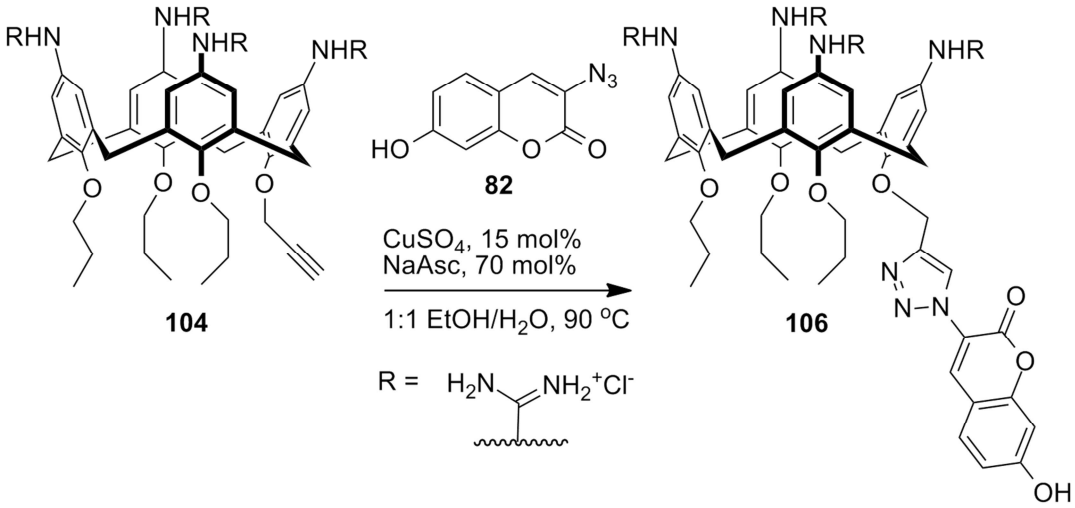

*Scheme 2.18: Click reaction of **104** with **82**.*

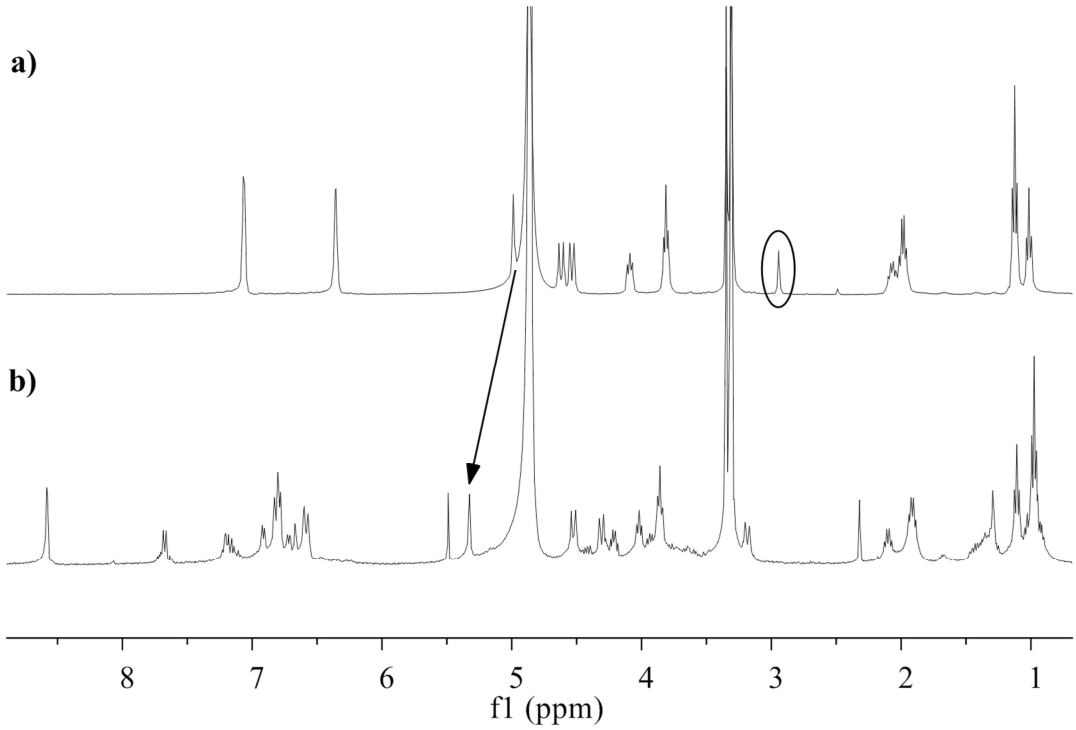

*Figure 2.24: ^{1}H-NMR-spectrum of a) **104** and b) crude **106** (CD_3OD) showing loss of terminal alkyne triplet (circled) and conversion of methylene doublet to a singlet.*

At this stage there was brown, amorphous solid present that was poorly soluble in both organic solvent and water unless treated with dilute HCl. Reverse-phase column chromatography was attempted, but solubility problems led to blockage of the column. No fractions were recovered that resembled the product.

Attention was turned to an alternative method for purifying the product. Since there should only be a single product from the CuAAC reaction, the presence of multiple products in the NMR could be attributed to the potential of the guanidinium groups to

interact with copper in the reaction, as well as the different anions present, resulting in a mixture of different species. The use of an anionic resin to bind the guanidinium product would allow the excess dye and the ascorbic acid to be readily removed as these would not bind to the resin. The product could then be separated from the copper catalyst, which would also bind to the matrix, by exploiting their different binding strengths. The compound would be eluted from the column in a single salt form with only one type of counter-anion (see Scheme 2.19).

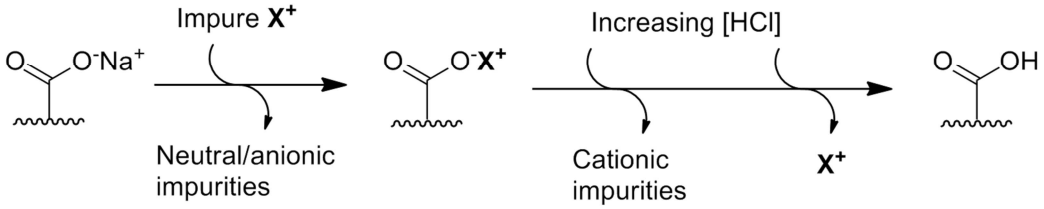

*Scheme 2.19: Principle of purification by ion-exchange chromatography (**X** = **106**).*

Commercially available cation-binding resins include those featuring strongly acidic groups such as sulphonic acid and weakly acidic groups such as carboxylic acid. Since four guanidinium moieties are clustered on each molecule, it would be expected that a strong-cation binder such as a sulphonic acid resin would bind the compound too strongly leading to harsh conditions to elute it. Therefore it was decided to use a carboxylic acid resin (Amberlite IRC-50) as a weak cation binder.

The crude product was applied to the sodium form of the resin. After washing with water, increasing concentrations of HCl solution were applied to the column to displace cations from the resin. However, even 2 M HCl failed to elute the product. Increasing concentrations of first ammonium chloride, then sodium chloride, up to saturated solutions of each, also failed to displace the product. The strength in binding could be attributed to a combination of the inherent tendency of guanidinium moieties to bind anions, as described previously, along with the clustering of four of these groups onto a single face of a molecule, with the potential to give binding that is greater than the sum of its parts.

Since applying cations to displace the product was not sufficient, it was reasoned that if the guanidinium groups of the compound could be deprotonated, then the binding strength could be lessened, allowing the product to be eluted. By using dilute sodium hydroxide, fluorescent fractions were indeed eluted from the column; however, the material recovered was a complex mixture by ^{1}H-NMR with no major species, suggesting significant degradation of the product. At this stage an alternative route to the product was sought.

2.3.2.4 Guanidinylation – Cbz protection route

Since the deprotected compound gave unforeseen problems and the Boc protecting groups were too labile for the synthesis, the possibility of using alternative protecting groups was investigated. A check of the commercially available thiourea- and isothiourea-type guanidinylation reagents turned up two additional possibilities in the form of carboxybenzyl (Cbz) and benzoyl (Bz) protected derivatives, both of which should have superior stability to the reaction and purification conditions than the Boc form. Since Cbz protecting groups have more options available for their cleavage compared with Bz groups, it was decided to follow this route.

Compound **80** was stirred with a mixture of N,N'-di-Cbz-S-methylisothiourea, $HgCl_2$ and triethylamine in dry DMF for 24 hours. The byproduct, HgSMe, appeared as a white precipitate over this time and was subsequently removed by filtration. The crude product was purified by column chromatography over silica gel, eluting with hexane/ethyl acetate (4:1 then 3:1) to give **107** as white crystals in 26% yield. Although the yield was relatively low, it is still higher than in the synthesis of pure **101**, which gave only 13% yield. This demonstrates the validity of this approach in increasing the stability of the fully protected species.

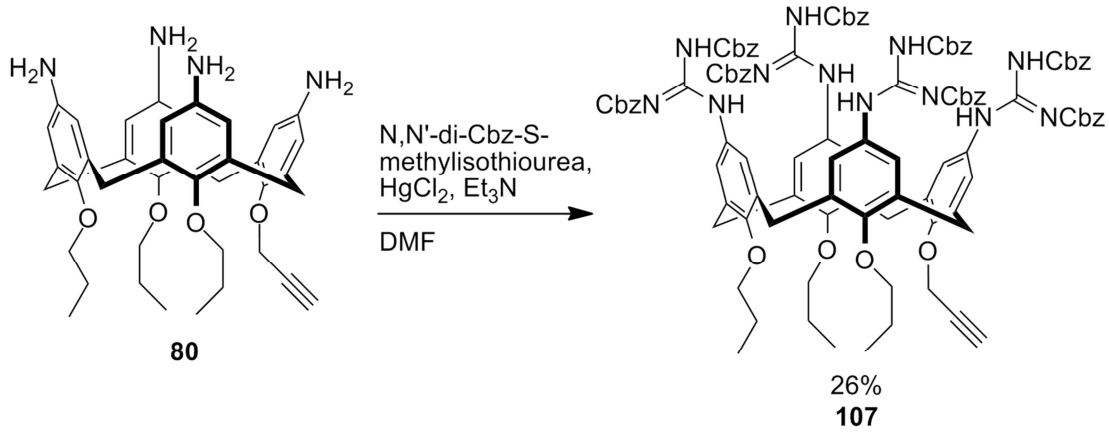

*Scheme 2.20: Synthesis of **107** from **80**.*

Confirmation of the correct product was provided by the ^{1}H-NMR spectrum (see Figure 2.25). The guanidinium N-H peaks can be seen around 11.8 ppm whilst the aryl N-H peaks are further upfield around 10.0 and 9.5 ppm. The aromatic hydrogens of the protecting groups give a complicated group of peaks around 7.2 ppm, whilst the methylene groups joining them to the carbamate are around 5 ppm, slightly downfield of the methylene of the alkyne.

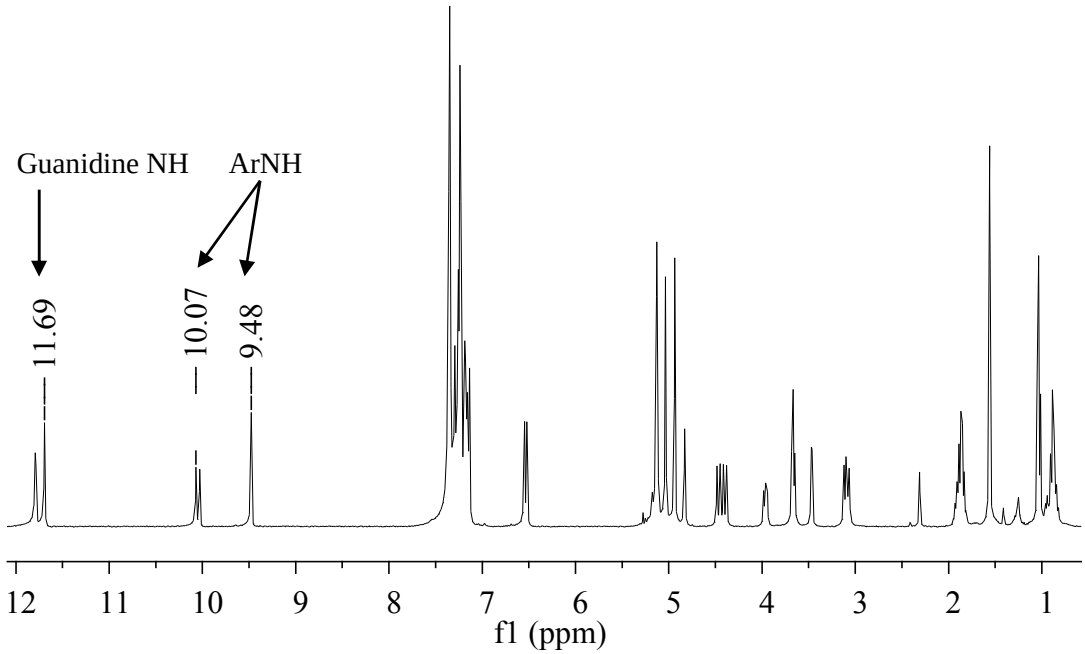

*Figure 2.25: ^{1}H-NMR spectrum of **107** ($CDCl_3$).*

2.3.2.5 Coumarin appended tetra-guanidine

With the stable guanidine compound in hand, the CuAAC reaction was implemented. A solution of **107** and **82** in DMF was treated with sodium ascorbate and catalytic $CuSO_4$, heating at 70 °C for 2 hours. Aqueous work up followed by purification by column chromatography over silica gel (eluting with 5-10% ethyl acetate in DCM) gave **108** as light yellow solid in 32% yield.

It was thought that the low yield was due to degradation of the product, so the reaction was repeated at room temperature for 24 hours. A modified work-up was used. Following removal of the DMF under reduced pressure, the solid was triturated with water and filtered to remove the catalyst, followed by washing with methanol to remove excess dye, exploiting the poor solubility of the Cbz protected compound in this solvent. After verifying that no product had been lost in the methanol wash, the product was purified by column chromatography over silica gel, eluting with 19:1 DCM/ethyl acetate to give **108** in 74% yield.

The correct product was confirmed by ^{1}H-NMR (see Figure 2.26). The methylene group adjacent to the triazole ring can no longer be differentiated from those of the Cbz groups around 5.1 ppm. However, the proton on the triazole ring itself can be seen at 8.54 ppm, confirmed by 2D-NMR. The dye peaks are also in evidence around 8.35 and 6.6 ppm, with the remaining dye peak obscured by the aromatic protons of the Cbz groups. In this case the guanidinium N-H protons give rise to one broad singlet, in contrast with **107**, possibly due to intermolecular interactions with the coumarin dye.

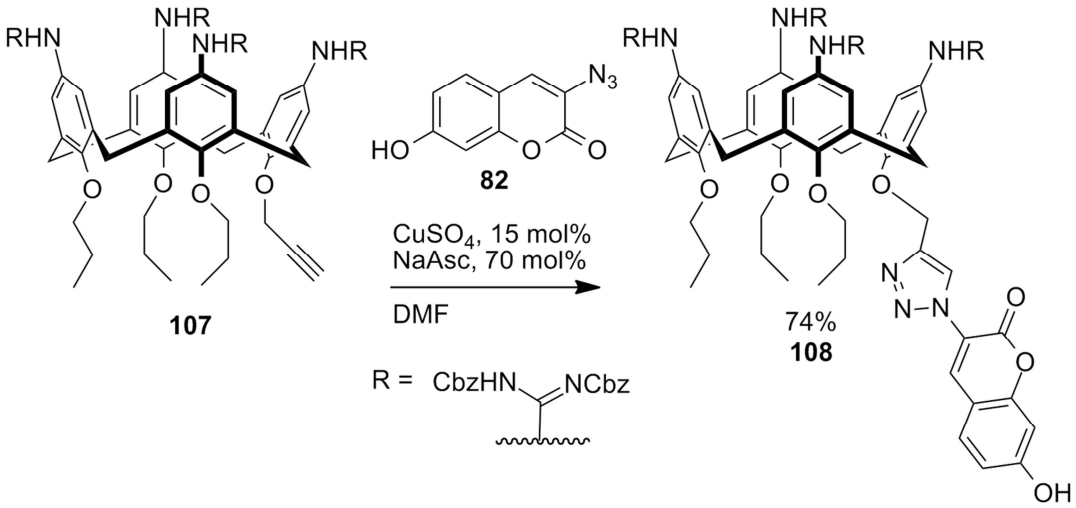

*Scheme 2.21: Click reaction of **107** with **82**.*

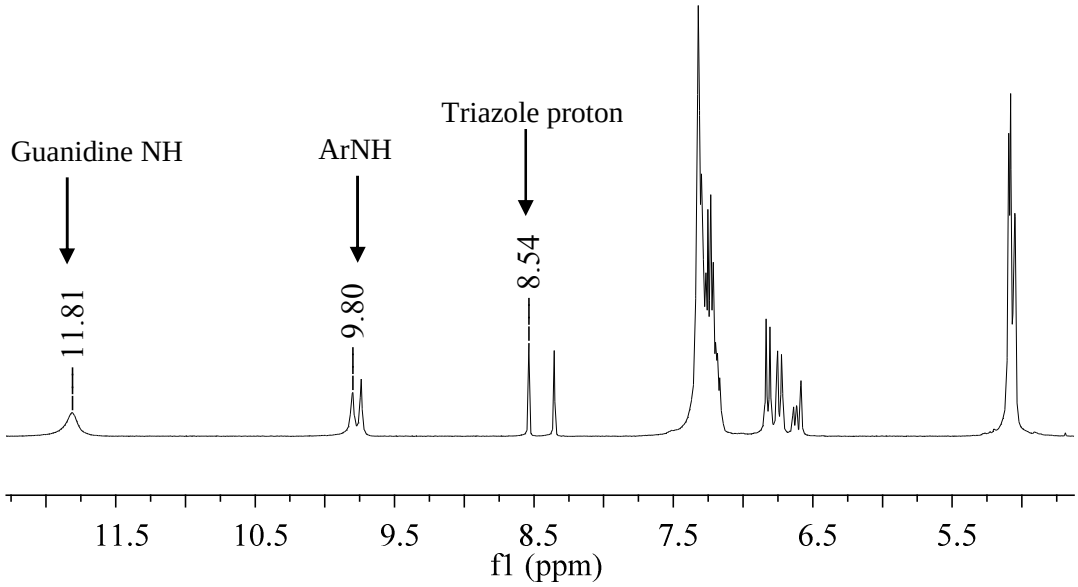

*Figure 2.26: ^{1}H-NMR spectrum of **108** ($CDCl_3$).*

2.3.2.6 Deprotection of Cbz protected guanidine derivative

A number of methods are available for cleavage of Cbz protecting groups. For aromatic Cbz-protected guanidines, catalytic hydrogenolysis with palladium on carbon[88] is the dominant literature method. However, this is unsuitable in this case due to the presence of the coumarin dye, which can be reduced under these conditions.[89]

For aliphatic Cbz-protected guanidines, methods that have been applied for removal of the protecting groups include the use of HBr in acetic acid[90] or thioanisole in TFA,[91] both of which utilise a combination of acidic conditions to protonate the carbonyl of the carbamate and a nucleophile to attack the methylene of the benzyl group. Another method simply heated the protected compound to reflux in 6 M HCl to remove the Cbz groups;[92] however it was decided to avoid such harsh conditions.

The first attempt at removal of the protecting groups from **108** was made by stirring the compound with HBr in acetic acid. After 18 hours, DCM was added to precipitate the product to separate it from the cleaved benzyl groups. However, the solid that precipitated was found to be a complex mixture of products by ^{1}H-NMR, suggesting considerable degradation of the product.

Following this, deprotection was attempted by stirring **108** with thioanisole in TFA. The colour of the solution immediately changed from yellow to green. After 24 hours the solvent was removed under reduced pressure and the residue triturated with diethyl ether. The progress of the reaction was assessed by ^{1}H-NMR, which showed a mixture of products with benzyl peaks still present, suggesting incomplete deprotection. After a further 48 hours under the same conditions the reaction still seemed to be incomplete, so the reaction mixture was heated to 40 °C for 48 hours, during which time the colour changed to grey-blue. This time the ^{1}H-NMR spectrum showed decomposition of the product.

At this stage, an alternative method was investigated which uses iodotrimethylsilane (TMSI), where TMS acts as a Lewis acid instead of a Brønsted acid, with iodide as a nucleophile.[93] Although TMSI is commercially available, it is commonly stabilised with copper, which could bind to the free guanidinium groups and cause problems with purification. TMSI can however be easily generated *in situ* from TMSCl and anhydrous sodium iodide,[94] with concomitant generation of sodium chloride. Anhydrous conditions are desirable for this reaction as TMSI is readily hydrolysed, generating HI, which could lead to undesired side-reactions.

The reaction was first attempted on **108** by stirring the compound with sodium iodide in acetonitrile under argon, followed by addition of TMSCl, resulting in a colour change to yellow-orange and precipitation of sodium chloride. After stirring at room temperature for 4 hours, methanol and dilute aqueous HCl were added to cleave the TMS still bound to the carbamate to allow decarboxylation to take place.

After removing the solvent under reduced pressure and triturating with diethyl ether, the ^{1}H-NMR spectrum showed that the integration height of the benzyl peaks had been halved, whilst the symmetry of the molecule was the same, suggesting that one Cbz had been removed from each guanidine. This is consistent with previous observations suggesting that the half-deprotected species is more stable than the fully protected compound.

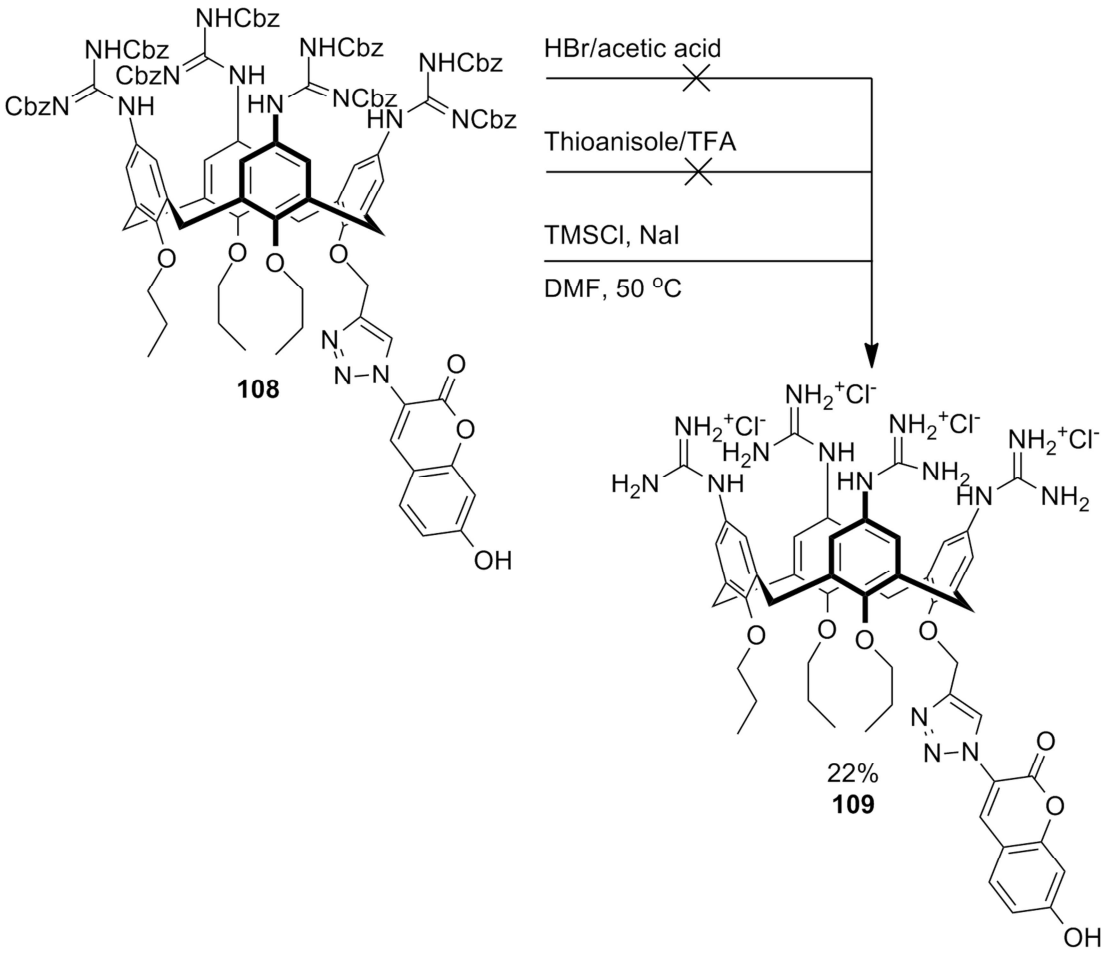

*Scheme 2.22: Deprotection of **108**.*

In an attempt to push the deprotection through to completion, two modified procedures were used. First, thioanisole was added to the reaction mixture to provide an additional nucleophile and a cation scavenger. However, after stirring overnight at room temperature the reaction still proceeded only halfway.

Second, the reaction was heated to 60 °C for 24 hours; this gave a complex mixture of products by NMR, suggesting decomposition of the product. This is likely due to side-reactions stemming from the variety of potential reactions that TMSI can carry out, including cleavage of lactones and ethers.[93] The cleavage of ethers on calixarenes by TMSI has in fact previously been investigated as a route towards mono-alkyl derivatives.[95] Therefore more caution is required to prevent undesired side-reactions.

Although it has been reasoned that acetonitrile participates in the reaction by forming a complex with the TMSI,[93] resulting in the observed colour-change, it was decided to investigate DMF as an alternative solvent. The deprotection was attempted at different temperatures and varying reaction times. Although reaction at room temperature gave only half-deprotected product after 24 hours, heating to 50 °C gave the fully-deprotected product that could, for the first time in this synthesis, be distinguished in the ^{1}H-NMR spectrum.

Stirring for 8 hours or 24 hours both gave fully-deprotected product as the major species, but longer reaction times generally gave a more complex mixture of products due to side-reactions. Reacting for 24 hours seemed to give the best compromise between maximising the desired product and avoiding side-products. The conditions that were tested for this deprotection are summarised in Table 2.1.

*Table 2.1: Conditions used in the deprotection of **108** with TMSCl/NaI*

Solvent	*Temperature / °C*	*Time / h*	*Result*
Acetonitrile	25	4	Half deprotected
Acetonitrile (with thioanisole)	25	18	Decomposition
Acetonitrile	60	24	Decomposition
DMF	25	24	Half deprotected
DMF	50	8	Fully deprotected
DMF	50	24	Fully deprotected
DMF	50	96	Fully deprotected, some decomposition

It is clear that DMF is a more appropriate solvent in this case than acetonitrile. It is possible that the complex that is formed between TMSI and acetonitrile activates the reagent, so that when it is heated to allow the more stable half-protected species to react, the incidence of side-reactions increases considerably. Without this activation, as with DMF, the reaction barrier of the half-protected species can be overcome with heating without compromising the rest of the molecule.

To obtain pure product, reverse-phase column chromatography was necessary to remove any side-products. To avoid loss of product during work-up, it was therefore decided to proceed to purification directly after removal of solvent under reduced pressure, so that impurities and cleaved protecting groups could be removed in the same step. Iodine also seemed to be generated during removal of the solvent and this could also be removed during purification. The product was purified by reverse-phase column chromatography, eluting with a gradient of methanol in 60 mM aqueous HCl. Pure deprotected compound **109** was isolated as off-white solid in 22% yield.

The ^{1}H-NMR of **109** is shown in Figure 2.27. The methylene adjacent to the triazole ring can now be resolved and is around 5.3 ppm. One methylene bridge doublet of the calixarene core is obscured by the residual methanol peak and was

found using 2D-COSY NMR to be at 3.3 ppm. In this case the peaks around 8.6 ppm corresponding to the proton on the triazole ring and one of the dye protons can barely be resolved as separate peaks and so cannot be differentiated due to the insufficient resolution of the 2D-NMR experiments.

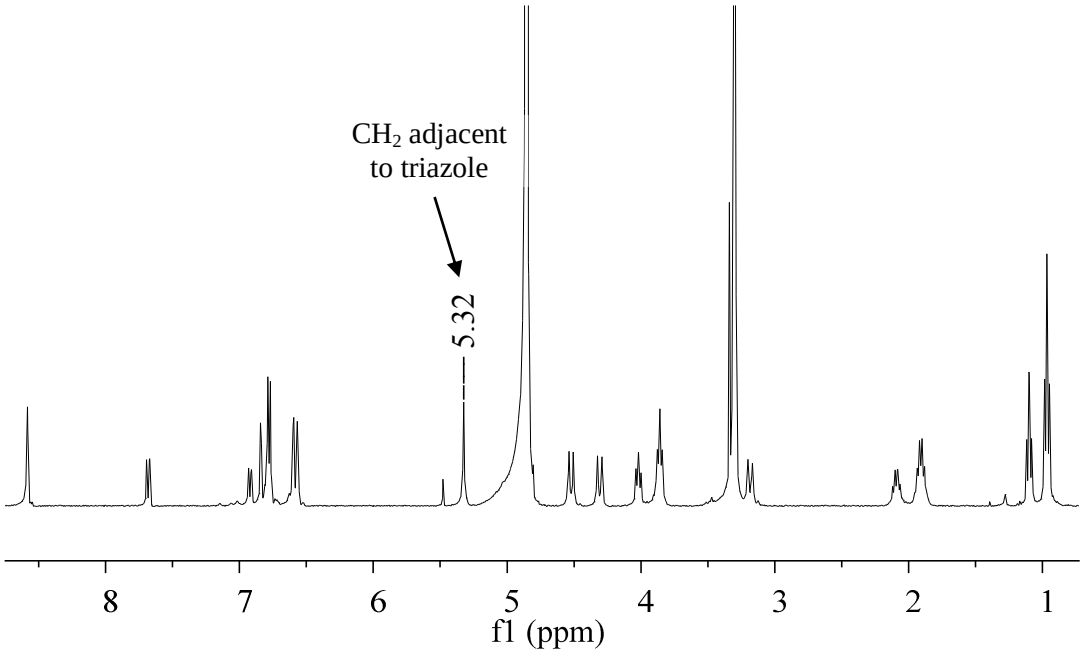

*Figure 2.27: ^{1}H-NMR spectrum of **109** (CD_3OD).*

2.3.3 Synthesis of dye-conjugates with variable linkers

In order to investigate the potential effect of changing the linkage method to a triazole ring, two compounds that were identical except for the type of linker were required. This gave two immediate possibilities as shown in Figure 2.28.

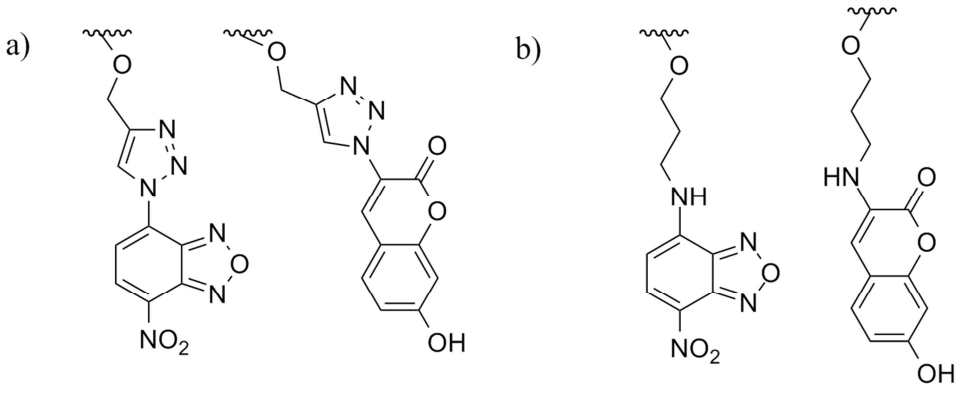

Figure 2.28: Analogues with NBD and coumarin dyes linked by a) triazole rings and b) secondary amines.

In order to make an analogue to a previously synthesised molecule with a different dye but the same linker, a triazole-linked NBD could be synthesised to compare with compound **94**, or an amine-linked coumarin to compare with NBDCalAm.

Investigation of the former showed that, whilst a derivative of NBD with an azide *para* to the nitro group can be synthesised, upon formation of the triazole ring the fluorescence is considerably quenched.[96] It was therefore decided to pursue the latter route.

Whilst the synthesis of the amine-linked NBD is straightforward due to the *para*-nitro group activating NBD-chloride to an S_NAr reaction, the analogous reaction with 3-halo-coumarin would require palladium catalysis.[97] Furthermore, there is no apparent evidence of such a reaction being carried out on 7-hydroxy-coumarin derivatives. A more straightforward synthesis would use 3-amino-7-hydroxycoumarin, which can easily be made from the previously synthesised **81**.[79] This could then be reacted with an alkyl halide (*via* an S_N2 reaction) or an acid (to give an intermediate amide bond) attached to the calixarene core to give the desired amine linkage.

2.3.3.1 Amine-linked coumarin *via* alkyl halide

The first route that was attempted was the formation of an amine-linked coumarin *via* an S_N2 reaction. This required an alkyl halide on the calixarene core, which could easily be installed on compound **77** using 1,3-dibromopropane in the ether formation reaction. In order to minimise dimerization of the calixarenes by reaction of the starting material with the product, a large excess of alkylating agent was used.

Compound **77** was treated with sodium hydride followed by 1,3-dibromopropane. After 24 hours, aqueous work-up followed by purification by column chromatography over silica gel, eluting with 8:3 hexane/DCM. Co-elution with an unknown impurity, even with varying eluents, made for inefficient purification, giving **110** as a powder in 39% yield.

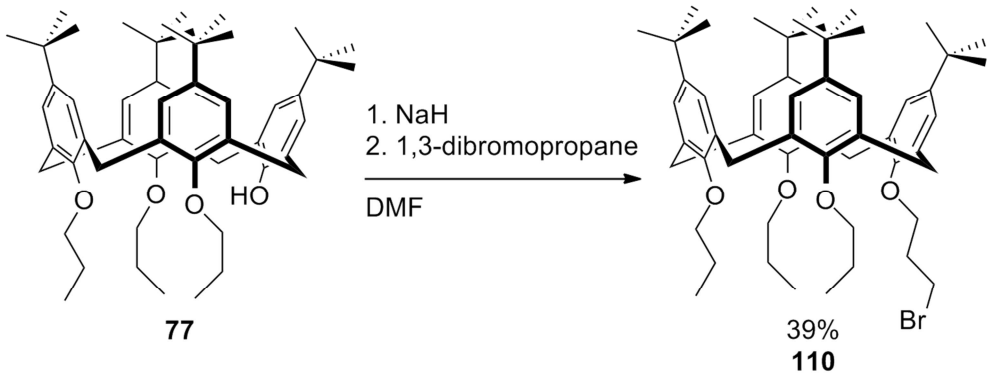

*Scheme 2.23: Alkylation of **77** to give **110**.*

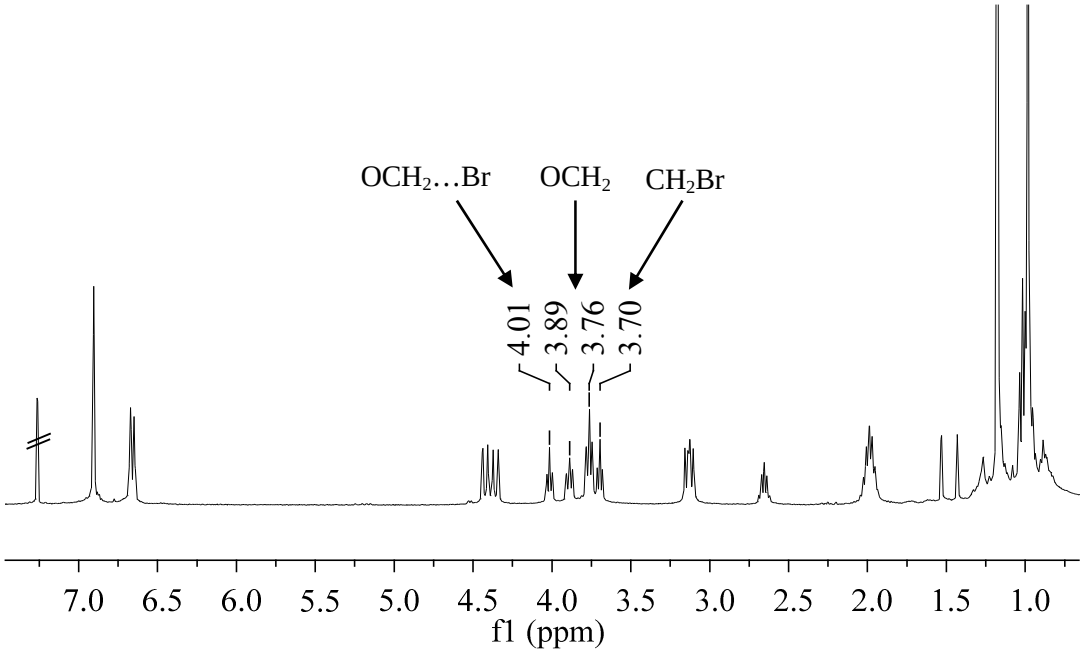

*Figure 2.29: [1]H-NMR spectrum of **110**.*

The [1]H-NMR spectrum of **110** is shown in Figure 2.29. In contrast to **77**, there is now an extra propyl chain, but since this is capped with an electron-withdrawing halide there are now two extra triplets in the spectrum around 3.75 ppm. Examination of the 2D-COSY spectrum allows these to be differentiated. It shows a mutual interaction of the peaks at 3.89 and 3.76 ppm with the multiplet around 2.0 ppm, which in turn shares a cross-peak with the CH_3 triplets obscured by the *tert*-butyl peaks around 1.0 ppm. These must therefore correspond to the three unfunctionalised propyl chains.

The triplets at 4.01 and 3.70 ppm have a mutual interaction with the multiplet around 2.7 ppm. These must correspond to the peaks of the bromopropyl group. Since the protons closest to the oxygen will be more deshielded compared with those adjacent to the bromine, the triplet at 3.7 ppm must correspond to the latter.

The conversion to the Boc-protected amine species was carried out the same as in the synthesis of **88**. Compound **110** was first nitrated by stirring with glacial acetic acid and 100% nitric acid for 6 hours, followed by aqueous work-up and trituration with methanol to give sufficiently pure tetra-nitrated product **111** as a light-orange powder in 87% yield.

This was then reduced by heating it to reflux in ethanol with tin chloride for 48 hours, followed by aqueous work-up with sodium hydroxide. The tetra-amine product **112** was isolated as brown-glass in 90% crude yield. Although the purity of this product was less than in previous reductions using this method, the crude material was taken through to the next reaction, after which it could be more easily purified.

Compound **112** was stirred with Boc-anhydride and DIPEA in DCM for 18 hours. The product was purified by column chromatography over silica gel, eluting with 19:1 DCM/ethyl acetate, giving the protected tetra-amine **113** as off-white glass in 59% yield.

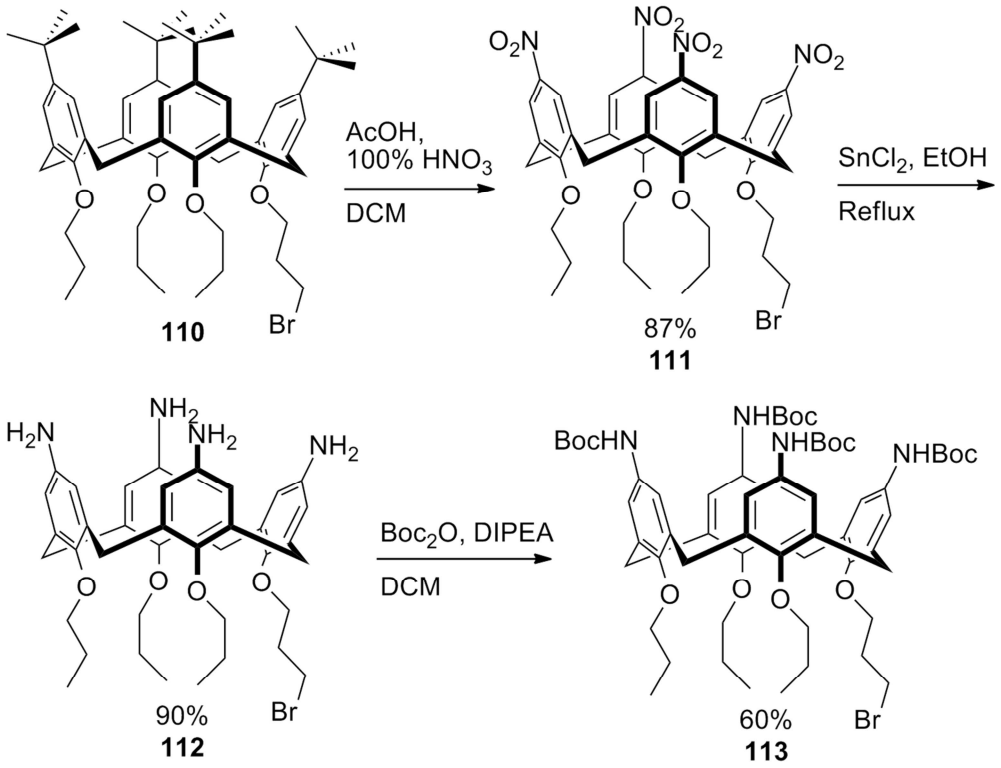

*Scheme 2.24: Conversion of **110** to **113** via nitration, reduction and Boc protection.*

With the alkyl-halide functionalised calixarene core in hand, the amino-coumarin was next synthesised. This was available in two steps from compound **81** using the hydrolysis-free synthesis of Kudale *et al*., which avoids the formation of 3-hydroxycoumarin which can occur under aqueous conditions.[79]

Compound **81** was first stirred with Boc-anhydride and DMAP in THF to afford an intermediate *N*-Boc imide, during which time the yellow suspension turned to a clearer brown solution. Hydrazine and methanol were then added to selectively hydrolyse the acetyl moieties whilst leaving the Boc group in place. Aqueous work-up followed by column chromatography over silica gel, eluting with 3:2 hexane/ethyl acetate gave the Boc-protected intermediate **114** as light yellow solid in 62% yield.

The Boc protecting group was then removed by stirring **114** in a mixture of TFA in chloroform for 6 hours. The product was purified by column chromatography over silica gel, eluting with 1:1 hexane/ethyl acetate, giving **115** as light orange-brown solid in 81% yield.

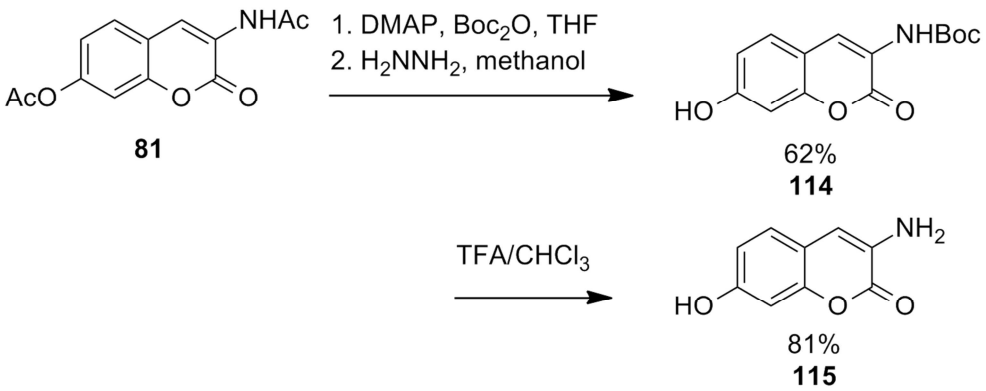

*Scheme 2.25: Synthesis of **115** from **81** using a hydrolysis-free method.*

The conjugation of the dye with the alkyl-halide functionalised calixarene to form the amine-linked coumarin (**116**) could now be attempted. First, a similar method to that used for the conjugation of NBD-chloride to an amino-calixarene[55] was attempted. Compounds **113** and **115** were stirred together at 70 °C in ethyl acetate, with pyridine added as a mild base. However, after 18 hours only the starting materials were present. It was reasoned that a stronger base may be required. However, due to the acidity of the phenolic proton on the coumarin dye, use of a stronger base could lead to deprotonation of this position and subsequent ether formation. Therefore it was decided to add a silyl protecting group to this phenol.

First, the same method used in the silylation of **78** was attempted. However, stirring **115** with LiHMDS gave an instant colour change to a brown solution. After stirring with TBDMSCl for 18 hours, followed by aqueous work up, no coumarin peaks could be discerned in the ^{1}H-NMR spectrum. It was reasoned that the pyrone portion of the coumarin could be acting as a Michael acceptor, giving rise to side-products.

The reaction was attempted again with a single equivalent of base added to a pre-mixed solution of **115** with TBDMSCl, so that the deprotonated phenol could immediately react with the silylating reagent rather than with the coumarin itself. This however gave no reaction. The same method with multiple equivalents of base gave a mixture of products.

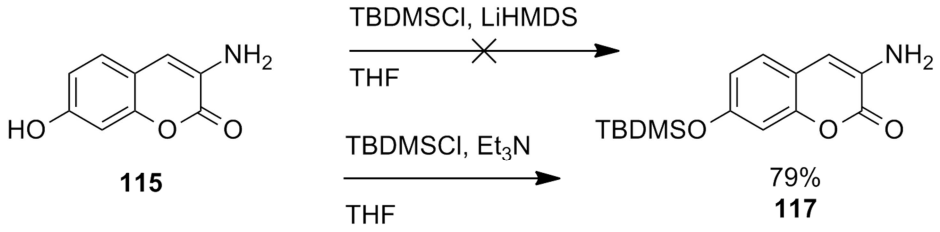

*Scheme 2.26: Silylation of **115** using TBDMSCl.*

Examination of the literature revealed that silylation of 7-hydroxy coumarin had been accomplished, but with milder bases such as triethylamine.[98] It could be that LiHMDS is simply too strong a base for this reaction and is deprotonating the aromatic amine, allowing additional side-reactions. The protection was attempted once more by adding triethylamine to a solution of **115** and TBDMSCl, this time giving no colour change. After stirring for 24 hours, aqueous work-up followed by purification by column chromatography over silica gel, eluting with 1:1 hexane/ethyl acetate, gave **117** as yellow needles in 79% yield.

Further attempts were now made at reacting the aminocoumarin with the calixarene core. A solution of **113** and **117** in acetone was heated to reflux with potassium carbonate for 18 hours, followed by removal of excess base by filtration and aqueous work-up. Only starting materials were recovered.

Finally, it was decided to attempt the alkylation using LiHMDS, based on the observation that this seemed to be able to deprotonate the amine of the coumarin and may therefore provide a stronger nucleophile. To a solution of **113** and **117** in THF was added LiHMDS and the mixture stirred for 18 hours. Once again, after aqueous work up there proved to have been no reaction.

It was concluded that the lone pair of the nitrogen on the coumarin is too delocalised over the ring system to be an effective nucleophile. At this stage it was decided to try an alternative approach.

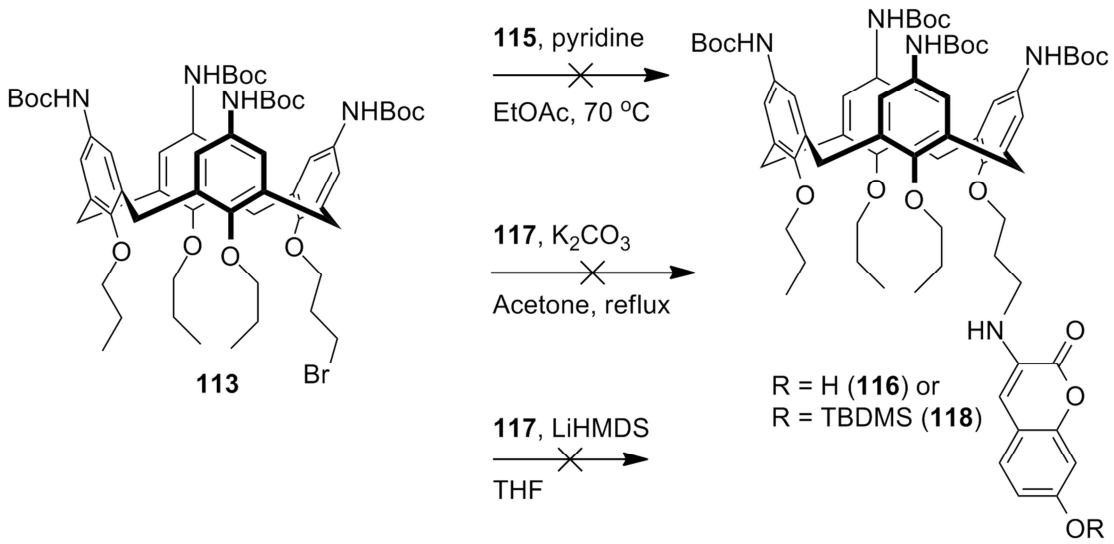

*Scheme 2.27: Conditions for the attempted synthesis of **116** or **118** by reaction of **113** with **115** or **117**.*

2.3.3.2 Amine-linked coumarin *via* amide

Although carrying out a simple S_N2 reaction with the aminocoumarin proved to be problematic, the formation of amide bonds with this type of compound has been accomplished.[99,100] This could be reacted with an acid moiety on the calixarene core and the intermediate amide bond could then be reduced to the desired secondary amine.

To form an end product with the correct length of linker, a C_3-acid was required on the calixarene. Initial attempts at installing this group were made using ethyl 3-bromopropanoate. Compound **77** was stirred with sodium hydride in DMF for 1 hour before adding the alkylating agent; at this stage, effervescence was observed. After 4 hours only starting material was present in the reaction mixture and the odour of ethyl acrylate could be detected. It was concluded that an acidic hydrogen adjacent to the carbonyl in the alkylating reagent was being removed by the sodium hydride, with evolution of hydrogen gas, followed by elimination of bromide to give ethyl acrylate.

To try to overcome this problem different reaction conditions were tested. Stirring with potassium carbonate as a weaker base in acetone gave no reaction, either at room temperature or at reflux. Using sodium hydride, but carrying out the addition of alkylating reagent at 0 °C, still gave evolution of hydrogen and likewise there was no ether formation.

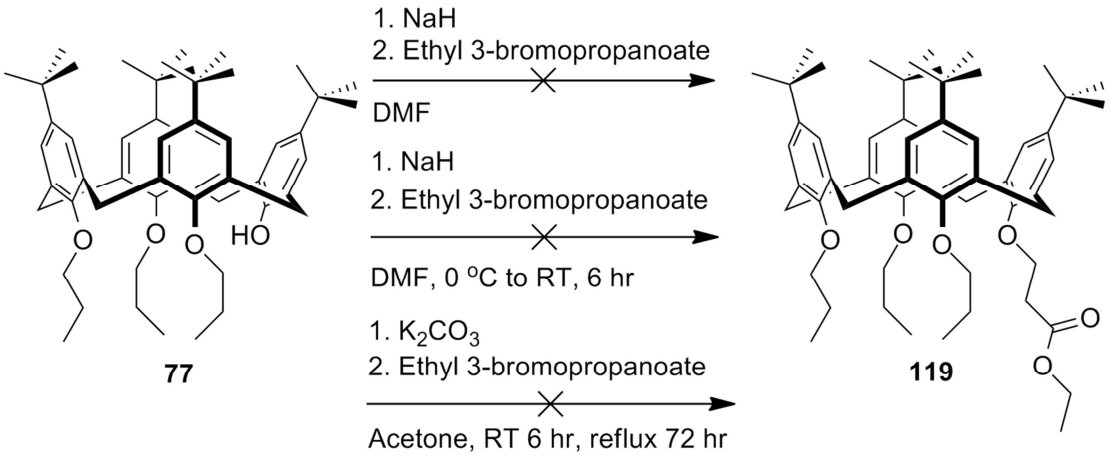

*Scheme 2.28: Attempted synthesis of **119** with ethyl 3-bromopropanoate.*

Since some of the base would be consumed in the deprotonation of the phenol, it was expected that some of the ethyl 3-bromopropanoate would remain intact to react with the calixarene. The lack of any reaction at all could be due to the phenoxide anion generated in the first stage of the reaction being sufficiently basic to deprotonate the alkylating agent rather than giving the desired S_N2 reaction.

Since ethyl 3-bromopropanoate could not be used directly, the possibility of carrying out a conjugate addition of the phenol on the calixarene to ethyl acrylate was investigated. Since stirring with base alone was insufficient, as demonstrated by the lack of product in the reactions where ethyl acrylate formed, it was decided to use a catalysed method.

Reaction of a number of different nucleophiles with ethyl acrylate was demonstrated by Yang *et al.*[101] using potassium fluoride supported on alumina, which could be prepared by stirring potassium fluoride with neutral alumina in water then drying thoroughly.[102] Compound **77** was then stirred with ethyl acrylate and 10 mol% of this catalyst in acetonitrile. After stirring for 3 hours, no reaction had occurred, raising concerns over the solubility of the calixarene in acetonitrile. Acetone was added to improve solubility and stirring continued for 18 hours. However after this time there was still only starting material present.

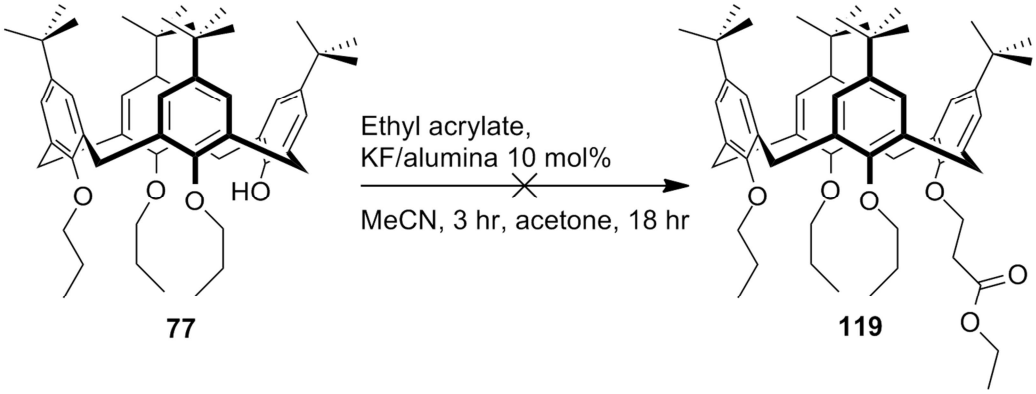

*Scheme 2.29: Attempted reaction of **77** with ethyl acrylate catalysed by KF/alumina.*

At this stage the strategy for creating two molecules with identical linkers was reconsidered. The problems surrounding the use of a 3-carbon acid could be easily circumvented by attaching a 4-carbon acid to the calixarene instead; the extra methylene between the α-position and the halide leaving group would reduce the acidity of the α-hydrogen and make elimination less favourable. In order to have an analogue of this with a different dye, the original NBDCalAm could be resynthesized using a 4-carbon linker *via* commercially available 4-bromobutylphthalimide.

2.3.3.2.1 Synthesis of NBD-conjugate with 4-carbon linker

The same strategy was used as for the synthesis of the original NBDCalAm.[55] The primary aliphatic amine required for the conjugation of the NBD dye would be installed using a phthalimide that could later be deprotected with hydrazine.

Compound **77** was stirred with sodium hydride in DMF for 30 minutes, followed by 4-bromobutylphthalimide for 24 hours. After removal of solvent under reduced

pressure and aqueous workup, the crude residue was triturated with hot methanol, filtered, and washed several times with methanol. Compound **120** was obtained as white solid in 51% yield.

The correct product is easily confirmed by the ^{1}H-NMR spectrum (see Figure 2.30), which shows a characteristic pair of doublet of doublets for the phthalimide group around 7.8 ppm. The peaks arising from the propyl and butyl chains can be differentiated using a 2D-COSY spectrum which shows an interaction between the triplet at 3.88 ppm with the multiplet at 2.08 ppm, which in turn interacts with the multiplet at 1.08 ppm. This latter peak has a further interaction within the cluster of peaks at 3.81 ppm. These must correspond to the butyl peaks, whilst the remainder of the cluster at 3.81 ppm, along with the multiplet at 2.00 ppm and the overlapping triplets at 0.97 ppm must correspond to the propyl chains.

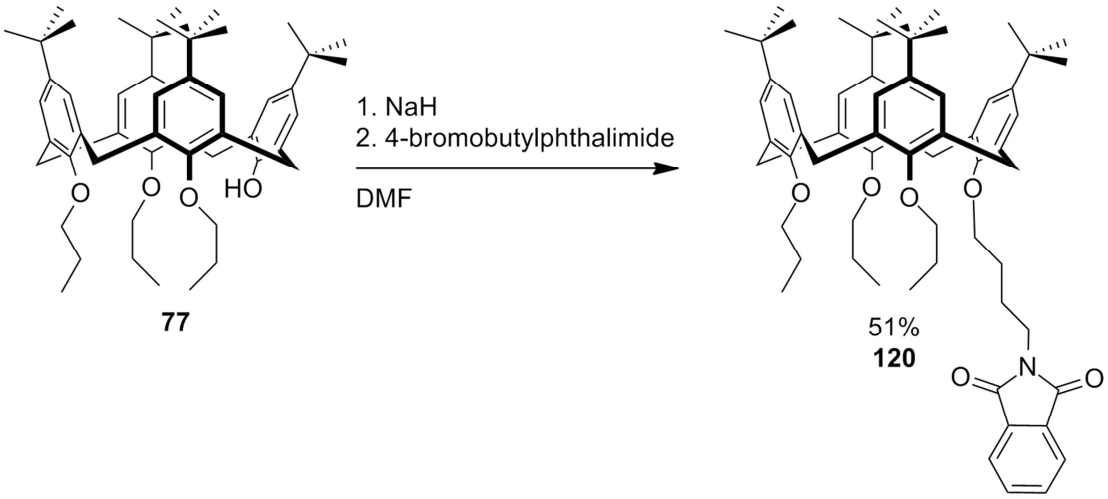

*Scheme 2.30: Synthesis of compound **120**.*

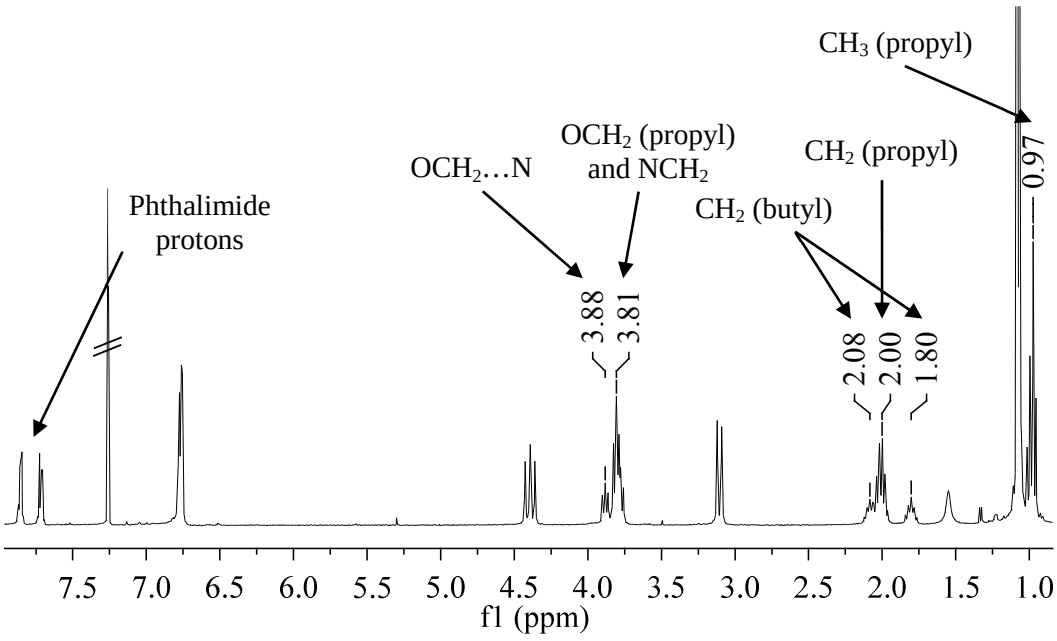

*Figure 2.30: ^{1}H-NMR spectrum of **120**.*

Elucidation of which peak corresponds to which methylene in the butyl chain requires a 2D-HSQC spectrum (see Figure 2.31). Examination of the peaks around 3.8 ppm reveals that within the cluster at 3.81 ppm there is an interaction with a secondary carbon that has a much lower chemical shift compared with the other carbon peaks that have interactions with this cluster. This suggests that this carbon is adjacent to a nitrogen, whereas the others around 75 ppm are adjacent to oxygen. This identifies the peak at 3.88 ppm as the methylene adjacent to the oxygen in the butyl chain, which in turn allows the differentiation of the peaks 2.08 and 1.80 ppm as the centre two methylene groups closest to the oxygen and the nitrogen, respectively.

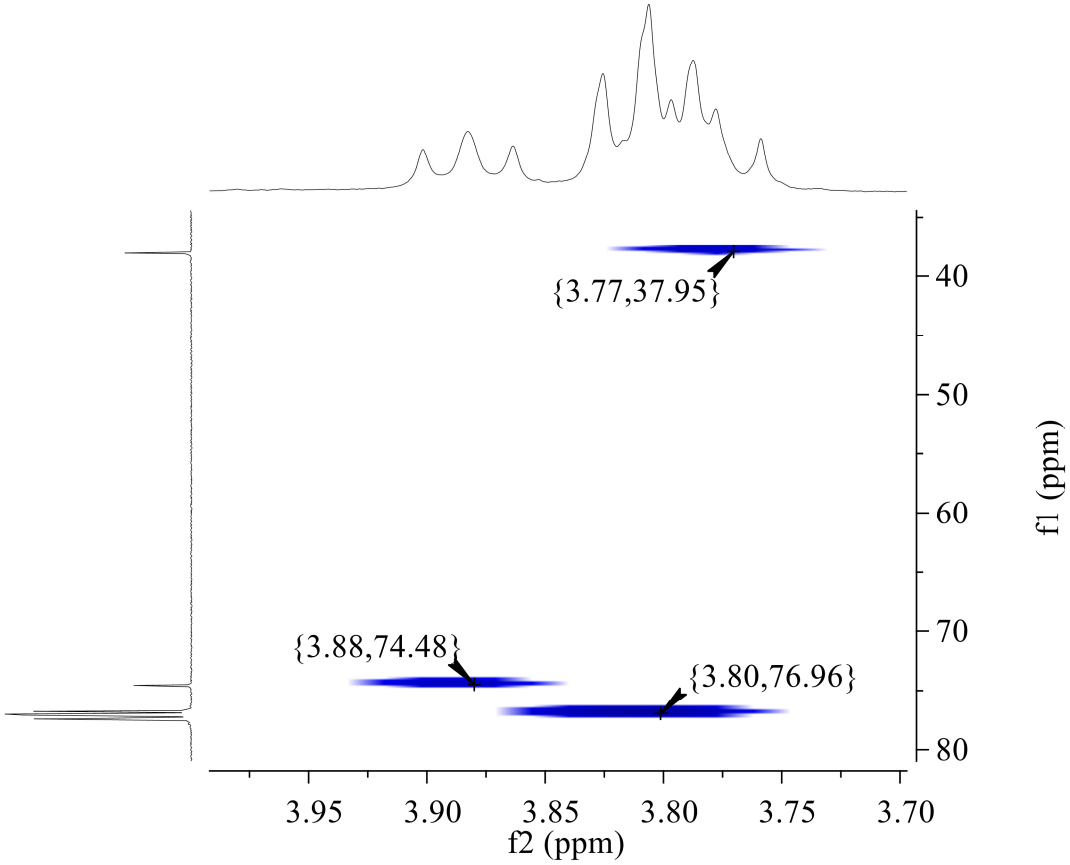

*Figure 2.31: 2D-HSQC spectrum of **120**.*

Conversion to the Boc-protected amine was carried out as previously. Compound **120** was stirred with 100% nitric acid and glacial acetic acid in DCM for 4 hours before quenching with water. Aqueous work-up followed by trituration with methanol gave sufficiently pure tetra-nitrated product **121** as light-yellow solid in 87% yield.

This product was heated to reflux in ethanol with tin chloride for 48 hours, followed by aqueous work-up with sodium hydroxide. The tetra-amine product **122** was isolated as brown glass in 88% yield

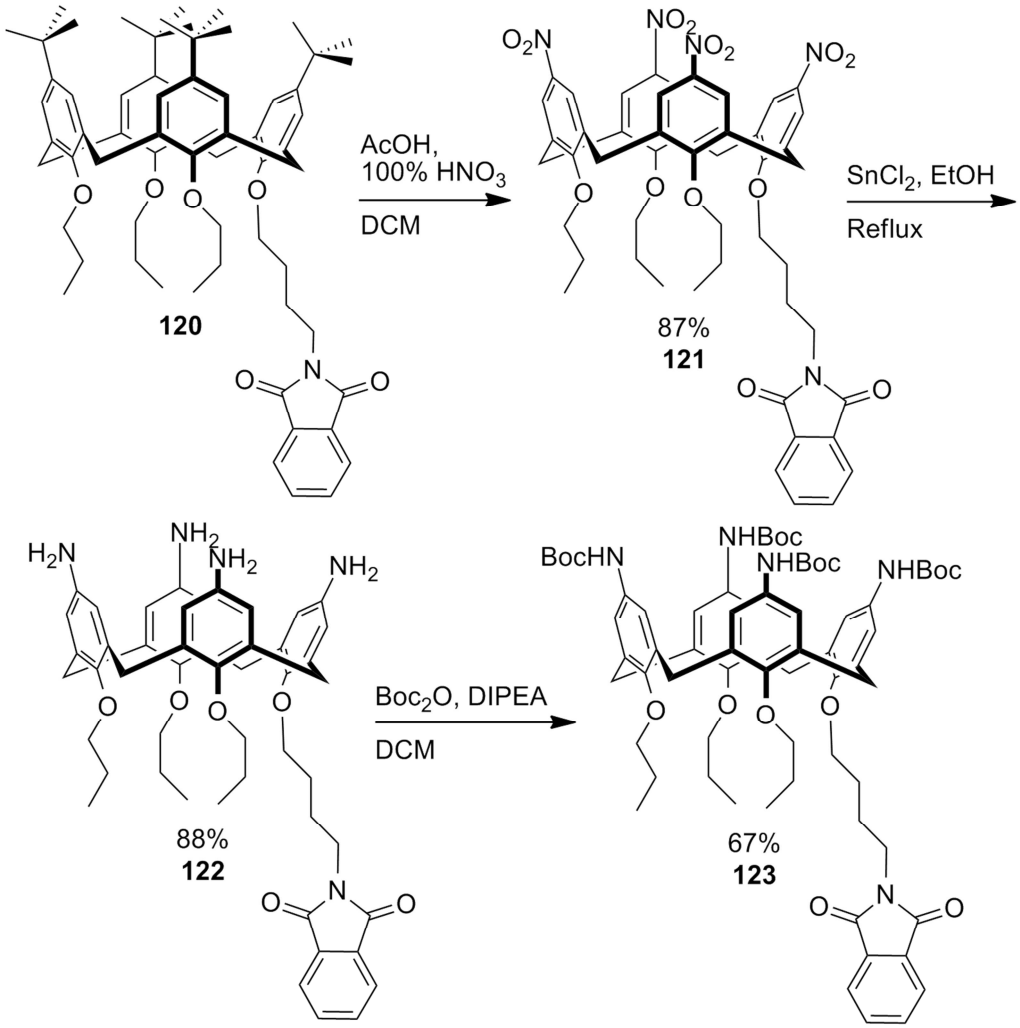

*Scheme 2.31: Conversion of **120** to **123** via nitration, reduction and Boc protection.*

Compound **122** was stirred with Boc-anhydride and DIPEA in DCM for 24 hours. The product was purified by column chromatography over silica gel, eluting with 19:1 DCM/ethyl acetate, giving the protected tetra-amine **123** as off-white glass in 67% yield.

The required lower-rim amine was next unmasked by cleaving the phthalimide. Compound **123** was stirred with hydrazine in ethanol for 18 hours. The resulting precipitate was removed by filtration and the solvent removed from the filtrate under reduced pressure. Due to the poor solubility of the product in organic solvent, aqueous work-up was avoided by precipitating the product from minimum methanol with water, filtering and drying under vacuum. Some of the solid was too fine to separate from the solvent by filtration so was salvaged by extracting from water with 10% methanol in ethyl acetate. The free-amine (**124)** was isolated as off-white solid in 72% yield and was carried forward as the crude product.

This product could now be reacted with the dye *via* a nucleophilic aromatic substitution reaction. Compound **124** was stirred with sodium hydrogencarbonate in

acetonitrile and a solution of NBDCl in acetonitrile was added dropwise, resulting in the formation of an intense brown-orange colour. The mixture was heated to 60 °C for 4 hours. Aqueous work-up followed by column chromatography over silica gel, eluting with 7:3 hexane/DCM, afforded the dye-conjugate **(125)** as a bright-orange solid in 53% yield.

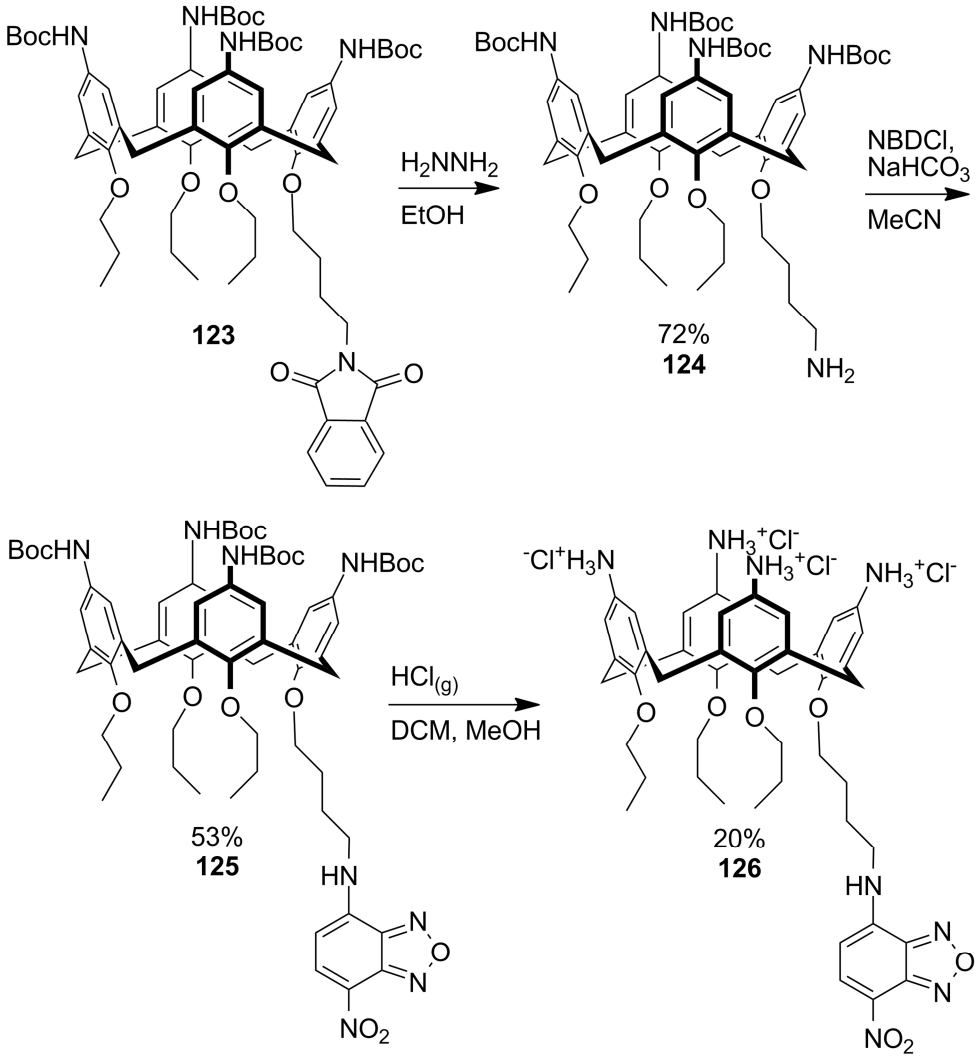

*Scheme 2.32: Synthesis of **126** from **123** via phthalimide cleavage, S_EAr reaction and removal of Boc groups.*

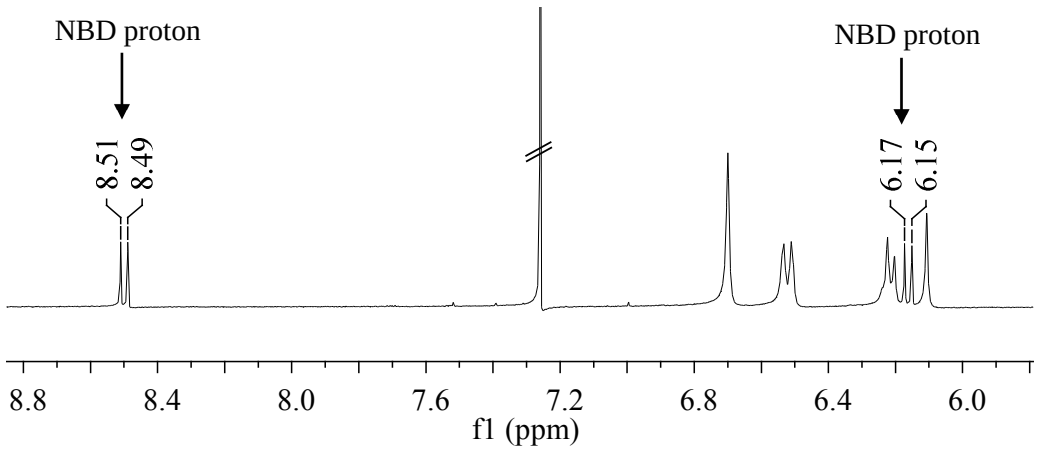

*Figure 2.32: ^{1}H-NMR spectrum of **125**.*

The ^{1}H-NMR spectrum of **125** (see Figure 2.32) confirms the incorporation of the NBD dye. At 8.50 ppm there is a doublet arising from one of the two aromatic protons on the dye. The 2D-COSY spectrum shows that the second doublet is at 6.16 ppm. The former, being more deshielded, must be the one adjacent to the nitro group.

Finally, the water soluble tetra-amine salt was formed by bubbling HCl gas through a solution of **125** in DCM for 10 minutes, followed by addition of methanol to dissolve the resulting precipitate and continuing the reaction for a further 20 minutes. The product was purified by reverse-phase column chromatography over C18, eluting with a gradient of 0-100% methanol in 60 mM aqueous HCl. Compound **126** was isolated as a bright-orange solid. Due to losses during purification, the final yield was just 20%.

2.3.3.2.2 Synthesis of amide-linked coumarin

The required butanoic acid group on the calixarene was put in place using ethyl 4-bromobutanoate. This ester can be hydrolysed once the upper rim has been functionalised with Boc-protected amines to expose the acid for the amide coupling. The synthesis of a *para*-nitro functionalised calixarene with a single C_4-acid on the lower rim has been previously reported.[103]

Compound **77** was stirred with sodium hydride in DMF for 30 minutes, followed by addition of ethyl 4-bromobutanoate. After 18 hours, the solvent was removed under reduced pressure. Aqueous work-up followed by trituration with methanol gave **127** as white powder in 68% yield.

This was then converted to the Boc-protected amine in the same manner as before. Compound **127** was stirred with 100% nitric acid and glacial acetic acid in DCM for 4 hours before quenching with water. Following aqueous work-up, the residue was triturated with methanol to give **128** as light-orange powder in 92% yield.

Compound **128** was heated to reflux in ethanol with tin chloride for 48 hours. After aqueous work-up with sodium hydroxide, the tetra-amine product **129** was isolated as light-brown solid in 79% yield.

Finally, **129** was stirred with Boc anhydride and DIPEA in DCM for 72 hours. Purification by column chromatography over silica gel, eluting with 19:1 DCM/ethyl acetate gave **130** as off-white glass in 78% yield.

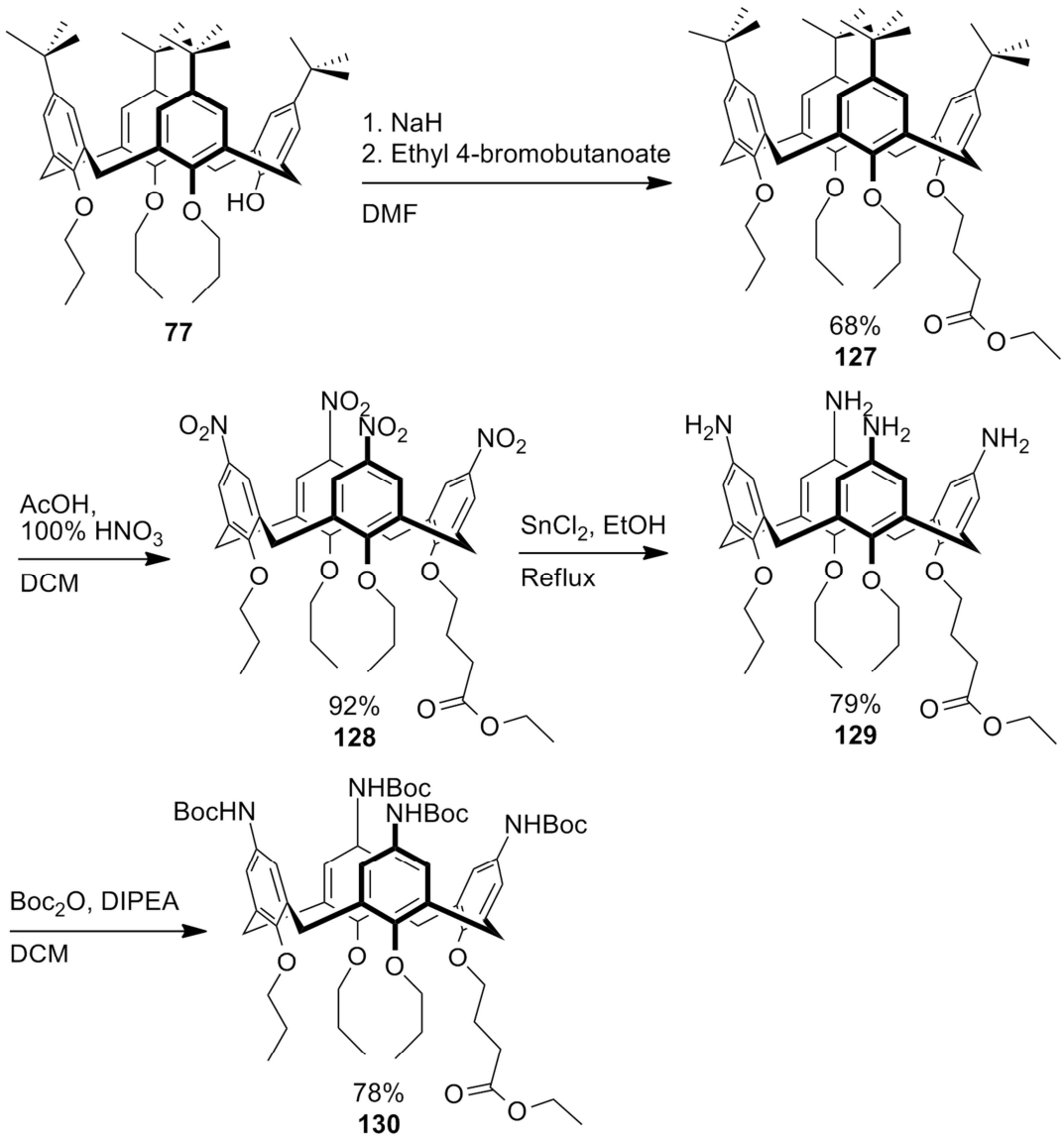

*Scheme 2.33: Conversion of **77** to **130** via alkylation, nitration, reduction and Boc protection.*

The ester that was masking the acid moiety could now be cleaved by base-catalysed hydrolysis. Although this has been accomplished on calixarene-based molecules using sodium hydroxide,[104] in this case a satisfactory solvent system that balanced the solubility of the sodium hydroxide and the calixarene could not be found at room temperature. Therefore it was decided to use tetramethylammonium hydroxide, which has been shown to be effective for this transformation and which can be used in organic solvent alone.[105]

To a solution of compound **130** in THF was added tetramethylammonium hydroxide solution in methanol and the mixture stirred for 6 hours at room temperature. After checking that no more starting material was present by TLC, the mixture was acidified with dilute HCl and extracted with ethyl acetate. Compound **131** was isolated as light-yellow glass in 96% yield.

With the free acid now present on the calixarene, the amide bond could be formed to the coumarin dye according to the literature.[99] Calixarene **131** was stirred with coumarin **115** and EDCI, using 30% pyridine in DCM as the solvent, for 18 hours before removing the solvent under reduced pressure. Dilute HCl was added and extraction attempted with ethyl acetate; this gave an emulsion that could only be broken by slowly adding methanol until two layers resolved. The solid isolated from the organic layer was purified by column chromatography over silica gel, eluting with 3:2 hexane/ethyl acetate, giving the amide-linked coumarin **132** as off-white solid in 49% yield.

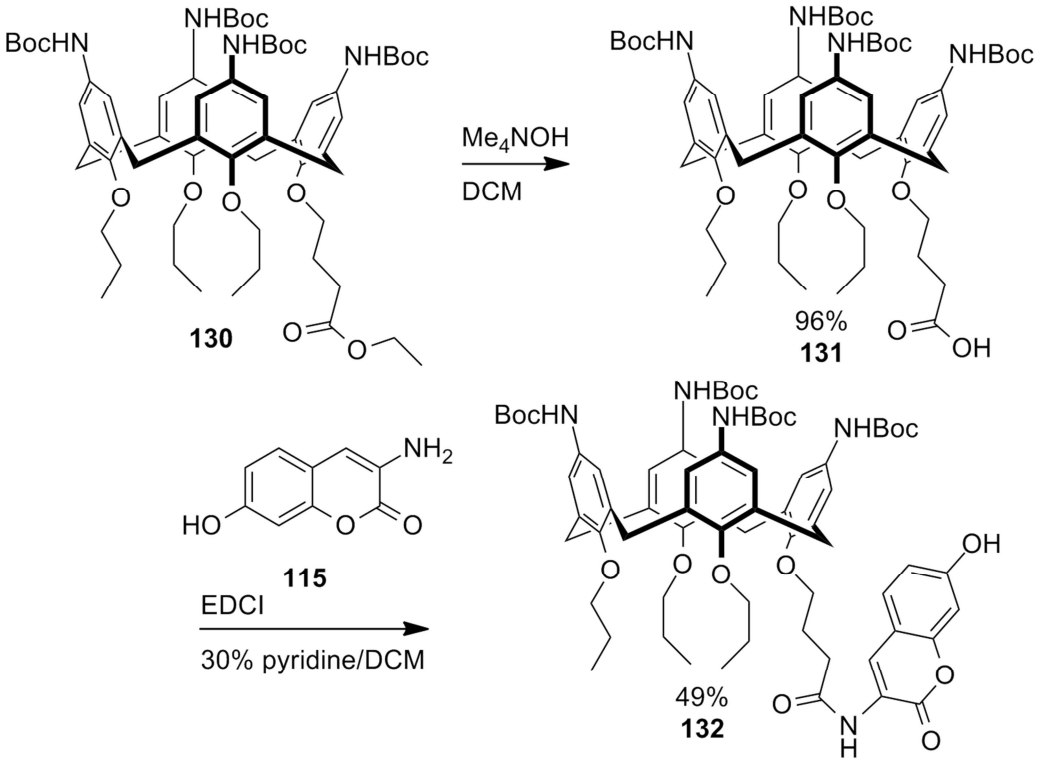

*Scheme 2.34: Synthesis of **132** from **130** via ester hydrolysis and amide bond formation.*

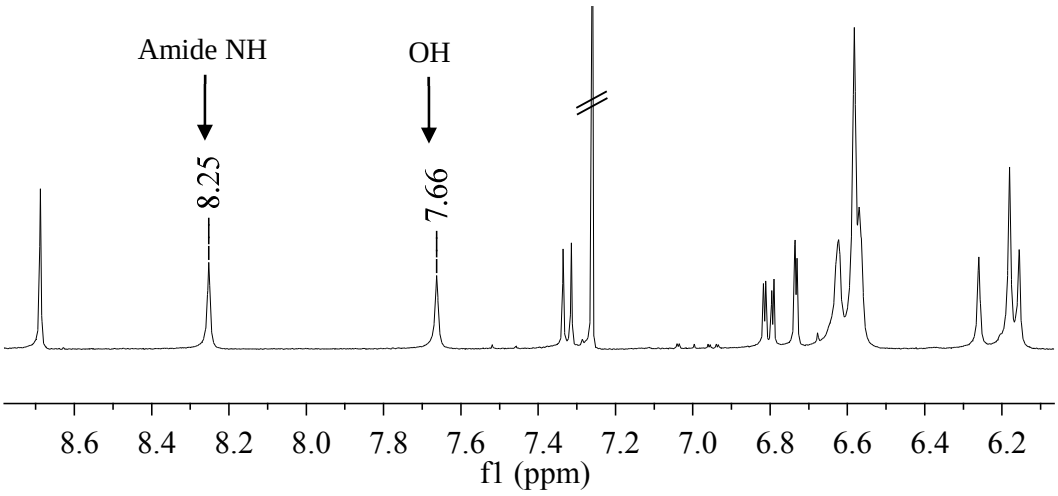

*Figure 2.33: ^{1}H-NMR spectrum of **132**.*

The ^{1}H-NMR spectrum (see Figure 2.33) confirms that the coumarin is present and joined by an amide bond. The characteristic peaks of the coumarin can be seen: a downfield singlet around 8.7 ppm, a doublet around 7.3 ppm, and a doublet of doublets next to a further doublet around 6.8 ppm. Two peaks are present at 8.25 and 7.66 ppm that give rise to no peaks in the 2D-HSQC, suggesting that these are the NH of the amide bond and the OH of the coumarin. According to the 2D-HMBC spectrum, the proton peak at 8.25 ppm and the proton peaks corresponding to the butyl chain share a long-range interaction with a highly deshielded carbon. This suggests that this carbon is the carbonyl of the amide and so the proton peak at 8.25 ppm would be the NH of the amide. By elimination, the peak at 7.66 ppm must be the OH of the coumarin.

2.3.3.2.3 Reduction of amide-linked coumarin

The reduction of an amide to an amine could theoretically be accomplished using a strong nucleophilic reducing agent such as lithium aluminium hydride. However, amides are more difficult to reduce in this way than esters due to the increased electron density at the carbonyl; therefore in the presence of an ester, it will be the latter that will be reduced first. The presence of the lactone in the coumarin dye precludes the use of such a method in this case.

Multiple methods exist for the selective reduction of amides in the presence of other functional groups, including esters. These include transition metal catalysed hydrosilation,[106] treatment with tetrabutylammonium hydride,[107] conversion to a thioamide prior to reduction[108] and reduction with borane.[109] The latter selectively delivers hydride to amide bonds in preference to esters by forming a coordination complex to the more electron-rich amide.[110] Borane reduction has been applied to a coumarin, albeit for the reduction of a carboxylic acid instead of an amide, without reducing the lactone.[111] For this reason, this reagent was selected for the reduction of the coumarin-amide.

A solution of **132** in dry THF was cooled to 0 °C and stirred under argon whilst borane-THF complex was added. This was then heated to 60 °C for 4 hours before quenching with methanol. At this stage the ^{1}H-NMR spectrum showed a complex mixture of products; this was also the case when the reaction was allowed to proceed at room temperature for 18 hours.

A mixture of products could arise from excess borane forming a complex with the carbamates on the upper rim. A mild method for the cleavage of borane adducts was

found which utilises palladium on carbon or Raney nickel as a catalyst for methanolysis, which can otherwise require a very long period of stirring in methanol.[112] The crude product was therefore stirred in methanol with 5 mol% of Raney nickel for 18 hours, followed by removal of the catalyst by filtration. The borate now present in the product was removed by azeotroping several times with methanol. However, the light-yellow glass that was obtained still proved to be a complex mixture by ^{1}H-NMR.

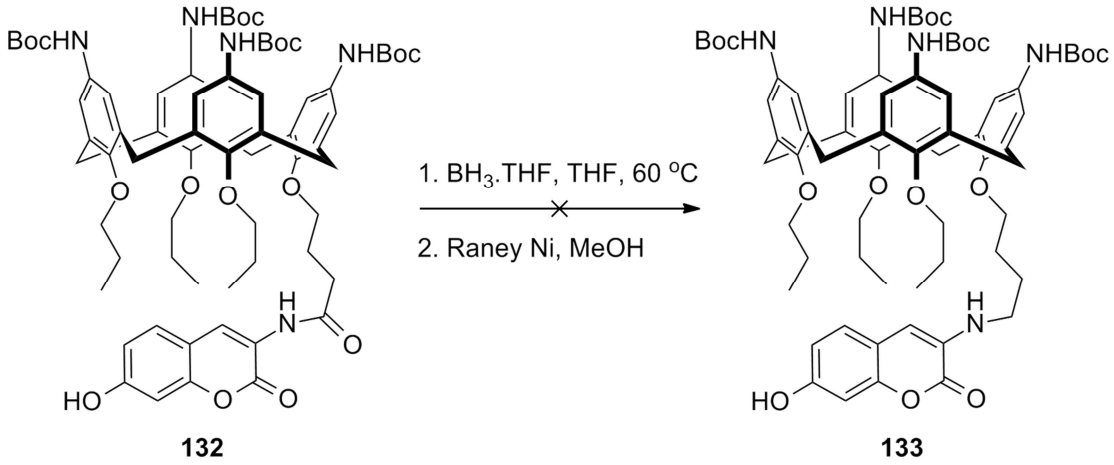

*Scheme 2.35: Attempted synthesis of **133** by reduction of **132**.*

Although examples are present in the literature of amide reductions being carried out in this way in the presence of Boc protecting groups,[113] it would appear in this case that the carbamates are not stable to these conditions. However, if these were removed then the resulting free amines would necessitate the use of a greater excess of borane, due to their propensity to form adducts with the reagent, and subsequently would poison the catalyst used to effect methanolysis. An alternative method of reduction would therefore be more suitable.

However, at this stage due to time constraints it was decided to proceed with the removal of the Boc protecting groups from **132** to provide a cationic molecule with an amide-linked coumarin. The cell-uptake properties could then be investigated to provide a comparison with the original triazole-linked coumarin.

2.3.3.2.4 Deprotection of amide-linked coumarin conjugate

Removal of the Boc protecting groups from **132** was initially attempted using the same procedure as in section 2.3.1.8. $HCl_{(g)}$ was bubbled through a solution of **132** in DCM for 10 minutes, followed by addition of methanol and stirring for a further 5 minutes. However, the solid obtained was a mixture of two distinct products by ^{1}H-NMR; when the reaction was continued for a further 15 minutes, the minor component increased in concentration. This led to the conclusion that the deprotection conditions

were also cleaving the amide bond to the coumarin.

A different deprotection protocol was therefore attempted, following the method used in the synthesis of the aminocoumarin.[79] Compound **132** was stirred in a mixture of TFA and DCM for 2 hours. This time a single product was obtained by ^{1}H-NMR. The product was then purified by reversed-phase column chromatography over C18, eluting with a gradient of 0-100% methanol in 60 mM aqueous HCl. This purification also converted the product to the hydrochloride salt and confirmed that the single product had not arisen from complete cleavage of the coumarin. Compound **134** was isolated as pale-orange solid in 88% yield.

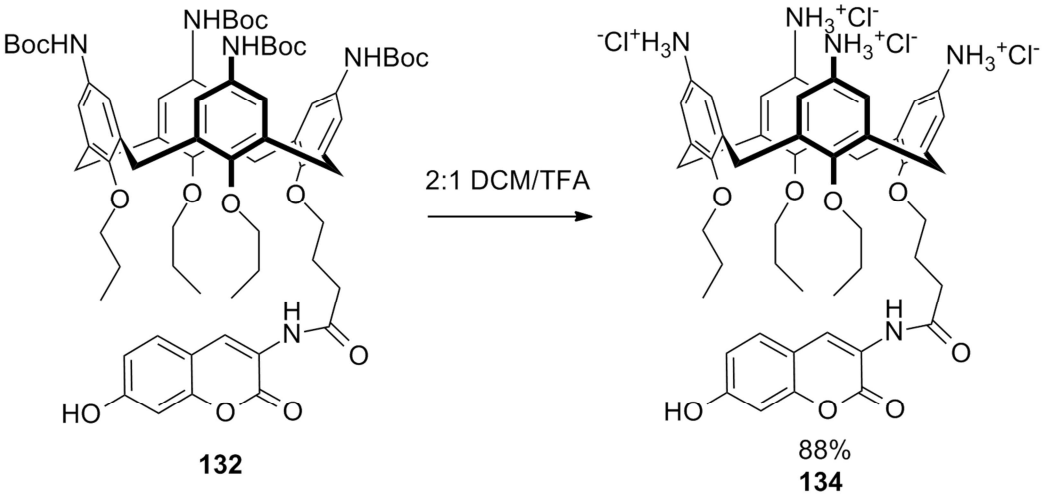

132 **134**

*Scheme 2.36: Boc-deprotection of **132** to give **134**.*

2.3.4 Biological analysis

The collection of compounds taken through to biological analysis are summarised in Figure 2.34. These are the triazole-linked coumarin-appended calixarenes, **87** (non-cationic control), **94** (aromatic amine functionalised), **97** (glycine functionalised) and **109** (guanidine functionalised); triazole-linked pyrene- (**95**) and anthracene-appended (**96**) calixarenes; NBD-appended calixarene with C_4 linker (**126**); and amide-linked coumarin-appended calixarene (**134**).

2.3.4.1 Toxicity assays

In order to assess the cell uptake and localisation properties of these compounds, the effect of the compounds on the viability of live cells first needed to be determined. Cell proliferation can be measured using a colorimetric assay by monitoring conversion of a tetrazolium dye to its formazan product by intracellular enzyme activity. For example, MTS (3-(4,5-dimethylthiazol-2-yl)-5-(3-carboxymethoxy-phenyl)-2-(4-sulfophenyl)-2H-tetrazolium) can be used in conjunction with phenazine

methosulphate (PMS). The activity of oxidoreductase enzymes, which is indicative of live cells, converts MTS to its formazan product to give an absorbance increase at 490-500 nm that is proportional to the number of live cells present.[114]

Selected cell-lines were incubated with increasing concentrations of the compounds to be tested for 72 hours before carrying out the MTS assays. Compounds **94**, **95**, **96**, **97**, **126** and **134** were compared to a control where only sterile water was added. Due to their poor solubility in water, compounds **87** and **109** were dissolved in DMSO and therefore this was used as the control.

The results of the MTS assays in THP-1 cells are shown in Figure 2.35 and are representative of the other cell lines tested.

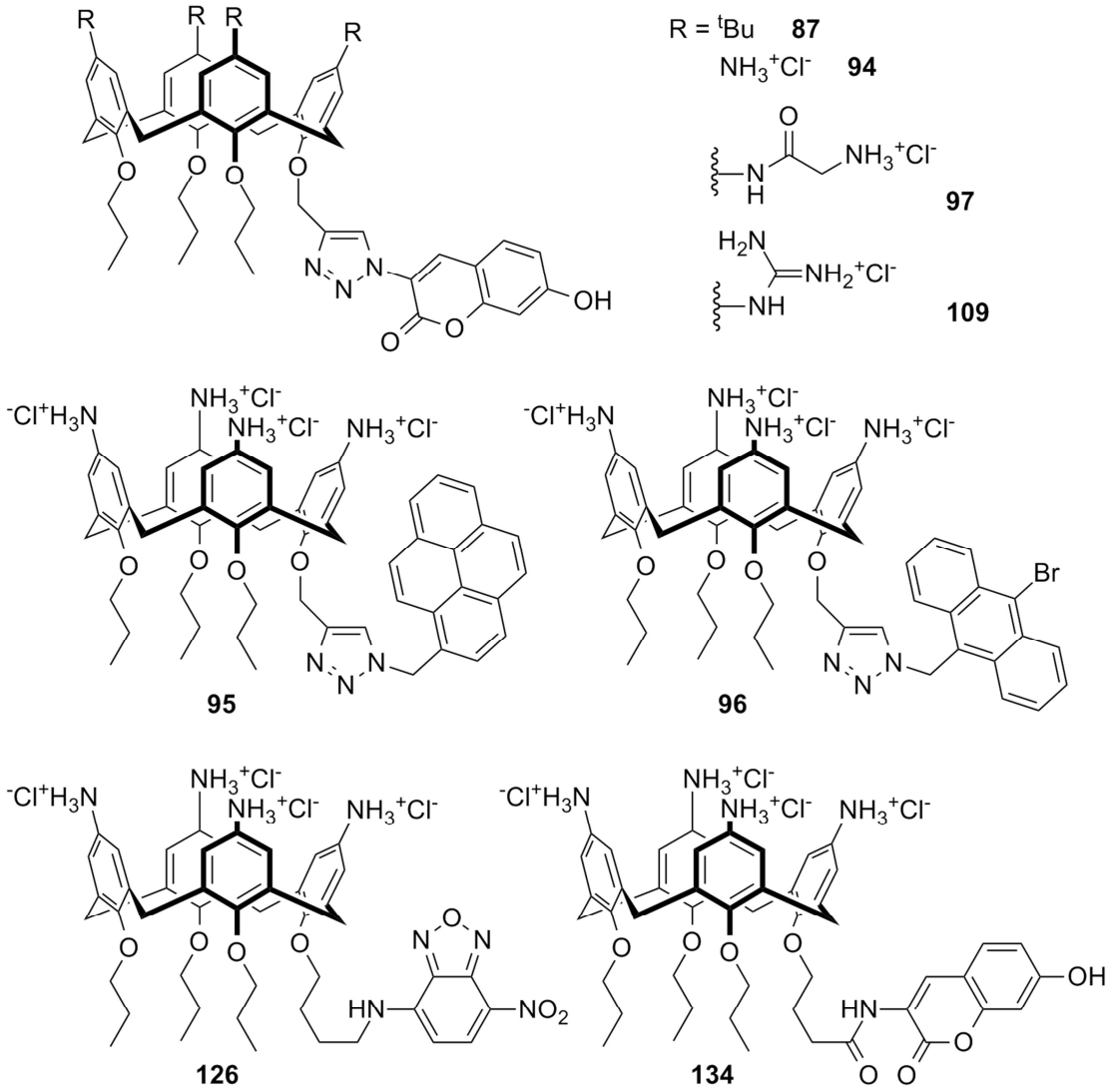

Figure 2.34: Summary of compounds subjected to in vivo testing.

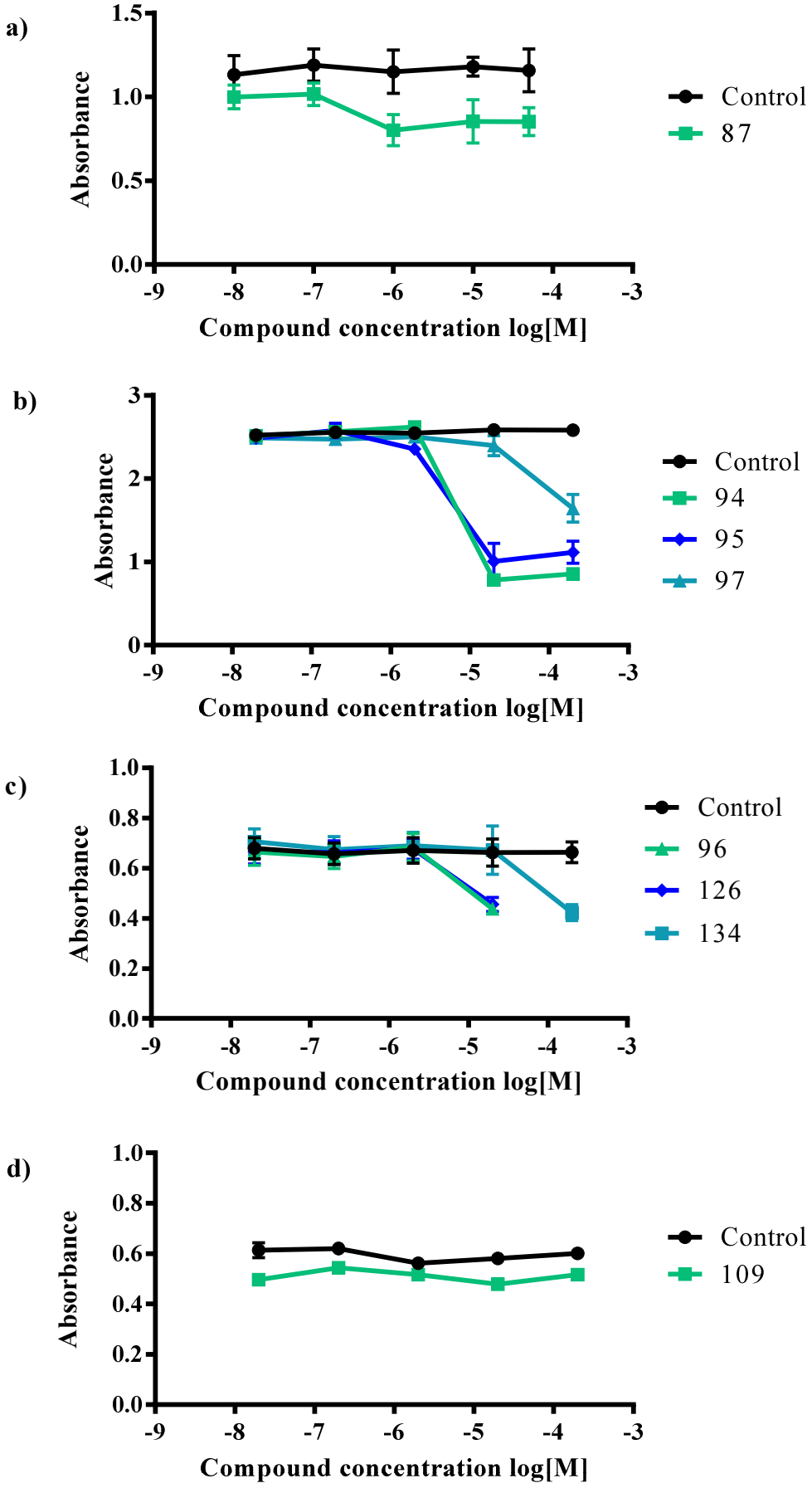

*Figure 2.35: MTS assays performed on THP-1 cells. a) Compound **87**; b) Compounds **94**, **95** and **97**; c) Compounds **96**, **126** and **134**; d) Compound **109**.*

In comparison with NBDCalAm,[55] which was only toxic at high concentrations (around 100 mM), most of the compounds began to inhibit cell proliferation at much lower concentrations (of the order of 10^{-6} to 10^{-5} M) . One explanation for this could be the change in dye molecule: compounds **94**, **95** and **96**, with a coumarin, pyrene and anthracene dye respectively, all began to display cytotoxic effects at around 10^{-6} M. However, the dye molecule clearly is not the only factor, as exemplified by the lower apparent toxicity of compound **97**, which in particular displayed no toxicity towards HeLa cells at the concentrations tested, and the lack of dose-dependent behaviour of compounds **87** and **109** at the concentrations used. These all bear a coumarin moiety, but the difference in functionality in the upper rim compared with the aromatic amine of **94** seems to influence the toxicity; compound **87** features only *tert*-butyl groups, whilst **97** and **109** are functionalised with aliphatic amine and aromatic guanidine groups, respectively.

The linker could also be a factor, since compounds **94**, **95** and **96** all have triazole-linked dyes, compared with the amine-linked dye of NBDCalAm. Compound **134**, which has an amide-linked coumarin, in comparison with **94**, begins to inhibit cell proliferation at a higher concentration in THP-1 cells (of the order of 10^{-5} M compared with 10^{-6} M), although this effect was not observed with HeLa cells. The sensitivity to the linker is particularly apparent in the case of **126**, which provides an interesting comparison with NBDCalAm. Although the only structural difference between these two compounds is an increase in the length of linker from C_3 to C_4, **126** displays cytotoxic effects at much lower concentrations (of the order of 10^{-6} M). The increased length of linker may allow the calixarene to form interactions that could not be made by NBDCalAm, resulting in increased impact on cell viability.

It is important to note that full characterisation of the cytotoxicity of these compounds would require collection of data at a larger number of concentrations, in order to determine IC_{50} values. Nevertheless, this data does reveal that at sub-micromolar concentrations the cells remained viable with no significant change in morphology (see section 2.3.4.2). Investigation of cell uptake and localisation could therefore be carried out with low concentrations of the compounds.

2.3.4.2 Cellular uptake

The ability of the tested compounds to penetrate living cells was subsequently tested. CHO cells were cultured on a glass coverslip followed by addition of the selected fluorescent compound and incubation for time intervals up to 72 hours. After washing to remove excess compound, these coverslips could directly be mounted onto glass slides and examined by fluorescence microscopy.

The non-cationic control (**87**) did not exhibit observable uptake into cells. This could be due to the particularly poor water solubility of this calixarene. Unexpectedly, of the seven cationic compounds tested, two of the compounds did not exhibit observable uptake. After incubation with the pyrene conjugate (**95**) for 48 hours, fluorescence could only be observed inside of the cells by increasing the exposure time of the camera; however, under the same conditions the control, to which only water had been added, also displayed intracellular fluorescence (see Figure 2.36). Therefore, the possibility that the observed fluorescence for **95** was due to background fluorescence from the cells could not be ruled out. This led to the investigation of anthracene as an alternative hydrophobic dye for investigation of dye effects. However, the anthracene conjugate (**96**) likewise did not give rise to any intracellular fluorescence, even after 48 hours.

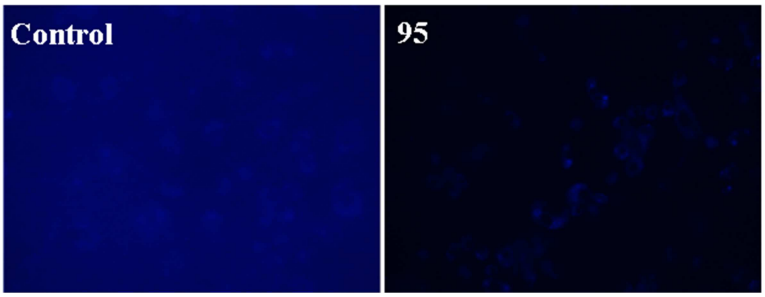

*Figure 2.36: Cellular uptake of **95** after 48 hours of incubation with CHO cells.*

The lack of increase in intracellular fluorescence relative to the controls for both compounds **95** and **96** could be due to either lack of uptake or poor fluorescence properties inside of cells. Given that Kumar *et al.*[59] demonstrated intracellular fluorescence of a non-cationic tetra-pyrene appended calixarene, it is unlikely that a single pyrene unit would prevent cellular uptake compared to the coumarin-appended calixarenes (*vide infra*). However, it is possible that the lack of π-π stacking interactions that occur with multiple pyrene units[59] results in insufficient intensity of emission to visualise in living cells. A similar principle could also apply to the anthracene-appended calixarene. Compounds **95** and **96** are therefore unsuitable for cellular imaging applications and were not investigated further.

By contrast, the coumarin-appended tetra-amino calixarene (**94**) showed clear uptake into CHO cells after 1 hour (see Figure 2.37). The initially diffuse intracellular fluorescence became more punctate after 24 hours and even more so from 48-72 hours. This suggests gradual sequestration of the compound into intracellular compartments.

Compound **97**, the tetra-glycine coumarin-appended derivative, exhibited slower cellular uptake than **94** (see Figure 2.38). At 1 hour, few cells showed intracellular fluorescence and at a lower intensity compared with **94**. This increased over the examined time intervals, but the uptake between different cells in the same culture remained inconsistent. From 24 hours onwards those cells that had taken up **97** began to show punctate rather than diffuse patterns of fluorescence. From 48 to 72 hours most cells were displaying uptake of the compound.

The guanidinium derivative (**109**) also seemed to be taken up more slowly into cells (see Figure 2.39). Interestingly, from 1-4 hours fluorescence was only visible in globular structures that appeared to be dying or dead cells. Since the MTS assays for this compound indicated low toxicity relative to the DMSO control, this suggests accumulation of **109** in such cells rather than cytotoxic action. From 24 hours onwards an increasing number of live cells exhibited intense intracellular fluorescence, with a more punctate pattern as time went on.

The different dynamics of **94**, **97**, **109** demonstrates the importance of upper-rim functionalisation in cellular uptake. Although the previous work on cell penetrating peptides suggests that guanidine groups give superior uptake to simple amines (see section 2.1.2.1.2), in this case the guanidine functionalised calixarene (**109**) did not give more rapid uptake compared with **94** or **97** as was expected. However, the aromatic guanidine groups of **109** may give different dynamics to the aliphatic guanidines of poly-arginine cell-penetrating peptides.

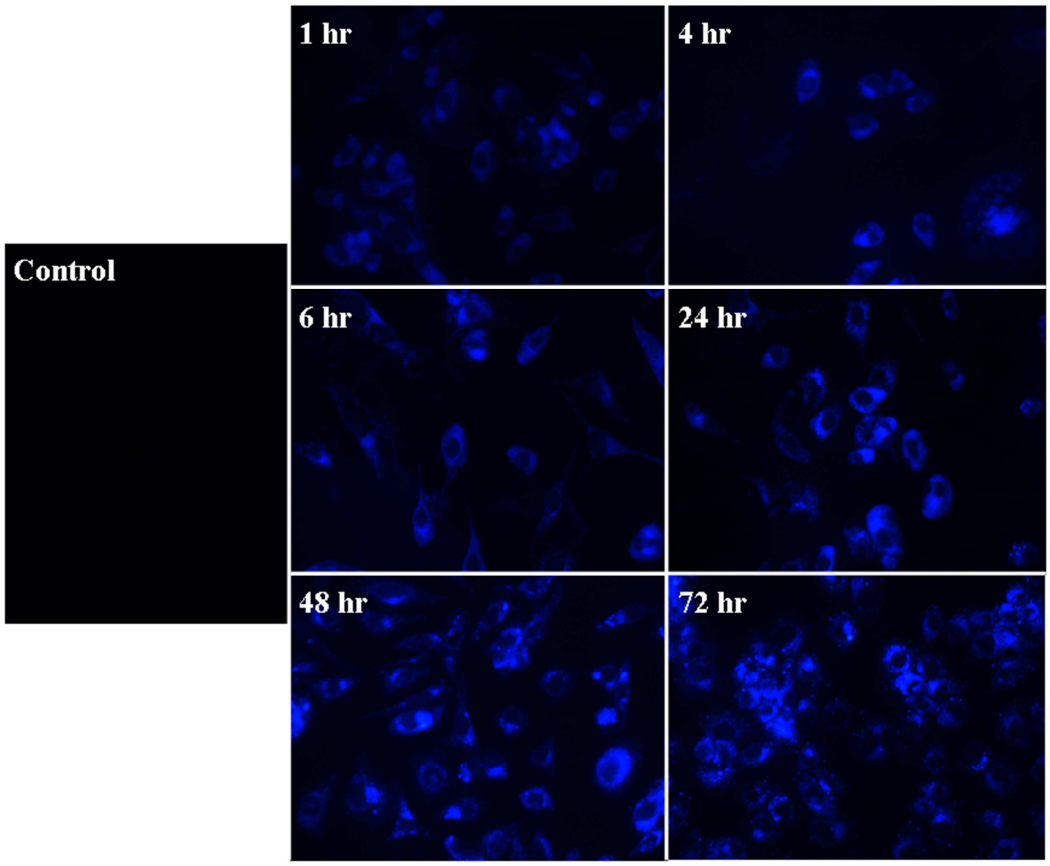

*Figure 2.37: Cellular uptake of **94** at given time intervals after addition of compound to CHO cells.*

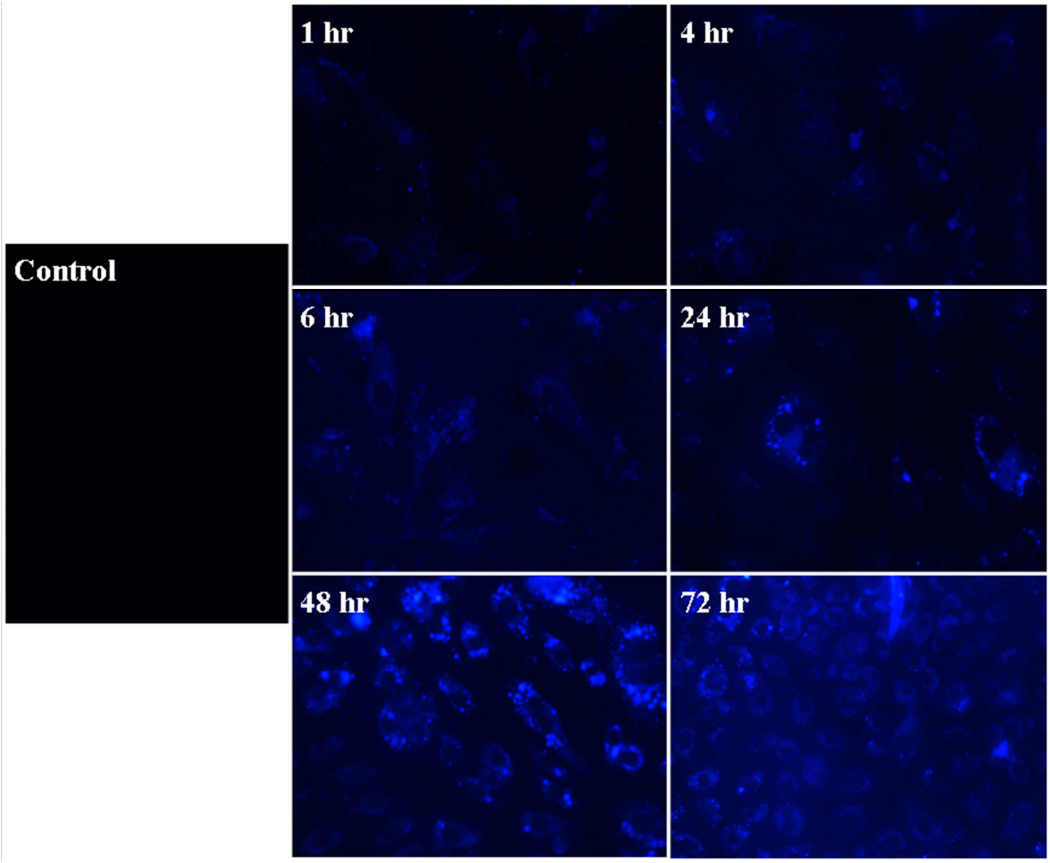

*Figure 2.38: Cellular uptake of **97** at given time intervals after addition of compound to CHO cells.*

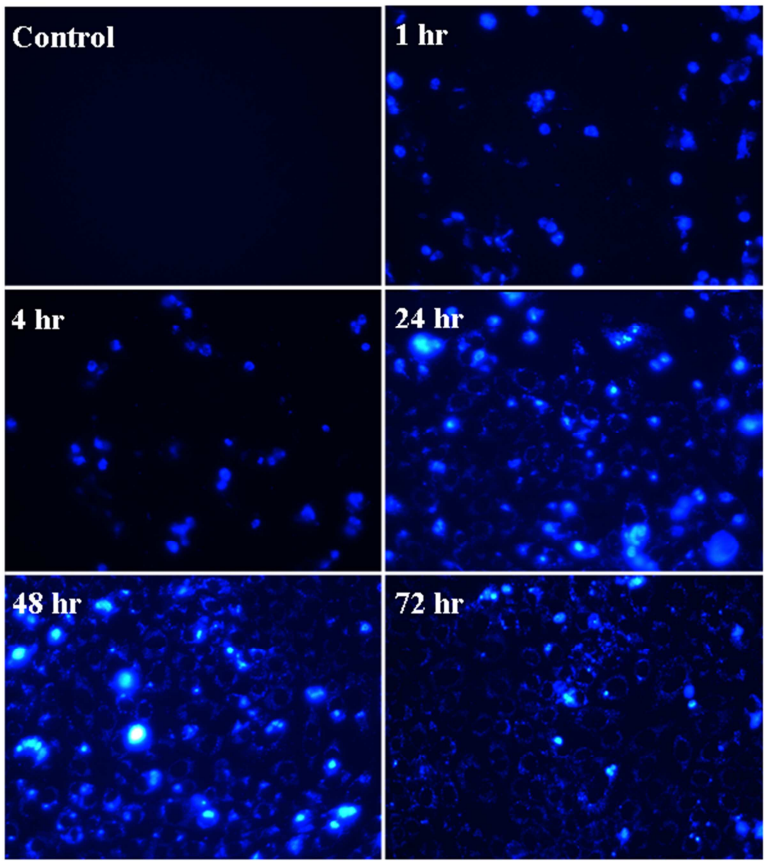

*Figure 2.39: Cellular uptake of **109** at given time intervals after addition of compound to CHO cells.*

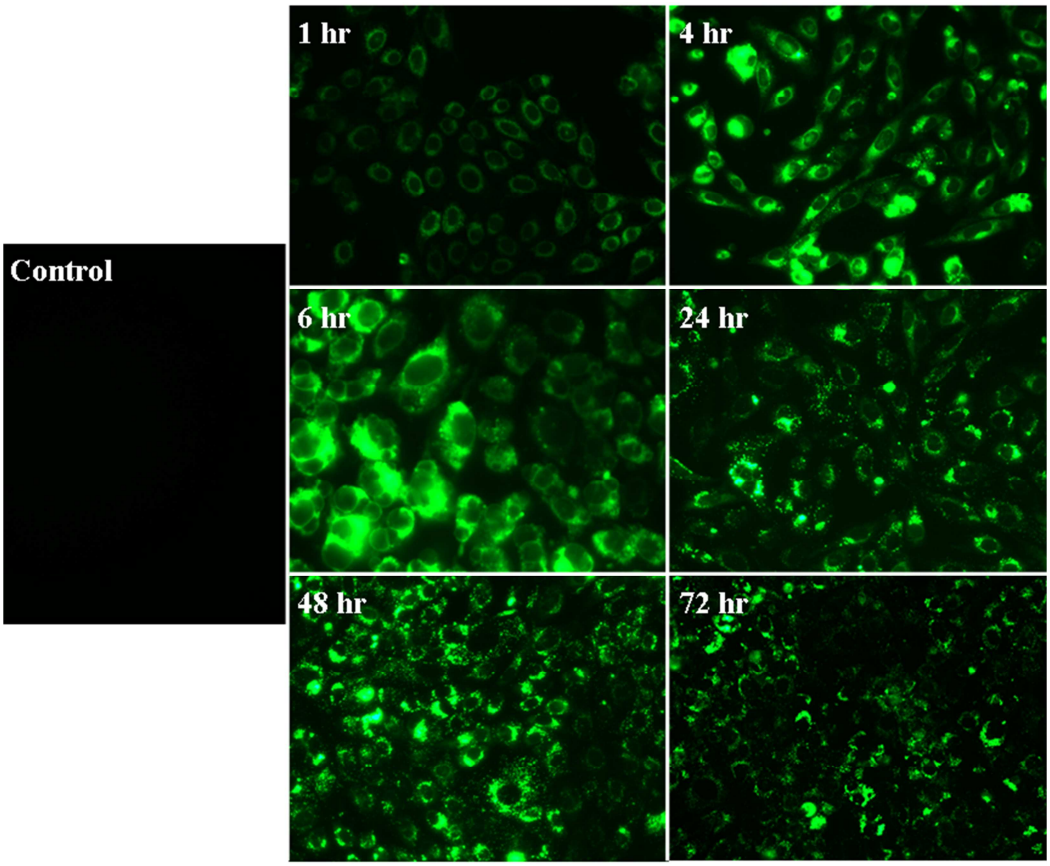

*Figure 2.40: Cellular uptake of **126** at given time intervals after addition of compound to CHO cells.*

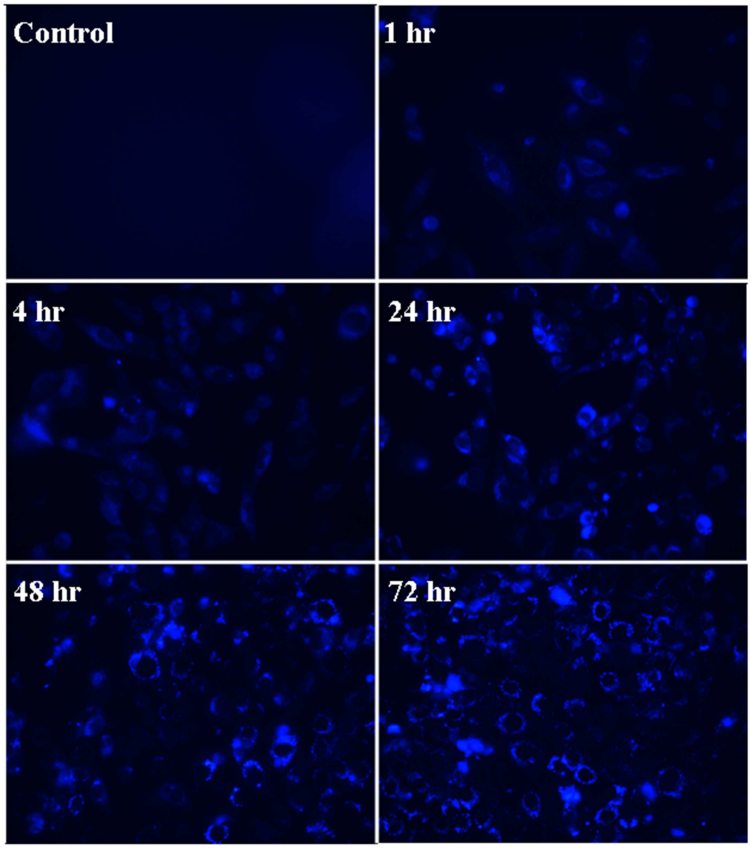

*Figure 2.41: Cellular uptake of **134** at given time intervals after addition of compound to CHO cells.*

Compound **126** allowed the effect of an increased length of linker to be tested compared with its previously investigated counterpart, NBDCalAm.[66] Although the increase in linker length resulted in higher cytotoxicity, the cellular uptake seemed to be similar: uptake was rapid, with intracellular fluorescence clearly visible after 1 hour and intense fluorescence exhibited after 4 hours, and increasingly punctate patterns visible from 24 hours onwards (see Figure 2.40).

Compound **134**, despite the change of linker from triazole to amide, displayed similar uptake to **94** (see Figure 2.41). Some intracellular fluorescence was visible after 1 hour, increasing in intensity over time, with the diffuse pattern changing to more punctate from 24 hours onwards. This suggests that the more rapid uptake exhibited by the NBD-appended compounds **126** and NBDCalAm compared with **94** could be due to the effect of the dye rather than that of the triazole ring.

It is important to note that these uptake studies give only qualitative information about the relative rate of uptake. In order to obtain accurate measurements of uptake kinetics, flow cytometry experiments would be required. However, the above experiments do reveal that an incubation time of 48 hours gives good uptake of all compounds and is therefore a suitable amount of time to allow in further experiments.

2.3.4.3 Mechanism of uptake

Incubation of cells with different inhibitors of endocytosis followed by incubation with the compounds under investigation allows the mechanism of their uptake to be investigated. As discussed in section 2.1.1, the two major pathways of endocytosis are *via* clathrin-coated pits or caveolae. Processes involving the latter can be inhibited by interfering with the function of cholesterol in the membrane. Suitable inhibitors include methyl-β-cyclodextrin (MCD),[115] which forms soluble inclusion complexes with cholesterol and so extracts it from the membrane, and the polyene antibiotics filipin[116] and nystatin,[117] which perturb the function of membrane domains by sequestering cholesterol within the membrane.

Clathrin-mediated processes can be inhibited by hypertonic sucrose, which disperses clathrin lattices.[118] The antibiotic monensin can also be used. This ionophore dissipates the proton gradient in lysosomes and interferes with transfer of compounds to these intracellular compartments; it therefore inhibits receptor-mediated uptake by interfering with receptor recycling.[119,120]

Investigations were carried out with these five inhibitors by incubating CHO cells grown on coverslips with each inhibitor followed by addition of the calixarene compounds under investigation and incubation for a further 48 hours. Excess inhibitor and calixarene was removed by washing before mounting on slides for imaging. In some cases incubation with monensin or MCD for 48 hours reduced cell viability and gave rounded dead or dying cells. In these cases the results are omitted since the possibility that uptake was due to the loss of viability could not be excluded.

The results for compound **94** are shown in Figure 2.42. Both MCD and nystatin resulted in a lower level of intracellular fluorescence, whilst filipin gave greatly diminished fluorescence. Conversely, monensin and sucrose had no inhibitory effect. This suggests that clathrin-mediated processes are not involved and that pathways involving caveolae are dominant in the uptake of **94**. Interestingly, although monensin and sucrose did not prevent uptake, both resulted in altered distribution of the calixarene within the cell. Whilst the cells treated with monensin displayed widely distributed fluorescence as in the control, the fluorescence seemed to be beginning to form into more aggregated structures. This can be attributed to perturbed intracellular trafficking due to dispersion of proton gradients within the cell.[120] Treatment with sucrose on the other hand gave a dramatically more punctate pattern of fluorescence; this could be due to side effects of hypertonic sucrose which include potential stimulation of rearrangement of the actin cytoskeleton.[121]

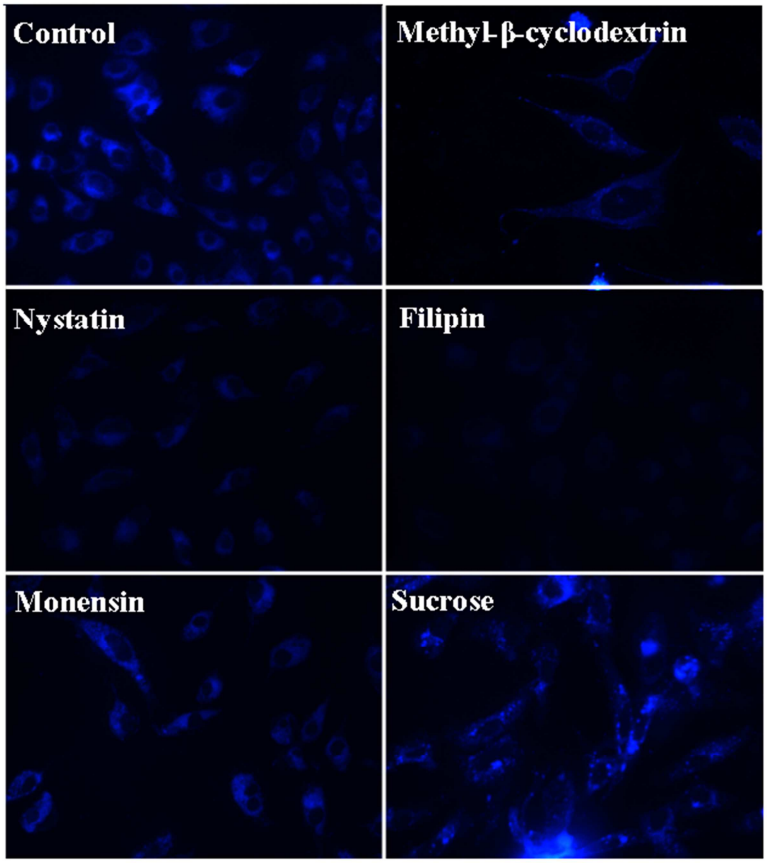

*Figure 2.42: Uptake of compound **94** after incubation with specified inhibitors.*

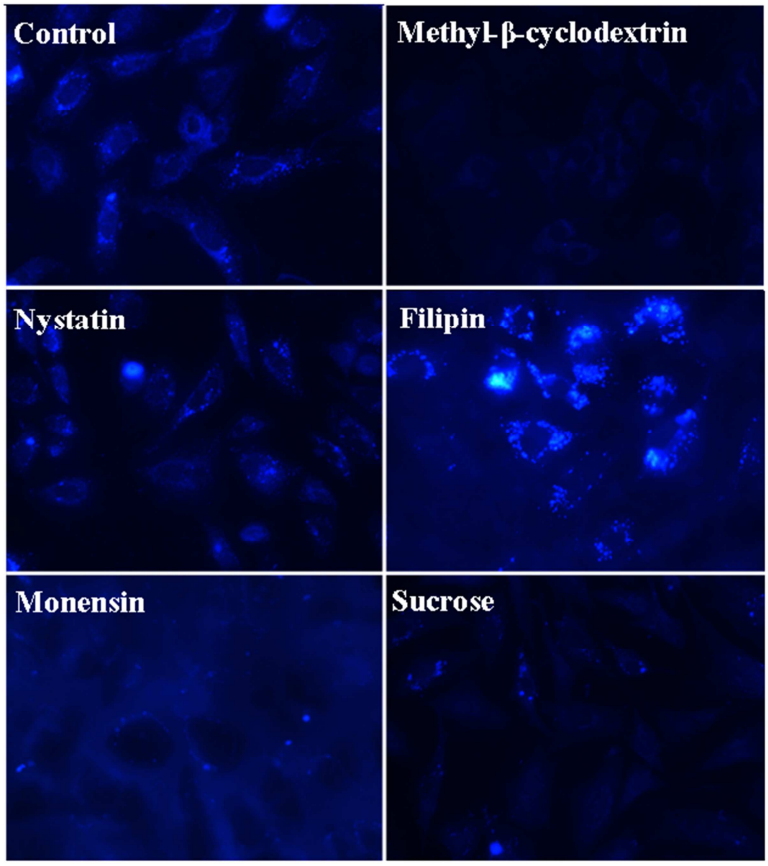

*Figure 2.43: Uptake of compound **97** after incubation with specified inhibitors.*

A different effect was observed with compound **97** (see Figure 2.43). Although treatment with MCD resulted in less intense, more diffuse intracellular fluorescence, both nystatin and filipin exhibited no inhibitory effect and did not alter the puntate pattern of fluorescence. However, the cells were not clearly visible when treated with monensin prior to **97**. Interestingly, in some cases punctate fluorescent outlines of cells were observed, suggesting that the calixarene had become bound to the exterior of the cell but not internalised. Sucrose also exhibited a negative effect on uptake, generally giving greatly diminished and diffused fluorescence with only a few cells showing a small amount of the familiar punctate fluorescence. This suggests that in this case clathrin and receptor-mediated processes are the dominant mechanism of uptake, whilst caveolae seem to not be involved. The diminished fluorescence in the case of MCD could be due to the potential for this inhibitor to also have an impact on invagination of clathrin-coated pits.[122]

The difference in apparent uptake mechanism between **94** and **97** highlights the importance in the upper rim functionalisation in the mode of internalisation. This also provides sharp contrast with NBDCalAm,[66] which despite being furnished with the same aromatic amines as **94** appeared to be taken up by direct translocation. Therefore the change from NBD to triazole-linked coumarin cargo has an impact on uptake mechanism.

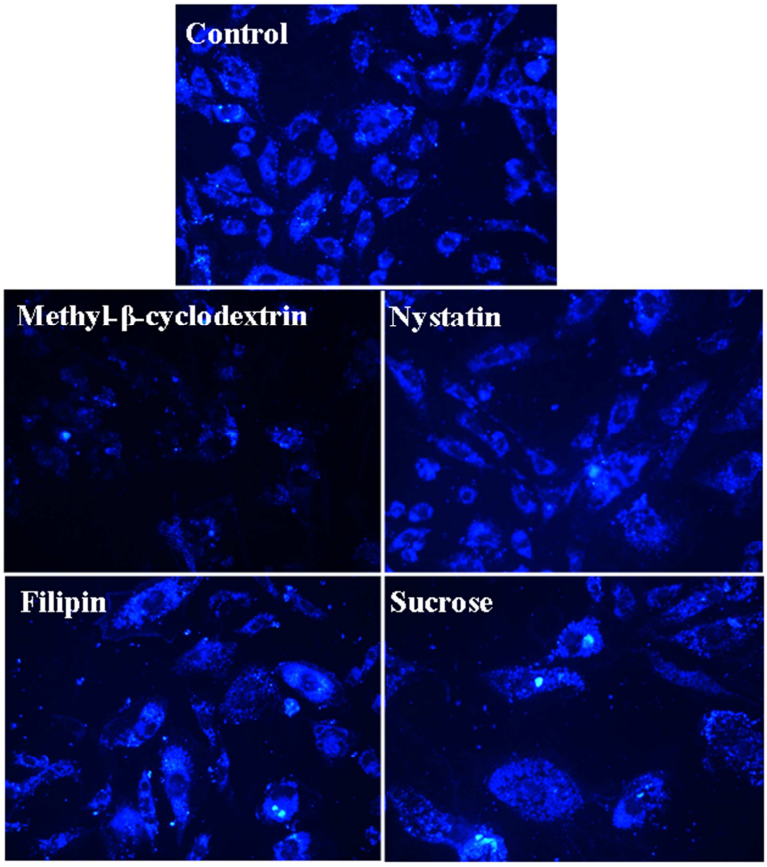

*Figure 2.44: Uptake of compound **109** after incubation with specified inhibitors.*

In the case of **109**, none of the inhibitors seemed to have any impact on internalisation. MCD, filipin, nystatin and sucrose all gave comparable fluorescence to the control (see Figure 2.39), although in some cases capturing the true level of fluorescence was difficult due to rapid photobleaching. This suggests a lack of involvement of endocytotic mechanisms in the uptake of this calixarene and potentially a direct translocation mechanism as was observed with NBDCalAm. This was unexpected, since the triazole-linked coumarin had resulted in uptake by endocytosis for **94** and **97**. The clustered guanidine residues therefore seem to allow this cargo to be directly translocated, although with slower apparent uptake than NBDCalAm.

As was observed for NBDCalAm,[66] internalisation of compound **126** was not significantly affected by the inhibitors tested, suggesting a similar direct translocation across the membrane. As with compound **94**, monensin and sucrose altered the distribution of the probe; this was particularly dramatic for the former, which gave the appearance of network-like structures within the cells. This could be due to inhibition of transfer to lysosomes from other cellular compartments such as the Golgi apparatus, which was previously observed for NBDCalAm on treatment with monensin.[66]

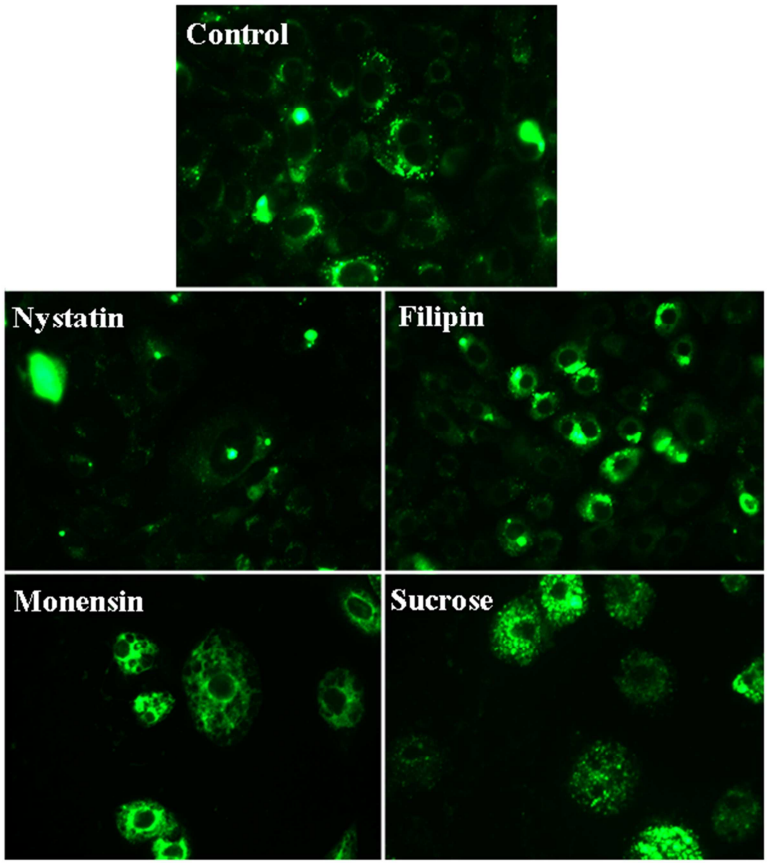

*Figure 2.45: Uptake of compound **126** after incubation with specified inhibitors.*

For compound **134**, no inhibition was observed with monensin or sucrose, suggesting that clathrin-mediated processes are not involved in uptake, although they did alter the distribution as observed for compounds **94** and **126**. However, although nystatin and filipin gave no significant effect relative to the control, MCD gave a different result. Some rounded cells were present, suggesting loss of viability of these cells as discussed previously. However, there were also cells present with normal morphology, which exhibited greatly diminished fluorescence relative to the control. This is unexpected, even with the potential for MCD to effect both clathrin and caveolae mediated processes, given that the other inhibitors of both of these types of endocytosis did not impact on uptake. This could be accounted for if both mechanisms were in use, resulting in a compensatory effect when one of the two was inhibited. However, given that some cells in the sample were already dead or dying, the anomalous result could simply be due to the remaining cells suffering non-visible abnormalities.

It does seem that the change in linker from a triazole to an amide has an impact on the uptake mechanism. Compound **134** is otherwise identical to **94** but uptake of the latter was inhibited by both nystatin and filipin, whilst **134** was not affected by either. The method of attachment of the cargo is therefore also an important factor.

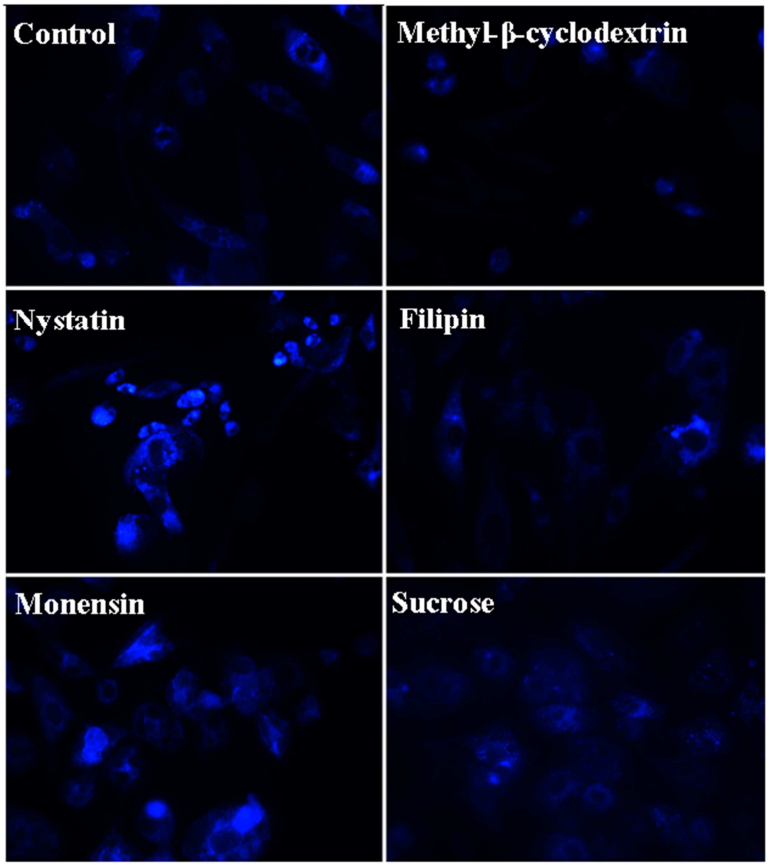

*Figure 2.46: Uptake of compound **134** after incubation with specified inhibitors.*

2.3.4.4 Intracellular localisation

To determine if the cellular fate of the compounds tested was the same as the previously investigated NBDCalAm, cells were incubated with the compounds for 48 hours followed by use of a selective lysosome stain. Weakly basic fluorescent probes are useful for this purpose, due to the tendency of weakly basic compounds to accumulate in lysosomes;[123] LysoTracker Red was used in this case. Double-stained cells were then photographed using a combination of a green excitation filter (for the LysoTracker) followed by either a UV (for the coumarin-appended calixarenes) or blue (for the NBD probe) excitation filter. By comparing the two images and examining the overlay of the two, the degree of probable overlap could be determined. Overlay of the red and blue emissions results in a pink colour, whereas overlay of red and green emissions gives yellow.

The results for compound **94** are shown in Figure 2.47. In general, the punctate fluorescence from the LysoTracker and **94** overlays, indicating co-localisation of the two compounds. However there is some diffuse blue fluorescence that does not overlay with red fluorescence of a similar intensity. This suggests that although some of **94** accumulates in acidic vesicles, not all of it is doing so.

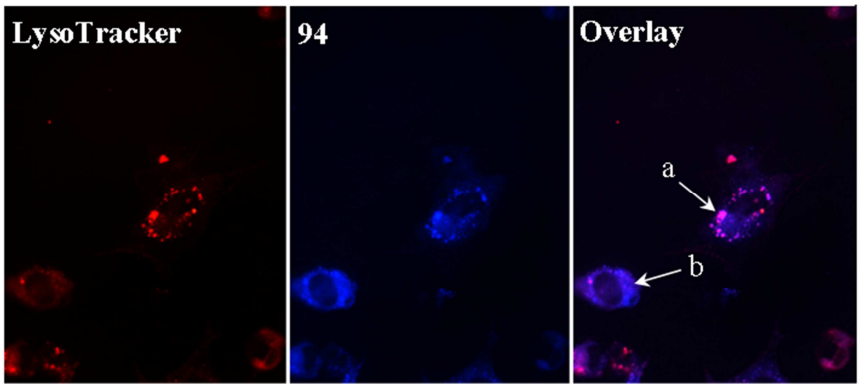

*Figure 2.47: Co-localisation of **94** with LysoTracker Red. White arrows indicate a pink spot of overlaid fluorescence (a) and an area of blue fluorescence with poor overlay (b).*

Compound **97** displayed more inconsistent results between cells. Figure 2.48a shows a sample which exhibited good overlay of fluorescence as indicated by the high proportion of pink punctate colouring, although some blue fluorescence is visible between these pink spots suggesting that not all of **97** has localised into the lysosomes. However, Figure 2.48b shows a sample where overlay was relatively poor; although there is some pink overlaid fluorescence, there are many spots of blue fluorescence, so some of the apparent overlay could be due to coincidental overlay in different planes of the three dimensional structure of the cell.

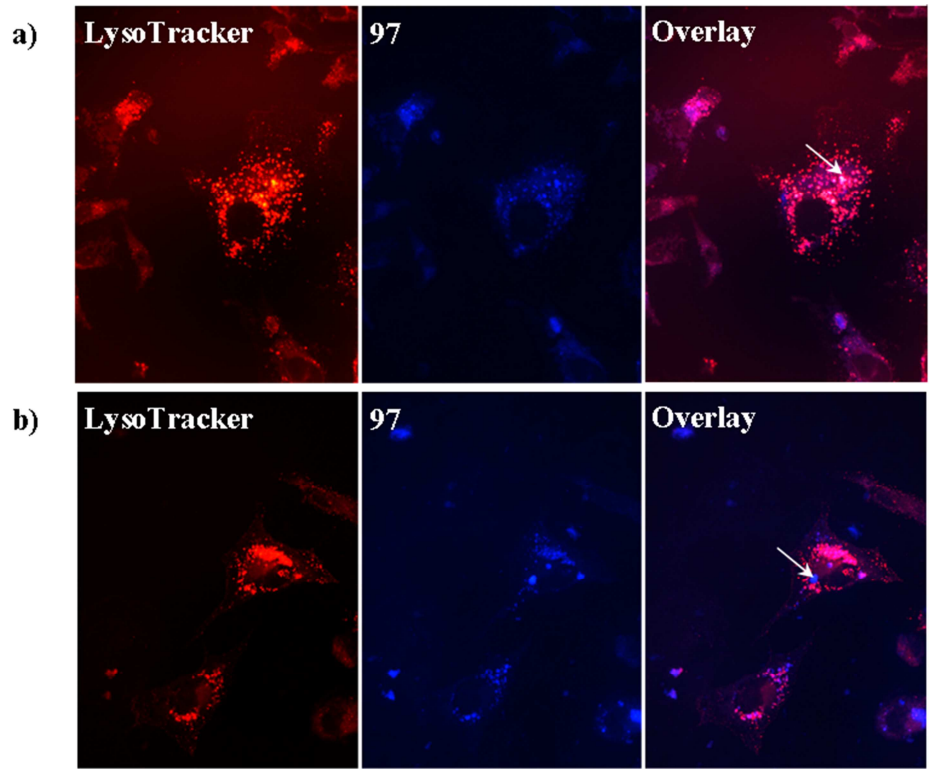

*Figure 2.48: a) Co-localisation of **97** with LysoTracker Red; white arrow indicates a pink spot of overlaid fluorescence. b) Cells showing limited overlay; white arrow indicates spot of blue fluorescence with no overlay.*

This inconsistency in localisation may correlate to the inconsistent rate of uptake observed for this compound (see section 2.3.4.2) between cells in the same sample and suggests that uptake and localisation could be sensitive to the state of the cell. If one cell begins to take up the calixarene before another in the sample, it stands to reason that the compound would reach its final cellular location earlier. Further experiments would be needed to confirm this; for example, samples could be taken at different time intervals to test for the proportion of cells displaying lysosome localisation. Co-localisation studies of other cellular compartments such as the Golgi apparatus could also help to elucidate the pathway of **97** inside the cell.

The results for compound **109** are shown in Figure 2.49. In this case, although there are areas of pink colour indicating overlay of red and blue fluorescence, there are numerous spots of blue fluorescence without overlay. Furthermore, in some of the pink areas there are spots that appear bluer in colour. This suggests that the apparent overlay could be coincidental. As a preliminary result, this suggests lack of localisation of **109** in lysosomes. This could be confirmed using confocal microscopy, which would allow individual planes of space through the cell to be sampled and allow apparently overlapping organelles to be differentiated. Further experiments with stains of other compartments would be required to determine the cellular fate of **109**.

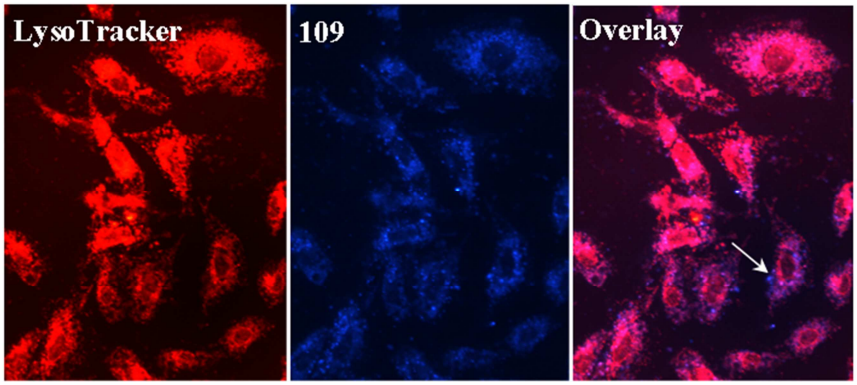

*Figure 2.49: Limited overlay of **109** with LysoTracker Red; white arrow indicates spot of blue fluorescence with no overlay.*

Compound **126** showed consistently good overlay with LysoTracker (see Figure 2.50). Although the staining from the LysoTracker was not as efficient in this case, resulting in lower intensity of red fluorescence and consequently a less dramatic yellow colour in the overlay, comparison of the fluorescence images from LysoTracker and **126** shows an almost identical pattern of staining. This suggests that like its analogue, NBDCalAm, **126** localises within acidic vesicles.

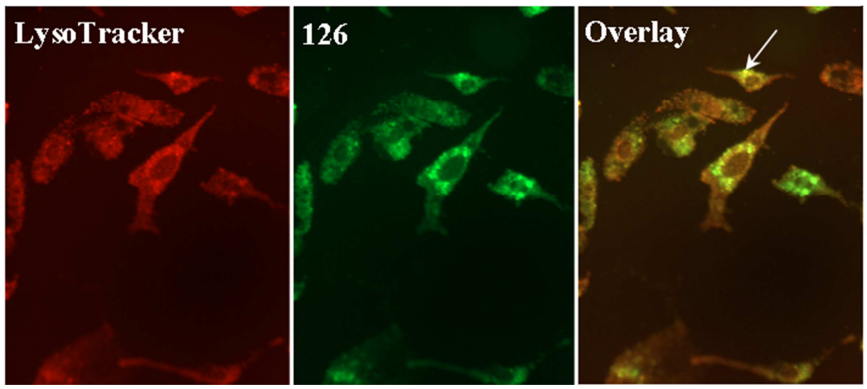

*Figure 2.50: Co-localisation of **126** with LysoTracker Red; white arrow indicates yellow spot of overlaid fluorescence.*

The results for compound **134** (see Figure 2.51) are similar to those of **94**. The fluorescence from the calixarene generally overlays with that of the LysoTracker, although some areas of diffuse blue fluorescence do not overlay with red fluorescence of a similar intensity. This suggests that most, but not all, of **134** has localised in acidic vesicles and that the change in linker from triazole to amide does not have a noticeable impact on localisation after the 48 hour incubation time.

As noted previously, the three dimensional nature of the cell means that the possibility of coincidental overlay cannot be ruled out. To confirm the obtained results and to obtain a quantitative measure of the degree of actual co-localisation of the compounds with LysoTracker, confocal microscopy would be required. From these preliminary results, it seems that the change in cargo from NBD to coumarin, whether

it is linked by a triazole or an amide bond, results in a slightly lower degree of localisation to acidic vesicles, although this could correlate to the slower uptake of the latter. Change in upper rim functionalisation from aromatic amine to aliphatic amine results in more inconsistent degree of localisation in acidic vesicles, whilst the guanidinium derivative did not seem to localise in acidic vesicles at all. This suggests that upper rim functionalisation has an impact on dynamics within the cell.

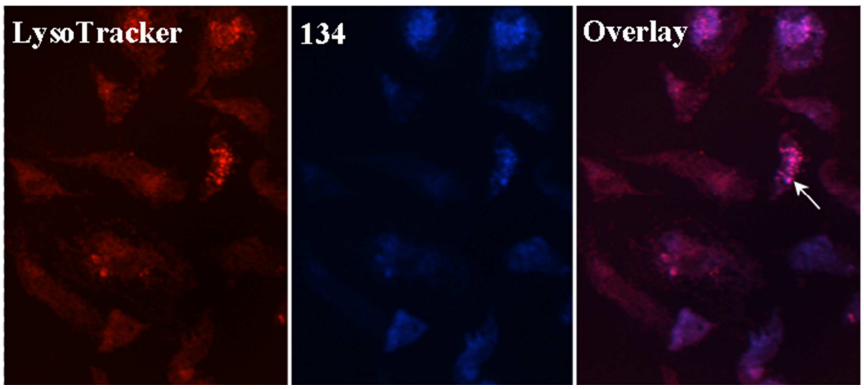

*Figure 2.51: Co-localisation of **134** with LysoTracker Red; white arrow indicates pink spot of overlaid fluorescence.*

2.4 Conclusions and further work

A method of synthesising diverse scaffolds has been developed using a common intermediate. This features aromatic amines on the upper rim which give access to other basic functionalities and an alkyne on the lower rim to which azide derivatives of various dyes (or potentially other cargo) can be attached using a CuAAC reaction. The utility of alkyne protecting groups in facilitating the synthesis of this intermediate in high purity has been demonstrated.

The synthesis of multifunctional scaffolds featuring aromatic guanidines on the upper rim is challenging due to the lability of the commonly utilised Boc protecting groups on this derivative. The validity of using Cbz protected guanidinylation agents has been demonstrated and has been shown to give improved integrity relative to the Boc protected analogue, allowing further reactions to take place on the guanidine-furnished scaffold. This may allow more complex guanidinylated calixarenes to be synthesised as analogues of cell penetrating peptides, although deprotection conditions must be carefully optimised to avoid degradation of the molecule. The suitability of the different deprotection methods available will depend on the nature of the cargo.

This approach may also allow the synthesis of the NBD-appended guanidinium derivative to be revisited. The decreased lability of the Cbz-protected guanidines on the upper rim should allow the phthalimide on the lower rim to be cleaved to expose

the amine required for coupling the NBD dye. A set of analogues to compare with the coumarin-appended calixarenes could be therefore be synthesised to determine if upper-rim functionalisation also effects the uptake and localisation of the NBD derivative.

Since the uptake and intracellular dynamics of these probes seems to be sensitive to the upper rim functionalisation, it is of interest to create an expanded library of compounds to test. Using the common intermediate, the amines on the upper rim could be coupled to alternative amino acids to glycine, for example lysine; such upper rim functionalisation has been accomplished by Bagnacani *et al*.[62] Similarly, coupling to arginine would provide a calixarene with aliphatic guanidine groups.

Alternatively, functionalisation with aliphatic guanidines could be achieved *via* chloromethylation of the upper rim followed by conversion to methylamines and ultimately guanidines. Previous work on this route within the group has encountered difficulties, with side reactions occurring during chloromethylation on the lower-rim functionalised calixarene and also if alkylation of the lower rim is attempted after chloromethylation. However, this synthesis could be achieved using the method of Mourer *et al*.,[86] which involves completing the guanidinylation of the upper rim prior to any functionalisation of the lower rim.

Biological tests of the compounds showed that the non-cationic control was not taken up into the cells tested, presumably due to the poor water solubility. The pyrene and anthracene derivatives proved to be unsuitable for cellular imaging, although it is possible that installation of multiple dye units on the lower rim may improve the fluorescence properties by allowing π-stacking between them.[59]

The coumarin derivatives were visibly taken up by cells and revealed sensitivity of the uptake, mechanism and localisation to the upper rim functionalisation. All of these derivatives were taken up more slowly than the NBD-appended calixarenes, but unexpectedly the guanidinium derivative seemed to be taken up most slowly, with probe only accumulating within dead or dying cells within the first 24 hours. The aliphatic amine derivative gave inconsistent uptake between cells in the same sample within this time frame, whilst the aromatic amine exhibited the fastest uptake of the three.

Caveolae mediated processes were implicated in the uptake of the aromatic amine, whilst the aliphatic amine seemed to be taken up *via* clathrin coated pits and the guanidinium derivative did not seem to be taken up by either endocytotic pathway. Localisation of the calixarenes seemed to be mostly within the lysosomes in the case

of the aromatic amine, whilst localisation of the aliphatic amine seemed to be more inconsistent. The guanidinium derivative did not seem to localise within acidic vesicles.

Comparison of the C_4-linked NBD derivative with NBDCalAm revealed no considerable difference in uptake or localisation, although toxicity was increased. This suggests that increasing the length of the linker does not affect uptake mechanism or localisation and therefore allows the amide-linked coumarin, featuring a C_4 length linker, to be compared with the triazole-linked coumarin, which has a C_3 length linker.

The triazole linker seemed to have no effect on relative rate of uptake or cellular localisation, since the amide-linked derivative was taken up in a similar time-frame and also seemed to localise within acidic vesicles; however, it resulted in uptake that was apparently not by endocytosis. The impact of the triazole ring was therefore limited. This suggests that the rapid uptake of NBDCalAm may have been due to the NBD dye, since the coumarin derivatives were taken up more slowly whether they featured a triazole or amide linker. The comparison of the triazole- and amide-linked compounds is also valuable in that it suggests that the triazole may be a suitable amide bioisostere in these compounds, although it can influence the mechanism of uptake.

To gain more information about the dynamics of these probes, flow cytometry experiments will be required to allow comparison of the quantitative uptake kinetics. Further investigation of the cellular localisation is needed for those probes that did not fully localise in the lysosomes, for example by using a Golgi apparatus stain such as BODIPY TR ceramide.[66] For those that did colocalise with LysoTracker, confocal microscopy experiments will be required to quantify the true degree of colocalisation.

In general, the current progress has elucidated some of the factors that influence the uptake and intracellular dynamics of calixarene-based cell-penetration agents. Synthesis of additional derivatives may allow more of the subtleties of the behaviour of such molecules to be determined. This in turn will inform the design of cell-penetration agents based on these scaffolds featuring other cargos such as antiviral or anticancer agents, or development of novel cellular imaging agents.

2.5 Experimental

2.5.1 General procedures - chemistry

All chemicals were purchased from Sigma-Aldrich, Alfa Aesar, Acrôs Organics or Novabiochem and were used without further purification. Deuterated solvents for NMR use were purchased from Cambridge Isotope Laboratories or Sigma-Aldrich.

Dry solvents were purchased from previously listed suppliers. Analytical thin layer chromatography (TLC) was performed using Merck or Machery-Nagel Alugram silica gel 60 F_{254} plates, with visualisation by UV light (254 nm). Column chromatography was run using silica gel 60 (230-400 mesh). NMR spectra were acquired using a Varian Unity Plus spectrometer (operating at 400 MHz for proton and 100 MHz for carbon), a Gemini 2000 spectrometer (operating at 300 MHz for proton and 75 MHz for carbon) or a Bruker Avance 400 Ultrashield spectrometer (operating at 400 MHz for proton or 100 MHz for carbon). Chemical shifts are referenced relative to tetramethylsilane (TMS) as the internal reference standard and expressed in parts per million (ppm or δ) downfield from the standard. Coupling constants (*J*) are expressed in Hz. Multiplicities are abbreviated as follows: s (singlet), br s (broad singlet), d (doublet), t (triplet), m (multiplet), app (apparent). MALDI-TOF mass spectra were recorded using a Kratos Axima CFR MALDI Mass Spectrometer using α-cyano-4-hydroxycinnamic acid as matrix. APCI and ESI or NSI mass spectra were recorded by the EPSRC National Mass Spectrometry Service, Swansea. Melting points were measured using an electrothermal Mel-temp® melting point apparatus and are reported uncorrected. Infrared spectra were recorded using a Perkin Elmer Spectrum BX or Spectrum 65 spectrometer fitted with an ATR attachment and are expressed in wavenumbers (cm^{-1}).

2.5.2 Synthesis

5,11,17,23-*p*-*tert*-Butylcalix[4]arene (2)[74]

In a 3 L flange flask, *p*-*tert*-butyl phenol (200.00 g, 1.33 mol), NaOH (2.40 g, 60 mmol) and 37 wt% formaldehyde (130 mL, 1.74 mol) were heated to 120 °C with mechanical stirring over 2 h. The resultant yellow solid was dissolved in diphenyl ether (980 mL). Water of condensation (100 mL) was removed by distillation under a stream of air, following which the solution was heated to reflux for 3 hours. After cooling, ethyl acetate (750 mL) was added to precipitate the crude product, which was collected by filtration, washed with ethyl acetate (2 x 150 mL), acetic acid (2 x 150 mL), water (2 x 150 mL) and acetone (1 x 150 mL) to give **2** as off-white crystals (143.63 g, 67%). **Mp** 338-340 °C; **IR** ν 3158.5, 3052, 3028.5, 2952.5, 2903.5, 2864.5, 1738, 1604, 1592, 1586, 1481.5, 1463, 1428, 1405.5, 1392, 1361.5, 1306, 1299, 1285.5, 1240.5, 1229.5, 1199, 1158.5, 1124, 1102.5, 1039 cm^{-1}; **^{1}H-NMR** (400 MHz, $CDCl_3$) δ 10.34 (s, 4H, O*H*), 7.05 (s, 8H, Ar*H*), 4.26 (d, *J* = 13 Hz, 4H, ArCH_2Ar), 3.49 (d, *J* = 13 Hz, 4H, ArCH_2Ar), 1.21 (s, 36H, C(CH_3)$_3$).

5,11,17,23-Tetra-*tert*-butyl-25,26,27-tripropoxy-28-hydroxy-calix[4]arene (77)[73]

p-tert-Butylcalix[4]arene (**2**) (20.11 g, 31.03 mmol) was dissolved in DMF (300 mL) and heated to 30 °C. BaO (7.15 g, 46.78 mmol) and $Ba(OH)_2.8H_2O$ (33.82 g, 107.35 mmol) were added and the mixture stirred for 30 mins. n-Propyl bromide (60 mL, 660 mmol) was added and the mixture stirred for 18 hrs. The solution was diluted with water (200 mL) and the product extracted with DCM (3 x 100 mL). After washing with water (2 x 200 mL) then brine (200 mL) the organic layer was dried ($MgSO_4$) and the solvent removed under reduced pressure. Precipitation from DCM with methanol and filtration gave **77** as white crystals (18.37 g, 79%). **Mp** 172-174 ^oC; **IR** ν 3479, 2956, 2898, 2684, 1584, 1480, 1462, 1431, 1385, 1360, 1295, 1239, 1194, 1121 cm^{-1}; **^{1}H-NMR** (400 MHz, $CDCl_3$) δ 7.07 (s, 2 H, Ar*H*), 6.99 (s, 2 H, Ar*H*), 6.45 (s, 4 H, Ar*H*), 4.30 (d, *J* = 13 Hz, 2 H, ArCH_2Ar), 4.27 (d, *J* = 13 Hz, 2 H, ArCH_2Ar), 3.78 (t, *J* = 8 Hz, 2 H, OC$H_2$$CH_2CH_3$), 3.69 (t, *J* = 7 Hz, 4 H, OC$H_2$$CH_2CH_3$), 3.17 (d, *J* = 13 Hz, 2 H, ArCH_2Ar), 3.10 (d, *J* = 13 Hz, 2 H, ArCH_2Ar), 2.36-2.26 (m, 2H, $OCH_2C$$H_2CH_3$), 1.99-1.78 (m, 4 H, $OCH_2C$$H_2CH_3$), 1.28 (s, 9 H, C(C$H_3$)$_3$), 1.27 (s, 9 H, C$H_3$), 1.03 (t, *J* = 7 Hz, 6 H, $OCH_2CH_2C$$H_3$), 0.89 (t, *J* = 8 Hz, 3 H, $OCH_2CH_2C$$H_3$), 0.76 (s, 18 H, C(C$H_3$)$_3$).

5,11,17,23-Tetra-*tert*-butyl-25,26,27-tripropoxy-28-propargyloxy-calix[4]arene (78)[124]

Compound **77** (12.51 g, 16.42 mmol) was dissolved in DMF (330 mL). NaH (1.54 g, 64.17 mmol) was added and the mixture stirred for 1 hour before addition of n-propargyl bromide (8.06 g, 80% w/w in toluene, 54.20 mmol). After stirring for 72 hours, the solution was diluted with water (200 mL) and the product extracted with DCM (3 x 100 mL). After washing with water (2 x 200 mL) then brine (200 mL), the organic layer was dried ($MgSO_4$) and the solvent removed under reduced pressure. Purification by column chromatography over silica (eluent: 1:1 DCM/hexane) gave **78** as off-white crystals (12.60 g, 95%). **Mp** 203-205 ^oC; **IR** ν 3539, 3285, 3261, 2950, 2900, 2860, 2123, 1585, 1582, 1477, 1391, 1360, 1299, 1258, 1237, 1193, 1120 cm^{-1}; **^{1}H-NMR** (400 MHz, $CDCl_3$): δ 7.02 (s, 4 H, Ar*H*), 6.58 (d, *J* = 2 Hz, 2 H, Ar*H*), 6.52 (d, *J* = 2 Hz, 2 H, Ar*H*), 4.97 (d, *J* = 2 Hz, 2 H, OCH_2CCH), 4.51 (d, *J* = 12 Hz, 2 H, ArCH_2Ar), 4.43 (d, *J* = 13 Hz, 2 H, ArCH_2Ar), 3.90 (t, *J* = 8 Hz, 2 H, OC$H_2$$CH_2CH_3$), 3.73 (t, *J* = 7 Hz, 4 H, OC$H_2$$CH_2CH_3$), 3.14 (d, *J* = 13 Hz, 2 H, ArCH_2Ar), 3.13 (d, *J* = 12 Hz, 2 H, ArCH_2Ar), 2.38 (t, *J* = 2 Hz, 1 H, OCH_2CC*H*), 2.14 (sextet, *J* = 8 Hz, 2H,

$OCH_2CH_2CH_3$), 2.04-1.91 (m, 4 H, $OCH_2CH_2CH_3$), 1.27 (s, 9 H, $C(CH_3)_3$), 1.26 (s, 9 H, $C(CH_3)_3$), 1.05 (t, *J* = 7 Hz, 6 H, $OCH_2CH_2CH_3$), 0.99 (t, *J* = 8 Hz, 3 H, $OCH_2CH_2CH_3$), 0.99 (s, 18 H, $C(CH_3)_3$).

5,11,17,23-Tetranitro-25,26,27-tripropoxy-28-propargyloxy-calix[4]arene (79)

Compound **78** (3.25 g, 4.00 mmol) was dissolved in 130 mL DCM. Glacial acetic acid (21.5 mL) and 100% nitric acid (21.5 mL) were added and the resulting blue-black solution was stirred until the colour changed to bright orange. Iced H_2O (45 mL) was added to quench. The product was extracted with DCM (3 x 100 mL) then washed with water (3 x 200 mL) then brine (200 mL). After drying ($MgSO_4$) the solvent was removed under reduced pressure and the product precipitated from DCM with methanol to give **79** as light yellow crystals (2.61 g, 85%). **Mp** > 180 °C (decomp.); **IR** ν 3285, 3069, 2959, 2921, 2867, 1722, 1638, 1597, 1583, 1514, 1449, 1338, 1301, 1262, 1205, 1156 cm^{-1}; **^{1}H-NMR** (400 MHz, $CDCl_3$): δ 8.07 (s, 2 H, Ar*H*), 8.06 (s, 2 H, Ar*H*), 7.16 (s, 4 H, Ar*H*), 4.92 (d, *J* = 2 Hz, 2 H, OCH_2CCH), 4.60 (d, *J* = 14 Hz, 2 H, $ArCH_2Ar$), 4.55 (d, *J* = 14 Hz, 2 H, $ArCH_2Ar$), 4.14 (t, *J* = 8 Hz, 2 H, $OCH_2CH_2CH_3$), 3.82 (t, *J* = 7 Hz, 4 H, $OCH_2CH_2CH_3$), 3.44 (d, *J* = 14 Hz, 2 H, $ArCH_2Ar$), 3.42 (d, *J* = 14 Hz, 2 H, $ArCH_2Ar$), 2.51 (t, *J* = 2 Hz, 1 H, OCH_2CCH), 1.98-1.87 (m, 6 H, $OCH_2CH_2CH_3$), 1.10 (t, *J* = 8 Hz, 6 H, $OCH_2CH_2CH_3$), 0.97 (t, *J* = 7 Hz, 3 H, $OCH_2CH_2CH_3$); **^{13}C-NMR** (100 MHz, $CDCl_3$) δ 162.8, 160.9, 160.2, 143.8, 142.9, 137.9, 136.6, 134.5, 134.2, 124.8, 124.7, 123.4, 123.3, 78.2, 78.2, 78.0, 77.1, 60.7, 31.5, 31.1, 23.5, 23.4, 10.6, 10.0; **ESI-MS** m/z: $[M]^+$ 768.2.

5,11,17,23-Tetraamino-25,26,27-tripropoxy-28-propargyloxy-calix[4]arene (80)

Compound **79** (2.4 g, 3.13 mmol) and $SnCl_2{\cdot}2H_2O$ (18.42 g, 81.64 mmol) were heated to reflux in ethanol (215 mL) for 48 hours. After removing the ethanol under reduced pressure, 10% NaOH (300 mL) was added, then the product extracted with DCM (3 x 100 mL). The organic layer was washed with water (200 mL) and brine (200 mL). After drying ($MgSO_4$) and removing the solvent under reduced pressure, **80** was obtained as an orange-brown glass (1.98 g, 98%). **Mp** >180 °C (decomp.); **IR** ν 3310, 2966, 2934, 2878, 1737, 1608, 1469, 1387, 1310, 1285, 1215, 1158, 1129 cm^{-1}; **^{1}H-NMR** (300 MHz, $CDCl_3$): δ 6.41 (s, 4 H, Ar*H*), 5.78 (s, 2 H, Ar*H*), 5.77 (s, 2 H, Ar*H*), 4.77 (d, *J* = 2 Hz, 2 H, OCH_2CCH), 4.39 (d, *J* = 14 Hz, 2 H, $ArCH_2Ar$), 4.32 (d, *J* = 13 Hz, 2 H, $ArCH_2Ar$), 3.86 (t, *J* = 8 Hz, 2 H, $OCH_2CH_2CH_3$), 3.61 (t, *J* = 7

Hz, 4 H, OC*H*$_2$CH$_2$CH$_3$), 2.95 (d, *J* = 14 Hz, 2 H, ArC*H*$_2$Ar), 2.92 (d, *J* = 13 Hz, 2 H, ArC*H*$_2$Ar), 2.31 (t, *J* = 2.4 Hz, 1 H, OCH$_2$CC*H*), 1.88 (sextet, *J* = 8 Hz, 2 H, OCH$_2$C*H*$_2$CH$_3$), 1.84 (sextet, *J* = 7 Hz, 4 H, OCH$_2$C*H*$_2$CH$_3$), 1.04 (t, *J* = 7 Hz, 6 H, OCH$_2$CH$_2$C*H*$_3$), 0.97 (t, *J* = 8 Hz, 3 H, OCH$_2$CH$_2$C*H*$_3$); **^{13}C-NMR** (100 MHz, CDCl$_3$): δ 150.6, 149.6, 147.9, 141.4, 140.4, 139.2, 138.1, 137.1, 134.3, 134.1, 116.2, 116.0, 115.8, 81.4, 74.2, 59.5, 31.6, 31.0, 23.5, 23.1, 10.9, 10.1; **HRMS** (NSI) m/z: $[M+H]^+$ Calcd for $C_{40}H_{49}N_4O_4$ 649.3748; Found 649.3745.

3-acetamido-7-acetoxy-chromen-2-one (81)[79]

4-Hydroxysalicylaldehyde (6.91 g, 50.01 mmol), *N*-acetyl glycine (5.85 g, 50.00 mmol), anhydrous sodium acetate (16.4 g, 19.99 mmol) and acetic anhydride (40 mL) were heated to 120 °C for 5 hours. Ice-cold H_2O was added and any solid broken up. After vacuum filtration and washing 3 times with cold water, the solid was air dried then triturated with ethyl acetate. Filtration under vacuum and air drying gave **81** as a yellow powder (6.33 g, 49%). **Mp** > 240 °C (decomp.); **IR** ν 3339, 3088, 1757, 1716, 1676, 1611, 1531, 1430, 1352, 1283, 1251, 1199, 1154, 1117 cm^{-1}; **^{1}H-NMR** (400 MHz, CDCl$_3$): δ 8.67 (s, 1 H, Ar*H*), 8.04 (s, 1 H, N*H*), 8.51 (d, *J* = 8 Hz, 1 H, Ar*H*), 7.12 (d, *J* = 2.3 Hz, 1 H, Ar*H*), 7.07 (dd, *J* = 8, 2.3 Hz, 1 H, Ar*H*), 2.34 (s, 3 H, C*H*$_3$), 2.25 (s, 3 H, C*H*$_3$).

3-Azido-7-hydroxy-chromen-2-one (82)[69]

Compound **81** (1 g, 3.83 mmol) was heated to reflux in a solution of 37% HCl and ethanol (2:1, 11 mL) for 1 hour. Iced H_2O (15 mL) was added and the mixture cooled in an ice bath. $NaNO_2$ (1 g, 14.5 mmol) was added in small portions then stirred for 10 minutes. After adding NaN_3 (1.4 g, 21.5 mmol) in small portions the mixture was stirred for a further 15 minutes then vacuum filtered. Washing with water several times then air drying gave crude **82** as a brown powder (0.64 g, 83%). Purification by column chromatography over silica (eluent: 3:2 hexane/ethyl acetate) gave pure **82** as yellow-orange needles (0.18 g, 23%). **Mp** 100-102 °C; **IR** ν 3276, 3047, 2105, 1679, 1609, 1593, 1449, 1370, 1340, 1315, 1256, 1217, 1153, 1119 cm^{-1}; **^{1}H-NMR** (400 MHz, DMSO) δ 10.52 (s, 1H, ArO*H*), 7.59 (s, 1H, Ar*H*), 7.48 (d, J = 8.5 Hz, 1H, Ar*H*), 6.81 (dd, J = 8.5, 2.3 Hz, 1H, Ar*H*), 6.76 (d, J = 2.3 Hz, 1H, Ar*H*).

1-Bromomethylpyrene (83)[70]

To a stirred suspension of 1-pyrene methanol (1.6 g, 6.83 mmol) in THF (8 mL) was added PBr_3 (2.77 g, 10.25 mmol). After 30 minutes the solid was filtered and washed with diethyl ether to give **83** as light yellow crystals (1.76 g, 87%). **Mp** 150-152 °C; **IR** ν 3333.5, 3037, 2892.5, 2836, 1602, 1588.5, 1497.5, 1464, 1435.5, 1418.5, 1386.5, 1373, 1312.5, 1269, 1243, 1222.5, 1204.5, 1180, 1138, 1107, 1093.5, 1083, 1027.5 cm^{-1}; **^{1}H-NMR** (300 MHz, $CDCl_3$): δ 8.41 (d, *J* = 9 Hz, 1 H, Ar*H*), 8.27-8.21 (m, 3 H, Ar*H*), 8.14-8.01 (m, 5 H, Ar*H*), 5.26 (s, 2 H, CH_2).

1-Azidomethylpyrene (84)[70]

To a stirred suspension of **83** in DMF (9 mL), NaN_3 (0.49 g, 7.54 mmol) was added and the mixture heated at 60 °C for 16 hours. The product was extracted into ether and washed with water 3 times. After drying and removing the solvent under reduced pressure, **84** was obtained as a waxy yellow solid (1.1 g, 88%). **Mp** 63-65 °C; **IR** ν 3041, 2992, 2942, 2888.5, 2507, 2482, 2455.5, 2425, 2099, 2079.5, 1925.5, 1901.5, 1875.5, 1861, 1793.5, 1724, 1678, 1652.5, 1603, 1596, 1589, 1509.5, 1489, 1456.5, 1435.5, 1418.5, 1392.5, 1372, 1340, 1314.5, 1270.5, 1252.5, 1245, 1226.5, 1194.5, 1181, 1169.5, 1150.5, 1136.5, 1100, 1059.5, 1026 cm^{-1}; **^{1}H-NMR** (300 MHz, $CDCl_3$): δ 8.31-8.17 (m, 5 H, Ar*H*), 8.13-7.98 (m, 4 H, Ar*H*), 5.05 (s, 2 H, CH_2).

Coumarin appended *tert*-butyl calix[4]arene (87)

A solution of **78** (0.5 g, 0.62 mmol), **82** (125 mg, 0.62 mmol), sodium ascorbate (132 mg, 0.67 mmol) and $CuSO_4.5H_2O$ (0.024 g, 0.095 mmol) in DMF (19 mL) was heated to 90 °C and stirred for 3 hours. After cooling, water (25 mL) was added and the product extracted with DCM (3 x 25 mL), washed with water (2 x 25 mL) then brine (25 mL), dried and the solvent removed under reduced pressure. The product was purified by column chromatography over silica (eluent: 49:1 DCM/methanol) to give **87** as a light yellow glass (0.38 g, 60%). **Mp** 175-180 °C; **IR** ν 2955, 2867, 1736, 1610, 1514, 1480, 1387, 1360, 1298, 1233, 1196, 1121 cm^{-1}; **^{1}H-NMR** (300 MHz, $CDCl_3$) δ 8.60 (s, 1H, Ar$H_{Triazole}$), 8.55 (s, 1H, Ar$H_{Coumarin}$), 7.55 (d, *J* = 9.2 Hz, 1H, Ar$H_{Coumarin}$), 6.97-6.93 (m, 2H, Ar$H_{Coumarin}$), 6.83 (s, 4H, Ar*H*), 6.74 (s 2H, Ar*H*), 6.70 (s, 2H, Ar*H*), 5.22 (s, 2H, OCH_2C), 4.39 (d, *J* = 12.4 Hz, 2H, ArCH_2Ar), 4.36 (d, *J* = 12.4 Hz, 2H, ArCH_2Ar), 3.83-3.73 (m, 6 H, OCH_2CH_2CH_3), 3.10 (d, *J* = 12.4 Hz, 4H, ArCH_2Ar), 2.06-1.85 (m, 4 H, OCH_2CH_2CH_3), 1.11 (s, 18H, C(CH_3)$_3$), 1.03 (s, 9H, C(CH_3)$_3$), 1.01(s, 9H, C(CH_3)$_3$), 0.88-0.81 (m, 9 H, OCH_2CH_2CH_3); **^{13}C-NMR** (100

MHz, $CDCl_3$): δ 162.8, 162.2, 159.8, 157.0, 155.0, 154.1, 154.0, 153.6, 152.2, 152.0, 151.5, 145.6, 145.4, 145.2, 145.2, 144.6, 144.5, 144.4, 135.1, 134.4, 134.1, 134.0, 133.8, 130.6, 125.3, 125.1, 125.0, 119.4, 115.6, 114.5, 110.9, 103.2, 102.8, 77.1, 66.5, 62.8, 34.1, 34.0, 32.0, 31.7, 31.6, 31.6, 31.5, 31.3, 29.3, 23.7, 23.7, 23.4, 23.4, 10.7, 10.6, 10.4, 10.3, 10.3; **MALDI-TOF** m/z: $[M+Na]^+$ 1039.95.

5,11,17,23-Tetra-Boc-amino-25,26,27-tripropoxy-28-propargyloxy-calix[4]arene (88)

To a solution of **80** (0.58 g, 0.89 mmol) in DCM (25 mL), Boc anhydride (1.99 g, 9.12 mmol) and DIPEA (0.33 mL, 2.00 mmol) were added. After stirring for 24 hours, the solvent was removed under reduced pressure and the product purified by column chromatography over silica (eluent: 15:1 DCM/ethyl acetate) to give **88** as off white crystals (0.78 g, 83%). **Mp** 179-181 °C; **IR** ν 3433, 3294, 2967, 2924, 2870, 1693, 1595, 1514, 1467, 1413, 1375, 1364, 1289, 1226, 1211, 1146 cm^{-1}; **^{1}H-NMR** (400 MHz, $CDCl_3$) δ 7.05 (s, 2 H, Ar*H*), 7.04 (s, 2 H, Ar*H*), 6.37 (s, 2 H, N*H*), 6.26 (s, 2 H, Ar*H*), 6.24 (s, 2 H, Ar*H*), 5.90 (s, 2 H, N*H*), 4.85 (d, *J* = 3 Hz, 2 H, OCH_2CCH), 4.43 (d, *J* = 13 Hz, 2 H, ArCH_2Ar), 4.36 (d, *J* = 13 Hz, 2 H, ArCH_2Ar), 3.92 (t, *J* = 8 Hz, 2 H, OCH_2CH$_2$CH$_3$), 3.63 (t, *J* = 6 Hz, 4 H, OCH_2CH$_2$CH$_3$), 3.10 (d, *J* = 13 Hz, 2 H, ArCH_2Ar), 3.08 (d, *J* = 13 Hz, 2 H, ArCH_2Ar), 2.31 (t, *J* = 3, 1 H, OCH$_2$CC*H*), 1.96-1.81 (m, 6 H, OCH$_2$CH_2CH$_3$), 1.53 (s, 9 H, C(CH_3)$_3$), 1.53 (s, 9 H, C(CH_3)$_3$), 1.43 (s, 18 H, C(CH_3)$_3$), 1.02 (t, *J* = 7 Hz, 6 H, OCH$_2$CH$_2$CH_3), 0.90 (t, *J* = 7 Hz, 3 H, OCH$_2$CH$_2$CH_3); **^{13}C NMR** (100 MHz, $CDCl_3$): δ 153.4, 153.3, 153.1, 152.3, 150.8, 137.7, 136.6, 133.9, 133.6, 133.3, 132.4, 131.9, 120.3, 120.2, 119.5, 119.0, 80.9, 80.3, 79.9, 77.2, 76.0, 74.7, 59.5, 31.7, 31.0, 28.5, 23.5, 23.1, 10.8, 10.1; **HRMS** (NSI) m/z: $[M+NH_4]^+$ Calcd for $C_{60}H_{84}N_5O_{12}$ 1066.6111; Found 1066.6101.

Coumarin appended tetra-Boc-amino calix[4]arene (89)

A solution of **88** (0.5 g, 0.48 mmol), **82** (0.15 g, 7.43 mmol), sodium ascorbate (0.10 g, 0.52 mmol) and $CuSO_4.5H_2O$ (0.018 g, 0.074 mmol) in DMF (15 mL) was heated to 90 °C and stirred for 20 hours. Water (20 mL) was added then the product extracted with DCM (3 x 25 mL), washed with water (2 x 25 mL) then brine (25 mL) before drying and removing the solvent under reduced pressure. The product was purified by column chromatography over silica gel (eluent: 49:1 DCM/methanol) to give **89** as a light yellow glass (0.39 g, 65%). **Mp** 170-172 °C; **IR** ν 2962, 2919, 2865, 1689, 1602, 1514, 1466, 1412, 1365, 1290, 1219, 1213, 1149 cm^{-1}; **^{1}H-NMR** (300

MHz, $CDCl_3$) δ 8.51 (s, 1H, Ar$H_{Triazole}$), 8.49 (s, 1H, Ar$H_{Coumarin}$), 7.50 (d, *J* = 8 Hz, 1H, Ar$H_{Coumarin}$), 6.89-6.84 (m, 2H, Ar$H_{Coumarin}$), 6.71 (s, 4H, Ar*H*), 6.52 (s, 4H, Ar*H*), 6.28 (s, 2H, N*H*), 6.21 (s, 2H, N*H*), 6.13 (s, 4H, N*H*), 5.21 (s, 2H, OCH_2C), 4.37 (d, *J* = 13 Hz, 2H, ArCH_2Ar), 4.25 (d, *J* = 13 Hz, 2H, ArCH_2Ar), 3.85 (t, *J* = 8 Hz, 2H, OCH_2CH$_2$CH$_3$), 3.67 (t, *J* = 7 Hz, 4H, OCH_2CH$_2$CH$_3$), 3.07 (d, *J* = 13 Hz, 2H, ArCH_2Ar), 3.02 (d, *J* = 13 Hz, 2H, ArCH_2Ar), 1.90 (sextet, *J* = 8 Hz, 2H, OCH$_2$CH_2CH$_3$), 1.81-1.70 (m, 4H, OCH$_2$CH_2CH$_3$), 1.50 (s, 9H, C(CH_3)$_3$), 1.49 (s, 9H, C(CH_3)$_3$), 1.47 (s, 18H, C(CH_3)$_3$), 0.96 (t, *J* = 7 Hz, 3H, OCH$_2$CH$_2$CH_3), 0.86 (t, *J* = 8 Hz, 6H, OCH$_2$CH$_2$CH_3); **^{13}C-NMR** (100 MHz, $CDCl_3$): δ 163.1, 162.8, 156.6, 155.0, 153.9, 153.8, 153.7, 153.1, 153.0, 151.2, 144.6, 136.1, 135.7, 135.1, 135.0, 134.7, 132.8, 132.1, 132.0, 130.4, 124.7, 120.4, 120.3, 120.1, 119.4, 115.2, 110.7, 103.2, 80.4, 77.3, 77.1, 77.0, 66.0, 37.0, 31.9, 31.6, 31.3, 28.6, 23.4, 23.2, 10.5, 10.5; **MALDI-TOF** m/z: $[M+Na]^+$ 1274.96.

Pyrene appended tetra-Boc-amino calix[4]arene (90)

A solution of **88** (0.69 g, 0.66 mmol), **84** (0.18 g, 0.69 mmol), sodium ascorbate (0.13 g, 0.66 mmol) and $CuSO_4.5H_2O$ (0.025 g, 0.099 mmol) in DMF (20 mL) were heated to 90 °C and stirred for 3 hours. After removal of solvent under reduced pressure, water (20 mL) was added then the product extracted with DCM (3 x 25 mL), washed with water (2 x 25 mL) then brine (25 mL) before drying and removing the solvent under reduced pressure. The product was purified by column chromatography over silica gel (eluent: 19:1 DCM/acetone) to give **90** as light yellow crystals (0.28 g, 32%). **Mp** 175-177 °C; **IR** ν 3499, 3480, 3445.5, 3416, 3323.5, 3292, 2973.5, 2932, 2872.5, 1698.5, 1694, 1605.5, 1595.5, 1519.5, 1475, 1456, 1415, 1390, 1365.5, 1293, 1241, 1214.5, 1150.5, 1059, 1045, 1000.5; **^{1}H-NMR** (400 MHz, $CDCl_3$) δ 8.28-8.25 (m, 3H, ArH_{Pyrene}), 8.17-8.14 (m, 3H, ArH_{Pyrene}), 8.11-8.06 (m, 2H, ArH_{Pyrene}), 7.90 (d, *J* = 8 Hz, 1H, ArH_{Pyrene}), 6.90 (s, 1H, Ar$H_{Triazole}$), 6.58 (s, 2H, Ar*H*), 6.53 (s, 2H, Ar*H*), 6.17 (s, 2H, CH_2), 6.12 (s, 2H, Ar*H*), 6.10 (s, 1H, N*H*), 6.04 (s, 2H, Ar*H*), 5.98 (s, 2H, N*H*), 5.84 (s, 1H, N*H*), 5.02 (s, 2H, OCH_2C), 4.28 (d, *J* = 13 Hz, 2H, ArCH_2Ar), 3.86 (d, *J* = 13 Hz, 2H, ArCH_2Ar), 3.73 (t, *J* = 7 Hz, 2H, OCH_2CH$_2$CH$_3$), 3.61-3.49 (m, 4H, OCH_2CH$_2$CH$_3$), 3.00 (d, *J* = 13 Hz, 2H, ArCH_2Ar), 2.41 (d, *J* = 13 Hz, 2H, ArCH_2Ar), 1.82 (sextet, *J* = 7 Hz, 2H, OCH$_2$CH_2CH$_3$), 1.68 (sextet, *J* = 7 Hz, 4H, OCH$_2$CH_2CH$_3$), 1.55 (s, 9H, C(CH_3)$_3$), 1.48 (s, 18H, C(CH_3)$_3$), 1.45 (s, 9H, C(CH_3)$_3$), 0.91 (t, *J* = 7 Hz, 3H, OCH$_2$CH$_2$CH_3), 0.77 (t, *J* = 7 Hz, 6H, OCH$_2$CH$_2$CH_3). **^{13}C-NMR** (100 MHz, $CDCl_3$) δ 153.43, 153.36, 153.22, 152.77,

150.13, 144.43, 135.66, 135.19, 135.16, 134.91, 132.37, 132.13, 131.99, 131.94, 131.24, 130.77, 129.29, 129.17, 128.43, 127.86, 127.48, 126.67, 126.08, 125.13, 124.58, 123.45, 122.29, 119.87, 119.81, 119.49, 119.40, 80.07, 80.05, 80.01, 77.36, 76.93, 76.72, 65.94, 52.40, 31.26, 31.14, 28.65, 28.56, 28.52, 23.26, 22.98, 22.98, 10.47, 10.30, 10.30; **MALDI-TOF** m/z: $[M+Na]^+$ 1329.41.

Anthracene appended tetra-Boc-amino calix[4]arene (91)

A solution of 9-bromomethyl-10-bromoanthracene (0.19 g, 0.70 mmol) and sodium azide (0.23 g, 3.50 mmol) in DMF (1.26 mL) was stirred under argon at 60 °C for 18 hours. After removal of the solvent under reduced pressure, water (20 mL) was added and the product extracted with ethyl acetate (3 x 10 mL). The combined organic extracts were washed with water (20 mL) then brine (20 mL), dried over $MgSO_4$ and the solvent removed under reduced pressure to give **86** as a yellow solid (0.12 g, 70%). **^{1}H-NMR** (400 MHz, $CDCl_3$) δ 8.67 – 8.63 (m, 2H, Ar*H*), 8.33 – 8.29 (m, 2H, Ar*H*), 7.66 – 7.62 (m, 4H, Ar*H*), 5.32 (s, 2H, CH_2). A solution of **88** (0.22 g, 0.21 mmol), **86** (0.054 g, 0.17 mmol), sodium ascorbate (0.032 g, 0.16 mmol) and $CuSO_4.5H_2O$ (0.008 g, 0.032 mmol) in DMF (3 mL) were heated to 90 °C and stirred for 3 hours. After removal of solvent under reduced pressure, water (20 mL) was added then the product extracted with DCM (3 x 25 mL), washed with water (2 x 25 mL) then brine (25 mL) before drying over $MgSO_4$ and removing the solvent under reduced pressure. The product was purified by column chromatography over silica gel (eluent: 2:1 hexane/ethyl acetate) to give **91** as light orange crystals (0.096 g, 47%). **Mp** 182-184 °C; **IR** ν 3416, 3325, 2970.5, 2930.5, 2874.5, 1698.5, 1595.5, 1519, 1470.5, 1415, 1390, 1365.5, 1324.5, 1292.5, 1242, 1215, 1151, 1062, 1001 cm^{-1}; **^{1}H-NMR** (400 MHz, $CDCl_3$) δ 8.70-8.68 (m, 2H, Ar$H_{Anthracene}$), 8.32-8.30 (m, 2H, Ar$H_{Anthracene}$), 7.69-7.62 (m, 4H, Ar$H_{Anthracene}$), 6.71 (s, 2H, Ar*H*), 6.60 (s, 1H, Ar$H_{Triazole}$), 6.49 (s, 2H, Ar*H*), 6.40 (s, 2H, Ar*H*), 6.32 (s, 2H, CH_2), 6.24 (s, 2H, Ar*H*), 6.17 (s, 1H, N*H*), 5.97 (s, 3H, N*H*), 4.99 (s, 2H, OCH_2C), 4.30 (d, *J* = 13 Hz, 2H, ArCH_2Ar), 3.81 (t, *J* = 8 Hz, 2H, OC$H_2$$CH_2CH_3$), 3.76 (d, *J* = 13 Hz, 2H, ArCH_2Ar), 3.52-3.39 (m, 4H, OC$H_2$$CH_2CH_3$), 3.02 (d, *J* = 13 Hz, 2H, ArCH_2Ar), 2.49 (d, *J* = 13 Hz, 2H, ArCH_2Ar), 1.90-1.90 (m, 2H, OCH_2CH_2CH_3), 1.66-1.55 (m, 4H, OCH_2CH_2CH_3), 1.57 (s, 9H, C(CH_3)$_3$), 1.49 (s, 9H, C(CH_3)$_3$), 1.44 (s, 18H, C(CH_3)$_3$), 0.90 (t, *J* = 7 Hz, 3H, OCH_2CH_2CH_3), 0.75 (t, *J* = 7 Hz, 6H, OCH_2CH_2CH_3). **^{13}C-NMR** (100 MHz, $CDCl_3$) δ 153.37, 153.25, 152.87, 152.83, 152.43, 149.92, 144.10, 136.07, 135.51, 134.47, 134.26, 132.40, 132.00, 131.76, 130.99, 130.22, 128.81,

127.83, 127.23, 126.03, 124.78, 123.29, 122.60, 119.91, 119.76, 119.58, 118.70, 79.89, 79.85, 79.74, 76.64, 76.56, 65.31, 60.34, 46.01, 31.05, 30.97, 28.48, 28.36, 23.01, 22.85, 10.27, 10.21; **MALDI-TOF** m/z: $[M+Na]^+$ 1383.67.

5,11,17,23-Tetra-Boc-glycine-25,26,27-tripropoxy-28-propargyloxy-calix[4]arene (92)

A solution of DCC (1.71 g, 8.29 mmol) in DCM (8 mL) was added to a solution of Boc-glycine (1.45 g, 8.29 mmol) in DCM (8 mL). This mixture was added to a stirred solution of **80** (0.6 g, 0.92 mmol) in DCM (8 mL). After 48 hours the precipitate was removed by filtration and the solvent removed under reduced pressure. The product was purified by column chromatography over silica gel (eluent: 19:1 DCM/methanol) to give **92** as a light orange glass (0.71 g, 61%). **Mp** 158-160 °C; **IR** ν 3292, 2968, 2925, 2869, 1668, 1599, 1501, 1465, 1416, 1389, 1364, 1268, 1242, 1211, 1157 cm^{-1}; **^{1}H-NMR** (300 MHz, DMSO) δ 9.77 (s, 2 H, ArN*H*), 9.31 (s, 2 H, ArN*H*), 7.29 (s, 4 H, Ar*H*), 7.05 (t, *J* = 6 Hz, 2 H, CH_2NH), 6.80 (s, *J* = 6 Hz, 2 H, CH_2NH), 6.60 (s, 4 H, Ar*H*), 4.94 (d, *J* = 2 Hz, 2 H, OCH_2CCH), 4.41 (d, *J* = 13 Hz, 2 H, $ArCH_2Ar$), 4.35 (d, *J* = 13 Hz, 2 H, $ArCH_2Ar$), 3.92 (t, *J* = 8 Hz, 2 H, $OCH_2CH_2CH_3$), 3.69-3.61 (m, 8 H, CH_2NH), 3.55-3.50 (m, 4 H, CH_2NH), 3.09 (d, *J* = 13 Hz, 4 H, $ArCH_2Ar$), 1.99-1.81 (m, 6 H, $OCH_2CH_2CH_3$), 1.40 (s, 18 H, $C(CH_3)_3$), 1.36 (s, 18 H, $C(CH_3)_3$), 1.03 (t, *J* = 7 Hz, 6 H, $OCH_2CH_2CH_3$), 0.91 (t, *J* = 7 Hz, 3 H, $OCH_2CH_2CH_3$); **^{13}C NMR** (100 MHz, CD_3OD): δ 168.9, 168.5, 157.3, 152.6, 151.5, 137.5, 136.3, 133.7, 133.5, 133.3, 132.5, 132.0, 120.9, 120.5, 120.4, 80.3, 79.5, 79.3, 77.3, 77.0, 75.4, 59.5, 53.7, 43.8, 43.5, 31.5, 30.8, 27.6, 27.5, 23.4, 23.3, 10.1, 9.3; **HRMS** (NSI) m/z: $[M+NH_4]^+$ Calcd for $C_{68}H_{96}N_9O_{16}$ 1294.6970; Found 1294.6967.

Coumarin appended tetra-Boc-glycine calix[4]arene (93)

A solution of **92** (0.39 g, 0.31 mmol), **82** (0.13 g, 0.64 mmol), sodium ascorbate (0.06 g, 0.30 mmol) and $CuSO_4.5H_2O$ (0.012 g, 0.04 mmol) in DMF (10 mL) were heated to 90 °C and stirred for 18 hours. After removal of solvent under reduced pressure, water (20 mL) was added. The product was extracted with 4:1 DCM/methanol before drying and removing the solvent under reduced pressure. The product was purified by column chromatography over silica gel (eluent: 97:3 DCM/methanol) to give **93** as a light yellow glass (0.15 g, 33%). **Mp** >250 °C (decomp.); **IR** ν 3301, 2981, 2939, 2883, 1682, 1609, 1519, 1475, 1423, 1394, 1368, 1226, 1164 cm^{-1}; **^{1}H-NMR** (400 MHz, CD_3OD) δ 8.58 (s, 1 H, $ArH_{Triazole}$), 8.57 (s, 1

H, Ar$H_{Coumarin}$), 7.70 (d, J = 9 Hz, 1 H, Ar$H_{Coumarin}$), 6.96-6.85 (m, 10 H, ArH), 5.28 (s, 2 H, OCH_2C), 4.49 (d, J = 13 Hz, 2 H, ArCH_2Ar), 4.40 (d, J = 13 Hz, 2 H, ArCH_2Ar), 3.93 (t, J = 7 Hz, 2 H, OCH_2CH$_2$CH$_{3)}$, 3.83 (t, J = 8 Hz, 4 H, OCH_2CH$_2$CH$_{3)}$, 3.77 (s, 8 H, CH_2NH), 3.14 (d, J = 13 Hz, 2 H, ArCH_2Ar), 3.10 (d, J = 13 Hz, 2 H, ArCH_2Ar), 2.04 (sextet, J = 7 Hz, 2 H, OCH$_2$CH_2CH$_3$), 1.97-1.85 (m, 4 H, OCH$_2$CH_2CH$_3$), 1.49 (s, 36 H, C(CH_3)$_3$), 1.08 (t, J = 7 Hz, 3 H, OCH$_2$CH$_2$CH_3), 0.96 (t, J = 8 Hz, 6 H, OCH$_2$CH$_2$CH_3); **^{13}C-NMR** (100 MHz, CD$_3$OD): δ 168.7, 163.1, 157.3, 156.7, 155.2, 153.4, 153.2, 151.6, 144.2, 135.6, 135.0, 132.8, 132.1, 130.9, 125.3, 120.6, 119.3, 114.5, 110.7, 102.2, 80.3, 79.6, 77.0, 66.1, 43.7, 31.3, 30.9, 29.6, 27.7, 23.4, 23.1, 9.9, 9.6; **MALDI-TOF** m/z: [M+Na]$^+$ 1503.38.

Coumarin appended tetra-amino calix[4]arene (·4HCl) (94)

$HCl_{(g)}$ was bubbled through a solution of **89** (0.16 g, 0.13 mmol) in DCM (12 mL). After 15 minutes, methanol (5 mL) was added to dissolve the precipitate and after a further 5 minutes the solvent was evaporated to give **94** as light orange-brown powder (0.12 g, 99%). **Mp** 280 °C (decomp.); **IR** ν 3391, 3064, 2958.5, 2927.5, 2872.5, 2589, 1729, 1699, 1608, 1575, 1516, 1466.5, 1386, 1310.5, 1281.5, 1228, 1217, 1148.5, 1124.5, 1042, 1000.5 cm^{-1}; **^{1}H-NMR** (400 MHz, CD$_3$OD) δ 8.54 (s, 2H, Ar$H_{Coumarin}$ and Ar$H_{Triazole}$), 7.67 (d, J = 9 Hz, 1H, Ar$H_{Coumarin}$), 6.92 (dd, J = 9, 2 Hz, 1H, Ar$H_{Coumarin}$), 6.84-6.79 (m, 9H, ArH and Ar$H_{Coumarin}$), 5.30 (s, 2H, OCH_2C), 4.54 (d, J = 13 Hz, 2H, ArCH_2Ar), 4.45 (d, J = 14 Hz, 2H, ArCH_2Ar), 3.98 (t, J = 7 Hz, 2H, OCH_2CH$_2$CH$_3$), 3.88 (t, J = 7 Hz, 4H, OCH_2CH$_2$CH$_3$), 3.36 (d, J = 13 Hz, 2H, ArCH_2Ar), 3.32 (d, J = 14 Hz, 2H, ArCH_2Ar), 2.01 (sextet, J = 7 Hz, 2H, OCH$_2$CH_2CH$_3$), 1.94-1.85 (m, 4H, OCH$_2$CH_2CH$_3$), 1.07 (t, J = 7 Hz, 3H, OCH$_2$CH$_2$CH_3), 0.95 (t, J = 7 Hz, 6H, OCH$_2$CH$_2$CH_3); **^{13}C-NMR** (100 MHz, CD$_3$OD) δ 164.53, 158.16, 158.08, 157.96, 156.57, 156.17, 144.46, 138.37, 137.70, 137.58, 137.23, 132.03, 126.86, 126.47, 125.87, 125.82, 124.54, 124.44, 124.40, 120.59, 115.72, 111.91, 103.45, 78.70, 78.63, 67.43, 31.99, 31.62, 24.53, 24.30, 10.77, 10.59; **HRMS** (NSI) m/z: [M+H]$^+$ Calcd for $C_{49}H_{54}N_7O_7$ 852.4079; Found 852.4055.

Pyrene appended tetra-amino calix[4]arene (·4HCl) (95)

$HCl_{(g)}$ was bubbled through a solution of **90** (0.16 g, 0.12 mmol) in DCM (12 mL). After 15 minutes, methanol (5 mL) was added to dissolve the precipitate and after a further 5 minutes the solvent was evaporated to give **95** as a brown solid (0.13 g, 99%). **Mp** 280 °C (decomp); **IR** ν 3382, 2958, 2919.5, 2870, 2594.5, 1603.5, 1586.5,

1523, 1465.5, 1385, 1309.5, 1280, 1249, 1216.5, 1147.5, 1129.5, 1062.5, 1041 cm^{-1}; **^{1}H-NMR** (400 MHz, CD_3OD) δ 8.38 (d, *J* = 9 Hz, 1H, ArH_{Pyrene}), 8.30-8.03 (m, 8H, ArH_{Pyrene}), 7.84 (s, 1H, Ar$H_{Triazole}$), 6.81 (d, *J* = 2 Hz, 2H, Ar*H*), 6.75 (d, *J* = 2 Hz, 2H, Ar*H*), 6.69 (s, 2H, Ar*H*), 6.67 (s, 2H, Ar*H*), 6.39 (s, 2H, CH_2), 5.06 (s, 2H, OCH_2C), 4.36 (d, *J* = 13.5 Hz, 2H, ArCH_2Ar), 4.11 (d, *J* = 13.5 Hz, 2H, ArCH_2Ar), 3.79 (t, *J* = 7 Hz, 2H, OCH_2CH$_2$CH$_3$), 3.54-3.41 (m, 4H, OCH_2CH$_2$CH$_3$), 3.21 (d, *J* = 13.5 Hz, 2H, ArCH_2Ar), 2.95 (d, *J* = 13.5 Hz, 2H, ArCH_2Ar), 1.83 (sextet, *J* = 7 Hz 2H, OCH$_2$CH_2CH$_3$), 1.52-1.42 (m, 4H, OCH$_2$CH_2CH$_3$), 0.94 (t, *J* = 7 Hz, 3H, OCH$_2$CH$_2$CH_3), 0.52 (t, *J* = 7 Hz, 6H, OCH$_2$CH$_2$CH_3); **^{13}C-NMR** (100 MHz, CD_3OD) δ 157.92, 157.44, 155.80, 144.63, 137.67, 137.60, 137.51, 137.08, 133.30, 132.40, 131.73, 130.22, 129.85, 129.19, 129.02, 128.95, 128.27, 127.47, 126.91, 126.74, 126.20, 126.10, 125.96, 125.68, 125.64, 125.40, 124.45, 124.34, 124.15, 123.23, 78.43, 78.13, 67.31, 53.17, 31.73, 31.33, 24.31, 23.85, 10.75, 10.23; **HRMS** (NSI) m/z: $[M+H]^+$ Calcd for $C_{57}H_{60}N_7O_4$ 906.4701; Found 906.4691.

Anthracene appended tetra-amino calix[4]arene (·4HCl) (96)

$HCl_{(g)}$ was bubbled through a solution of **91** (0.096 g, 0.075 mmol) in DCM (2 mL). After 15 minutes, methanol (5 mL) to dissolve the precipitate and after a further 5 minutes the solvent was evaporated to give **96** as a brown solid (0.077 g, 99%). **Mp** 240 °C (decomp.); **IR** ν 3390, 2958.5, 2921, 2871.5, 2592.5, 2356.5, 2343, 1583.5, 1526, 1465.5, 1445, 1385, 1323, 1310, 1280, 1257.5, 1216.5, 1147.5, 1129.5, 1117.5, 1063, 1038 cm^{-1}; **^{1}H-NMR** (400 MHz, CD_3OD) δ 8.69-8.66 (m, 2H, Ar$H_{Anthracene}$), 8.59-8.57 (m, 2H, Ar$H_{Anthracene}$), 7.74-7.71 (m, 5H, Ar$H_{Anthracene}$), 7.59 (s, 1H, Ar$H_{Triazole}$), 6.80 (d, *J* = 2.0 Hz, 3H, Ar*H*), 6.73 (s, 2H Ar*H*), 6.71 (d, *J* = 1.9 Hz, 2H, Ar*H*), 6.67 (s, 2H, CH_2), 6.59 (s, 2H, Ar*H*), 5.00 (s, 2H, OCH_2C), 4.38 (d, *J* = 13.5 Hz, 2H, ArCH_2Ar), 4.02 (d, *J* = 13.5 Hz, 2H, ArCH_2Ar), 3.79 (t, *J* = 7 Hz, 2H, OCH_2CH$_2$CH$_3$), 3.58-3.41 (m, 4H, OCH_2CH$_2$CH$_3$), 3.23 (d, *J* = 13.5 Hz, 2H, ArCH_2Ar), 2.83 (d, *J* = 13.5 Hz, 2H, ArCH_2Ar), 1.84 (sextet, *J* = 7 Hz, 2H, OCH$_2$CH_2CH$_3$), 1.50-1.40 (m, 4H, OCH$_2$CH_2CH$_3$), 0.96 (t, *J* = 7 Hz, 3H, OCH$_2$CH$_2$CH_3), 0.53 (t, *J* = 7 Hz, 6H, OCH$_2$CH$_2$CH_3); **^{13}C-NMR** (100 MHz, CD_3OD) δ 157.96, 157.58, 155.75, 144.60, 137.75, 137.62, 137.50, 137.25, 132.55, 131.69, 129.78, 129.04, 128.58, 127.07, 126.76, 125.81, 125.27, 125.17, 124.42, 124.32, 124.18, 78.53, 78.23, 67.24, 47.37, 31.74, 31.45, 24.41, 23.94, 10.76, 10.41; **HRMS** (NSI) m/z: $[M+H]^+$ Calcd for $C_{55}H_{59}BrN_7O_4$ 960.3806; Found 960.3810.

Coumarin appended tetra-glycine calix[4]arene (·4HCl) (97)

$HCl_{(g)}$ was bubbled through a solution of **93** (0.088 g, 0.059 mmol) in DCM (6 mL). After 15 minutes, methanol (5 mL) to dissolve the precipitate and after a further 5 minutes the solvent was evaporated to give **97** as beige powder (0.072 g, 99%). **Mp** >300 °C (decomp.); **^{1}H-NMR** (400 MHz, CD_3OD) δ 8.56 (s, 1H, Ar$H_{Triazole}$), 8.56 (s, 1H, Ar$H_{Coumarin}$), 7.67 (d, *J* = 9 Hz, 1H, Ar$H_{Coumarin}$), 6.97 (s, 2H, Ar*H*), 6.95 (s, 2H, Ar*H*), 6.91 (dd, *J* = 9, 2 Hz, 1H, Ar$H_{Coumarin}$), 6.91 (s, 2H, Ar*H*), 6.90 (s, 2H, Ar*H*), 6.83 (d, *J* = 2 Hz, 1H, Ar$H_{Coumarin}$), 5.27 (s, 2H, OCH_2C), 4.49 (d, *J* = 13 Hz, 2H, ArCH_2Ar), 4.41 (d, *J* = 13 Hz, 2H, ArCH_2Ar), 3.91 (t, *J* = 8 Hz, 2H, OCH_2CH$_2$CH$_3$), 3.82 (t, *J* = 8 Hz, 4H, OCH_2CH$_2$CH$_3$), 3.76 (s, 8H, CH_2NH$_3^+$), 3.14 (d, *J* = 13 Hz, 2H, ArCH_2Ar), 3.11 (d, *J* = 13 Hz, 2H, ArCH_2Ar), 2.06-1.97 (m, 2H, OCH$_2$CH_2CH$_3$), 1.94-1.83 (m, 4H, OCH$_2$CH_2CH$_3$), 1.05 (t, *J* = 7 Hz, 3H, OCH$_2$CH$_2$CH_3), 0.93 (t, *J* = 7 Hz, 6H, OCH$_2$CH$_2$CH_3); **^{13}C-NMR** (100 MHz, CD_3OD) δ 164.93, 164.39, 157.98, 156.48, 154.75, 154.62, 152.94, 145.22, 137.00, 136.82, 136.40, 136.26, 136.21, 133.59, 132.90, 131.99, 126.57, 121.78, 120.61, 115.65, 111.92, 103.42, 78.30, 67.20, 42.12, 32.43, 32.01, 24.53, 24.29, 10.86, 10.69; **MALDI-TOF** m/z: $[M+H]^+$ 1081.17, $[M+Na]^+$ 1103.16.

5,11,17,23-Tetra-*tert*-butyl-25,26,27-tripropoxy-28-[*tert*-butyl(dimethyl)silyl]-propargyloxy-calix[4]arene (98)

To a stirred solution of **78** (7.31 g, 9.00 mmol) in THF (63 mL) cooled to -80 °C was added 1 M LiHMDS in THF (9.45 mL, 9.45 mmol). After 5 minutes, TBDMSCl (2.03 g, 13.50 mmol) in 3 mL of THF was added dropwise. The reaction mixture was allowed to warm to room temperature and stirred for 18 hours. The reaction was quenched with saturated ammonium chloride, extracted with DCM (3 x 100 mL) and the combined organic extracts washed with water (200 mL) then brine (200 mL). After drying over $MgSO_4$ the solution was concentrated under reduced pressure to an orange oil and **98** was precipitated with methanol as white crystals (7.77 g, 93%). **Mp** 152-154 °C; **IR** ν 2957.5, 2933.5, 2902.5, 2873, 2860, 2175.5, 1601.5, 1583.5, 1505, 1480, 1470.5, 1415, 1389.5, 1361, 1300, 1279, 1248, 1239.5, 1200, 1121, 1105.5, 1070.5, 1045, 1032.5, 1010 cm^{-1}; **^{1}H-NMR** (400 MHz, $CDCl_3$) δ 7.42 (s, 2H, Ar*H*), 7.36 (s, 2H, Ar*H*), 6.89 (d, *J* = 2 Hz, 2H, Ar*H*), 6.82 (d, *J* = 2 Hz, 2H, Ar*H*), 5.42 (s, 2H, OCH_2C), 4.83 (d, *J* = 12.5 Hz, 2H, ArCH_2Ar), 4.77 (d, *J* = 12.5 Hz, 2H, ArCH_2Ar), 4.30 – 4.26 (m, 2H, OCH_2CH$_2$CH$_3$), 4.09 – 4.00 (m, 4H, OCH_2CH$_2$CH$_3$), 3.48 (d, *J* = 12.5 Hz, 2H, ArCH_2Ar), 3.46 (d, *J* = 12.5 Hz, 2H, ArCH_2Ar), 2.52– 2.42

(m, 2H, $OCH_2CH_2CH_3$), 2.39 – 2.24 (m, 4H, $OCH_2CH_2CH_3$), 1.65 (s, 9H, $C(CH_3)_3$), 1.64 (s, 9H, $C(CH_3)_3$), 1.42 (t, *J* = 7.5 Hz, 6H, $OCH_2CH_2CH_3$), 1.32 (t, *J* = 7.5 Hz, 3H, $OCH_2CH_2CH_3$), 1.22 (s, 18H, $C(CH_3)_3$), 1.17 (s, 9H, $SiC(CH_3)_3$), 0.37 (s, 6H, $SiCH_3$); **^{13}C-NMR** (100 MHz, $CDCl_3$) δ 154.56, 153.23, 151.74, 145.34, 144.75, 144.13, 136.69, 135.59, 132.62, 132.27, 125.46, 125.11, 124.64, 124.47, 104.31, 89.73, 77.54, 59.48, 34.17, 33.73, 32.37, 31.87, 31.81, 31.70, 31.55, 31.49, 31.35, 31.11, 26.13, 23.78, 23.63, 16.56, 10.90, 10.21, -4.57; **HRMS** (NSI) m/z: $[M+NH_4]^+$ Calcd for $C_{62}H_{94}O_4SiN$ 944.6947; Found 944.6936.

5,11,17,23-Tetranitro-25,26,27-tripropoxy-28-[*tert*-butyl(dimethyl)silyl]-propargyloxy-calix[4]arene (99)

Compound **98** (4.08 g, 4.40 mmol) was dissolved in 100 mL DCM. Glacial acetic acid (23 mL) and 100% nitric acid (23 mL) were added and the resulting blue-black solution was stirred until the colour changed to bright orange. Water (100 mL) was added to quench. The product was extracted with DCM (3 x 100 mL) then washed with water (3 x 200 mL) and brine (200 mL). After drying over $MgSO_4$ the solvent was removed under reduced pressure and the product triturated with methanol to give **99** as light yellow powder (3.22 g, 83%). **Mp** 238-240 °C; **IR** ν 3079.5, 2958.5, 2936, 2927.5, 2877.5, 2857, 2170, 1609, 1586.5, 1523.5, 1455.5, 1343.5, 1299.5, 1286.5, 1263.5, 1233, 1209.5, 1202, 1159, 1096.5, 1060, 1041.5, 1018.5 cm^{-1}; **^{1}H-NMR** (300 MHz, $CDCl_3$) δ 8.08 (s, 2H, Ar*H*), 8.07 (s, 2H, Ar*H*), 7.16 (s, 4H, Ar*H*), 5.00 (s, 2H, OCH_2C), 4.57 (d, *J* = 14 Hz, 2H, $ArCH_2Ar$), 4.54 (d, *J* = 14 Hz, 2H, $ArCH_2Ar$), 4.15 – 4.10 (m, 2H, $OCH_2CH_2CH_3$), 3.87 – 3.75 (m, 4H, $OCH_2CH_2CH_3$), 3.41 (d, *J* = 14 Hz, 2H, $ArCH_2Ar$), 3.41 (d, *J* = 14 Hz, 2H, $ArCH_2Ar$), 2.00 – 1.84 (m, 6H, $OCH_2CH_2CH_3$), 1.10 (t, *J* = 7 Hz, 6H, $OCH_2CH_2CH_3$), 0.97 (t, *J* = 7 Hz, 3H, $OCH_2CH_2CH_3$), 0.80 (s, 9H, $SiC(CH_3)_3$), 0.01 (s, 6H, $SiCH_3$); **^{13}C-NMR** (100 MHz, $CDCl_3$) δ 162.81, 160.84, 159.81, 143.75, 143.08, 138.34, 136.61, 134.62, 134.08, 124.85, 124.46, 123.45, 123.32, 99.91, 93.45, 78.17, 78.02, 60.79, 31.64, 31.07, 25.84, 23.53, 23.34, 16.36, 10.63, 10.02, -4.82; **HRMS** (NSI) m/z: $[M+H]^+$ Calcd for $C_{46}H_{55}N_4O_{12}Si$ 883.3580, Found 883.3586.

5,11,17,23-Tetraamino-25,26,27-tripropoxy-28-[*tert*-butyl(dimethyl)silyl]-propargyloxy-calix[4]arene (100)

A solution of **99** (2.86 g, 3.24 mmol) and $SnCl_2{\cdot}2H_2O$ (19.01 g, 84.24 mmol) in ethanol (216 mL) were heated to reflux for 48 hours. After removing the solvent under

reduced pressure, 10% NaOH (200 mL) was added, then the product extracted with DCM (3 x 100 mL). The organic layer was washed with water (200 mL) and brine (200 mL). After drying over $MgSO_4$ and removing the solvent under reduced pressure, **100** was obtained as an orange-brown glass (2.22 g, 90%). **Mp** 157-159 °C; **IR** ν 3415.5, 3349, 3215.5, 2999.5, 2958.5, 2926, 2900, 2874, 2853.5, 2171, 1608, 1467.5, 1384.5, 1361.5, 1304.5, 1281, 1247, 1212, 1164.5, 1152, 1130.5, 1106.5, 1068, 1035.5, 1026, 1005.5 cm^{-1}; **^{1}H-NMR** (400 MHz, $CDCl_3$) δ 6.37 (s, 2H, Ar*H*), 6.33 (s, 2H, Ar*H*), 5.80 (s, 2H, Ar*H*), 5.80 (s, 2H, Ar*H*), 4.81 (s, 2H, OCH_2C), 4.36 (d, *J* = 13 Hz, 2H, ArCH_2Ar), 4.32 (d, *J* = 13 Hz, 2H, ArCH_2Ar), 3.86 – 3.82 (m, 2H, OCH_2CH$_2$CH$_3$), 3.61 (t, *J* = 7 Hz, 4H, OCH_2CH$_2$CH$_3$), 2.92 (d, *J* = 13 Hz, 4H, ArCH_2Ar), 1.95 – 1.81 (m, 6H, OCH$_2$CH_2CH$_3$), 1.02 (t, *J* = 7 Hz, 6H, OCH$_2$CH$_2$CH_3), 0.90 (t, *J* = 7.5 Hz, 3H, OCH$_2$CH$_2$CH_3), 0.85 (s, 9H, SiC(CH_3)$_3$), 0.03 (s, 6H, SiCH_3); **^{13}C-NMR** (100 MHz, $CDCl_3$) δ 150.63, 149.37, 147.76, 141.10, 140.46, 140.40, 138.19, 137.07, 134.48, 133.97, 115.95, 115.67, 115.58, 115.44, 104.19, 89.26, 77.12, 76.84, 59.85, 31.86, 31.10, 26.05, 23.51, 23.13, 16.50, 10.84, 10.23, -4.61; **HRMS** (NSI) m/z: $[M+H]^+$ Calcd for $C_{46}H_{63}N_4O_4Si$ 763.4613; Found 763.4613.

5,11,17,23-Tetraamino-25,26,27-tripropoxy-28-propargyloxy-calix[4]arene (80)

To a stirred solution of **100** (1.05 g, 1.38 mmol) in THF (10 mL) was added 1 M TBAF in THF (6.9 mL, 6.9 mmol) and the mixture stirred for 18 hours. The reaction was quenched with saturated ammonium chloride, extracted with DCM (3 x 100 mL) and the combined organic extracts washed with water (200 mL) then brine (200 mL). After drying over $MgSO_4$ the solvent was removed under reduced pressure and the residue triturated with hexane. After filtration and air drying **80** was obtained as light brown powder (0.7 g, 79%). **Mp** >180 °C (decomp.); **IR** ν 3310, 2966, 2934, 2878, 1737, 1608, 1469, 1387, 1310, 1285, 1215, 1158, 1129 cm^{-1}; **^{1}H-NMR** (300 MHz, $CDCl_3$): δ 6.41 (s, 4 H, Ar*H*), 5.78 (s, 2 H, Ar*H*), 5.77 (s, 2 H, Ar*H*), 4.77 (d, *J* = 2 Hz, 2 H, OCH_2CCH), 4.39 (d, *J* = 14 Hz, 2 H, ArCH_2Ar), 4.32 (d, *J* = 13 Hz, 2 H, ArCH_2Ar), 3.86 (t, *J* = 8 Hz, 2 H, OCH_2CH$_2$CH$_3$), 3.61 (t, *J* = 7 Hz, 4 H, OCH_2CH$_2$CH$_3$), 2.95 (d, *J* = 14 Hz, 2 H, ArCH_2Ar), 2.92 (d, *J* = 13 Hz, 2 H, ArCH_2Ar), 2.31 (t, *J* = 2.4 Hz, 1 H, OCH$_2$CC*H*), 1.88 (sextet, *J* = 8 Hz, 2 H, OCH$_2$CH_2CH$_3$), 1.84 (sextet, *J* = 7 Hz, 4 H, OCH$_2$CH_2CH$_3$), 1.04 (t, *J* = 7 Hz, 6 H, OCH$_2$CH$_2$CH_3), 0.97 (t, *J* = 8 Hz, 3 H, OCH$_2$CH$_2$CH_3); **^{13}C-NMR** (100 MHz, $CDCl_3$): δ 150.6, 149.6, 147.9, 141.4, 140.4, 139.2, 138.1, 137.1, 134.3, 134.1, 116.2,

116.0, 115.8, 81.4, 74.2, 59.5, 31.6, 31.0, 23.5, 23.1, 10.9, 10.1; **HRMS** (NSI) m/z: $[M+H]^+$ Calcd for $C_{40}H_{49}N_4O_4$ 649.3748; Found 649.3745.

5,11,17,23-Tetrakis[(N,N′-di-Boc)guanidine]-25,26,27-tripropoxy-28-propargyloxy-calix[4]arene (101)

A mixture of **80** (0.30 g, 0.46 mmol), bis-Boc-methylthiopseudourea (0.64 g, 2.21 mmol) and $HgCl_2$ (0.6 g, 2.21 mmol) were stirred under argon in dry DMF (10 mL). Triethylamine (0.77 mL, 5.52 mmol) was added and the mixture stirred for 48 hours. The solvent was removed under reduced pressure and the product dissolved in DCM (10 mL). The HgSMe was removed by filtration, washed with DCM and the filtrate washed with water (100 mL) and brine (100 mL). After drying over $MgSO_4$, the solvent was removed under reduced pressure and the solid recrystallized from minimum hexane, the excess reagent filtered off, then the filtrate purified by column chromatography over silica gel (eluent: 8:1:1 hexane/diethyl ether/triethylamine) to give **101** as white crystals (0.10 g, 13%). **IR** ν 3263, 2972, 2878, 1716, 1621, 1455, 1409, 1393, 1366, 1249, 1214, 1142, 1102, 1057, 1003; **^{1}H-NMR** (400 MHz, $CDCl_3$) δ 11.62 (s, 1H, N*H*$_{Guanidine}$), 11.60 (s, 1H, N*H*$_{Guanidine}$), 11.46 (s, 2H, N*H*$_{Guanidine}$), 10.22 (s, 1H, ArN*H*), 10.14 (s, 1H, ArN*H*), 9.41 (s, 2H, ArN*H*), 7.20 (s, 2H, Ar*H*), 7.19 (s, 2H, Ar*H*), 6.63 (d, *J* = 2.4 Hz, 2H, Ar*H*), 6.56 (d, *J* = 2.4 Hz, 2H, Ar*H*), 4.94 (d, *J* = 2 Hz, 2H, OC*H*$_2$CCH), 4.44 (d, *J* = 13 Hz, 2H, ArC*H*$_2$Ar), 4.36 (d, *J* = 13 Hz, 2H, ArC*H*$_2$Ar), 3.96 – 3.90 (m, 2H, OC*H*$_2$CH$_2$CH$_3$), 3.60 (t, *J* = 7 Hz, 4H, OC*H*$_2$CH$_2$CH$_3$), 3.12 (d, *J* = 13 Hz, 2H, ArC*H*$_2$Ar), 3.11 (d, *J* = 13 Hz, 2H, ArC*H*$_2$Ar), 2.27 (t, *J* = 2 Hz, 1H, OCH$_2$CC*H*), 2.00 – 1.79 (m, 6H, OCH$_2$C*H*$_2$CH$_3$), 1.46 (s, 18H, C(CH$_3$)$_3$), 1.44 (s, 9H, C(CH$_3$)$_3$), 1.43 (s, 9H, C(CH$_3$)$_3$), 1.39 (s, 18H, C(CH$_3$)$_3$), 1.36 (s, 18H, C(CH$_3$)$_3$), 0.97 (t, *J* = 7 Hz, 6H, OCH$_2$CH$_2$C*H*$_3$), 0.87 (t, *J* = 7 Hz, 3H, OCH$_2$CH$_2$C*H*$_3$); **^{13}C-NMR** (100 MHz, $CDCl_3$) δ 163.64, 163.47, 154.43, 153.66, 153.39, 153.33, 153.19, 152.87, 151.88, 137.02, 135.89, 133.22, 133.12, 131.91, 130.93, 130.67, 123.35, 122.90, 122.30, 83.28, 83.22, 82.77, 81.07, 79.33, 79.26, 78.93, 77.44, 76.87, 74.83, 59.38, 31.95, 31.21, 28.22, 28.15, 28.06, 23.37, 23.04, 10.63, 9.96; **MALDI-TOF** m/z: $[M+NH_4]^+$ 1634.9.

5,11,17,23-Tetraguanidine-25,26,27-tripropoxy-28-propargyloxy-calix[4]arene (104)

Route 1:

A mixture of **100** (0.50 g, 0.66 mmol), bis-Boc-methylthiopseudourea (0.92 g, 3.17

mmol) and $HgCl_2$ (0.86 g, 3.17 mmol) were stirred under argon in dry DMF (9 mL). Triethylamine (1.10 mL, 7.92 mmol) was added and the mixture stirred for 24 hours. The solvent was removed under reduced pressure and the product dissolved in DCM (10 mL). The HgSMe was removed by filtration, washed with DCM and the filtrate washed with water (2 x 100 mL) and brine (100 mL). After drying over $MgSO_4$, the solvent was removed under reduced pressure to give a light orange solid, the identity of which was verified by ^{1}H-NMR as **102** with residual reagent. **^{1}H-NMR** (400 MHz, $CDCl_3$) δ 11.68 (s, 1H, N*H*$_{Guanidine}$), 11.64 (s, 1H, N*H*$_{Guanidine}$), 11.53 (s, 2H, N*H*$_{Guanidine}$), 10.20 (s, 1H, ArN*H*), 10.17 (s, 1H, ArN*H*), 9.52 (s, 2H, ArN*H*), 7.28 (s, 2H, Ar*H*), 7.21 (s, 2H, Ar*H*), 6.74 (d, *J* = 2 Hz, 2H, Ar*H*), 6.65 (d, *J* = 2 Hz, 2H, Ar*H*), 4.99 (s, 2H, OC*H*$_2$C), 4.51 (d, *J* = 13 Hz, 2H, ArC*H*$_2$Ar), 4.42 (d, *J* = 13 Hz, 2H, ArC*H*$_2$Ar), 3.99 – 3.95 (m, 2H, OC*H*$_2$CH$_2$CH$_3$), 3.67 (t, *J* = 7 Hz, 4H, OC*H*$_2$CH$_2$CH$_3$), 3.17 (d, *J* = 13 Hz, 2H, ArC*H*$_2$Ar), 3.16 (d, *J* = 13 Hz, 2H, ArC*H*$_2$Ar), 2.01 – 1.88 (m, 6H, OCH$_2$C*H*$_2$CH$_3$), 1.52 (s, 9H, C(CH$_3$)$_3$), 1.51 (s, 9H, C(CH$_3$)$_3$), 1.49 (s, 9H, C(CH$_3$)$_3$), 1.49 (s, 9H, C(CH$_3$)$_3$), 1.45 (s, 18H, C(CH$_3$)$_3$), 1.43 (s, 18H, C(CH$_3$)$_3$), 1.02 (t, *J* = 7 Hz, 6H, OCH$_2$CH$_2$C*H*$_3$), 0.93 (t, *J* = 7 Hz, 3H, OCH$_2$CH$_2$C*H*$_3$), 0.87 (s, 9H, Si(CH$_3$)$_3$), 0.05 (s, 6H, SiC*H*$_3$). Half of this material was dissolved in THF (3 mL) and stirred with TBAF (3.3 mL, 1 M in THF, 3.3 mmol) for 18 hours. The reaction was quenched with saturated aqueous ammonium chloride and the product extracted with diethyl ether (3 x 50 mL). After washing with water (100 mL) then brine (100 mL) and drying with $MgSO_4$, the solvent was removed under reduced pressure. ^{1}H-NMR verified the reappearance of the terminal alkyne. The residue was redissolved in DCM (10 mL) and $HCl_{(g)}$ bubbled through the solution for 30 minutes. Methanol was added to dissolve the resulting precipitate and the solution stirred for a further 1.5 hours. The solvent was removed under reduced pressure and the product purified by column chromatography over C18 (eluent: methanol in water, 5-65%, 65%, then 65-100%) to give **104** as off white solid (0.07 g, 21% over three steps).

Route 2:

A mixture of **100** (0.70 g, 0.92 mmol), bis-Boc-methylthiopseudourea (1.20 g, 4.14 mmol) and $HgCl_2$ (1.12 g, 4.14 mmol) were stirred under argon in dry DMF (25 mL). Triethylamine (1.53 mL, 11.04 mmol) was added and the mixture stirred for 24 hours. The solvent was removed under reduced pressure and the product dissolved in DCM (10 mL). The HgSMe was removed by filtration, washed with DCM and the filtrate washed with water (2 x 100 mL) and brine (100 mL). After drying over $MgSO_4$, the

solvent was removed under reduced pressure to give a light orange solid, the identity of which was verified by ^{1}H-NMR as **102** with residual reagent. The solid was dissolved in DCM (30 mL) and $HCl_{(g)}$ bubbled through the solution for 30 minutes. Methanol was added to dissolve the resulting precipitate and the solution stirred for 1 hour. Removal of solvent under reduced pressure gave a light grey-green solid. Complete removal of Boc groups was verified by ^{1}H-NMR. The solid was suspended in THF (9 mL) and stirred with TBAF (9.2 mL, 1 M in THF, 9.2 mmol) for 18 hours. The reaction was quenched with saturated aqueous ammonium chloride and the precipitate filtered and washed with THF. The solvent was removed from the filtrate under reduced pressure and the residue purified by column chromatography over C18, 0-100% methanol in water to give **104** as off-white solid (0.21 g, 24% over three steps). **Mp** 280 °C (decomp.); **IR** ν 3310.5, 3144.5, 2961, 2934.5, 2874.5, 1667, 1651, 1644.5, 1633.5, 1621.5, 1615, 1581.5, 1463.5, 1386, 1286, 1218.5, 1175.5, 1123.5, 1104.5, 1065, 1042, 1001 cm^{-1}; **^{1}H-NMR** (400 MHz, CD_3OD) δ 7.07 (s, 2H, Ar*H*), 7.06 (s, 2H, Ar*H*), 6.36 (s, 4H, Ar*H*), 4.99 (d, *J* = 2 Hz, 2H, OC*H*$_2$CCH), 4.62 (d, *J* = 13 Hz, 2H, ArC*H*$_2$Ar), 4.54 (d, *J* = 13 Hz, 2H, ArC*H*$_2$Ar), 4.11 – 4.07 (m, 2H, OC*H*$_2$CH$_2$CH$_3$), 3.82 (t, *J* = 7 Hz, 4H, OC*H*$_2$CH$_2$CH$_3$), 2.95 (t, *J* = 2 Hz, 1H, OCH$_2$CC*H*), 2.12 – 1.95 (m, 6H, OCH$_2$C*H*$_2$CH$_3$), 1.13 (t, *J* = 7 Hz, 6H, OCH$_2$CH$_2$C*H*$_3$), 1.02 (t, *J* = 7 Hz, 3H, OCH$_2$CH$_2$C*H*$_3$); **^{13}C-NMR** (100 MHz, CD_3OD) δ 157.97, 157.86, 157.78, 157.49, 156.19, 155.42, 139.76, 138.63, 136.49, 136.24, 131.09, 130.18, 129.84, 127.32, 126.87, 125.61, 125.56, 80.87, 78.60, 78.42, 77.35, 61.23, 32.09, 31.47, 24.49, 24.44, 11.14, 10.38; **HRMS** (NSI) m/s: $[M+H]^+$ Calcd for $C_{44}H_{57}N_{12}O_4$ 817.4620; Found 817.4603.

Coumarin appended tetraguanidine calix[4]arene (106)

A mixture of **104** (0.050 g, 0.052 mmol), **82** (0.013 g, 0.062 mmol), $CuSO_4.5H_2O$ (2 mg, 8 μmol) and sodium ascorbate (7 mg, 0.036 mmol) were stirred in 1:1 ethanol/water (2 mL) at 90 °C for 4 hours. The mixture was allowed to cool to room temperature before filtering off the brown insoluble material and washing it with ethanol. Solvent was removed under reduced pressure from the filtrate. ^{1}H-NMR confirmed reaction had taken place. Attempted purification by column chromatography over C18 (eluent: 0-100% methanol in water) and by ion exchange chromatography over Amberlite IRC-50 resin failed to give product.

5,11,17,23-Tetrakis[(N,N′-di-CBz)guanidine]-25,26,27-tripropoxy-28-propargyloxy-calix[4]arene (107)

A mixture of **80** (0.60 g, 0.92 mmol), bis-CBz-methylthiopseudourea (1.58 g, 4.42 mmol) and $HgCl_2$ (1.20 g, 4.42 mmol) were stirred under argon in dry DMF (13 mL). Triethylamine (1.53 mL, 4.42 mmol) was added and the mixture stirred for 24 hours. The solvent was removed under reduced pressure and the product dissolved in DCM (10 mL). The HgSMe was removed by filtration, washed with DCM and the filtrate washed with water (2 x100 mL) and brine (100 mL). After drying over $MgSO_4$, the solvent was removed under reduced pressure and the residue purified by column chromatography over silica gel (eluent: 4:1 to 3:1 hexane/ethyl acetate) to give **107** as white crystals (0.5 g, 28%). **Mp** 105-107 °C; **IR** ν 3280.5, 3164, 3092, 3064.5, 3034, 2960, 2936, 2875, 1724.5, 1622, 1575, 1497.5, 1454, 1422.5, 1380, 1367.5, 1335.5, 1309.5, 1250.5, 1234.5, 1204.5, 1167, 1103, 1081.5, 1053.5, 1028.5, 1003 cm^{-1}; **^{1}H-NMR** (400 MHz, $CDCl_3$) δ 11.79 (s, 2H, N*H*$_{Guanidine}$), 11.69 (s, 2H, N*H*$_{Guanidine}$), 10.07 (s, 1H, ArN*H*), 10.03 (s, 1H, ArN*H*), 9.48 (s, 2H, ArN*H*), 7.35 – 7.14 (m, 44H, Ar*H* and OCH_2Ar*H*), 6.55 (s, 2H, Ar*H*), 6.52 (s, 2H, Ar*H*), 5.14 – 5.12 (m, 8H, OC*H*$_2$Ar), 5.03 (s, 4H, OC*H*$_2$Ar), 4.93 (s, 4H, OC*H*$_2$Ar), 4.83 (d, *J* = 2 Hz, 2H, OC*H*$_2$CCH), 4.47 (d, *J* = 13.5 Hz, 2H, ArC*H*$_2$Ar), 4.40 (d, *J* = 13 Hz, 2H, ArC*H*$_2$Ar), 3.98 – 3.94 (m, 2H, OC*H*$_2$CH$_2$CH$_3$), 3.66 (t, *J* = 7 Hz, 4H, OC*H*$_2$CH$_2$CH$_3$), 3.10 (d, *J* = 13.5 Hz, 2H, ArC*H*$_2$Ar), 3.08 (d, *J* = 13 Hz, 2H, ArC*H*$_2$Ar), 2.31 (app. s, 1H, OCH_2CCH), 1.95 – 1.82 (m, 6H, $OCH_2CH_2CH_3$), 1.03 (t, *J* = 7 Hz, 6H, $OCH_2CH_2CH_3$), 0.89 (t, *J* = 7 Hz, 3H, $OCH_2CH_2CH_3$); **^{13}C-NMR** (100 MHz, $CDCl_3$) δ 164.07, 163.92, 155.11, 153.85, 153.51, 153.45, 153.39, 153.27, 153.10, 152.58, 137.35, 137.13, 136.90, 136.23, 134.64, 134.53, 133.79, 133.59, 131.35, 130.48, 130.37, 128.88, 128.76, 128.63, 128.48, 128.40, 128.31, 127.97, 127.95, 127.85, 127.64, 127.43, 123.25, 122.79, 122.47, 122.43, 80.73, 77.36, 77.24, 76.99, 74.88, 68.34, 68.32, 68.17, 67.45, 67.37, 67.08, 59.82, 31.71, 31.64, 31.22, 23.47, 23.14, 10.79, 10.05; **ESI-MS** m/z: $[M+H]^+$ 1889.8.

Coumarin appended tetrakis[(N,N′-di-CBz)guanidine-calix[4]arene (108)

A mixture of **107** (1.02 g, 0.54 mmol), **82** (0.13 g, 0.65 mmol), $CuSO_4.5H_2O$ (0.027 g, 0.11 mmol) and sodium ascorbate (0.075 g, 0.38 mmol) were stirred in DMF (20 mL) for 24 hours at room temperature. Solvent was removed under reduced pressure and the residue triturated with water before filtering. The solid was washed with H_2O (2 x 10 mL) and methanol (10 mL) then purified by column

chromatography over silica gel (eluent: 19:1 DCM/ethyl acetate) to give **108** as a light yellow solid (0.83 g, 74%). **Mp** 133-135 °C; **IR** ν 3275.5, 3164.5, 3087.5, 3065, 3033.5, 2961, 2934.5, 2874, 1727.5, 1621.5, 1574.5, 1497, 1455, 1417.5, 1380, 1367, 1335, 1311, 1292, 1234, 1205, 1167.5, 1155.5, 1103.5, 1081.5, 1053.5, 1028.5, 1001.5 cm^{-1}; **^{1}H-NMR** (400 MHz, $CDCl_3$) δ 11.81 (br s, 4H, N$H_{Guanidine}$), 9.80 (s, 2H, ArN*H*), 9.74 (s, 2H, ArN*H*), 8.54 (s, 1H, Ar$H_{Triazole}$), 8.35 (s, 1H, Ar$H_{Coumarin}$), 7.32 – 7.17 (m, 41H, Ar$H_{Coumarin}$ and OCH_2Ar*H*), 6.84 (s, 2H, Ar*H*), 6.81 (s, 2H, Ar*H*), 6.75 (s, 2H, Ar*H*), 6.72 (s, 2H, Ar*H*), 6.63 (dd, *J* = 8, 2 Hz, 1H, Ar$H_{Coumarin}$), 6.58 (d, *J* = 2 Hz, 1H, Ar$H_{Coumarin}$), 5.09 – 5.05 (m, 18H, OCH_2Ar and OCH_2C), 4.33 (d, *J* = 13 Hz, 2H, ArCH_2Ar), 4.25 (d, *J* = 13 Hz, 2H, ArCH_2Ar), 3.79 (t, *J* = 7 Hz, 2H, OC$H_2$$CH_2CH_3$), 3.64 – 3.53 (m, 4H, OC$H_2$$CH_2CH_3$), 3.05 (d, *J* = 13 Hz, 2H, ArCH_2Ar), 3.02 (d, *J* = 13 Hz, 2H, ArCH_2Ar), 1.86 (sextet, *J* = 7 Hz, 2H, OCH_2CH_2CH_3), 1.75 – 1.57 (m, 4H, OCH_2CH_2CH_3), 0.95 (t, *J* = 7 Hz, 3H, OCH_2CH_2CH_3), 0.74 (t, *J* = 7 Hz, 6H, OCH_2CH_2CH_3); **^{13}C-NMR** (100 MHz, $CDCl_3$) δ 163.96, 163.84, 162.69, 156.34, 154.61, 154.37, 153.89, 153.68, 153.57, 153.04, 144.29, 136.70, 136.57, 135.44, 135.13, 135.04, 134.86, 134.49, 134.35, 130.67, 130.07, 129.84, 129.67, 128.83, 128.73, 128.58, 128.32, 127.96, 127.89, 127.83, 124.23, 123.61, 123.47, 123.20, 119.00, 115.17, 110.16, 103.22, 77.36, 76.89, 68.37, 67.37, 60.50, 31.43, 31.22, 23.25, 23.03, 21.11, 14.26, 10.38, 10.12; **ESI-MS** m/z: $[M+H]^+$ 2092.8.

Coumarin appended tetraguanidine-calix[4]arene (·4HCl) (109)

A mixture of **108** (25 mg, 12 μmol) and NaI (57 mg, 380 μmol) was stirred under argon in dry DMF (0.5 mL). To this was added dry chlorotrimethylsilane (48 μL, 380 μmol) and the mixture heated to 50 °C for 24 hours. Methanol (1 mL) and dilute HCl (5 mL) were added and the mixture stirred for 15 minutes. Solvent was removed under reduced pressure and the major impurities removed by column chromatography over C18 (eluent: methanol in 60 mM $HCl_{(aq)}$, 30-70%) to give crude product (40 mg, 93%). This was purified by further column chromatography over C18 (eluent: methanol in 60 mM $HCl_{(aq)}$, 0-50%) to give pure **109** as off-white powder (9.3 mg, 22%). **Mp** 280 °C (decomp.); **IR** ν 3312, 3142, 2965.5, 2934, 2874, 1733, 1668.5, 1606.5, 1582.5, 1516.5, 1464, 1429, 1385.5, 1312, 1285, 1219, 1170.5, 1154.5, 1116, 1043 cm^{-1}; **^{1}H-NMR** (400 MHz, CD_3OD) δ 8.59-8.58 (2s, 2H, Ar$H_{Coumarin}$ and Ar$H_{Triazole}$), 7.68 (d, *J* = 8.5 Hz, 1H, Ar$H_{Coumarin}$), 6.92 (dd, *J* = 8.5, 2 Hz, 1H, Ar$H_{Coumarin}$), 6.84 (d, *J* = 2 Hz, 1H, Ar$H_{Coumarin}$), 6.79 (s, 2H, Ar*H*), 6.77 (s, 2H, Ar*H*),

6.60 (s, 2H, Ar*H*), 6.57 (s, 2H, Ar*H*), 5.32 (s, 2H, OCH_2C), 4.52 (d, *J* = 13 Hz, 2H, ArCH_2Ar), 4.31 (d, *J* = 13 Hz, 2H, ArCH_2Ar), 4.02 (t, *J* = 7 Hz, 2H, OCH_2CH_2CH_3), 3.86 (t, *J* = 7 Hz, 4H, OCH_2CH_2CH_3), 3.32 (d, *J* = 13 Hz, 2H, ArCH_2Ar), 3.18 (d, *J* = 13 Hz, 2H, ArCH_2Ar), 2.09 (sextet, *J* = 7 Hz, 2H, OCH$_2$CH_2CH_3), 1.91 (sextet, *J* = 7 Hz, 4H, OCH$_2$CH_2CH_3), 1.10 (t, *J* = 7 Hz, 3H, OCH$_2$CH$_2$CH_3), 0.97 (t, *J* = 7 Hz, 6H, OCH$_2$CH$_2$CH_3). **^{13}C-NMR** (100 MHz, CD_3OD) δ 164.56, 158.19, 158.07, 157.91, 157.79, 157.32, 156.97, 156.58, 155.53, 144.73, 138.56, 137.92, 137.32, 137.23, 132.10, 130.55, 129.89, 129.76, 127.39, 127.07, 126.96, 126.53, 126.38, 120.59, 115.73, 111.92, 103.43, 78.59, 78.46, 67.17, 32.01, 31.73, 24.63, 24.37, 10.75, 10.68; **MALDI-TOF** m/z: $[M+H]^+$ 1020.78.

5,11,17,23-Tetra-*tert*-butyl-25,26,27-tripropoxy-28-bromopropoxy-calix[4]arene (110)[125]

To a stirred solution of **77** (2.00 g, 2.58 mmol) in DMF (60 mL) was added NaH (0.25 g, 10.32 mmol) and the mixture stirred for 30 minutes before addition of 1,3-dibromopropane (5.26 mL, 51.60 mmol). The mixture was stirred for 24 hours then the solvent was removed under reduced pressure. Water (200 mL) was added and the solid filtered, washed with water (3 x 50 mL) and air dried. The product was purified by column chromatography over silica gel (eluent: 8:3 hexane/DCM) to give **110** as white powder (0.91 g, 39%). **Mp** 209-211 °C; **IR** ν 3039, 2959, 2903.5, 2873, 1601.5, 1578, 1480, 1463, 1434, 1415, 1388, 1360, 1299, 1279, 1255.5, 1248, 1237, 1198.5, 1122.5, 1107.5, 1068.5, 1037.5, 1009 cm^{-1}; **^{1}H-NMR** (400 MHz, $CDCl_3$) δ 6.90 (s, 2H, Ar*H*), 6.90 (s, 2H, Ar*H*), 6.67 (d, *J* = 2.5 Hz, 2H, Ar*H*), 6.64 (d, *J* = 2.5 Hz, 2H, Ar*H*), 4.42 (d, *J* = 12.5 Hz, 2H, ArCH_2Ar), 4.35 (d, *J* = 12.5 Hz, 2H, ArCH_2Ar), 4.01 (t, *J* = 7 Hz, 2H, OCH_2CH_2CH_2Br), 3.91 – 3.87 (m, 2H, OCH_2CH$_2$CH$_3$), 3.78 – 3.74 (m, 4H, OCH_2CH$_2$CH$_3$), 3.69 (t, *J* = 7 Hz, 2H, OCH$_2$CH$_2$CH_2Br), 3.14 (d, *J* = 12.5 Hz, 2H, ArCH_2Ar), 3.12 (d, *J* = 12.5 Hz, 2H, ArCH_2Ar), 2.65 (quintet, *J* = 7 Hz, 2H, OCH$_2$CH_2CH$_2$Br), 2.02 – 1.93 (m, 6H, OCH$_2$CH_2CH$_3$), 1.18 (s, 9H, C(CH$_3$)$_3$), 1.17 (s, 9H, C(CH$_3$)$_3$), 1.03 – 0.97 (m, 27H, OCH$_2$CH$_2$CH_3 and C(CH$_3$)$_3$).

5,11,17,23-Tetra-nitro-25,26,27-tripropoxy-28-bromopropoxy-calix[4]arene (111)

To a stirred solution of **110** (0.58 g, 0.68 mmol) in DCM (40 mL) was added glacial acetic acid (4 mL) and 100% nitric acid (4 mL). After 6 hours water (100 mL) was added to quench. The organic layer was separated and washed with water (2 x

200 mL) and brine (200 mL). After drying over $MgSO_4$, the solvent was removed under reduced pressure and the residue triturated with methanol. The product was filtered and air dried to give **111** as light orange powder (0.50 g, 87%). **Mp** 270 °C; **IR** ν 3075, 2968.5, 2932, 2877, 1607, 1585, 1513.5, 1463, 1450.5, 1435, 1385.5, 1341, 1303, 1287, 1262.5, 1221.5, 1211, 1160.5, 1094, 1060, 1034.5 cm^{-1}; **^{1}H-NMR** (400 MHz, $CDCl_3$) δ 7.58 (s, 2H, Ar*H*), 7.58 (s, 2H, Ar*H*), 7.57 (s, 4H, Ar*H*), 4.53 (d, *J* = 14 Hz, 2H, ArC*H*$_2$Ar), 4.50 (d, *J* = 14 Hz, 2H, ArC*H*$_2$Ar), 4.17 (t, *J* = 7 Hz, 2H, OC*H*$_2$CH$_2$CH$_2$Br), 4.01 – 3.93 (m, 6H, OC*H*$_2$CH$_2$CH$_3$), 3.57 (t, *J* = 6.5 Hz, 2H, OCH$_2$CH$_2$C*H*$_2$Br), 3.44 (d, *J* = 14 Hz, 2H, ArC*H*$_2$Ar), 3.41 (d, *J* = 14 Hz, 2H, ArC*H*$_2$Ar), 2.43 (quintet, *J* = 6.5 Hz, 2H, OCH$_2$C*H*$_2$CH$_2$Br), 1.96 – 1.85 (m, 6H, OCH$_2$C*H*$_2$CH$_3$), 1.03 (t, *J* = 7 Hz, 6H, OCH$_2$CH$_2$C*H*$_3$), 1.02 (t, *J* = 7 Hz, 3H, OCH$_2$CH$_2$C*H*$_3$); **^{13}C-NMR** (100 MHz, $CDCl_3$) δ 161.74, 161.71, 161.28, 143.17, 142.95, 135.60, 135.55, 135.39, 124.20, 124.17, 124.09, 124.06, 77.88, 73.95, 32.52, 31.20, 29.11, 23.40, 23.29, 10.29, 10.23; **HRMS** (APCI) m/z: $[M]^+$ Calcd for $C_{40}H_{43}BrN_4O_{12}$ 850.2055; Found 850.2058; $[M+H]^+$ Calcd for $C_{40}H_{44}BrN_4O_{12}$ 851.2134; Found 851.2129.

5,11,17,23-Tetra-Boc-amino-25,26,27-tripropoxy-28-bromopropoxy-calix[4]arene (113)

A mixture of **111** (0.45 g, 0.50 mmol) and $SnCl_2 \cdot 2H_2O$ (2.93 g, 13.00 mmol) was heated to reflux in ethanol (30 mL) for 48 hours. The solvent was removed under reduced pressure and 10% NaOH (100 mL) added. The product was extracted with DCM (3 x 100 mL) then washed with water (2 x 200 mL) and brine (200 mL). After drying over $MgSO_4$, the solvent was removed under reduced pressure to give the intermediate tetra-amine (**112**) as a brown glass (crude yield: 0.33 g, 90%). **^{1}H-NMR** (400 MHz, $CDCl_3$) δ 6.15 (s, 2H, Ar*H*), 6.14 (s, 2H, Ar*H*), 5.98 (app. s, 2H, Ar*H*), 5.97 (app. s, 2H, Ar*H*), 4.30 (d, *J* = 13 Hz, 2H, ArC*H*$_2$Ar), 4.25 (d, *J* = 13 Hz, 2H, ArC*H*$_2$Ar), 3.92 (t, *J* = 6.5 Hz, 2H, OC*H*$_2$CH$_2$CH$_2$Br), 3.77 – 3.74 (m, 2H, OC*H*$_2$CH$_2$CH$_3$), 3.69 (t, *J* = 7 Hz, 4H, OC*H*$_2$CH$_2$CH$_3$), 3.60 (t, *J* = 6.5 Hz, 2H, OCH$_2$CH$_2$C*H*$_2$Br), 2.94 (d, *J* = 13 Hz, 2H, ArC*H*$_2$Ar), 2.92 (d, *J* = 13 Hz, 2H, ArC*H*$_2$Ar), 2.42 (quintet, *J* = 6.5 Hz, 2H, OCH$_2$C*H*$_2$CH$_2$Br), 1.90 – 1.79 (m, 6H, OCH$_2$C*H*$_2$CH$_3$), 0.97 (t, *J* = 7 Hz, 6H, OCH$_2$CH$_2$C*H*$_3$), 0.93 (t, *J* = 7 Hz, 3H, OCH$_2$CH$_2$C*H*$_3$). A solution of crude **112** (0.28 g, 0.38 mmol), Boc-anhydride (0.66 g, 3.04 mmol) and DIPEA (0.25 mL, 3.04 mmol) in DCM (10 mL) was stirred for 48 hours. After diluting with DCM (20 mL), the product was washed with water (2 x50

mL) then brine (50 mL) before drying over $MgSO_4$. The solvent was removed under reduced pressure and the product purified by column chromatography over silica gel (eluent: 19:1 DCM/ethyl acetate) to give **113** as off-white glass (0.26 g, 60%). **Mp** 231-233 °C; **IR** ν 3425.5, 3340, 3318.5, 3253, 3164, 2972.5, 2930.5, 2874, 1698, 1595.5, 1532, 1511, 1470.5, 1416.5, 1389.5, 1365, 1294.5, 1241, 1214.5, 1151, 1060.5, 1036.5, 1003.5 cm^{-1}; **^{1}H-NMR** (400 MHz, $CDCl_3$) δ 6.71 (s, 4H, Ar*H*), 6.51 (s, 4H, Ar*H*), 6.18 (s, 2H, N*H*), 6.06 (s, 2H, N*H*), 4.36 (d, *J* = 13 Hz, 2H, ArC*H*$_2$Ar), 4.32 (d, *J* = 13 Hz, 2H, ArC*H*$_2$Ar), 3.97 (t, *J* = 7 Hz, 2H, OC*H*$_2$CH$_2$CH$_2$Br), 3.82 – 3.78 (m, 2H, OC*H*$_2$CH$_2$CH$_3$), 3.73 (t, *J* = 7 Hz, 4H, OC*H*$_2$CH$_2$CH$_3$), 3.57 (t, *J* = 7 Hz, 2H, OCH$_2$CH$_2$C*H*$_2$Br), 3.11 (d, *J* = 13 Hz, 2H, ArC*H*$_2$Ar), 3.09 (d, *J* = 13 Hz, 2H, ArC*H*$_2$Ar), 2.42 (quintet, *J* = 7 Hz, 2H, OCH$_2$C*H*$_2$CH$_2$Br), 1.96 – 1.76 (m, 6H, OCH$_2$C*H*$_2$CH$_3$), 1.50 (s, 18H, C(CH$_3$)$_3$), 1.47 (s, 18H, C(CH$_3$)$_3$), 0.97 (t, *J* = 7 Hz, 6H, OCH$_2$CH$_2$C*H*$_3$), 0.93 (t, *J* = 7 Hz, 3H, OCH$_2$CH$_2$C*H*$_3$); **^{13}C-NMR** (100 MHz, $CDCl_3$) δ 153.50, 153.41, 153.37, 152.88, 152.52, 152.48, 135.59, 135.49, 134.90, 134.67, 132.54, 132.18, 132.09, 120.12, 119.99, 119.89, 119.77, 80.10, 80.04, 79.98, 76.89, 76.72, 72.83, 32.97, 31.12, 30.36, 28.48, 23.23, 22.99, 10.45, 10.31; **MALDI-TOF** m/z: [M+Na] 1154.49.

(7-Hydroxy-2-oxo-2H-chromen-3-yl)carbamic acid t-butyl ester (114)[79]

To a stirred solution of **81** (3.00 g, 11.49 mmol) and DMAP (0.28 g, 2.30 mmol) in THF (60 mL) was added Boc anhydride (10.53 g. 48.26 mmol). After stirring for 30 minutes, hydrazine hydrate (7.02 mL, 114.90 mmol) and methanol (50 mL) were added and stirring continued for 20 minutes. Solvent was removed under reduced pressure and the residue dissolved in DCM (100 mL). The product was washed with dilute HCl (100 mL), 1 M $CuSO_4$ (100 mL), saturated $NaHCO_3$ (100 mL) then brine (100 mL). After drying over $MgSO_4$, the solvent was removed under reduced pressure and the product purified by column chromatography over silica gel (eluent: 3:2 hexane/ethyl acetate) to give **114** as light yellow solid (0.36 g, 62%). **Mp** 163-165 °C; **IR** 3314.5, 3080, 2999, 2978.5, 2933, 1719.5, 1701.5, 1681, 1651, 1633, 1607.5, 1534, 1510.5, 1455, 1392.5, 1366, 1341, 1288, 1268, 1242, 1224, 1198.5, 1159, 1124, 1045, 1020.5 cm^{-1}; **^{1}H NMR** (400 MHz, $CDCl_3$) δ 8.23 (s, 1H, O*H*), 7.33 (d, *J* = 8 Hz, 1H, Ar*H*), 7.28 (s, 1H, N*H*), 6.83 (d, *J* = 2 Hz, 1H, Ar*H*), 6.81 (dd, *J* = 8, 2 Hz, 1H, Ar*H*), 5.73 (s, 1H, Ar*H*), 1.53 (s, 9H, C(CH$_3$)$_3$).

3-Amino-7-hydroxy-2H-chromen-2-one (115)[79]

A solution of **114** (1.29 g, 4.65 mmol) in 15% TFA/chloroform (57 mL) was stirred for 6 hours. The solvent was removed under reduced pressure and the product purified by column chromatography over silica gel (eluent: 1:1 hexane/ethyl acetate) to give **115** as light orange-brown solid (0.67 g, 81%). **Mp** 250-252 °C; **IR** ν 3435, 3343.5, 3210.5, 1678.5, 1651, 1615, 1605.5, 1556.5, 1508, 1455.5, 1416.5, 1360, 1330.5, 1280.5, 1241.5, 1197.5, 1152, 1124.5 cm^{-1}; **^{1}H-NMR** (400 MHz, DMSO) δ 9.80 (s, 1H, O*H*), 7.23 (d, *J* = 8 Hz, 1H, Ar*H*), 6.70 – 6.65 (m, 3H, Ar*H*), 5.22 (s, 2H, NH_2).

5,11,17,23-Tetra-Boc-amino-25,26,27-tripropoxy-28-[(7'-hydroxy-2'-oxo-2H-chromen-3'-ylamino)propoxy-calix[4]arene (116)

A stirred solution of **113** (0.05 g, 0.044 mmol), **115** (0.016 g, 0.088 mmol) and pyridine (3.9 μL, 0.044 mmol) in ethyl acetate (1 mL) was heated at 70 °C for 18 hours. Removal of solvent under reduced pressure gave a mixture of the starting materials with no product.

3-Amino-7-(*tert*-butyl-dimethyl)silylether-2H-chromen-2-one (117)

To a stirred solution of **115** (0.5 g, 2.82 mmol) and TBDMSCl (0.64 g, 4.23 mmol) in THF (14 mL) was added triethylamine (0.59 mL, 4.23 mmol) and the mixture stirred for 24 hours. Saturated ammonium chloride (25 mL) was added and the product extracted with ethyl acetate (3 x 50 mL) then washed with water (150 mL) and brine (150 mL). After drying over $MgSO_4$, the solvent was removed under reduced pressure and the product purified by column chromatography over silica gel (eluent: 1:1 hexane/ethyl acetate) to give **117** as yellow needles (0.65 g, 79%). **Mp** 109-110 °C; **IR** ν 3452.5, 3405, 3354, 2954, 2929, 2883.5, 2858.5, 1689, 1634, 1615.5, 1593.5, 1504.5, 1471, 1432, 1408, 1389, 1361, 1335.5, 1309.5, 1298, 1269.5, 1258, 1250.5, 1199.5, 1159, 1118.5, 1008.5, 1003 cm^{-1}; **^{1}H-NMR** (400 MHz, CD_3OD) δ 7.23 (d, *J* = 8 Hz, 1H, Ar*H*), 6.78 – 6.73 (m, 3H, Ar*H*), 1.00 (s, 9H, $SiC(CH_3)_3$), 0.22 (s, 6H, $SiCH_3$); **^{13}C-NMR** (100 MHz, CD_3OD) δ 161.34, 155.91, 150.99, 132.23, 126.92, 118.63, 117.21, 112.30, 108.08, 26.08, 19.06, -4.38; **HRMS** (NSI) m/z: $[M+H]^+$ Calcd for $C_{15}H_{22}NO_3Si$ 292.1363; Found 292.1364.

5,11,17,23-Tetra-Boc-amino-25,26,27-tripropoxy-28-[(7'-(*tert*-butyl-dimethyl)silylether-2'-oxo-2H-chromen-3'-yl)amino]propoxy-calix[4]arene (118)

Method A: A stirred solution of **113** (0.046 g, 0.041 mmol), **117** (0.012 g, 0.041

mmol) and K_2CO_3 (0.017 g, 0.12 mmol) in acetone (1 mL) was heated at reflux for 18 hours. After cooling to room temperature, excess K_2CO_3 was removed by filtration. Water (20 mL) was added and the product extracted with ethyl acetate (3 x 20 mL) then washed with water (50 mL) and brine (50 mL). After drying over $MgSO_4$, the solvent was removed under reduced pressure to give a mixture of starting materials and no product.

Method B: To a stirred solution of **113** (0.030 g, 0.027 mmol) and **117** (0.015 g, 0.053 mmol) in THF (1 mL) was added 1 M LiHMDS in THF (0.053 mL g, 0.053 mmol) and the mixture stirred for 18 hours. The reaction was quenched with saturated ammonium chloride (20 mL) and the product extracted with ethyl acetate (3 x 20 mL) then washed with water (50 mL) and brine (50 mL). After drying over $MgSO_4$, the solvent was removed under reduced pressure to give a mixture of starting materials and no product.

5,11,17,23-Tetra-*tert*-butyl-25,26,27-tripropoxy-28-[(ethoxycarbonyl)propoxy-calix[4]arene (119)

Method A:

To a stirred solution of **77** (5.00 g, 6.45 mmol) in DMF (150 mL) was added NaH (0.62 g, 25.80 mmol) and the mixture stirred for 1 hour before addition of ethyl 4-bromopropionate (3.30 mL, 25.80 mmol). The mixture was stirred for 6 hours before addition of water (150 mL). The resulting precipitate was filtered and washed with methanol. ^{1}H-NMR showed starting material only.

Method B:

A stirred solution of **77** (5.00 g, 6.45 mmol) in DMF (150 mL) was cooled to 0 °C before adding NaH (0.62 g, 25.80 mmol). After 30 mins ethyl 4-bromopropionate (3.30 mL, 25.80 mmol) was added. The mixture was stirred for 6 hours before addition of water (150 mL). The resulting precipitate was filtered and washed with methanol. ^{1}H-NMR showed starting material only.

Method C:

A mixture of **77** (5.00 g, 6.45 mmol) and K_2CO_3 (3.57 g, 25.80 mmol) was heated to reflux in acetone (100 mL). After 30 mins ethyl 4-bromopropionate (3.30 mL, 25.80 mmol) was added. The mixture was stirred for 72 hours then cooled to room temperature. After removal of base by filtration, the product was precipitated with water (100 mL), filtered and washed with methanol. ^{1}H-NMR showed starting material only.

Method D:

A mixture of **77** (1.00 g, 1.29 mmol), KF/Al_2O_3 (21 mg, 0.13 mmol) and ethyl acrylate (0.28 mL, 2.58 mmol) was stirred in acetonitrile for 3 hours. Acetone (5 mL) was added to improve solubility and the mixture stirred for a further 18 hours. The catalyst was removed by filtration and the product precipitated with water (20 mL), filtered and washed with methanol. ^{1}H-NMR showed starting material only.

5,11,17,23-Tetra-*tert*-butyl-25,26,27-tripropoxy-28-phthalimidobutoxy-calix[4]arene (120)

To a stirred solution of **77** (5.00 g, 6.45 mmol) in DMF (200 mL) was added NaH (0.62 g, 25.80 mmol) and the mixture stirred for 30 minutes before addition of 4-bromobutylphthalimide (4.55 g, 16.13 mmol). The mixture was stirred for 24 hours then the solvent was removed under reduced pressure. The residue was dissolved in DCM (100 mL) and washed with water (3 x 200 mL) then brine (200 mL). After drying over $MgSO_4$, the solvent was removed under reduced pressure and the solid triturated with hot methanol, filtered, washed with methanol and air dried to give **120** as white powder (3.19 g, 51%). **Mp** 108-110 °C; **IR** ν 2958, 2904, 2871.5, 1773.5, 1714.5, 1480.5, 1467, 1437, 1394.5, 1360, 1299, 1278.5, 1247.5, 1196, 1122.5, 1108, 1088, 1069, 1043, 1009 cm^{-1}; **^{1}H-NMR** (400 MHz, $CDCl_3$) δ 7.86 (dd, *J* = 5.5, 3.0 Hz, 2H, Ar$H_{Phthalimide}$), 7.72 (dd, *J* = 5.5, 3.0 Hz, 2H, Ar$H_{Phthalimide}$), 6.79 – 6.76 (m, 8H, Ar*H*), 4.41 (d, *J* = 12.5 Hz, 2H, ArCH_2Ar), 4.38 (d, *J* = 12.5 Hz, 2H, ArCH_2Ar), 3.88 (t, *J* = 7.5 Hz, 2H, OCH_2CH$_2$CH$_2$CH$_2$N), 3.83 – 3.76 (m, 8H, OCH_2CH$_2$CH$_3$ and OCH$_2$CH$_2$CH$_2$CH_2N), 3.11 (d, *J* = 12.5 Hz, 4H, ArCH_2Ar), 2.12 – 1.96 (m, 8H, OCH$_2$CH_2CH$_2$CH$_2$N and OCH$_2$CH_2CH$_3$), 1.84 – 1.76 (m, 2H, OCH$_2$CH$_2$CH_2CH$_2$N), 1.08 (s, 18H, C(CH_3)$_3$), 1.07 (s, 9H, C(CH_3)$_3$), 1.06 (s, 9H, C(CH_3)$_3$), 1.02 – 0.96 (m, 9H, OCH$_2$CH$_2$CH_3). **^{13}C-NMR** (100 MHz, $CDCl_3$) δ 168.34, 153.74, 153.69, 153.50, 144.38, 144.20, 133.90, 133.85, 133.79, 132.26, 124.96, 124.94, 124.90, 123.22, 77.42, 77.10, 77.02, 76.78, 74.55, 38.07, 33.85, 31.53, 31.13, 27.59, 25.46, 23.42, 23.36, 10.41, 10.37; **HRMS** (APCI) m/z: $[M+H]^+$ Calcd for $C_{65}H_{86}NO_6$ 976.6450; Found 976.6447.

5,11,17,23-Tetranitro-25,26,27-tripropoxy-28-phthalimidobutoxy-calix[4]arene (121)

To a stirred solution of **120** (2.00 g, 2.05 mmol) in DCM (300 mL) was added glacial acetic acid (11 mL) and 100% nitric acid (11 mL). After 4 hours water (200

mL) was added to quench. The organic layer was separated and washed with water (3 x 300 mL) and brine (300 mL). After drying over $MgSO_4$, the solvent was removed under reduced pressure and the residue triturated with methanol. The product was filtered and air dried to give **121** as light yellow powder (1.67 g, 87%). **Mp** 164-166 °C; **IR** ν 3075, 2963, 2934.5, 2876, 1770, 1710.5, 1607.5, 1585, 1518, 1448.5, 1434.5, 1396, 1340.5, 1302.5, 1286.5, 1262.5, 1209.5, 1170.5, 1159, 1092, 1038 cm^{-1}; **^{1}H-NMR** (400 MHz, $CDCl_3$) δ 7.84 (dd, *J* = 5.5, 3.0 Hz, 2H, Ar*H*$_{Phthalimide}$), 7.74 (dd, *J* = 5.5, 3.0 Hz, 2H, Ar*H*$_{Phthalimide}$), 7.66 – 7.64 (m, 4H, Ar*H*), 7.49 (s, 2H, Ar*H*), 7.46 (s, 2H, Ar*H*), 4.51 (d, *J* = 14.0 Hz, 2H, ArC*H*$_2$Ar), 4.48 (d, *J* = 14.0 Hz, 2H, ArC*H*$_2$Ar), 4.01 (t, *J* = 7.0 Hz, 2H, OC*H*$_2$CH$_2$CH$_2$CH$_2$N), 3.98 – 3.90 (m, 6H, OC*H*$_2$CH$_2$CH$_3$), 3.75 (t, *J* = 7.0 Hz, 2H, OCH$_2$CH$_2$CH$_2$C*H*$_2$N), 3.40 (d, *J* = 14.0 Hz, 2H, ArC*H*$_2$Ar), 3.39 (d, *J* = 14.0 Hz, 2H, ArC*H*$_2$Ar), 1.97 – 1.77 (m, 10H, OCH$_2$C*H*$_2$CH$_3$ and OCH$_2$C*H*$_2$C*H*$_2$CH$_2$N), 1.03 (t, *J* = 7.5 Hz, 3H, OCH$_2$CH$_2$C*H*$_3$), 0.97 (t, *J* = 7.5 Hz, 6H, OCH$_2$CH$_2$C*H*$_3$); **^{13}C-NMR** (100 MHz, $CDCl_3$) δ 168.35, 162.00, 161.61, 161.30, 142.91, 142.84, 142.82, 135.72, 135.67, 135.29, 134.26, 131.96, 124.20, 124.17, 123.87, 123.85, 123.32, 77.87, 77.80, 75.33, 37.48, 31.19, 31.15, 27.40, 25.14, 23.34, 23.29, 10.28, 10.07; **HRMS** (APCI) m/z: $[M+H]^+$ Calcd for $C_{49}H_{50}N_5O_{14}$ 932.3349; Found 932.3348.

5,11,17,23-Tetraamino-25,26,27-tripropoxy-28-phthalimidobutoxy-calix[4]arene (122)

A mixture of **121** (1.50 g, 1.61 mmol) and $SnCl_2{\cdot}2H_2O$ (9.44 g, 41.86 mmol) was heated to reflux in ethanol (90 mL) for 48 hours. The solvent was removed under reduced pressure and 10% NaOH (300 mL) added. The product was extracted with DCM (3 x 100 mL) then washed with water (200 mL) and brine (200 mL). After drying over $MgSO_4$, the solvent was removed under reduced pressure to give **122** as brown glass (1.15 g, 88%). **Mp** 154-156 °C; **IR** ν 3418.5, 3347.5, 3210.5, 2956.5, 2930.5, 2873, 1769, 1707, 1607.5, 1465.5, 1396, 1370.5, 1333, 1306, 1279, 1260, 1213.5, 1188.5, 1169, 1149, 1130, 1106, 1088.5, 1067, 1040.5, 1007 cm^{-1}; **^{1}H-NMR** (400 MHz, $CDCl_3$) δ 7.85 – 7.83 (m, 2H, Ar*H*$_{Phthalimide}$), 7.72 – 7.69 (m, 2H, Ar*H*$_{Phthalimide}$), 6.07 (s, 4H, Ar*H*), 6.03 – 6.02 (m, 4H, Ar*H*), 4.30 (d, *J* = 13.0 Hz, 2H, ArC*H*$_2$Ar), 4.27 (d, *J* = 13.0 Hz, 2H, ArC*H*$_2$Ar), 3.79 (t, *J* = 7.0 Hz, 2H, OC*H*$_2$CH$_2$CH$_2$CH$_2$N), 3.75 – 3.70 (m, 8H, OC*H*$_2$CH$_2$CH$_3$ and OCH$_2$CH$_2$CH$_2$C*H*$_2$N), 2.91 (d, *J* = 13.0 Hz, 4H, ArC*H*$_2$Ar), 1.95 – 1.73 (m, 10H, OCH$_2$C*H*$_2$CH$_3$ and OCH$_2$C*H*$_2$C*H*$_2$CH$_2$N), 0.98 – 0.89 (m, 9H, OCH$_2$CH$_2$C*H*$_3$); **^{13}C-NMR** (100 MHz,

$CDCl_3$) δ 168.29, 150.07, 150.01, 149.74, 140.21, 140.02, 135.75, 135.69, 135.57, 135.53, 133.87, 132.15, 123.16, 115.90, 76.68, 74.19, 38.00, 31.14, 27.48, 25.50, 23.13, 10.43, 10.34; **HRMS** (NSI) m/z: $[M+H]^+$ Calcd for $C_{49}H_{58}N_5O_6$ 812.4382; Found 812.4380.

5,11,17,23-Tetra-Boc-amino-25,26,27-tripropoxy-28-phthalimidobutoxy-calix[4]arene (123)

A solution of **122** (1.00 g, 1.23 mmol), Boc anhydride (2.15 g, 9.84 mmol) and DIPEA (0.81 mL, 4.92 mmol) in DCM (34 mL) was stirred for 24 hours. The solvent was removed under reduced pressure and the product purified by column chromatography over silica gel (eluent: 19:1 DCM/ethyl acetate) to give **123** as light-yellow glass (0.99 g, 67%). **Mp** 146-148 °C; **IR** ν 3332, 2975, 2931, 2874, 1772, 1708.5, 1596, 1519, 1468, 1415, 1392, 1365.5, 1291.5, 1241, 1214.5, 1151, 1061.5, 1042.5, 1002 cm^{-1}; **^{1}H-NMR** (400 MHz, $CDCl_3$) δ 7.84 (dd, *J* = 5.5, 3.0 Hz, 2H, Ar$H_{Phthalimide}$), 7.70 (dd, *J* = 5.5, 3.0 Hz, 2H, Ar$H_{Phthalimide}$), 6.63 (s, 2H, Ar*H*), 6.62 (s, 2H, Ar*H*), 6.57 (s, 2H, Ar*H*), 6.56 (s, 2H, Ar*H*), 6.16 (s, 2H, N*H*), 6.13 (s, 1H, N*H*), 6.12 (s, 1H, N*H*), 4.35 (d, *J* = 13 Hz, 2H, ArCH_2Ar), 4.32 (d, *J* = 13 Hz, 2H, ArCH_2Ar), 3.82 (t, *J* = 7 Hz, 2H, OCH_2CH$_2$CH$_2$CH$_2$N), 3.77 – 3.71 (m, 8H, OCH_2CH$_2$CH$_3$ and OCH$_2$CH$_2$CH$_2$CH_2N), 3.07 (d, *J* = 13 Hz, 4H, ArCH_2Ar), 1.95 – 1.73 (m, 10H, OCH$_2$CH_2CH$_3$ and OCH$_2$CH_2CH_2CH$_2$N), 1.48 (s, 18H, C(CH$_3$)$_3$), 1.48 (s, 18H, C(CH$_3$)$_3$), 0.95 (t, *J* = 7.5 Hz, 3H, OCH$_2$CH$_2$CH_3), 0.91 (t, *J* = 7.5 Hz, 6H, OCH$_2$CH$_2$CH_3); **^{13}C-NMR** (100 MHz, $CDCl_3$) δ 168.40, 153.52, 153.47, 152.98, 152.90, 152.63, 135.45, 135.37, 135.24, 135.19, 134.00, 132.25, 132.09, 123.31, 119.98, 119.94, 80.09, 76.84, 74.40, 38.02, 31.23, 28.56, 27.53, 25.53, 23.24, 23.21, 10.48, 10.36; **MALDI-TOF** m/z: $[M+Na]^+$ 1235.48, $[M+K]^+$ 1251.52.

NBD appended tetra-Boc-amino calix[4]arene (125)

To a solution of **123** (0.9 g, 0.74 mmol) in ethanol (5 mL) was added hydrazine hydrate (0.14 mL, 80%, 2.22 mmol) and the mixture stirred for 24 hours. The resulting precipitate was removed by filtration. Solvent was removed from the filtrate under reduced pressure and the residue dissolved in minimum methanol followed by precipitation of the product with water. After separation of the product by filtration, the filtrate was extracted with 10% methanol in ethyl acetate (3 x 10 mL). After removal of solvent from the organic extracts under reduced pressure, the solid was combined with the previously isolated product and the two dried under reduced

pressure to give crude **124** as off-white solid (0.57 g, 72%). To a stirred mixture of this intermediate and $NaHCO_3$ (45 mg, 0.53 mmol) in acetonitrile (4 mL), NBDCl (0.12 g, 0.58 mmol) in acetonitrile (2 mL) was added dropwise. The mixture was stirred at 60 °C for 4 hours. Water (20 mL) was added and the product extracted with DCM (3 x 20 mL), then washed with brine (20 mL). After removal of solvent under reduced pressure, the product was purified by column chromatography over silica gel (eluent: 7:3 hexane/DCM) to give **125** as bright orange solid (0.35 g, 53%). **Mp** 154-156 °C; **IR** ν 3328, 2975, 2926, 2875, 2854, 1726.5, 1696, 1623.5, 1576.5, 1517.5, 1472, 1414.5, 1388, 1365.5, 1349.5, 1296.5, 1242, 1214.5, 1151.5, 1063.5, 1035 cm^{-1}; **^{1}H-NMR** (400 MHz, $CDCl_3$) δ 8.50 (d, *J* = 8.5 Hz, 1H, ArH_{NBD}), 6.70 (s, 4H, Ar*H*), 6.53 (s, 2H, Ar*H*), 6.51 (s, 2H, Ar*H*), 6.22 (s, 2H, N*H*), 6.20 (s, 1H, N*H*), 6.16 (d, *J* = 8.5 Hz, 1H, ArH_{NBD}), 6.11 (s, 2H, N*H*), 4.34 (d, *J* = 13 Hz, 2H, ArCH_2Ar), 4.32 (d, *J* = 13 Hz, 2H, ArCH_2Ar), 3.95 (t, *J* = 7 Hz, 2H, OC$H_2$$CH_2CH_2CH_2$N), 3.81 – 3.67 (m, 6H, OC$H_2$$CH_2CH_3$), 3.52 (q, *J* = 7 Hz, 2H, $OCH_2CH_2CH_2$CH_2N), 3.11 (d, *J* = 13 Hz, 2H, ArCH_2Ar), 3.09 (d, *J* = 13 Hz, 2H, ArCH_2Ar), 2.06 – 1.99 (m, 2H, CH_2C$H_2$$CH_2CH_2$), 1.91 – 1.79 (m, 8H, CH_2C$H_2$$CH_2CH_2$ and OCH_2C$H_2$$CH_3$), 1.50 (s, 18H, C$(CH_3)_3$), 1.48 (s, 18H, C$(CH_3)_3$), 0.96 – 0.91 (m, 9H, OCH_2CH_2CH_3); **^{13}C-NMR** (100 MHz, $CDCl_3$) δ 153.55, 153.50, 152.78, 152.57, 152.46, 144.21, 143.97, 136.61, 135.25, 135.21, 134.97, 134.67, 132.34, 132.12, 132.10, 123.39, 120.10, 119.94, 119.86, 98.68, 80.09, 80.01, 76.69, 73.86, 44.07, 31.15, 31.05, 28.41, 27.37, 25.23, 23.16, 23.06, 10.39, 10.37; **MALDI-TOF** m/z: $[M+Na]^+$ 1268.99, $[M+K]^+$ 1285.02.

NBD appended tetra-amino calix[4]arene (·4HCl) (126)

$HCl_{(g)}$ was bubbled through a solution of **125** (0.22 g, 0.18 mmol) in DCM (16 mL). After 10 minutes, methanol was added to dissolve the precipitate and stirring continued for 30 minutes. After removing solvent under reduced pressure the product was purified by reverse-phase column chromatography over C18 (eluent: 0-100% methanol in 60 mM HCl) to give **126** as bright orange solid (30 mg, 20%). **Mp** 245 °C (decomp.); **IR** ν 3379, 3196, 3134, 2921, 2873, 2592, 1617, 1576.5, 1529, 1507, 1496.5, 1405, 1385, 1349.5, 1293, 1253.5, 1217, 1185.5, 1146.5, 1131, 1103, 1065.5, 1035.5 cm^{-1}; **^{1}H-NMR** (400 MHz, CD_3OD) δ 8.51 (d, *J* = 9 Hz, 1H, ArH_{NBD}), 6.86 (s, 2H, Ar*H*), 6.85 (s, 2H, Ar*H*), 6.77 (s, 4H, Ar*H*), 6.40 (d, *J* = 9 Hz, 1H, ArH_{NBD}), 4.50 (d, *J* = 13 Hz, 2H, ArCH_2Ar), 4.47 (d, *J* = 13 Hz, 2H, ArCH_2Ar), 4.03 (t, *J* = 7 Hz, 2H, OC$H_2$$CH_2CH_2CH_2$N), 3.91 – 3.86 (m, 6H, OC$H_2$$CH_2CH_3$), 3.66 (app br s, 2H,

$OCH_2CH_2CH_2CH_2N$), 2.12 – 2.05 (m, 2H, $CH_2CH_2CH_2CH_2$), 1.98-1.85 (m, 8H, $CH_2CH_2CH_2CH_2$ and $OCH_2CH_2CH_3$), 1.02 (t, *J* = 7 Hz, 3H, $OCH_2CH_2CH_3$), 0.94 (t, *J* = 7 Hz, 6H, $OCH_2CH_2CH_3$); **^{13}C-NMR** (100 MHz, CD_3OD) δ 157.98, 157.78, 157.67, 146.52, 145.84, 145.53, 138.47, 137.75, 137.64, 137.42, 125.93, 125.89, 125.83, 124.54, 124.49, 124.42, 124.37, 122.99, 99.68, 78.57, 78.51, 76.42, 44.61, 31.69, 31.57, 28.74, 26.03, 24.41, 24.36, 10.79, 10.63; **HRMS** (NSI) m/z: $[M+H]^+$ Calcd for $C_{47}H_{57}N_8O_7$ 845.4345; Found 845.4345.

5,11,17,23-Tetra-*tert*-butyl-25,26,27-tripropoxy-28-[(ethoxycarbonyl)butoxy-calix[4]arene (127)[103]

To a solution of **77** (5.00 g, 6.45 mmol) in DMF (200 mL) was added NaH (0.62 g, 25.80 mmol) and the mixture stirred for 1 hour before addition of ethyl 4-bromobutyrate (3.7 mL, 25.80 mmol). The mixture was stirred for 18 hours then the solvent was removed under reduced pressure. The residue was dissolved in DCM (100 mL) and washed with water (200 mL) then brine (200 mL). After drying over $MgSO_4$, the solvent removed under reduced pressure and the residue repeatedly triturated with methanol until a solid was obtained, which was filtered and air dried to give **127** as white powder (3.92 g, 68%). **Mp** 122-124 °C; **IR** ν 2959, 2903.5, 2872.5, 1737.5, 1604, 1582, 1480, 1390.5, 1373, 1360.5, 1299, 1278, 1247.5, 1197.5, 1175.5, 1123, 1109, 1090, 1069.5, 1036, 1009 cm^{-1}; **^{1}H-NMR** (400 MHz, $CDCl_3$) δ 6.80 (s, 2H, Ar*H*), 6.79 (s, 2H, Ar*H*), 6.75 – 6.75 (m, 4H, Ar*H*), 4.42 (d, *J* = 13 Hz, 2H, $ArCH_2Ar$), 4.38 (d, *J* = 13 Hz, 2H, $ArCH_2Ar$), 4.17 (q, *J* = 7 Hz, 2H, $CO_2CH_2CH_3$), 3.89 (t, *J* = 7.5 Hz, 2H, $OCH_2CH_2CH_2CO_2$), 3.85 – 3.79 (m, 6H, $OCH_2CH_2CH_3$), 3.12 (d, *J* = 13 Hz, 2H, $ArCH_2Ar$), 3.11 (d, *J* = 13 Hz, 2H, $ArCH_2Ar$), 2.52 (t, *J* = 7.5 Hz, 2H, $OCH_2CH_2CH_2CO_2$), 2.33 (quintet, *J* = 7.5 Hz, 2H, $OCH_2CH_2CH_2CO_2$), 2.06 – 1.95 (m, 6H, $OCH_2CH_2CH_3$), 1.28 (t, *J* = 7 Hz, 3H, $CO_2CH_2CH_3$), 1.10 (s, 9H, $C(CH_3)_3$), 1.09 (s, 9H, $C(CH_3)_3$), 1.06 (s, 18H, $C(CH_3)_3$), 0.99 (t, *J* = 7.5 Hz, 6H, $OCH_2CH_2CH_3$), 0.99 (t, *J* = 7.5 Hz, 3H, $OCH_2CH_2CH_3$).

5,11,17,23-Tetra-nitro-25,26,27-tripropoxy-28-[(ethoxycarbonyl)butoxy-calix[4]arene (128)[103]

To a stirred solution of **127** (2.36 g, 2.65 mmol) in DCM (300 mL) was added glacial acetic acid (15 mL) and 100% nitric acid (15 mL). After 4 hours water (200 mL) was added to quench. The organic layer was separated and washed with water (3 x 300 mL) and brine (300 mL). After drying over $MgSO_4$, the solvent was removed

under reduced pressure and the residue triturated with methanol. The product was filtered and air dried to give **128** as light orange powder (2.06 g, 92%). **Mp** 240-241 °C; **IR** ν 3078, 2969.5, 2934.5, 2877, 1731, 1609, 1585.5, 1519, 1451, 1386, 1341.5, 1301.5, 1286, 1262.5, 1210, 1180, 1092, 1061.5, 1034 cm^{-1}; **^{1}H-NMR** (400 MHz, $CDCl_3$) δ 7.62 (s, 4H, Ar*H*), 7.54 (s, 4H, Ar*H*), 4.52 (d, *J* = 14 Hz, 2H, ArCH_2Ar), 4.50 (d, *J* = 14 Hz, 2H, ArCH_2Ar), 4.16 (q, *J* = 7 Hz, 2H, $CO_2CH_2CH_3$), 4.02 (t, *J* = 7 Hz, 2H, $OCH_2CH_2CH_2CO_2$), 3.99 – 3.93 (m, 6H, $OCH_2CH_2CH_3$), 3.41 (d, *J* = 14 Hz, 2H, ArCH_2Ar), 3.41 (d, *J* = 14 Hz, 2H, ArCH_2Ar), 2.45 (t, *J* = 7 Hz, 2H, $OCH_2CH_2CH_2CO_2$), 2.21 (quintet, *J* = 7 Hz, 2H, $OCH_2CH_2CH_2CO_2$), 1.95 – 1.85 (m, 6H, $OCH_2CH_2CH_3$), 1.26 (t, *J* = 7 Hz, 3H, $CO_2CH_2CH_3$), 1.03 (t, *J* = 8 Hz, 3H, $OCH_2CH_2CH_3$), 1.01 (t, *J* = 8 Hz, 6H, $OCH_2CH_2CH_3$).

5,11,17,23-Tetra-amino-25,26,27-tripropoxy-28-[(ethoxycarbonyl)butoxy-calix[4]arene (129)

A mixture of **128** (2.06 g, 2.44 mmol) and $SnCl_2{\cdot}2H_2O$ (14.31 g, 63.44 mmol) was heated to reflux in ethanol (140 mL) for 48 hours. The solvent was removed under reduced pressure and 10% NaOH (300 mL) added. The product was extracted with DCM (3 x 100 mL) then washed with water (200 mL) and brine (200 mL). After drying over $MgSO_4$, the solvent was removed under reduced pressure to give **129** as light brown solid (1.39 g, 79%). **Mp** 139 °C; **IR** ν 3418.5, 3344.5, 3214.5, 2958.5, 2930.5, 2873.5, 2736, 1730, 1607, 1465, 1383, 1373.5, 1346, 1302.5, 1279.5, 1258.5, 1213.5, 1175.5, 1131.5, 1106.5, 1096, 1067, 1038.5, 1007 cm^{-1}; **^{1}H-NMR** (400 MHz, $CDCl_3$) δ 6.07 (s, 4H, Ar*H*), 6.04 (s, 2H, Ar*H*), 6.03 (s, 2H, Ar*H*), 4.30 (d, *J* = 13.5 Hz, 2H, ArCH_2Ar), 4.27 (d, *J* = 13.5 Hz, 2H, ArCH_2Ar), 4.14 (q, *J* = 7 Hz, 2H, $CO_2CH_2CH_3$), 3.79 (t, *J* = 7 Hz, 2H, $OCH_2CH_2CH_2CO_2$), 3.74 – 3.70 (m, 6H, $OCH_2CH_2CH_3$), 2.92 (d, *J* = 13.5 Hz, 2H, ArCH_2Ar), 2.91 (d, *J* = 13.5 Hz, 2H, ArCH_2Ar), 2.46 (t, *J* = 8 Hz, 2H, $OCH_2CH_2CH_2CO_2$), 2.20 – 2.12 (m, 2H, $OCH_2CH_2CH_2CO_2$), 1.90 – 1.79 (m, 6H, $OCH_2CH_2CH_3$), 1.25 (t, *J* = 7 Hz, 3H, $CO_2CH_2CH_3$), 0.95 (t, *J* = 7 Hz, 3H, $OCH_2CH_2CH_3$), 0.94 (t, *J* = 7 Hz, 6H, $OCH_2CH_2CH_3$); **^{13}C-NMR** (100 MHz, $CDCl_3$) δ 173.45, 149.94, 149.64, 140.53, 140.29, 135.70, 135.63, 135.54, 135.51, 115.85, 115.82, 115.78, 76.74, 76.70, 73.83, 60.26, 31.29, 31.14, 30.93, 25.52, 23.13, 14.25, 10.41, 10.32; **HRMS** (NSI) m/z: $[M+H]^+$ Calcd for $C_{43}H_{57}N_4O_6$ 725.4273; Found 725.4282.

5,11,17,23-Tetra-Boc-amino-25,26,27-tripropoxy-28-[(ethoxycarbonyl)butoxy-calix[4]arene (130)

A solution of **129** (1.39 g, 1.92 mmol), Boc anhydride (6.70 g, 30.72 mmol) and DIPEA (1.27 mL, 7.68 mmol) in DCM (50 mL) was stirred for 72 hours. The solvent was removed under reduced pressure and the product purified by column chromatography over silica gel (eluent: 19:1 DCM/ethyl acetate) to give **130** as an off-white glass (1.68 g, 78%). **Mp** 144-146 °C; **IR** ν 3446, 3328, 2975, 2930.5, 2875.5, 1698.5, 1597.5, 1519.5, 1470.5, 1415.5, 1390, 1365.5, 1291.5, 1241.5, 1214.5, 1150.5, 1061.5, 1037, 1004 cm^{-1}; **^{1}H-NMR** (400 MHz, $CDCl_3$) δ 6.62 (s, 4H, Ar*H*), 6.59 (s, 4H, Ar*H*), 6.16 (s, 2H, N*H*), 6.15 (s, 2H, N*H*), 4.36 (d, *J* = 13 Hz, 2H, ArC*H*$_2$Ar), 4.33 (d, *J* = 13 Hz, 2H, ArC*H*$_2$Ar), 4.14 (q, *J* = 7 Hz, 2H, $CO_2CH_2CH_3$), 3.83 (t, *J* = 7.5 Hz, 2H, $OCH_2CH_2CH_2CO_2$), 3.48 – 3.74 (m, 6H, $OCH_2CH_2CH_3$), 3.09 (d, *J* = 13 Hz, 2H), 3.08 (d, *J* = 13 Hz, 2H), 2.45 (t, *J* = 7.5 Hz, 2H, $OCH_2CH_2CH_2CO_2$), 2.17 (quintet, *J* = 7.5 Hz, 2H, $OCH_2CH_2CH_2CO_2$), 1.85 (sextet, *J* = 7 Hz, 6H, $OCH_2CH_2CH_3$), 1.48 (s, 18H $C(CH_3)_3$), 1.48 (s, 18H, $C(CH_3)_3$), 1.25 (t, *J* = 7 Hz, 3H, $CO_2CH_2CH_3$), 0.95 (t, *J* = 7 Hz, 3H, $OCH_2CH_2CH_3$), 0.94 (t, *J* = 7 Hz, 6H, $OCH_2CH_2CH_3$); **^{13}C-NMR** (100 MHz, $CDCl_3$) δ 172.95, 153.42, 153.39, 152.47, 152.22, 134.97, 134.90, 134.80, 132.21, 132.01, 119.78, 119.72, 79.66, 76.53, 73.68, 60.10, 30.98, 30.92, 28.28, 25.28, 22.89, 14.04, 10.17, 10.09; **MALDI-TOF** m/z: $[M+Na]^+$ 1148.15, $[M+K]^+$ 1164.17.

5,11,17,23-Tetra-Boc-amino-25,26,27-tripropoxy-28-[(hydroxycarbonyl)-propoxycalix[4]arene (131)

A solution of **130** (1.30 g, 1.06 mmol) and tetramethylammonium hydroxide (2.23 mL, 2.2 5.30) in THF (10 mL) was stirred for 6 hours. Water (50 mL) was added and the pH adjusted to < 7 by addition of dilute HCl. The product was extracted with ethyl acetate (3 x 50 mL) then washed with water (100 mL) and brine (100 mL). After drying over $MgSO_4$, the solvent was removed under reduced pressure to give **131** as a light yellow glass (1.12 g, 96%). **Mp** 165-167 °C; **IR** ν 3444, 3327.5, 2975, 2930.5, 2875.5, 1698, 1596.5, 1518, 1470, 1414.5, 1390, 1365.5, 1292.5, 1242, 1214.5, 1150.5, 1063, 1036.5, 1002 cm^{-1}; **^{1}H-NMR** (400 MHz, $CDCl_3$) δ 6.63 (s, 4H, Ar*H*), 6.60 (s, 2H, Ar*H*), 6.55 (s, 2H, Ar*H*), 6.30 (s, 1H, N*H*), 6.29 (s, 1H, N*H*), 6.22 (s, 2H, N*H*), 4.36 (d, *J* = 13 Hz, 2H, ArC*H*$_2$Ar), 4.33 (d, *J* = 13 Hz, 2H, ArC*H*$_2$Ar), 3.88 (t, *J* = 7.5 Hz, 2H, $OCH_2CH_2CH_2CO_2$), 3.79 – 3.73 (m, 6H, $OCH_2CH_2CH_3$), 3.09 (d, *J* = 13 Hz, 2H, ArC*H*$_2$Ar), 3.08 (d, *J* = 13 Hz, 2H, ArC*H*$_2$Ar), 2.50 (t, *J* = 7.5 Hz, 2H,

$OCH_2CH_2CH_2CO_2$), 2.20 (quintet, *J* = 7.5 Hz, 2H, $OCH_2CH_2CH_2CO_2$), 1.90 – 1.81 (m, 6H, $OCH_2CH_2CH_3$), 1.48 (s, 9H, $C(CH_3)_3$), 1.48 (s, 27H, $C(CH_3)_3$), 0.94 (t, *J* = 7 Hz, 6H, $OCH_2CH_2CH_3$), 0.94 (t, *J* = 7 Hz, 3H, $OCH_2CH_2CH_3$); **^{13}C-NMR** (100 MHz, $CDCl_3$) δ 178.42, 153.64, 152.74, 152.71, 152.45, 135.21, 135.17, 134.98, 132.36, 132.06, 119.88, 80.11, 76.78, 76.70, 73.84, 31.12, 30.98, 28.44, 25.22, 23.11, 23.06, 10.32, 10.29; **MALDI-TOF** m/z: $[M+Na]^+$ 1120.45.

5,11,17,23-Tetra-Boc-amino-25,26,27-tripropoxy-28-[(7-hydroxy-2-oxo-2H-chromen-3-yl)carbamoyl]propoxy-calix[4]arene (132)

A solution of **131** (0.84 g, 0.77 mmol), **115** (0.32 g, 1.82 mmol) and EDCI·HCl (0.34 g, 1.82 mmol) in 30% pyridine in DCM (43 mL) was stirred for 18 hours. Solvent was removed under reduced pressure and dilute HCl (100 mL) was added followed by ethyl acetate (200 mL). Methanol was then added in small portions, with shaking, until the mixture resolved into two layers. The organic layer was collected, the solvent removed under reduced pressure and the product purified by column chromatography over silica gel (eluent: 3:2 hexane/ethyl acetate) to give **132** as off-white solid (0.48 g, 49%). **Mp** 175-177 °C; **IR** ν 3327.5, 2975, 2930.5, 2875.5, 1685, 1607.5, 1521.5, 1476.5, 1465.5, 1414.5, 1388, 1365.5, 1319, 1293, 1242.5, 1214.5, 1151.5, 1063.5, 1035.5, 1002 cm^{-1}; **^{1}H-NMR** (400 MHz, $CDCl_3$) δ 8.69 (s, 1H, Ar$H_{Coumarin}$), 8.25 (s, 1H, O*H*), 7.66 (s, 1H, N$H_{Coumarin}$), 7.32 (d, *J* = 8.5 Hz, 1H, Ar$H_{Coumarin}$), 6.80 (dd, *J* = 8.5, 2 Hz, 1H, Ar$H_{Coumarin}$), 6.73 (d, *J* = 2 Hz, 1H, Ar$H_{Coumarin}$), 6.62 (s, 2H, Ar*H*), 6.58 (s, 4H, Ar*H*), 6.57 (s, 2H, Ar*H*), 6.27 (s, 1H, N*H*), 6.19 (s, 2H, N*H*), 6.17 (s, 1H, N*H*), 4.34 (d, *J* = 13 Hz, 4H, ArCH_2Ar), 3.90 (t, *J* = 7.5 Hz, 2H, $OCH_2CH_2CH_2CO_2$), 3.82 – 3.64 (m, 6H, $OCH_2CH_2CH_3$), 3.06 (d, *J* = 13 Hz, 4H, ArCH_2Ar), 2.54 (t, *J* = 7.5 Hz, 2H, $OCH_2CH_2CH_2CO_2$), 2.26 (quintet, *J* = 7.5 Hz, 2H, $OCH_2CH_2CH_2CO_2$), 1.94 – 1.72 (m, 6H, $OCH_2CH_2CH_3$), 1.49 (s, 9H, $C(CH_3)_3$), 1.49 (s, 27H, $C(CH_3)_3$), 0.95 (t, *J* = 7 Hz, 3H, $OCH_2CH_2CH_3$), 0.92 (t, *J* = 7 Hz, 6H, $OCH_2CH_2CH_3$). **^{13}C-NMR** (100 MHz, $CDCl_3$) δ 171.94, 159.28, 159.22, 153.87, 153.74, 153.69, 152.85, 152.67, 151.47, 135.25, 135.21, 135.02, 132.02, 131.91, 131.87, 128.73, 125.00, 120.99, 120.41, 120.21, 120.09, 119.97, 114.29, 112.25, 102.89, 80.40, 80.24, 73.99, 34.32, 31.11, 28.45, 25.83, 23.13, 23.07, 10.39, 10.32; **MALDI-TOF** m/z: $[M+Na]^+$ 1279.74, $[M+K]^+$ 1295.77.

5,11,17,23-Tetra-amino-25,26,27-tripropoxy-28-[(7-hydroxy-2-oxo-2H-chromen-3-yl)amino]butoxy-calix[4]arene

A solution of **132** (20 mg, 0.016 mmol) in THF (1 mL) was cooled to 0 °C before addition of BH_3.THF (0.16 mL, 1 M in THF, 0.16 mmol) under argon. The mixture was heated to 60 °C and stirred for 4 hours. After cooling to room temperature, the reaction was quenched with methanol and the solvent removed under reduced pressure. Methanol (1 mL) was added followed by Raney nickel (1 mg, 0.8 μmol) and the mixture stirred for 18 hours. After removal of the catalyst by filtration, solvent was removed from the filtrate under reduced pressure and residual borate removed by co-evaporation with methanol three times. ^{1}H-NMR showed a complex mixture of products.

5,11,17,23-Tetra-amino-25,26,27-tripropoxy-28-[(7-hydroxy-2-oxo-2H-chromen-3-ylcarbamoyl)butoxy-calix[4]arene (·4HCl) (134)

A solution of **132** (0.20 g, 0.16 mmol) in 2:1 DCM/TFA (3 mL) was stirred for 2 hours. The solvent was removed under reduced pressure and the product purified by column chromatography over C18 (eluent: 0-100% methanol in 60mM HCl) to give **134** as pale orange solid (0.14 g, 88%). **Mp** 260 °C (decomp.); **IR** ν 3390, 2958.5, 2920.5, 2870.5, 2847, 2584.5, 1685, 1607.5, 1576.5, 1523, 1465, 1374, 1309.5, 1263.5, 1249.5, 1216.5, 1180, 1148.5, 1127.5, 1063.5, 1035.5, 1000 cm^{-1}; **^{1}H-NMR** (400 MHz, CD_3OD) δ 8.56 (s, 1H, Ar$H_{Coumarin}$), 7.40 (d, *J* = 8.5 Hz, 1H, Ar$H_{Coumarin}$), 6.91 (s, 2H, Ar*H*), 6.90 (s, 2H, Ar*H*), 6.82 (dd, *J* = 8.5, 2 Hz, 1H, Ar$H_{Coumarin}$), 6.79 (s, 4H, Ar*H*), 6.73 (d, *J* = 2 Hz, 1H, Ar$H_{Coumarin}$), 4.55 (d, *J* = 13.5 Hz, 2H, ArCH_2Ar), 4.54 (d, *J* = 13.5 Hz, 2H, ArCH_2Ar), 4.09 (t, *J* = 7 Hz, 2H, OCH_2CH$_2$CH$_2$CO$_2$), 3.97 (t, *J* = 7 Hz, 2H, OCH_2CH$_2$CH$_3$), 3.91 (t, *J* = 7 Hz, 4H, OCH_2CH$_2$CH$_3$), 3.36 (d, *J* = 13.5 Hz, 2H, ArCH_2Ar), 3.34 (d, *J* = 13.5 Hz, 2H, ArCH_2Ar), 2.61 (t, *J* = 7 Hz, 2H, OCH$_2$CH$_2$CH_2CO$_2$), 2.33 (quintet, *J* = 7 Hz, 2H, OCH$_2$CH_2CH$_2$CO$_2$), 2.02 – 1.91 (m, 6H, OCH$_2$CH_2CH$_3$), 1.04 (t, *J* = 7 Hz, 9H, OCH$_2$CH$_2$CH_3); **^{13}C-NMR** (100 MHz, CD_3OD) δ 173.97, 161.48, 160.19, 158.02, 157.86, 157.83, 153.42, 137.89, 137.86, 137.47, 137.43, 130.07, 127.83, 126.09, 125.90, 125.84, 124.66, 124.57, 124.46, 124.44, 122.21, 114.99, 113.18, 103.33, 78.74, 78.57, 75.92, 34.06, 31.73, 31.63, 26.98, 24.49, 24.38, 10.85, 10.80; **HRMS** (NSI) m/z: $[M+H]^+$ Calcd for $C_{50}H_{58}N_5O_8$ 856.4280; Found 856.4268.

2.5.3 General procedures - biology

THP-1, HL60, HeLa RC-49 and CHO.CCR5 cells have been described previously.[55,126,127] CHO-K1 cells were purchased from ATCC. THP-1 cells were cultured in RPMI medium (Invitrogen) with 10% bovine calf serum, 100 units of penicillin/mL, 100 µg of streptomycin/mL and 2 mM L-glutamine at pH 7.4. The remaining cell lines were cultured in DMEM medium (Invitrogen) with 10% bovine calf serum, 100 units of penicillin/mL, 100 µg of streptomycin/mL and 2mM L-glutamine at pH 7.4. All cell lines were incubated at 37 °C in a water-saturated 5% CO_2 atmosphere. Nystatin, filipin, sucrose and methyl-β-cyclodextrin were purchased from Sigma-Aldrich. Monensin was purchased from Calbiochem. LysoTracker® Red (Invitrogen) was purchased from Molecular Probes. Remaining chemicals and reagents were purchased from Fisher Scientific. Fluorescence images were obtained using a Leica DM IL HC microscope.

2.5.4 Toxicity assays

MTS assays were performed using a CellTiter 96® AQ_{ueous} Non-Radioactive Cell Proliferation Assay (Promega). THP-1 cells were suspended in RPMI medium and HL60, HeLa RC-49 and CHO.CCR5 cells were suspended in DMEM at a concentration of 1 x 10^5 cells/mL. Cell suspension (100 µL) was incubated with calixarene (2 µL) dissolved in sterile water or DMSO (for **87** and **109**) at concentrations of 200 µM, 20 µM, 2 µM, 0.2 µM and 0.02 µM. After 72 hours, 10 µL (for compounds **87**, **96**, **109**, **126** and **134**) or 20 µL (for compounds **94**, **95** and **97**) of MTS was added followed by incubation for 4 hours. Absorbance readings were taken at 492 nm using a BMG Labtech Fluostar Galaxy 96 well plate reader.

2.5.5 Cellular uptake

CHO.CCR5 cells were grown on coverslips in 3 mL of DMEM for 24 hours then incubated with calixarene (10 µM) for time periods of 1, 4, 6, 24, 48 or 72 hours. After removal of medium, the cells were washed with phosphate buffered saline (PBS) (3 x 1 mL) and applied to glass slides with DPX mounting medium for imaging.

2.5.6 Inhibition studies

CHO.CCR5 or CHO-K1 cells were grown on coverslips in 3 mL of DMEM for 24 hours then incubated with monensin (50 µg/mL), sucrose (0.4 M), methyl-β-cyclodextrin (10 mM), filipin (5 µg/mL) or nystatin (5 µg/mL) for 1 hour. This was

followed by incubation with calixarene (10 μM) for 48 hours. After removal of medium, the cells were washed with PBS (3 x 1 mL) and applied to glass slides with DPX mounting medium for imaging.

2.5.7 Co-localisation studies

CHO.CCR5 or CHO-K1 cells were grown on coverslips in 3 mL of DMEM for 24 hours then incubated with calixarene (10 μM) for 48 hours. The cells were then incubated with LysoTracker® Red (50 nM) for 15 minutes. After removal of medium, the cells were washed with PBS (3 x 1 mL) and applied to glass slides with DPX mounting medium for imaging.

2.6 References

(1) Underhill, D. M.; Ozinsky, A.; Hajjar, a M.; Stevens, A.; Wilson, C. B.; Bassetti, M.; Aderem, A. *Nature* **1999**, *401*, 811–5.

(2) Hupalowska, A.; Miaczynska, M. *Traffic* **2012**, *13*, 9–18.

(3) Bonazzi, M.; Cossart, P. *FEBS Lett.* **2006**, *580*, 2962–7.

(4) Mayor, S.; Pagano, R. E. *Nat. Rev. Mol. Cell Biol.* **2007**, *8*, 603–612.

(5) Brodin, L.; Low, P.; Shupliakov, O. *Curr. Opin. Neurobiol.* **2000**, *10*, 312–320.

(6) Russell-Jones, G. J. *Adv. Drug Deliv. Rev.* **2001**, *46*, 59–73.

(7) Schmid, E. M.; McMahon, H. T. *Nature* **2007**, *448*, 883–888.

(8) Collawn, J. F.; Stangel, M.; Kuhn, L. A.; Esekogwu, V.; Jing, S. Q.; Trowbridge, I. S.; Tainer, J. A. *Cell* **1990**, *63*, 1061–1072.

(9) Lundmark, R.; Carlsson, S. R. *Semin. Cell Dev. Biol. 21*, 363–370.

(10) Schmid, S. L.; McNiven, M. A.; De Camilli, P. *Curr. Opin. Cell Biol.* **1998**, *10*, 504–512.

(11) Wigge, P.; Vallis, Y.; McMahon, H. T. *Curr. Biol.* **1997**, *7*, 554–560.

(12) Ungewickell, E. *Proc. Natl. Acad. Sci. U. S. A.* **1999**, *96*, 8809–8810.

(13) Parton, R. G.; Simons, K. *Nat. Rev. Mol. Cell Biol.* **2007**, *8*, 185–194.

(14) Fra, A. M.; Williamson, E.; Simons, K.; Parton, R. G. *J. Biol. Chem.* **1994**, *269*, 30745–30748.

(15) Kurzchalia, T. V; Parton, R. G. *Curr. Opin. Cell Biol.* **1999**, *11*, 424–431.

(16) Parton, R. G.; Hanzal-Bayer, M.; Hancock, J. F. *J. Cell Sci.* **2006**, *119*, 787–796.

(17) Sandvig, K.; Torgersen, M. L.; Raa, H. A.; Van Deurs, B. *Histochem. Cell Biol.* **2008**, *129*, 267–276.

(18) Sabharanjak, S.; Sharma, P.; Parton, R. G.; Mayor, S. *Dev. Cell* **2002**, *2*, 411–423.

(19) Sharma, D. K.; Brown, J. C.; Choudhury, A.; Peterson, T. E.; Holicky, E.; Marks, D. L.; Simari, R.; Parton, R. G.; Pagano, R. E. *Mol. Biol. Cell* **2004**, *15*, 3114–3122.

(20) Kirkham, M.; Parton, R. G. *Biochim. Biophys. Acta, Mol. Cell Res.* **2005**, *1746*, 349–363.

(21) Watts, C. *Annu. Rev. Immunol.* **1997**, *15*, 821–850.

(22) Johannes, L.; Lamaze, C. *Traffic* **2002**, *3*, 443–451.

(23) Grimmer, S.; van Deurs, B.; Sandvig, K. *J. Cell Sci.* **2002**, *115*, 2953–2962.

(24) Derossi, D.; Joliot, A. H.; Chassaing, G.; Prochiantz, A. *J. Biol. Chem.* **1994**, *269*, 10444–10450.

(25) Vives, E.; Brodin, P.; Lebleu, B. *J. Biol. Chem.* **1997**, *272*, 16010–16017.

(26) Richard, J. P.; Melikov, K.; Vives, E.; Ramos, C.; Verbeure, B.; Gait, M. J.; Chernomordik, L. V; Lebleu, B. *J. Biol. Chem.* **2003**, *278*, 585–590.

(27) Nakase, I.; Takeuchi, T.; Tanaka, G.; Futaki, S. *Adv. Drug Deliv. Rev.* **2008**, *60*, 598–607.

(28) Potocky, T. B.; Menon, A. K.; Gellman, S. H. *J. Biol. Chem.* **2003**, *278*, 50188–50194.

(29) Richard, J. P.; Melikov, K.; Brooks, H.; Prevot, P.; Lebleu, B.; Chernomordik, L. V *J. Biol. Chem.* **2005**, *280*, 15300–15306.

(30) Fittipaldi, A.; Ferrari, A.; Zoppe, M.; Arcangeli, C.; Pellegrini, V.; Beltram, F.; Giacca, M. *J. Biol. Chem.* **2003**, *278*, 34141–34149.

(31) Fretz, M. M.; Penning, N. A.; Al-Taei, S.; Futaki, S.; Takeuchi, T.; Nakase, I.; Storm, G.; Jones, A. T. *Biochem. J.* **2007**, *403*, 335–342.

(32) Wender, P. A.; Galliher, W. C.; Goun, E. A.; Jones, L. R.; Pillow, T. H. *Adv. Drug Deliv. Rev.* **2008**, *60*, 452–472.

(33) Tünnemann, G.; Martin, R. M.; Haupt, S.; Patsch, C.; Edenhofer, F.; Cardoso, M. C. *FASEB J.* **2006**, *20*, 1775–84.

(34) Derossi, D.; Calvet, S.; Trembleu, A.; Brunissen, A.; Chassaing, G.; Prochiantz,

A. *J. Biol. Chem.* **1996**, *271*, 18188–18193.

(35) Sakai, N.; Futaki, S.; Matile, S. *Soft Matter* **2006**, *2*, 636–641.

(36) Schmidt, N.; Mishra, A.; Lai, G. H.; Wong, G. C. L. *FEBS Lett.* **2010**, *584*, 1806–1813.

(37) Wender, P. A.; Jessop, T. C.; Pattabiraman, K.; Pelkey, E. T.; VanDeusen, C. L. *Org. Lett.* **2001**, *3*, 3229–3232.

(38) Steel, R.; Cowan, J.; Payerne, E.; O'Connell, M. A.; Searcey, M. *ACS Med. Chem. Lett.* **2012**, *3*, 407–410.

(39) Rothbard, J. B.; Garlington, S.; Lin, Q.; Kirschberg, T.; Kreider, E.; McGrane, P. L.; Wender, P. A.; Khavari, P. A. *Nat. Med.* **2000**, *6*, 1253–7.

(40) Chiu, Y. L.; Ali, A.; Chu, C. Y.; Cao, H.; Rana, T. M. *Chem. Biol.* **2004**, *11*, 1165–1175.

(41) Moschos, S. A.; Jones, S. W.; Perry, M. M.; Williams, A. E.; Erjefalt, J. S.; Turner, J. J.; Barnes, P. J.; Sproat, B. S.; Gait, M. J.; Lindsay, M. A. *Bioconjug. Chem.* **2007**, *18*, 1450–1459.

(42) Veldhoen, S.; Laufer, S. D.; Trampe, A.; Restle, T. *Nucleic Acids Res.* **2006**, *34*, 6561–6573.

(43) Andaloussi, S. E. L.; Lehto, T.; Mäger, I.; Rosenthal-Aizman, K.; Oprea, I. I.; Simonson, O. E.; Sork, H.; Ezzat, K.; Copolovici, D. M.; Kurrikoff, K.; Viola, J. R.; Zaghloul, E. M.; Sillard, R.; Johansson, H. J.; Said Hassane, F.; Guterstam, P.; Suhorutšenko, J.; Moreno, P. M. D.; Oskolkov, N.; Hälldin, J.; Tedebark, U.; Metspalu, A.; Lebleu, B.; Lehtiö, J.; Smith, C. I. E.; Langel, U. *Nucleic Acids Res.* **2011**, *39*, 3972–87.

(44) Kim, S. W.; Kim, N. Y.; Choi, Y. Bin; Park, S. H.; Yang, J. M.; Shin, S. *J. Controlled Release* **2010**, *143*, 335–43.

(45) Kirschberg, T. A.; VanDeusen, C. L.; Rothbard, J. B.; Yang, M.; Wender, P. A. *Org. Lett.* **2003**, *5*, 3459–3462.

(46) Liang, J. F.; Yang, V. C. *Bioorg. Med. Chem. Lett.* **2005**, *15*, 5071–5075.

(47) Jiang, T.; Olson, E. S.; Nguyen, Q. T.; Roy, M.; Jennings, P. A.; Tsien, R. Y. *Proc. Natl. Acad. Sci. U. S. A.* **2004**, *101*, 17867–17872.

(48) Dodd, C. H.; Hsu, H. C.; Chu, W. J.; Yang, P. G.; Zhang, H. G.; Mountz, J. D.; Zinn, K.; Forder, J.; Josephson, L.; Weissleder, R.; Mountz, J. M. *J. Immunol. Methods* **2001**, *256*, 89–105.

(49) Wender, P. A.; Mitchell, D. J.; Pattabiraman, K.; Pelkey, E. T.; Steinman, L.; Rothbard, J. B. *Proc. Natl. Acad. Sci. U. S. A.* **2000**, *97*, 13003–13008.

(50) Wender, P. A.; Rothbard, J. B.; Jessop, T. C.; Kreider, E. L.; Wylie, B. L. *J.*

Am. Chem. Soc. **2002**, *124*, 13382–13383.

(51) Huang, K.; Voss, B.; Kumar, D.; Hamm, H. E.; Harth, E. *Bioconjug. Chem.* **2007**, *18*, 403–9.

(52) Maiti, K. K.; Jeon, O.-Y.; Lee, W. S.; Chung, S.-K. *Chem.--Eur. J.* **2007**, *13*, 762–75.

(53) Paclet, M.-H.; Rousseau, C. F.; Yannick, C.; Morel, F.; Coleman, A. W. *J. Incl. Phenom. Macrocycl. Chem.* **2006**, *55*, 353–357.

(54) Bagnacani, V.; Franceschi, V.; Fantuzzi, L.; Casnati, A.; Donofrio, G.; Sansone, F.; Ungaro, R. *Bioconjug. Chem.* **2012**.

(55) Lalor, R.; Baillie-Johnson, H.; Redshaw, C.; Matthews, S. E.; Mueller, A. *J. Am. Chem. Soc.* **2008**, *130*, 2892–2893.

(56) Pathak, R. K.; Hinge, V. K.; Rai, A.; Panda, D.; Rao, C. P. *Inorg. Chem.* **2012**, *51*, 4994–5005.

(57) Pathak, R. K.; Tabbasum, K.; Rai, A.; Panda, D.; Rao, C. P. *Anal. Chem.* **2012**, *84*, 5117–23.

(58) Pathak, R. K.; Hinge, V. K.; Mahesh, K.; Rai, A.; Panda, D.; Rao, C. P. *Anal. Chem.* **2012**, *84*, 6907–13.

(59) Kumar, M.; Kumar, R.; Bhalla, V.; Sharma, P. R.; Kaur, T.; Qurishi, Y. *Dalton Trans.* **2012**, *41*, 408–12.

(60) Sansone, F.; Dudic, M.; Donofrio, G.; Rivetti, C.; Baldini, L.; Casnati, A.; Cellai, S.; Ungaro, R. *J. Am. Chem. Soc.* **2006**, *128*, 14528–14536.

(61) Lalor, R.; DiGesso, J. L.; Mueller, A.; Matthews, S. E. *Chem. Commun.* **2007**, 4907.

(62) Bagnacani, V.; Franceschi, V.; Bassi, M.; Lomazzi, M.; Donofrio, G.; Sansone, F.; Casnati, A.; Ungaro, R. *Nat. Commun.* **2013**, *4*, 1721.

(63) Eggers, P. K.; Becker, T.; Melvin, M. K.; Boulos, R. A.; James, E.; Morellini, N.; Harvey, A. R.; Dunlop, S. A.; Fitzgerald, M.; Stubbs, K. A.; Raston, C. L. *RSC Adv.* **2012**, *2*, 6250.

(64) Rodik, R. V; Klymchenko, A. S.; Jain, N.; Miroshnichenko, S. I.; Richert, L.; Kalchenko, V. I.; Mély, Y. *Chem.--Eur. J.* **2011**, *17*, 5526–38.

(65) Redshaw, C.; Elsegood, M. R. J.; Wright, J. A.; Baillie-Johnson, H.; Yamato, T.; De Giovanni, S.; Mueller, A. *Chem. Commun.* **2012**, *48*, 1129–31.

(66) Mueller, A.; Lalor, R.; Cardaba, C. M.; Matthews, S. E. *Cytometry, Part A* **2011**, *79*, 126–36.

(67) Kolb, H. C.; Sharpless, K. B. *Drug Discov. Today* **2003**, *8*, 1128–37.

(68) Brik, A.; Alexandratos, J.; Lin, Y.-C.; Elder, J. H.; Olson, A. J.; Wlodawer, A.; Goodsell, D. S.; Wong, C.-H. *Chembiochem* **2005**, *6*, 1167–9.

(69) Sivakumar, K.; Xie, F.; Cash, B. M.; Long, S.; Barnhill, H. N.; Wang, Q. *Org. Lett.* **2004**, *6*, 4603–4606.

(70) Park, S. Y.; Yoon, J. H.; Hong, C. S.; Souane, R.; Kim, J. S.; Matthews, S. E.; Vicens, J. *J. Org. Chem.* **2008**, *73*, 8212–8218.

(71) Xie, F.; Sivakumar, K.; Zeng, Q.; Bruckman, M. A.; Hodges, B.; Wang, Q. *Tetrahedron* **2008**, *64*, 2906–2914.

(72) Groenen, L. C.; Ruel, B. H. M.; Casnati, A. *Tetrahedron* **1991**, *41*, 8379–8384.

(73) Iwamoto, K.; Araki, K.; Shinkai, S. *Tetrahedron* **1991**, *47*, 4325–4342.

(74) Gutsche, C. D.; Iqbal, M. *Org. Synth.* **1990**, *68*, 234–236.

(75) Kumar, S.; Varadarajan, R.; Chawla, H. M. M.; Hundal, G.; Hundal, M. S. S. *Tetrahedron* **2004**, *60*, 1001–1005.

(76) Klimentová, J.; Vojtíšek, P. *J. Mol. Struct.* **2007**, *826*, 48–63.

(77) Sansone, F.; Chierici, E.; Casnati, A.; Ungaro, R. *Org. Biomol. Chem.* **2003**, *1*, 1802–1809.

(78) Budka, J.; Lhotak, P.; Michlova, V.; Stibor, I. *Tetrahedron Lett.* **2001**, *42*, 1583–1586.

(79) Kudale, A. A.; Kendall, J.; Warford, C. C.; Wilkins, N. D.; Bodwell, G. J. *Tetrahedron Lett.* **2007**, *48*, 5077–5080.

(80) Rostovtsev, V. V; Green, L. G.; Fokin, V. V; Sharpless, K. B. *Angew. Chem., Int. Ed.* **2002**, *41*, 2596–9.

(81) Baldini, L.; Melegari, M.; Bagnacani, V.; Casnati, A.; Dalcanale, E.; Sansone, F.; Ungaro, R. *J. Org. Chem.* **2011**, *76*, 3720–32.

(82) Saadioui, M.; Shivanyuk, A.; Böhmer, V.; Vogt, W.; Bohmer, V. *J. Org. Chem.* **1999**, *64*, 3774–3777.

(83) Boyko, V.; Rodik, R.; Danylyuk, O.; Tsymbal, L.; Lampeka, Y.; Suwinska, K.; Lipkowski, J.; Kalchenko, V. *Tetrahedron* **2005**, *61*, 12282–12287.

(84) Casnati, A.; Della Ca, N.; Fontanella, M.; Sansone, F.; Ugozzoli, F.; Ungaro, R.; Liger, K.; Dozol, J. F. *European J. Org. Chem.* **2005**, 2338–2348.

(85) Mecca, T.; Cunsolo, F. *Tetrahedron* **2007**, *63*, 10764–10767.

(86) Mourer, M.; Dibama, H. M.; Fontanay, S.; Grare, M.; Duval, R. E.; Finance, C.; Regnouf-de-Vains, J.-B. *Bioorg. Med. Chem.* **2009**, *17*, 5496–509.

(87) Chen, X. M.; Dings, R. P. M.; Nesmelova, I.; Debbert, S.; Haseman, J. R.; Maxwell, J.; Hoye, T. R.; Mayo, K. H. *J. Med. Chem.* **2006**, *49*, 7754–7765.

(88) Itoh, K.; Sekizaki, H.; Toyota, E.; Tanizawa, K. *Bioorg. Chem.* **1997**, *25*, 307–319.

(89) Lee, J. H.; Bang, H. B.; Han, S. Y.; Jun, J.-G. *Tetrahedron Lett.* **2007**, *48*, 2889–2892.

(90) Kaur, K.; Jain, M.; Khan, S. I.; Jacob, M. R.; Tekwani, B. L.; Singh, S.; Singh, P. P.; Jain, R. *Eur. J. Med. Chem.* **2012**, *52*, 230–41.

(91) Białas, A.; Grembecka, J.; Krowarsch, D.; Otlewski, J.; Potempa, J.; Mucha, A. *J. Med. Chem.* **2006**, *49*, 1744–53.

(92) Le Corre, L.; Kizirian, J.-C.; Levraud, C.; Boucher, J.-L.; Bonnet, V.; Dhimane, H. *Org. Biomol. Chem.* **2008**, *6*, 3388–98.

(93) Olah, G. A.; Narang, S. C. *Tetrahedron* **1982**, *38*, 2225–2277.

(94) Olah, G. A.; Narang, S. C.; Gupta, B. G. B.; Malhotra, R. *J. Org. Chem.* **1979**, *44*, 1247–1251.

(95) Casnati, A.; Arduini, A.; Ghidini, E.; Pochini, A.; Ungaro, R. *Tetrahedron* **1991**, *47*, 2221–2228.

(96) Key, J. A.; Cairo, C. W. *Dyes Pigm.* **2011**, *88*, 95–102.

(97) Soussi, M. A.; Audisio, D.; Messaoudi, S.; Provot, O.; Brion, J.-D.; Alami, M. *European J. Org. Chem.* **2011**, 5077–5088.

(98) Carta, F.; Maresca, A.; Scozzafava, A.; Supuran, C. T. *Bioorg. Med. Chem.* **2012**, *20*, 2266–73.

(99) Burlison, J. a; Blagg, B. S. J. *Org. Lett.* **2006**, *8*, 4855–8.

(100) Wan, X.; Joullié, M. M. *J. Am. Chem. Soc.* **2008**, *130*, 17236–7.

(101) Yang, L.; Xu, L.-W.; Xia, C.-G. *Tetrahedron Lett.* **2005**, *46*, 3279–3282.

(102) Schmittling, E.; Sawyer, J. *Tetrahedron Lett.* **1991**, *32*, 7207–7210.

(103) Gattuso, G.; Grasso, G.; Marino, N.; Notti, A.; Pappalardo, A.; Pappalardo, S.; Parisi, M. F. *European J. Org. Chem.* **2011**, *2011*, 5696–5703.

(104) Kim, H. J.; Bok, J. H.; Vicens, J.; Suh, I.-H.; Ko, J.; Kim, J. S. *Tetrahedron Lett.* **2005**, *46*, 8765–8768.

(105) Bu, J.-H.; Zheng, Q.-Y.; Chen, C.-F.; Huang, Z.-T. *Tetrahedron* **2005**, *61*, 897–902.

(106) Das, S.; Addis, D.; Junge, K.; Beller, M. *Chem.--Eur. J.* **2011**, *17*, 12186–92.

(107) Narasimhan, S.; Swarnalakshmi, S.; Balakumar, R.; Velmathi, S. *Synlett* **1999**, 1321–1322.

(108) Raucher, S.; Klein, P. *Tetrahedron Lett.* **1980**, *21*, 4061–4064.

(109) Brown, H. C.; Heim, P. *J. Org. Chem.* **1973**, *38*, 912–916.

(110) Alcântara, A. F. de C.; Barroso, H. dos S.; Piló-Veloso, D. *Quim. Nova* **2002**, *25*, 300–311.

(111) Pisani, L.; Muncipinto, G.; Miscioscia, T. F.; Nicolotti, O.; Leonetti, F.; Catto, M.; Caccia, C.; Salvati, P.; Soto-Otero, R.; Mendez-Alvarez, E.; Passeleu, C.; Carotti, A. *J. Med. Chem.* **2009**, *52*, 6685–706.

(112) Couturier, M.; Tucker, J. L.; Andresen, B. M.; Dubé, P.; Negri, J. T. *Org. Lett.* **2001**, *3*, 465–7.

(113) Mochizuki, A.; Nagata, T.; Kanno, H.; Suzuki, M.; Ohta, T. *Bioorg. Med. Chem.* **2011**, *19*, 1623–42.

(114) Cory, A. H.; Owen, T. C.; Barltrop, J. A. Cory, J. G. *Cancer Commun.* **1991**, *3*, 207–212.

(115) Kilsdonk, E. P. C.; Yancey, P. G.; Stoudt, G. W.; Bangerter, F. W.; Johnson, W. J.; Phillips, M. C.; Rothblat, G. H. *J. Biol. Chem.* **1995**, *270*, 17250–17256.

(116) Orlandi, P. a; Fishman, P. H. *J. Cell Biol.* **1998**, *141*, 905–15.

(117) Kitajima, Y.; Sekiya, T.; Nozawa, Y. *Biochim. Biophys. Acta, Biomembr.* **1976**, *455*, 452–465.

(118) Hansen, S. H.; Sandvig, K.; van Deurs, B. *J. Cell Biol.* **1993**, *121*, 61–72.

(119) Dickson, R. B.; Willingham, M. C.; Pastan, I. H. *Ann. N. Y. Acad. Sci.* **1982**, *401*, 38–49.

(120) Stenseth, K.; Thyberg, J. *Eur. J. Cell Biol.* **1989**, *49*, 326–333.

(121) Malek, A. M.; Xu, C.; Kim, E. S.; Alper, S. L. *Am. J. Physiol. Cell Physiol.* **2007**, *292*, C1645–59.

(122) Rodal, S. K.; Skretting, G.; Garred, O.; Vilhardt, F.; van Deurs, B.; Sandvig, K. *Mol. Biol. Cell* **1999**, *10*, 961–74.

(123) De Duve, C.; De Barsy, T.; Poole, B.; Trouet, A.; Tulkens, P.; Van Hoof, F. *Biochem. Pharmacol.* **1974**, *23*, 2495–2531.

(124) Cecioni, S.; Lalor, R.; Blanchard, B.; Praly, J.-P.; Imberty, A.; Matthews, S. E.; Vidal, S. *Chem.--Eur. J.* **2009**, *15*, 13232–13240.

(125) Lhotak, P.; Shinkai, S. *Tetrahedron* **1995**, *51*, 7681–7696.

(126) Mueller, A.; Kelly, E.; Strange, P. G. *Blood* **2002**, *99*, 785–791.

(127) Mueller, A.; Strange, P. G. *FEBS Lett.* **2004**, *570*, 126–32.

Chapter 3: Calixarene-Based Glycoconjugates

3.1 Introduction

Protein-carbohydrate interactions are involved in a range of biological processes,[1] including binding of bacterial toxins to cells, bacterial adhesion, viral infection, leukocyte trafficking and the response of the immune system to pathogens. Although the interactions of individual carbohydrate moieties can be weak, when they are clustered on a single scaffold the increase in binding strength can be much greater than that associated with an equivalent increase in concentration of the monomer; this is termed the glycoside cluster effect.[2] This occurs due to pre-arrangement of multiple binding moieties so that they are optimally presented to a multivalent target.

Due to the biological relevance of such interactions, there has been much interest in producing synthetic glycoconjugates to target specific biological processes. Various types of scaffold have been exploited to this end, including proteins,[3] polymers,[4] dendrimers[5] and fullerenes.[6] Calixarenes are also an attractive choice as a scaffold since the conformation and the type and degree of functionalisation can be controlled, allowing the synthesis of glycoconjugates with selected valency and finely tuned orientation and flexibility of the presented sugar moieties in space.

The use of these scaffolds as multivalent glycoconjugates will be examined in the following sections.

3.1.1 Calixarene-based glycoconjugates

A number of different biological targets have been pursued using calixarene-based glycoconjugates. For example, C-type lectin-like receptors found on the surface of NK cells have been targeted as they are involved in the activation of the immune response against tumours and intracellular pathogens, such as viruses. *N*-acetylglucosamine (GlcNAc) based glycoconjugates were synthesised[7] and tested against NKR-P1 and CD69 receptors. Although binding was observed in both cases, a glycoside cluster effect was only observed with the latter. The conjugate with the greatest binding strength, compound **135** (see Figure 3.1), was also able to stimulate NK-mediated cytotoxicity against tumor cells.

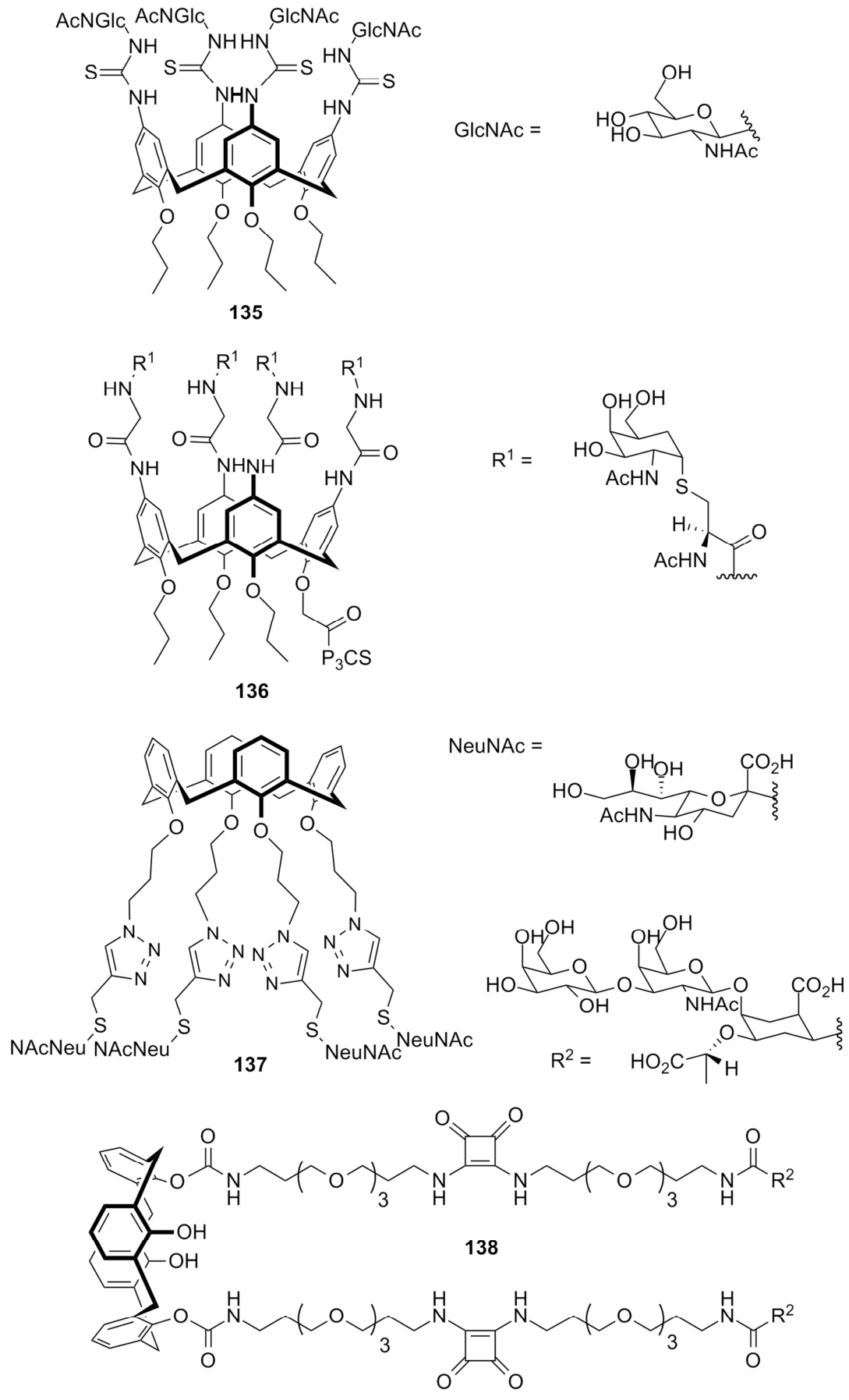

*Figure 3.1: Calixarene-based glycoconjugates for receptor binding (**135**)*[7]*, an artificial antibody (**136**)*[8]*, antiviral activity (**137**)*[9] *and toxin binding (**138**).*[10]

Certain cell-surface glycosyltransferases are involved in cell adhesion and mediation of cell-matrix interactions and have enhanced expression on metastatic cells, their activity being associated with increased invasiveness. A calix[8]arene analogue of compound **135** was tested against rat glioma cells and was found to inhibit wound closure in a scratch-wound model, with greater efficacy than monomeric GlcNAc even at high concentrations of the latter.[11] Although this conjugate was found to affect proliferation of the cells as well as migration, comparison to a butyl-ureido control suggested that the sugar moieties were not responsible for this inhibition.

A further potential anti-cancer application is the construction of an artificial antigen. A tumor associated antigen, Tn, is overexpressed on epithelial cancer cells due to incomplete glycosylation on the cell surface; however, it is a weak immunogen. To overcome this, glycoconjugate **136** (see Figure 3.1), featuring Tn moieties on the upper rim and tripalmitoyl-S-glycerylcysteinylserine (P_3CS) on the lower rim as an immunoadjuvant, was synthesised.[8] This combination resulted in stimulation of antibody production in mice with an apparent glycoside cluster effect when compared with a monovalent analogue.

The use of glycoconjugates as antiviral agents against BK virus (BKV) and influenza A has also been investigated.[9] BKV is known to bind to the sialic acid 5-acetylneuraminic acid (Neu5Ac) on host cells. Influenza A also forms interactions with this epitope *via* hemagluttinin (HA) and a glycosidase (NA), allowing the virus to bind to host cells and proliferate. To interfere with these processes, tetrameric sialoside clusters were synthesised; the lower-rim tetravalent cluster **137** is shown in Figure 3.1.

Although these conjugates displayed binding towards BKV, the opposite of the glycoside cluster effect was achieved, with a loss of activity per sugar unit relative to the monomer. This was attributed to a low concentration of viral hemagglutinin on the virus surface. However, a moderate glycoside cluster effect was apparent for the binding to influenza A. For both BKV and influenza A, infection of cells could be prevented by pre-incubation with the glycoconjugate. This demonstrates that the infection process can be interfered with by competing with the natural ligands of the viral proteins.

Common targets for glycoconjugates are lectins. These are proteins that are characterised by binding to specific sugars with a lack of catalytic activity and are not the product of an immune response.[12] For example, the cholera toxin, a pentavalent

protein-based toxin, presents sugar-binding sites on a single face of the molecule which it uses to bind to host cells. This process is mediated by the ganglioside GM1, which interacts *via* terminal galactose and sialic acid groups. To target this interaction, a GM1 oligosaccharide (GM1os) mimic (**138**) was synthesised[10] with two pseudotrisaccharide moieties presented at the upper rim of a calixarene core, using long linkers to give the necessary flexibility (see Figure 3.1). This divalent glycoconjugate demonstrated superior binding to cholera toxin compared with GM1os, and was also better able to inhibit binding of cholera toxin to its natural target. Such a conjugate could potentially be applied to modulating the effect of such toxins.

The targeting of lectins could potentially have applications in treatment of bacterial infections, for example *Pseudomonas aeruginosa*. This will be examined in more detail in the following section.

3.1.2 Glycoconjugates against *Pseudomonas aeruginosa*

Pseudomonas aeruginosa is an opportunistic pathogen that is capable of infecting most tissues when their defences are compromised.[13] It is the predominant cause of nosocomial pneumonia[14] and lung infections in cystic fibrosis patients.[15] It is a highly adaptable pathogen and multiple drug-resistant strains have developed.[13] This, along with its ability to form biofilms,[16] makes treatment of infections with antibiotics difficult. This has led to the investigation of alternative means of treatment.

Amongst the virulence factors of *P. aeruginosa* are two lectins, PA-IL and PA-IIL (sometimes referred to as LecA and LecB, respectively). Both are homo-tetramers featuring one Ca^{2+} dependent carbohydrate binding site per monomer (see Figure 3.2). PA-IL is selective for D-galactose and its derivatives, which it binds with moderate affinity, whereas PA-IIL has wider specificity, though it binds most strongly to L-fucose and its derivatives. Both of these lectins have hemagglutination activity.[17]

These lectins have inherent cytotoxicity and can inhibit ciliary beating. However, they are primarily implicated in the early stages of infection by binding to glycoconjugates on host cells, allowing other virulence factors to reach their targets. They have been shown to contribute to pathogenicity when acting in synergy with other factors.[18] PA-IIL in particular has also been shown to play a role in the formation of protective biofilms.[16]

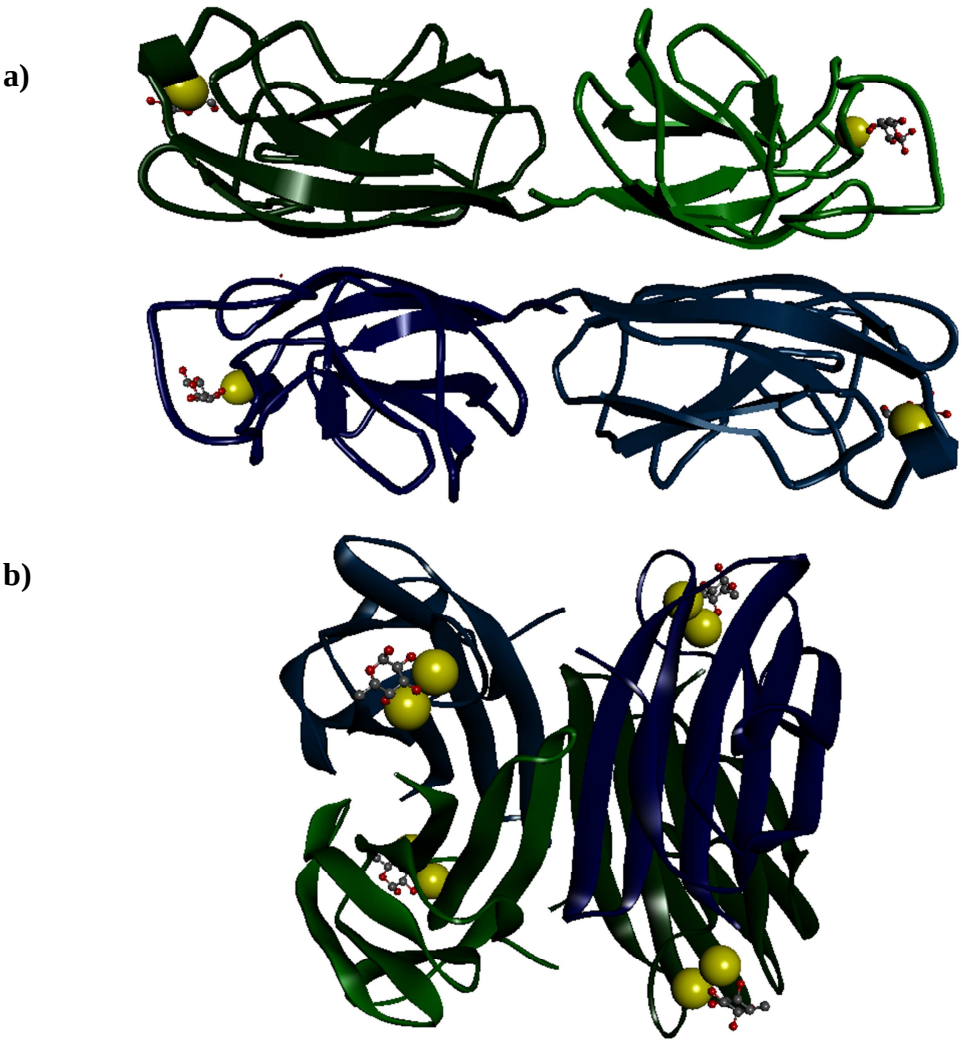

Figure 3.2: Crystal structures of a) PA-IL (PDB code: 1OKO) and b) PA-IIL (PDB code: 1UZV) showing Ca^{2+} binding sites in yellow and ball and stick representations of monosaccharides.

Their contribution to pathogenicity makes these lectins attractive targets. Early investigation showed the potential to inhibit the interaction of the lectins with the host cells using their natural ligands. *In vivo* tests with lung epithelial cells showed reduced cytotoxicity in the presence of the preferred ligand, whilst tests in a mouse model showed a reduction in bacterial load and lung injury, along with improved survival.[18] Investigations were also carried out with cystic fibrosis patients, who were treated by inhalation of fucose or galactose; each of these resulted in reduction of bacterial load, although combination with antibiotic therapy did not give any further improvement, possibly due to antibiotic-related suppression of lectin synthesis.[19]

Together, these studies showed that there was potential to treat infections by *P. aeruginosa* by competitive inhibition of lectin binding. However, the binding

strengths of the individual monosaccharides would make this an inefficient process. This led to the investigation of the use of artificial glycoconjugates to exploit the glycoside cluster effect. Those clusters utilising calixarene scaffolds will be the focus of the remainder of this chapter.

An early attempt at exploiting the glycoside cluster effect with a multivalent calixarene was made with a scaffold functionalised at the upper rim with galactose using click chemistry.[20] The calixarene (**139**) was conformationally locked using three propyl chains on the lower rim with the remaining phenolic position providing a linker to an oligonucleotide, which in turn was used to bind the scaffold to a DNA-based microarray (see Figure 3.3). A fluorescent dye (Cy3) on the oligonucleotide was used to confirm the presence of the glycoconjugates, whilst a different fluorescent dye (Alexa947) on PA-IL was used to measure the degree of binding between the lectin and the glycoconjugates. However, no binding of PA-IL was observed with the calixarene-based scaffold. It was concluded that the steric hindrance caused by the short linkers to the sugars was responsible for this lack of binding to the lectin.

Following on from this, lower rim functionalised calixarenes were synthesised using propargylated scaffolds and sugars with triethyleneglycol linkers, to give greater flexibility whilst improving water solubility.[21] A variety of scaffolds were synthesised with different valencies (mono-, 1,2-di-, 1,3-di-, tri- and tetra-functionalised) and geometries (tetra-functionalised in cone, partial cone and 1,3-alternate conformations). The 1,3-alternate tetravalent scaffold (**140**) is shown in Figure 3.3. The monovalent calixarene was insufficiently water-soluble for testing. Out of the remainder, the tetravalent conjugates gave the best binding to PA-IL (measured by isothermal titration calorimetry, ITC) and displayed a glycoside cluster effect when compared to the corresponding monomer. A mannose-functionalised analogue gave no binding, confirming that there was no non-specific binding from the calixarene core.

The 1,3-alternate compound gave the strongest binding of all and it was found that all four galactose moieties were each binding to one monomer. Since the geometry of the lectin would not allow for the simultaneous binding of all four sugars to a single lectin and the aggregation that would be expected if they were binding to four different lectins was not observed, an aggregative chelate binding mode was proposed where the two pairs of sugars were each binding to one face of two different lectins. Molecular modelling supported this binding mode.[21]

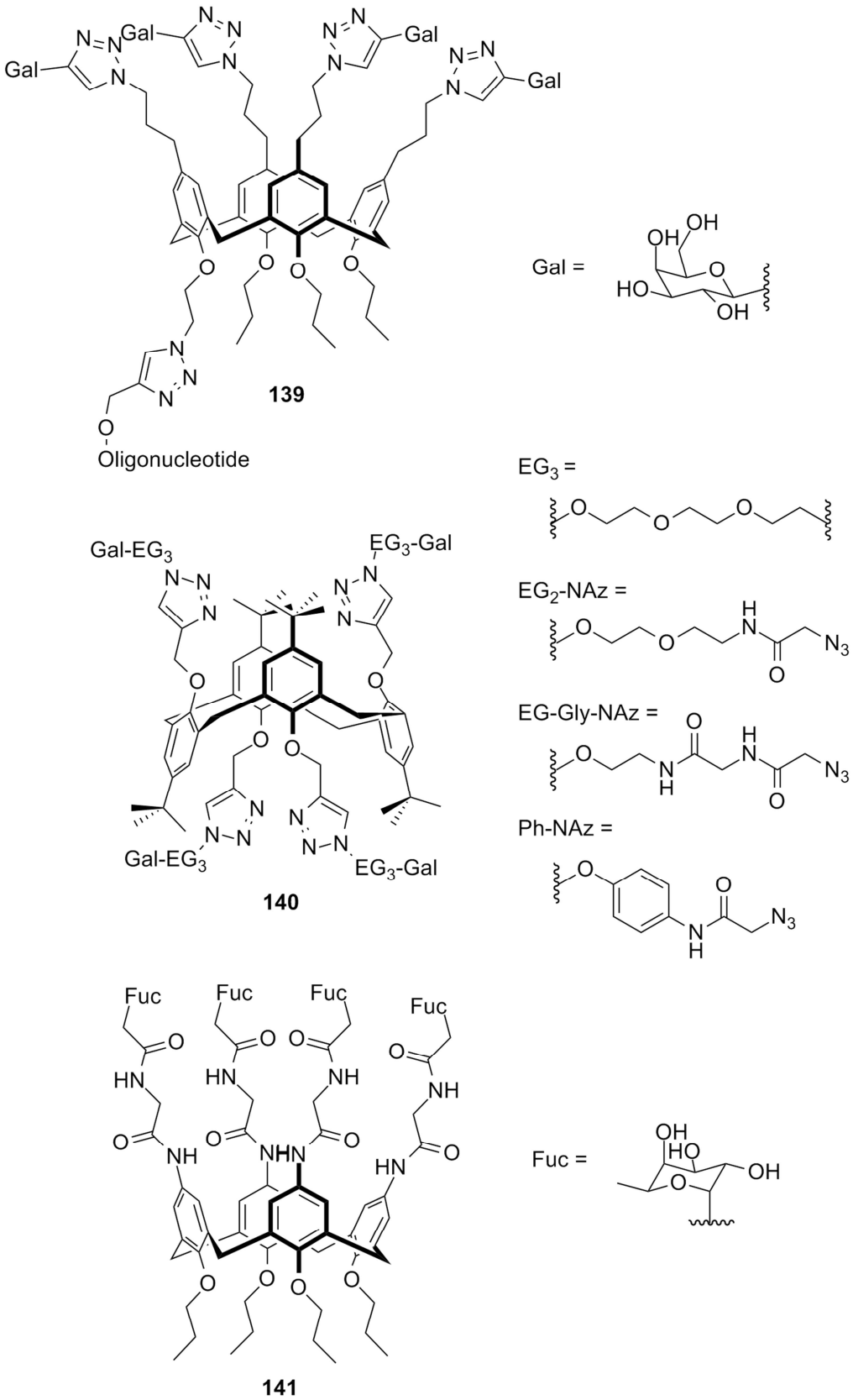

*Figure 3.3: Calixarene-based glycoconjugates for targeting Pseudomonas aeruginosa lectins: compounds **139**,[20] **140**,[21] and **141**[22] and the variable linkers[23] applied to **140**.*

An analogue of the cone conformer of **140** based on calix[6]arene was also synthesised.[24] Although this gave superior binding to PA-IL according to ITC and surface plasmon resonance (SPR), a hemagglutination inhibition assay (HIA) suggested that this hexavalent glycoconjugate was no better than a porphyrin-based tetravalent cluster that was also tested. This hexameric scaffold also lacks the conformational control that is possible with calix[4]arene.

Further investigation of the binding mode of **140** was carried out using atomic force microscopy (AFM).[25] A 1:1 mixture of PA-IL and **140** with $CaCl_2$ was deposited on mica and dried. This revealed long filaments with occasional branch-points. It was proposed that these arose from rare defects in the symmetry of the conjugate, giving one free galactose that could bind to a third lectin. Molecular modelling confirmed that this was possible.

Finally, work was carried out to attempt to optimise the interactions of this conjugate with PA-IL by varying the linker arms to the sugars.[23] It was postulated that greater rigidity would reduce the entropic cost during multivalent binding and also provide additional contacts for binding. A series of four linkers were tested: the original triethyleneglycol (EG_3), diethyleneglycol with an amide bond (EG_2-NAz, where NAz is *N*-azidoacetyl), ethyleneglycol with two amide bonds (EG-Gly-NAz) and a phenyl linker with an amide bond (Ph-NAz). The structures of these linkers are shown in Figure 3.3.

Although the monosaccharide featuring the Ph-NAz linker gave the strongest binding out of the set of monomers, the calixarene conjugates featuring this linker resulted in haemolysis in HIA and were insufficiently soluble for ITC studies. In some cases, for example with the partial cone and 1,3-alternate scaffolds with the EG-Gly-NAz linker, there was a change in binding stoichiometry, with binding to 2-3 monomers instead of 4 as with the EG_3 linker. However, with the 1,3-alternate scaffold with the EG_2-NAz linker, the 1:4 stoichiometry was retained; this was also the highest affinity glycol-conjugate to be synthesised thus far, with a K_D of 90 nM. Contrary to the objective of the investigation, the entropic cost of binding had greatly increased relative to **140**; however this failed to counterbalance the increase in the enthalpic contribution observed with this conjugate, postulated to be due to hydrogen bonds between the amide of the linker with the backbone of the lectin.

Calix[4]arene glycoconjugates based on the propargylated scaffold are currently subject to a patent.[26] The scope of this covers variation of the sugars, the linkers, the

functionalisation of the calixarene upper-rim and also the substitution of the calixarene methylene bridges with heteroatomic groups.

Although PA-IIL has received less attention within the scope of calixarene-based glycoconjugates, some investigation has taken place with a fucose-functionalised calixarene (**141**).[22] The sugars were installed *via* an amide bond to the upper rim, with glycine as a spacer. The calixarene was conformationally locked by exhaustive propylation of the lower rim. Although the conjugate had no direct antimicrobial effect, it was able to inhibit biofilm formation in a dose-dependent manner. With only the free amines on the upper rim, inhibition only occurred at higher concentrations, and to a lesser degree than the glycoconjugate. This research suggests that PA-IIL is a valid target, as well as PA-IL.

It might be assumed that targeting both lectins would give an even more effective treatment. However, the experiments with the free sugars in the mouse model showed no improvement when both galactose and fucose were used. Although a multivalent scaffold could behave differently, there is little evidence of heteroglycoconjugates targeting PA-IL and PA-IIL in the literature. Non-calixarene based examples of glycoconjugates bearing both fucose and galactose show that although such a glycoconjugate can simultaneously bind both lectins, there is in fact a slight loss of binding affinity.[27,28]

3.2 Aims

Although the probable binding mode of compound **140** to free PA-IL in solution has been determined, and the ability of a fucose glycoconjugate (**141**) to inhibit *P. aeruginosa* biofilm formation has been demonstrated, no direct observation of the binding of a calixarene-based glycoconjugate to the bacterium has been made. To confirm the binding of a glycoconjugate to cell-surface exposed lectins, a bifunctional conjugate featuring a fluorescent tag in addition to the sugar units would be desirable. This would allow binding to bacterium, instead of just the free lectins, to be observed.

The aim of this chapter was to synthesise a calixarene core featuring attachment points for sugars *via* a CuAAC reaction, preferably by propargylation of the calixarene, and to also attach a fluorescent dye, preferably on the opposite face to avoid interference with the binding of the sugars to the target lectin, PA-IL. The sugars could then be attached to the scaffold in collaboration with the research group of Sebastien Vidal in Lyon.

In summary, the aims are:

- To suitably functionalise a calixarene for a CuAAC reaction;
- To install a fluorescent dye on the calixarene, preferable on the opposite face to the groups installed for the CuAAC reaction;
- To attach sugars via an ethyleneglycol linker, functionalised for the CuAAC reaction.

3.3 Results and Discussion

3.3.1 Design of the fluorescent glycoconjugate

In order to synthesise the fluorescent glycoconjugate, attachment sites for both the sugars and the fluorescent dye were needed. It was decided to use the methodology of Vidal and coworkers[21] to install the sugars, i.e. by using a CuAAC reaction between propargyl groups on the calixarene and an azide linked to the sugar *via* a triethyleneglycol chain. This linker would improve solubility and give the requried flexibility in the arrangement of the sugars.

The required propargyl groups are easily installed on the lower rim of the calixarene using an ether formation as described in Chapter 2. The dye should therefore be placed on the upper rim to avoid interfering with the binding of the sugars to PA-IL, with the mode of attachment being dependent on the dye. A preference was expressed for fluorescent dyes with emission wavelengths above 570 nm, preferably red. Although red fluorescent dyes are commercially available, those commonly used for biological applications such as Cy5 and Alexa Fluor 633 were prohibitively expensive in this case. It was therefore decided to synthesise a suitable dye.

Various Nile Red derivatives have been synthesised[29] with different emission wavelengths. Of these, derivative **142** (see Figure 3.4) displayed suitable properties for this synthesis, with a carboxylic acid group providing a convenient point for attachment *via* an amide coupling reaction, and with an emission wavelength of its amide conjugates of around 580 nm. The synthesis of this dye uses a straightforward, one-pot procedure.

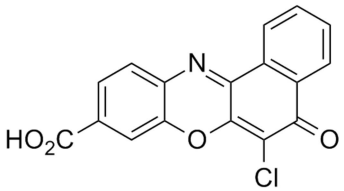

*Figure 3.4: Nile Red derivative (NRD) **142**.*

With the selection of this dye, an amine is required on the upper rim of the calixarene. This is easily accessible by reduction of the corresponding nitro group. The requirement for a single nitro group on the upper rim leads to two possibilities: regioselective nitration, using the functionalisation of the lower rim to control the substitution reaction, or non-selective nitration controlled by reaction time. Both of these routes will be examined.

3.3.2 Route 1: Regioselective mono-nitration

By selectively alkylating the lower-rim of the calixarene, the subsequent electrophilic aromatic substitution reaction can be controlled by the greater electron density donated by a free phenol compared with alkyl ethers. This has been demonstrated for the selective mono-nitration of calixarenes using a multistep process involving temporary installation of benzoyl groups on the lower rim,[30] and also more directly by nitration[31] or *ipso*-nitration[32] of the desired alkyl ether. The latter procedure, containing the fewest synthetic steps, was selected.

The required tripropargyl ether for the selective *ipso*-nitration was available from tetra-*tert*-butylcalix[4]arene (**2**) using a selective trialkylation as described in Chapter 2. Compound **2** was stirred with a mixture of barium oxide and barium hydroxide, followed by addition of propargyl bromide. The mixture was stirred for 18 hours. Aqueous work up followed by column chromatography over silica (eluting with 2:1 DCM/Hexane) gave **143** in the cone conformation as a white powder in 28% yield.

Compound **143** was then reacted with a mixture of glacial acetic acid and 65% nitric acid in proportions used in the literature.[32] The nitric acid was added dropwise over 2 minutes, then the solution stirred for a further 4 minutes, during which time the reaction mixture gained a blue-black colour, before quenching. Aqueous work up followed by purification by column chromatography over silica (eluting with 2:1 DCM/Hexane) gave **144** as yellow crystals in 44% yield.

The ^{1}H-NMR spectrum of **144** (see Figure 3.5b) confirms the correct symmetry and the successful mono nitration. The single plane of symmetry results in a pair of triplets around 2.5 ppm corresponding to the terminal hydrogens of the alkynes, one for the propargyl groups adjacent to the phenol ring and one for the distal propargyl group. However, the same pattern is not observed for the methylene groups of the propargyl ethers.

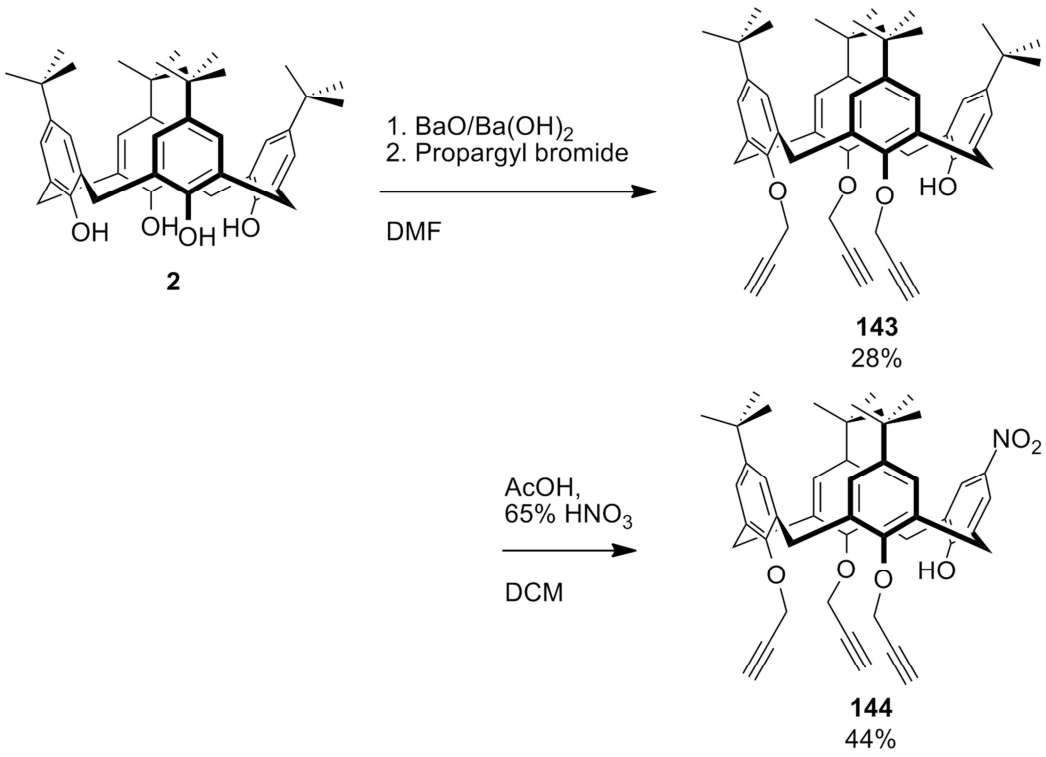

*Scheme 3.1: Synthesis of **144** via selective trialkylation and mono-nitration.*

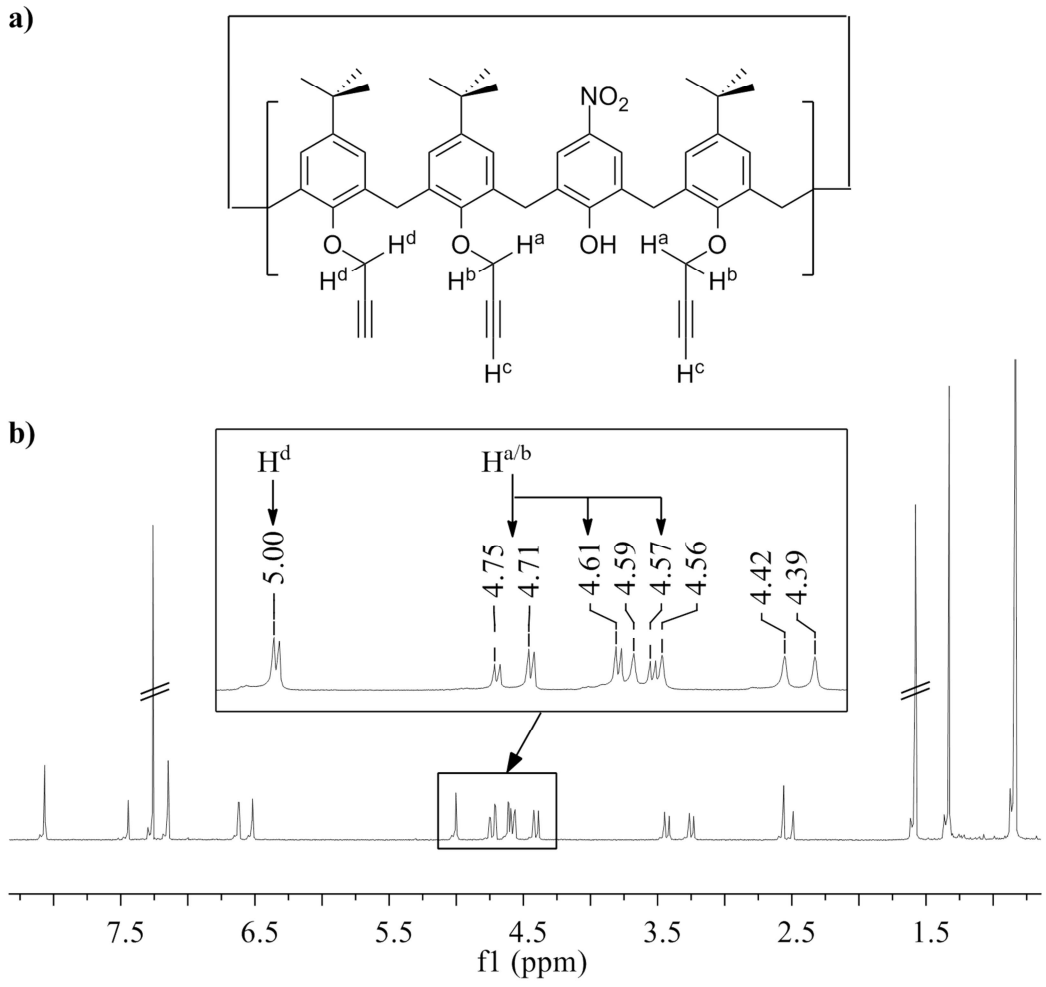

*Figure 3.5: a) Diagram of **144** showing diastereotopic hydrogens on the propargyl groups adjacent to the nitrophenol group; b) ^{1}H-NMR spectrum of **144** ($CDCl_3$).*

The doublet corresponding to the distal propargyl methylene is seen at 5 ppm. The proximal propargyl groups instead give rise to a pair of doublet of doublets at 4.73 and 4.59 ppm, the latter overlapping slightly with one of the methylene bridge doublets at 4.57 ppm. This occurs because the hydrogens on the propargyl methylenes adjacent to the nitrophenol are diastereotopic (see Figure 3.5a); this was not observed for **143**, but seems to be enhanced by the presence of the *para* nitro group on the adjacent phenol in **144**. Therefore there are two couplings, one long range to the terminal hydrogen (with a *J* value around 2.4 Hz) and a second to the geminal hydrogen (with a larger *J* value of around 16 Hz). This gives one doublet of doublets for H^a and a second one for H^b. The mono-nitration is confirmed by the shift of one of the aromatic peaks to around 8.1 ppm. This shift to higher ppm results from the deshielding effect of the nearby nitro group.

With the mono-nitro compound in hand, the lower rim now required exhaustive alkylation. The obvious choice was to use sodium hydride, as in the complete alkylations of Chapter 2. However, previous attempts to carry out this reaction within the group were met with limited success, achieving yields of less than 5% of the desired tetra-propargyl derivative. Although alkylations on partially nitrated calixarenes have been demonstrated,[33,34] there is no evidence in the literature of this being accomplished with propargyl groups. The difficulties associated with installing the final propargyl group could be due to the propargyl ethers that are already present on the calixarene; under basic conditions, it is possible to effect isomerisation to an allene,[35] facilitated by the phenolic oxygen. Therefore, milder alkylation conditions were sought to achieve this transformation.

The Mitsunobu reaction presented one possible route to fully alkylating the lower rim. In this case, alkylation can be achieved using a mixture of triphenylphosphine (TPP) and a dialkylazodicarboxylate to mediate an S_N2 type reaction between a nucleophile and an alcohol, using the loss of phosphine oxide as a leaving group as a driving force. The *O*-alkylation of calix[4]arene with allyl and benzyl alcohols using the Mitsunobu reaction has previously been investigated.[36] The reaction has also been used to apply a bridging crown ether between two phenolic units of a calixarene.[37] In this case, it was hoped that propargyl alcohol could be coupled to phenol, using the latter as the nucleophile.

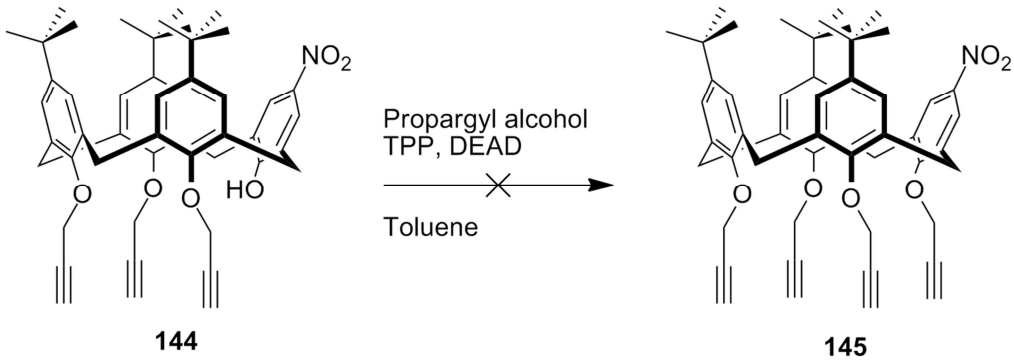

144 **145**

*Scheme 3.2: Attempted synthesis of **145** via a Mitsunobu reaction on **144**.*

Propargyl alcohol was treated with TPP and diisopropylazodicarboxylate (DIAD); the latter was added dropwise to the cooled reaction mixture. After stirring for 10 minutes **144** was added and the mixture stirred overnight at room temperature. Trituration with MeOH/H_2O gave only starting material. The same procedure was attempted with diethylazodicarboxylate (DEAD) instead of DIAD and with no cooling. The reaction mixture was stirred for 3 days. Trituration with MeOH/H_2O gave an oil, so the product was extracted into DCM, though this again gave a red-brown oil. The ^{1}H-NMR spectrum showed starting material.

The lack of reactivity of **144** may be due to the inactivation of the phenol ring by the electron withdrawing nitro group in the *para* position. This would reduce the reactivity of the phenolic oxygen as a nucleophile, such that even the activated intermediate provided by the Mitsunobu reaction could not promote the reaction. At this stage, instead of pursuing this route it was decided to attempt the alternative, non-selective method.

3.3.3 Route 2: Non-selective mono-nitration

In order to access the desired upper-rim mono-nitro calixarene, the reaction can be performed in a non-selective manner, controlling the proportions of the different products of the nitration by varying the amount of time allowed for the reaction. The optimisation of such a reaction by monitoring it over time has been demonstrated on calix[4]arene with no *t*-butyl groups on the upper rim, where during the search for optimal yield of trinitro product it was found that maximum yield of mono-nitro (38%) could be achieved at around 25 minutes, with the return of 45% of starting material.[38]

It was decided to attempt to carry out this transformation on a similarly unfunctionalised calixarene, which required the removal of the *t*-butyl groups from the

previously synthesised **2**. This could be accomplished *via* a reverse Friedel-Crafts reaction with $AlCl_3$ and phenol.[39]

To a stirred mixture of **2** and phenol in toluene was added $AlCl_3$ in small portions. After 4 hours the cloudy suspension had turned brown. The reaction mixture was poured onto ice followed by extraction of the product with DCM. After removal of solvent under reduced pressure, trituration of the residue with methanol gave **146** as off-white powder in 79% yield.

This calixarene could be exhaustively alkylated at the lower rim with sodium hydride as described in Chapter 2, using sodium hydride followed by propargyl bromide. After stirring for 72 hours, aqueous work-up followed by column chromatography over silica gel (eluting with 2:1 hexane/toluene) gave **147** as white powder in 37%.

The mono-nitration reaction was then tested. After stirring **147** in DCM with glacial acetic acid and 65% nitric acid for 30 minutes, the reaction was quenched. Aqueous work up gave only the starting material.

It was decided to use a stronger nitrating mixture and monitor the reaction over time by TLC. To a solution of **147** in DCM, 100% nitric acid and a few drops of 95% sulphuric acid were added, giving an immediate colour change to purple-black. After stirring for 1 hour the reaction was quenched with water; aqueous work up followed by purification by column chromatography over silica (eluting with 1:1 DCM/hexane) gave **148** as light yellow solid and returned **147** in 60% yield.

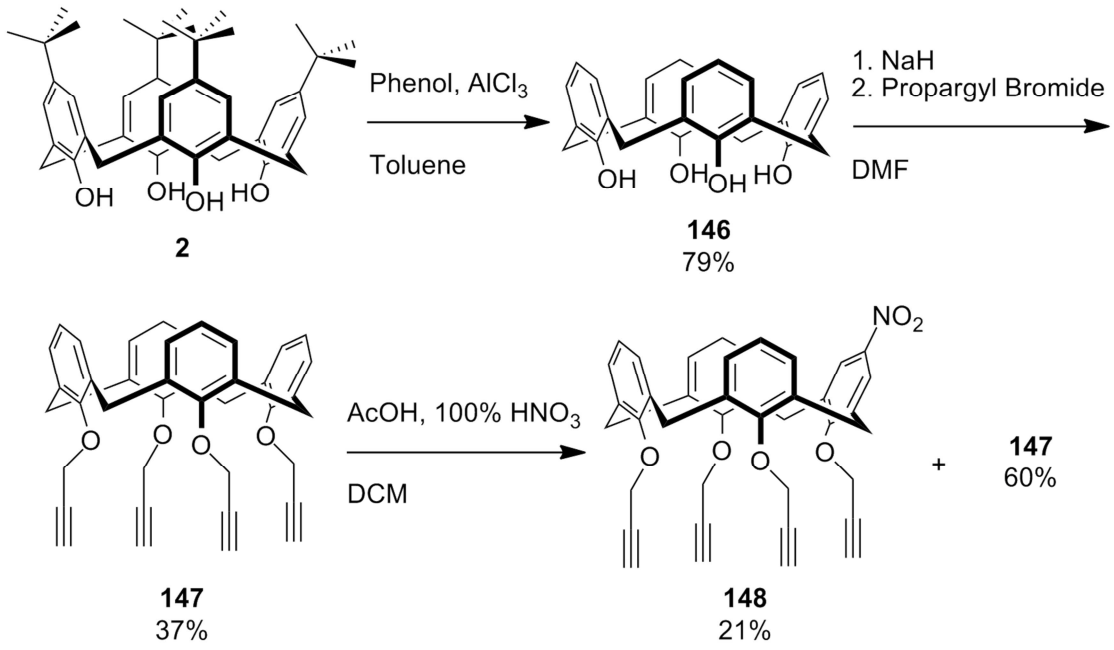

*Scheme 3.3: Synthesis of **148** from **2** via de-tert-butylation, tetraalkyation and time-controlled nitration.*

Purification in this way was complicated by an unknown impurity that co-eluted with the product. This problem could be mitigated by re-crystallising impure column fractions from DCM/methanol, but it still led to a poor yield (total 21%) and made the synthesis less efficient. Once again, in the ^{1}H-NMR spectrum the pattern of two doublets of doublets for the alkyne methylenes on the positions adjacent to the nitrated ring was observed.

Although the overall yield over the three steps was lower than that achieved so far from the first route, the latter synthesis was incomplete. The final alkylation would have needed to have a yield of at least 50% to compare favourably, assuming that a successful method could be found. The second route could potentially be improved if the number of steps was reduced by carrying out an *ipso*-nitration on the *tert*-butyl derivative. However, at this stage, the synthesis was continued with product **148**.

3.3.3.1 Dye synthesis

The selected NRD was synthesised according to the literature.[29] A mixture of 2,3-dichloro-1,4-napthoquinone, 4-amino-3-hydroxybenzoic acid and sodium acetate in methanol was heated to reflux for 24 hours, during which time the suspension turned from yellow to red. After cooling in ice, the solid was filtered and washed with water. The solid was triturated with hot methanol, filtered and washed with further methanol to give **142** as brick-red solid in 66% yield.

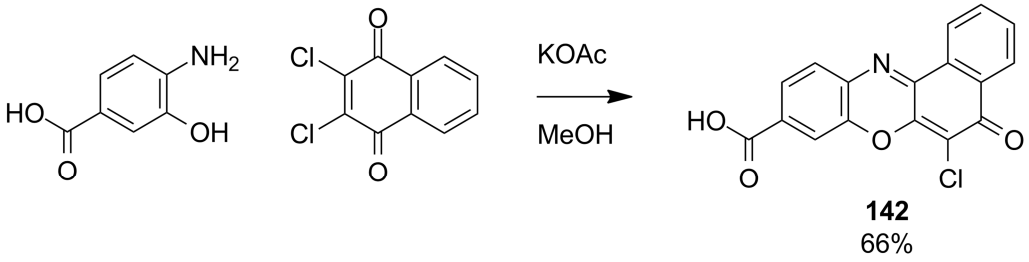

142
66%

*Scheme 3.4: Synthesis of NRD **142**.*

3.3.3.2 Sugar synthesis

To selectively synthesise the target β-anomer of the azide-derivatised sugar, neighbouring group participation can be exploited. Lewis-acid promoted elimination of the leaving group at the anomeric centre can be accomplished with sugar-halides, for example using silver or mercury salts;[40] however, for the installation of the azido-triethyleneglycol linker, it has been found that the use of peracetylated sugar in combination with tin (IV) chloride and silver trifluoroacetate gave superior yield of the desired anomer with short reaction times and on large scales.[41]

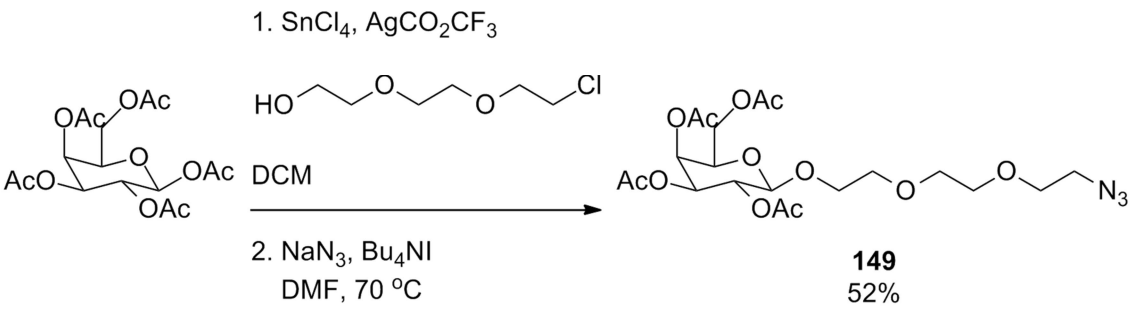

*Scheme 3.5: Synthesis of **149** from pentaacetyl-β-D-galactose.*

To a stirred solution of pentaacetyl-β-D-galactose, $AgCO_2CF_3$ and 2-[2-(2-chloroethoxy)ethoxy]ethanol in dry DCM, $SnCl_4$ was added dropwise. After 2.5 hours, the reaction was quenched with sodium hydrogen carbonate and stirred for a further 12 hours. After aqueous work-up, the intermediate glycosylated product was isolated as a yellow oil. This was stirred with NaN_3 and Bu_4NI in DMF for 18 hours at 70 °C. After filtration of excess reagent, aqueous work-up and flash column chromatography over silica gel (eluting with 1:1 petroleum ether/ethyl acetate), **149** was isolated as viscous, light yellow oil in 52% yield.

3.3.3.3 Conjugation of the dye

In preparation for the reaction with carboxylic acid group of **142**, the nitro group of **148** was next reduced to the amine. As in the reductions carried out during Chapter 2, the tin (II) chloride method was used.

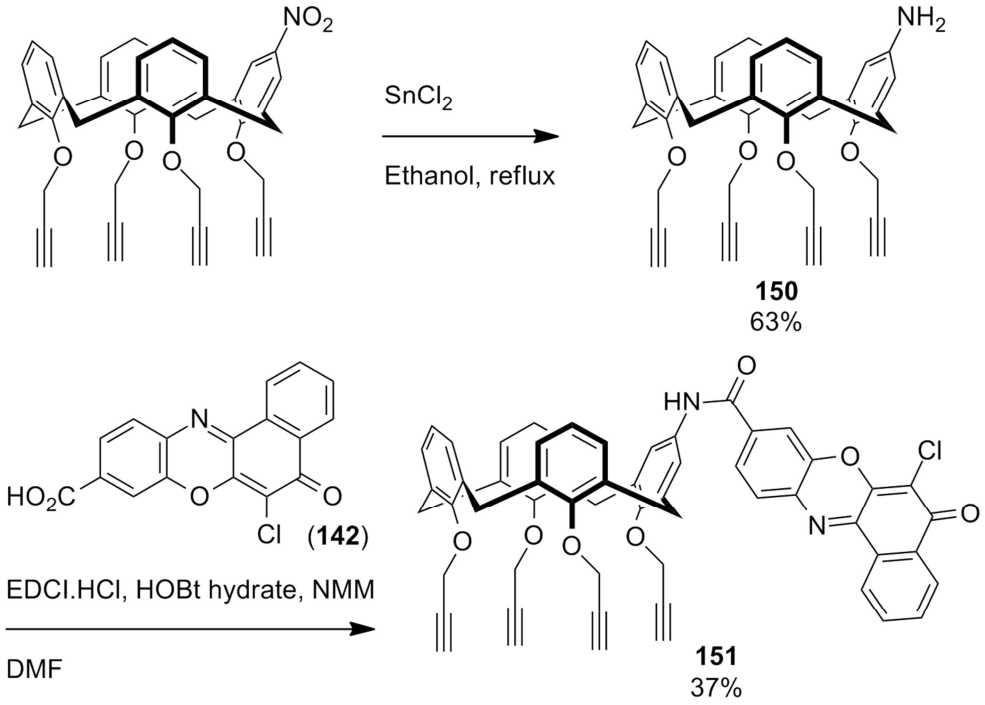

*Scheme 3.6: Reduction of **148** and subsequent conjugation with **142** to give **151**.*

A mixture of **148** and $SnCl_2$ was heated to reflux in ethanol for 48 hours. After removal of solvent under reduced pressure, aqueous work-up with sodium hydroxide gave the mono-amine **150** of moderate purity as brown glass in 63% yield. This crude product was taken through to the next step without further purification to minimise loss of product.

Procedures that have been applied to the conjugation of **142** to amines include the use of amide coupling reagents and a one-pot acid-chloride mediated coupling using Ghosez's reagent.[29] Due to availability of reagents, amide coupling using EDCI was used.

A mixture of **150**, **142**, EDCI, HOBt and *N*-methylmorpholine (NMM) were stirred in DMF for 18 hours. Aqueous work-up followed by column chromatography over silica gel (eluting with DCM) gave **151** as brick-red solid in 37% yield.

The correct product was confirmed by ^{1}H-NMR spectroscopy. The protons on the dye give rise to two multiplets around 8.5 ppm and a cluster of peaks around 8.0 ppm. The N-H of the amide bond can be observed at 7.59 ppm, and the aromatic protons adjacent to this on the calixarene are visible as a singlet at 7.03 ppm, separated from the cluster corresponding to the other aromatic protons around 6.75 ppm. Interestingly, in the ^{1}H-NMR spectra of both the amine and the amide, the peaks corresponding to the alkyene methylene groups do not give rise to the previously observed doublets of doublets; this indicates a lack of inequivalence between the protons on the methylene bridges adjacent to the dye-appended ring.

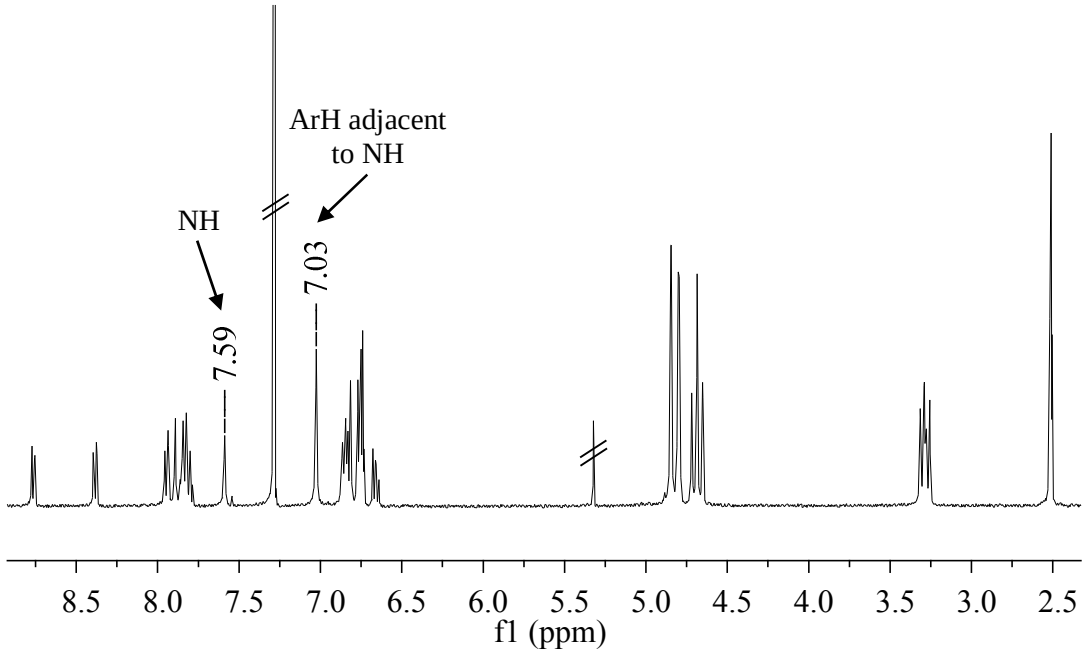

*Figure 3.6: ^{1}H-NMR spectrum of **151** ($CDCl_3$).*

At this stage, a serious problem with this scaffold was identified; although the dye absorbed long-wave UV light, there was no fluorescence. The previously synthesised fluorescent amide-conjugates of **142** were synthesised using aliphatic amines; therefore it was concluded that the loss of fluorescence was due to the extension of the conjugation onto the aromatic ring of the calixarene. The design of the scaffold therefore needed to be modified.

However, with both a dye-conjugated scaffold and the required sugars in hand, it was decided to test the applicability of the sugar conjugation and deacetylation to this new scaffold.

3.3.3.4 Sugar conjugation

It was decided to first test the CuAAC conditions previously used for the conjugation of **149** to alkyne-functionalised calixarenes.[21] This method utilised copper (I) iodide to directly provide the catalytic copper. This method also exploited microwave heating to accelerate the reaction.

A mixture of **149**, **151**, CuI and DIPEA in DMF was heated to 100 °C for 20 minutes. To avoid loss of product during aqueous work-up, the solvent was removed under reduced pressure and the residue directly subjected to column chromatography over silica gel. After eluting the excess sugar with 3:2 ethyl acetate/petroleum ether, the polarity was increased to first neat ethyl acetate and finally a gradient of methanol in ethyl acetate (1-13%) to elute the product. However, this failed to give pure product according to ^{1}H-NMR and low-resolution mass spectrometry showed a mixture of products with lower than expected mass, suggesting that the scaffold had not been fully functionalised.

The presence of poorly-soluble red material also raised concerns as to the stability of the dye conjugate to these conditions. Therefore, at this stage it was decided to carry out the reaction at room temperature, with a long reaction time to allow complete functionalisation. It was also decided to use copper (II) sulphate with sodium ascorbate for *in situ* generation of the copper catalyst, as this gave reliable results in Chapter 2.

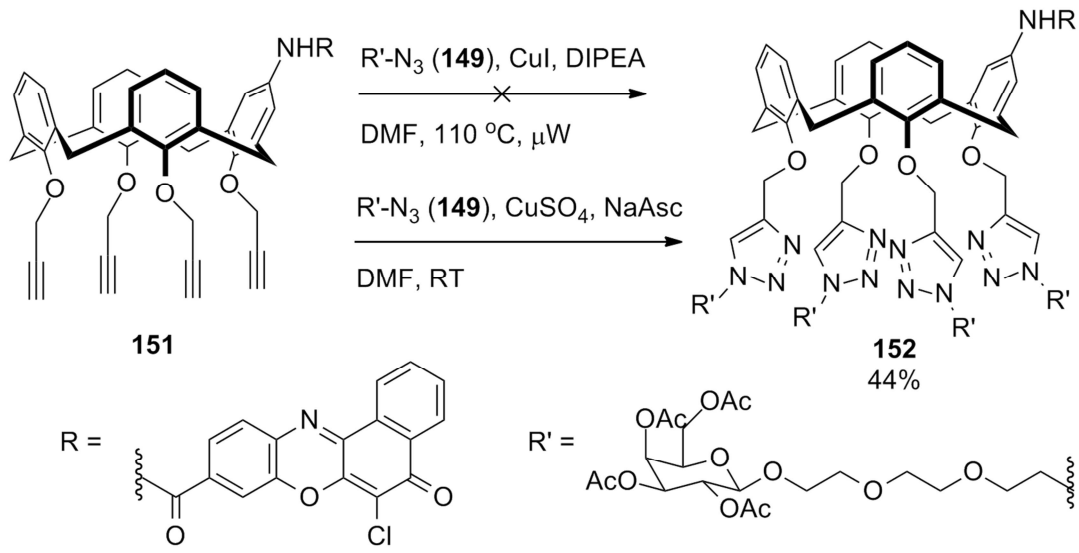

*Scheme 3.7: CuAAC reaction between **149** and **151** to give **152**.*

A mixture of **149** and **151** were stirred with sodium ascorbate and catalytic copper sulphate in DMF for 24 hours, followed by addition of fresh catalyst and **149** and stirring for a further 24 hours. The product was purified by column chromatography over silica gel (eluting with 1:1 ethyl acetate/petroleum ether, ethyl acetate, and 19:1 ethyl acetate/methanol) to give a dark-orange solid. Full substitution was confirmed by low resolution mass spectrometry indicating that **152** had been isolated. The yield of 44% is comparable with the yield previously obtained[21] for conjugation of **149** to the tetra-propargyl calixarene in the cone confirmation; the lower yield obtained for this conformation compared with the others was proposed to be due to steric hindrance on the lower rim.

The correct product is further confirmed by the ^{1}H-NMR spectrum (see Figure 3.7). The characteristic pair of multiplets on the dye can be seen at 8.74 and 8.34 ppm, whilst the remaining dye peaks are around 7.9 ppm, along with the protons on the newly-formed triazole rings. The NH of the amide can be seen as a broad singlet at 8.14 ppm. Interestingly, the aromatic protons adjacent to the NH appear as a pair of peaks around 7.1 ppm instead of just a singlet as expected from the symmetry of the molecule. The lack of any correlation to other peaks in the 2D-COSY spectrum suggests that these are two singlets rather than a doublet, although the loss of symmetry that would give two environments for these protons is not observed in the rest of the spectrum.

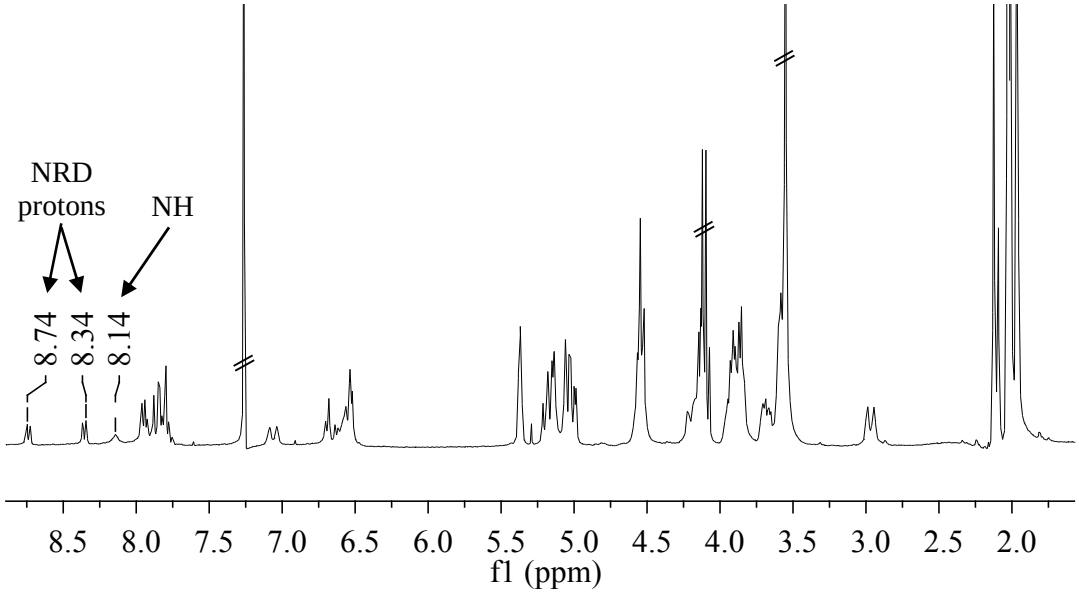

*Figure 3.7: ^{1}H-NMR spectrum of **152** ($CDCl_3$).*

The sugar peaks are present as a complex series of multiplets due to the multiple environments on the lower rim of the calixarene. These obscure the methylene peaks between the triazole ring and the calixarene core around 5.1 ppm, and also one of the calixarene methylene bridge peaks around 4.2 ppm. The peaks corresponding to the ethylene glycol linker are present around 3.6, 3.9 and 4.5 ppm, with the latter two multiplets overlapping with two of the sugar environments. Finally, the acetyl protecting groups on the sugars can be seen around 2.0 ppm.

3.3.3.5 Deprotection

The protecting groups on the sugars could now be removed to give the final product. Commonly employed methods for deacetylation of sugars include the use of sodium ethoxide in methanol[42] or triethylamine catalysed methanolysis.[21] The latter method was selected as this was previously employed in the synthesis of galactose functionalised calixarenes. It provides simple, mild reaction conditions with reagents and byproducts that are easily removed under vacuum.

A solution of **152** in a mixture of triethylamine, methanol and water was stirred under argon for 42 hours before removing solvent under reduced pressure. However, at this stage both the ^{1}H-NMR and low resolution mass spectra indicated a mixture of products and were inconclusive. The reaction was therefore continued for a further 48 hours to ensure that the compound had been fully deacetylated as partial deprotection would give rise to a wide range of different products. The ^{1}H-NMR spectrum showed little change.

Purification by reversed-phase column chromatography over C18 (eluting with a gradient of 5-95% methanol in water) failed to give pure product. In addition, a fraction containing an unknown aromatic compound as the major component raised concerns as to the stability of the dye under the deprotection conditions.

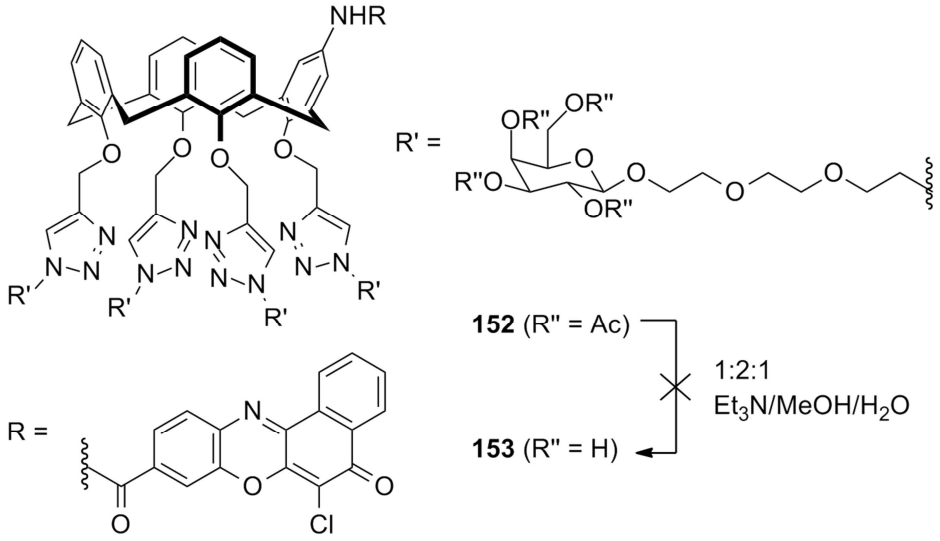

*Scheme 3.8: Attempted deacetylation of **152** to give **153**.*

At this stage, further investigation of the effect of the relative proportions of triethylamine, methanol and water may have yielded suitable deprotection conditions whilst maintaining the integrity of the dye-conjugated scaffold. Alternatively, deacetylation of the sugars prior to carrying out the CuAAC reaction may circumvent the problem of instability of the scaffold to deacetylation conditions; this procedure has been utilised in the synthesis of fullerene-based glycoconjugates.[6] However, it was decided to focus attention on the synthesis of a scaffold with the correct fluorescent properties, which could then be conjugated to the sugars utilising the knowledge attained in sections 3.3.3.4 and 3.3.3.5.

3.3.4 Route 3: Non-selective mono-nitration on *tert*-butyl calixarene

In response to the loss of fluorescence on the conjugation of **142** to the aromatic amine, it was decided to put in place an aliphatic linker in the form of a glycine residue, which could be added via an amide bond to the mono-amine funtionalised calixarene. This would interrupt the extended conjugation across the amide bond and on to the aromatic ring of the calixarene. This also provided the opportunity to revisit the synthesis of the mono-nitrated product.

To increase the efficiency of the synthesis of the scaffold, it was decided to attempt the mono-nitration directly on the *tert*-butyl calixarene. A time-controlled *ipso*-

nitration has been accomplished previously using acetic acid and 100% nitric acid in much smaller amounts than used in the corresponding tetra-nitration.[43]

Compound **2** was first tetra-alkylated in the same way as in the synthesis of **147**. After stirring the reaction mixture for 48 hours the product was precipitated with excess water, filtered and washed with water to give **154** as light-brown powder in 53% yield. This product was sufficiently pure to use in further reactions.

The nitration reaction was tested on **154** by stirring it in DCM with acetic acid and 100% nitric acid. After a 30, 60 or 90 minutes, the reaction was quenched by addition of water. After aqueous washes, the product (now identical to **145**, the synthesis of which was previously attempted in section 3.3.2) was purified by column chromatography over silica gel (eluting with 8-10% ethyl acetate in hexane) and the proportions of starting material and products were assessed.

The results are shown in Table 3.1. A reaction time of 30 minutes gave the optimum yield of **145** whilst returning maximal **154**. Longer reaction times did not improve the yield of product, whilst returning less starting material. At 90 minutes, a significant amount of material was lost to a mixture of over-nitrated products.

*Table 3.1: Change in proportions of product **145** and recovered **154** over time.*

Reaction time / mins	*% recovery of **154***	*% yield of **145***
30	40	26
60	13	23
90	2	22

In addition to removing one step from the synthesis, a noteworthy improvement in this route was the ease of purification relative to that of **148**. This made this synthetic step a much more simple and efficient process.

Reduction was carried out as in section 3.3.3. Compound **145** was heated to reflux with $SnCl_2$ in ethanol for 18 hours, followed by removal of solvent and aqueous work up with sodium hydroxide, giving **155** as yellow solid in 83% yield. However, in this case, a small amount of unknown impurity was consistently found in the product. When the reaction was allowed to continue for 48 hours, the purity of the product was greatly diminished. Therefore 18 hours seems to be the optimum to allow the reaction to run to completion without diminishing the yield due to impurities.

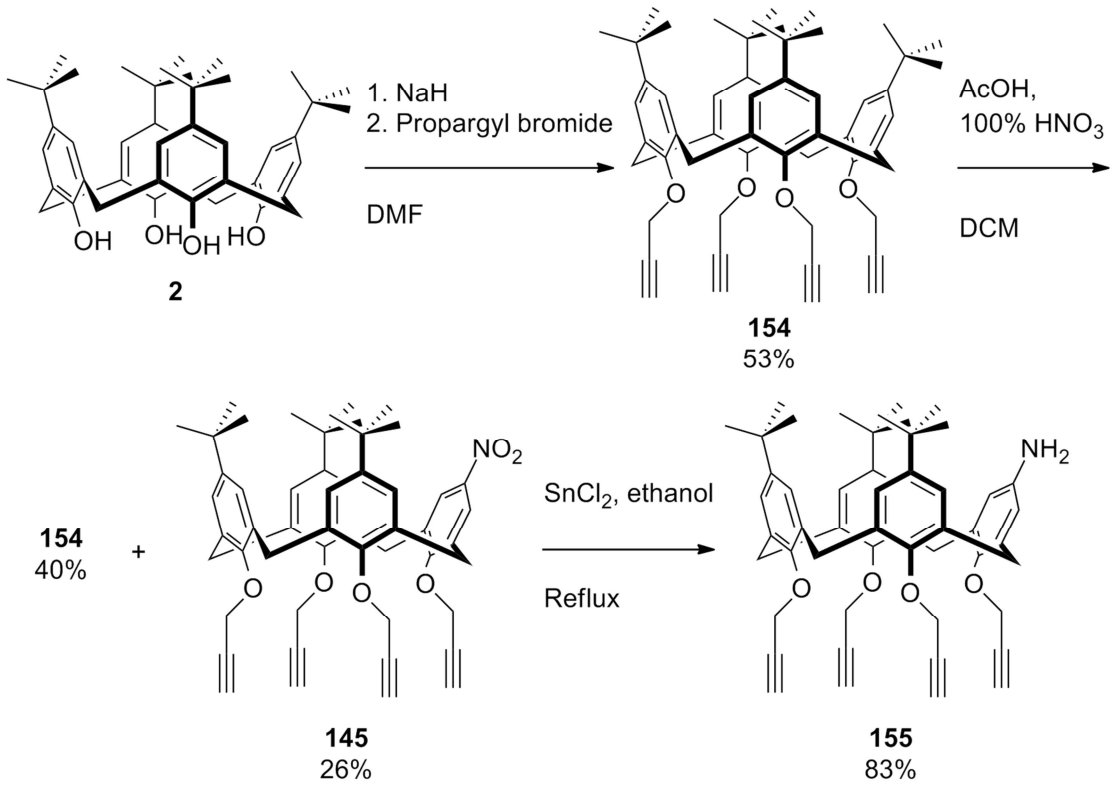

*Scheme 3.9: Synthesis of **155** via alkylation, mono-nitration and reduction.*

The addition of the glycine linker was accomplished in a similar manner to the conjugation of the dye molecule. To a stirred mixture of Boc-glycine, EDCI and HOBt in dry DMF under argon was added **155** in DMF, followed by DIPEA. This was stirred for 24 hours, followed by aqueous work-up and purification by column chromatography over silica gel (eluting with 5-7% ethyl acetate in DCM) to give **156** as yellow solid in 64% yield.

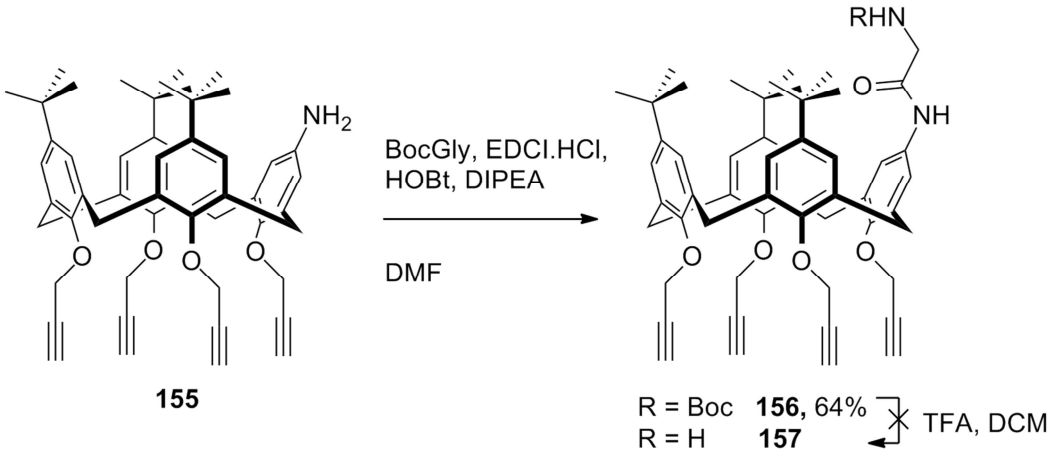

*Scheme 3.10: Synthesis of **156** by amide coupling reaction of **155** with Boc-glycine; attempted deprotection to give **157**.*

The ^{1}H-NMR spectrum of **156** (see Figure 3.8) shows a doublet corresponding to the methylene of the glycine group at 3.71 ppm, which is coupled to the Gly-NH visible at 5.00 ppm as a broad singlet. The aromatic NH proton is visible at 7.23 ppm.

The methylenes of the alkynes adjacent to the functionalised ring once again give rise to a pair of doublet of doublets around 4.9 ppm; however, in this case there is a pronounced 'rooftop' effect due to the proximity of the two multiplets. The doublets of the other two alkynes are overlapping with one of the methylene bridge peaks at 4.60 ppm.

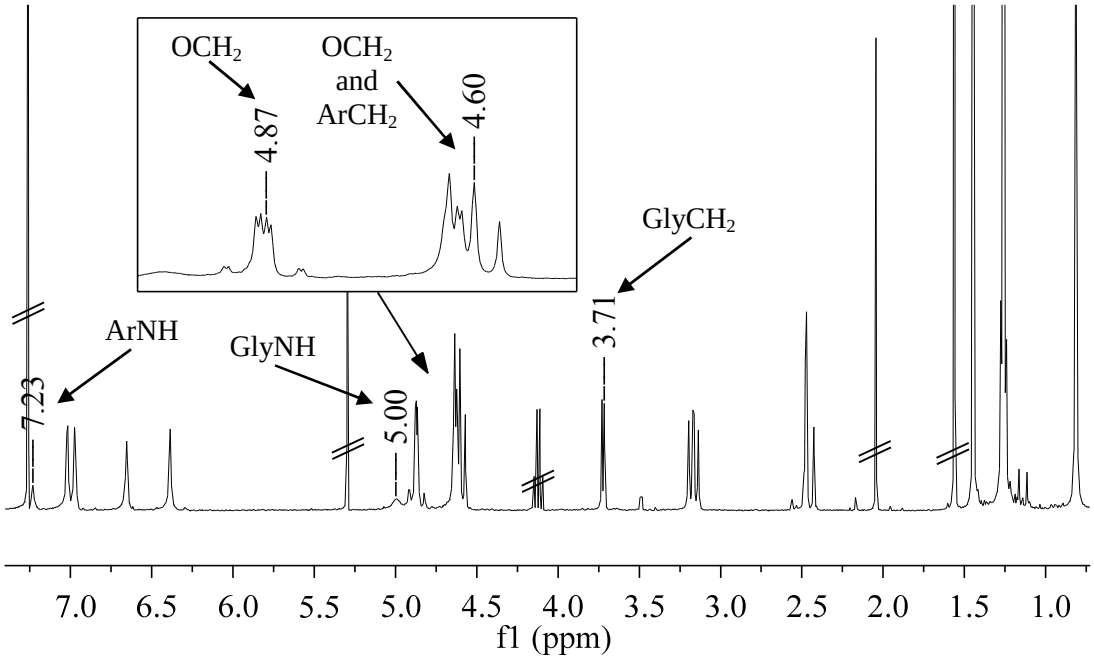

*Figure 3.8: ^{1}H-NMR spectrum of **156** ($CDCl_3$).*

In order to perform the conjugation reaction with **142**, the Boc protecting group next needed to be removed to reveal the required amine. Based on the deprotection of the amide-linked coumarin conjugate (**132**) carried out in Chapter 2, it was decided to use the TFA deprotection method instead of using gaseous HCl as this appeared to be a milder method and better suited to compounds featuring amide bonds. Compound **156** was stirred with TFA in DCM, resulting in a change in colour of the light orange-yellow solution to orange then brown, finally gaining a pink hue. After 40 minutes the reaction was quenched with water to give a grey emulsion. The acid was neutralised with saturated aqueous $NaHCO_3$; on shaking the emulsion resolved to give an orange organic layer. However, the isolated orange-brown solid proved to be a complex mixture of products by ^{1}H-NMR.

It was unclear exactly what unexpected transformation was taking place in this reaction. However, it was reasoned that such a complex mixture would likely arise from side-reactions of the alkynes. The potential of propargyl ethers to give rise to side-reactions was noted in Chapter 2. It was therefore decided to synthesise an analogous structure with TBDMS-protected alkynes to determine if these groups were resulting in the failure of this Boc deprotection reaction.

3.3.5 Route 4: Synthesis of scaffold using TBDMS-protected alkynes

The TBDMS groups could be installed as in Chapter 2 using LiHMDS as a strong base and TBDMSCl as a silylating reagent. This was first attempted on compound **145** as this compound was already available.

To a solution of **145** in THF, cooled to -70 °C, LiHMDS solution in THF was added followed by TBDMSCl, also dissolved in minimum THF. The mixture was allowed to warm to room temperature and stirred for 24 hours. After aqueous work-up with saturated NH_4Cl, a dark orange oil was isolated, from which the product could not be precipitated with methanol. Instead of the TBDMS protected mono-nitro product (**158**), the ^{1}H-NMR spectrum of this residue revealed a complex mixture of products, which could not be accounted for by mixtures of partially protected products since the triplets corresponding to the terminal alkyne protons were not present.

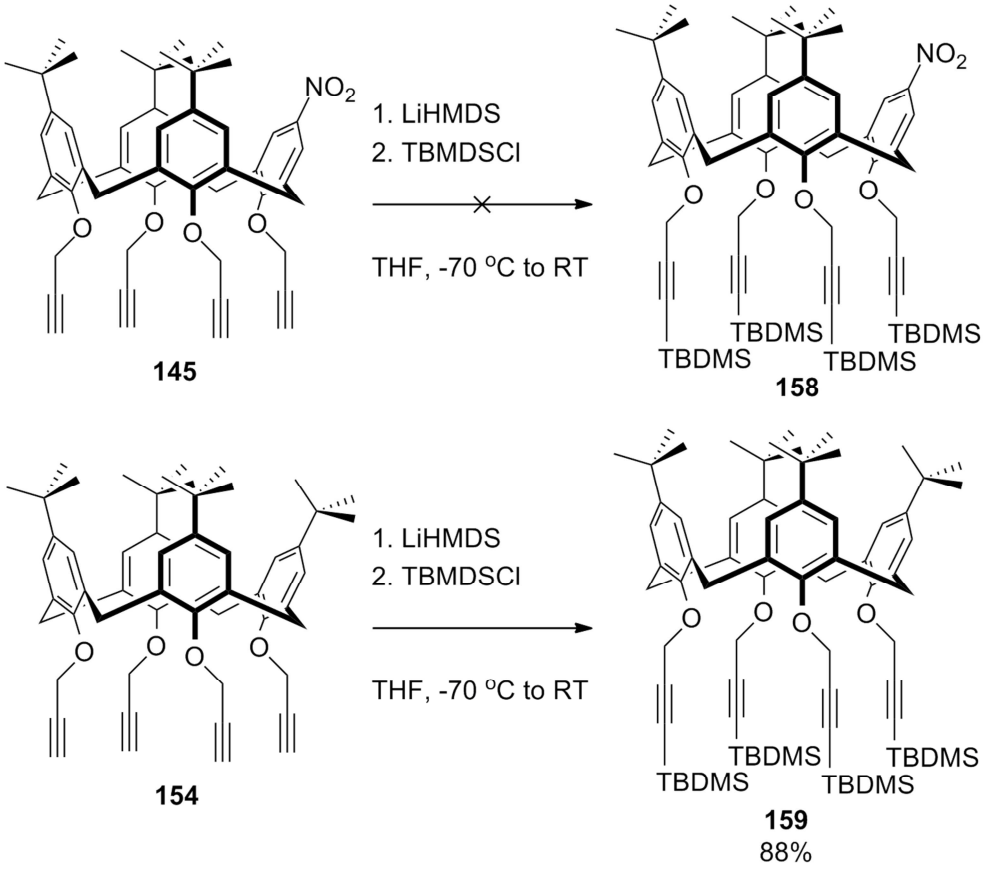

*Scheme 3.11: Attempted TBDMS protection of **145** to give **158**; analogous protection of **154** to give **159**.*

Due to the apparent incompatibility of the protection reaction with the nitrated calixarene, the TBDMS groups were applied instead to the precursor **154**. To a stirred solution of this compound in THF, cooled to -80 °C, LiHMDS solution in THF was added followed by TBDMSCl, also dissolved in minimum THF. The mixture was allowed to warm to room temperature and stirred for 18 hours. After aqueous work-up

with saturated NH_4Cl, the product was precipitated from the isolated residue with methanol to give **159** as light brown powder in 88% yield.

The ^{1}H-NMR spectrum of **159** compared with that of **154** (see Figure 3.9) shows exhaustive protection of the lower rim alkynes. The doublet around 4.8 ppm is now a singlet, and the triplet corresponding to the terminal alkyne position around 2.4 ppm is now absent. The symmetry of the molecule is preserved, giving rise to just two doublets for the methylene bridges due to the equivalence between each pair of diastereotopic hydrogens. Finally, the integrals of the TBDMS peaks (not shown) are correct for 4 protecting groups.

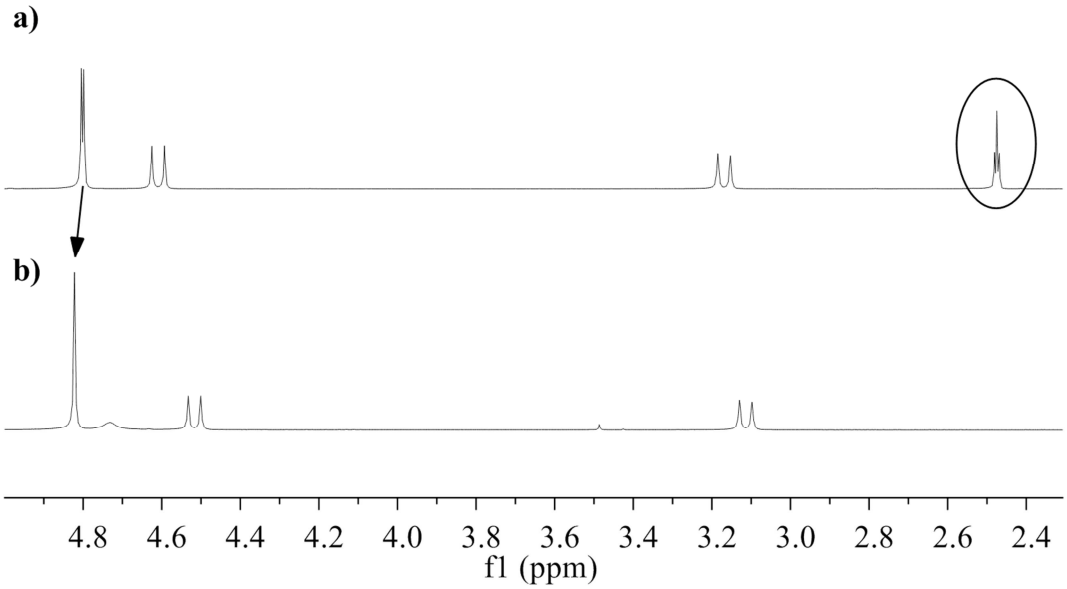

*Figure 3.9: ^{1}H-NMR spectra of a) compound **154** and b) compound **159** showing loss of terminal alkyne triplet (circled) and change of methylene doublet in a) to singlet in b).*

The mono-nitration of **159** was then performed as in 3.3.4. To a stirred solution of **159** in DCM was added glacial acetic acid and 100% nitric acid. After 45 or 60 minutes, the reaction was quenched by addition of water. After aqueous washes the product was purified by column chromatography over silica gel (eluting with 4:1 then 2:1 hexane/DCM) and the proportions of starting material and products assessed. Slightly longer reaction times were required in this case with 60 minutes being the optimum, as shown in Table 3.2.

*Table 3.2: Change in proportions of product **158** and recovered **159** over time.*

Reaction time / mins	*% recovery of **159***	*% yield of **158***
45	71	15
60	70	29

The ^{1}H-NMR spectrum of **158** (see Figure 3.10a) shows that the singlet corresponding to the protons on the nitrated ring has been shifted downfield to 7.37 ppm as expected. The methylene groups of two of the alkynes give rise to singlets at 4.78 and 4.58 ppm; however, the other two peaks around 4.94 ppm have satellite peaks. This indicates the presence of diastereotopic hydrogens on the two alkynes adjacent to the functionalised ring as previously observed for the non-TBDMS protected compounds. In this case, with the loss of the long range coupling to the terminal alkyne position, a pair of doublets is observed, with a pronounced 'rooftop' effect due to their proximity to one other.

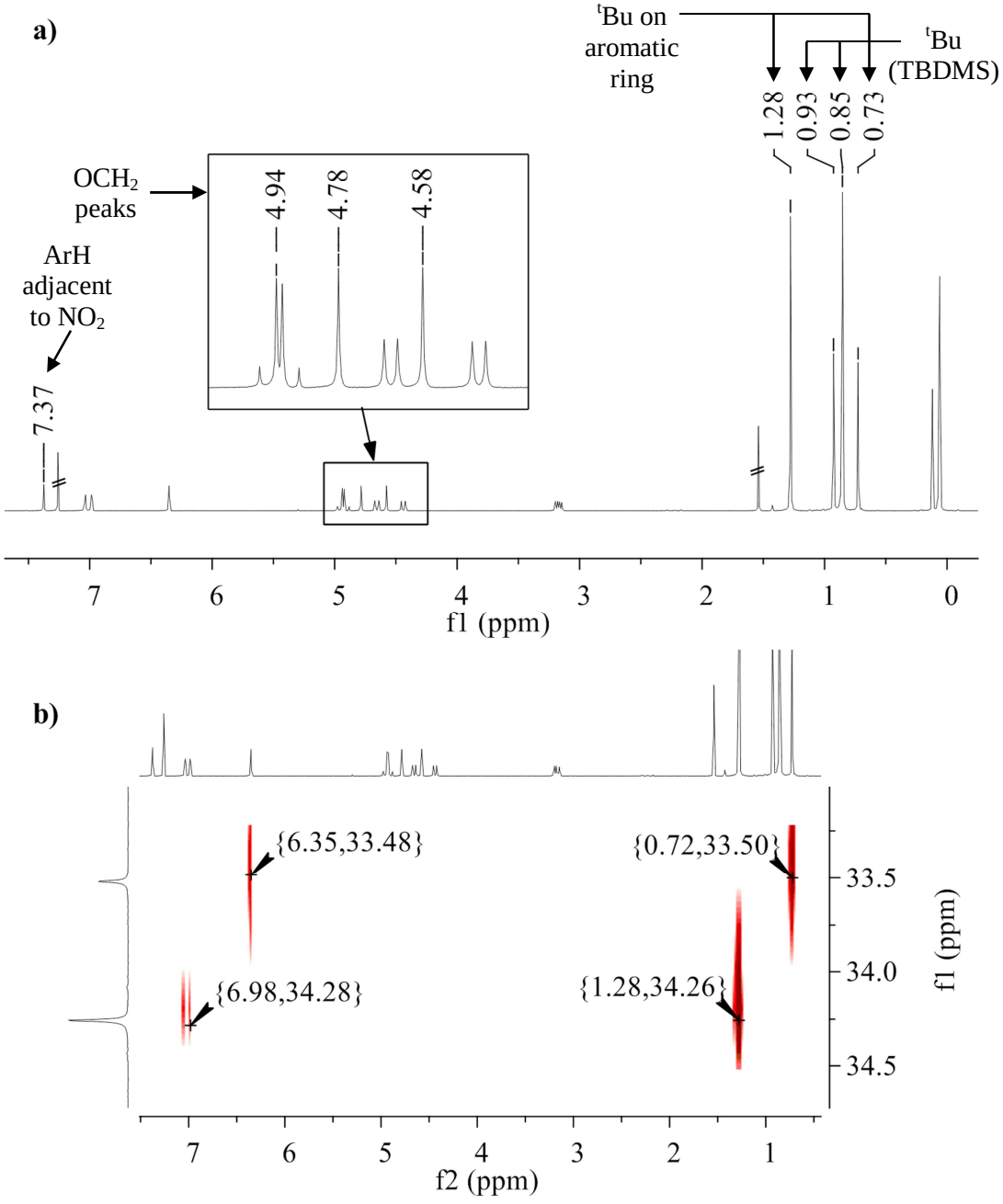

*Figure 3.10: a) ^{1}H-NMR spectrum and b) 2D-HMBC spectrum of **158**.*

Although the methyl peaks of the TBDMS groups are easily identified around 0 ppm, in this instance the *tert*-butyl peaks on the protecting groups are in the same region as the aromatic *tert*-butyl peaks. These can be differentiated using the 2D-HMBC spectrum (see Figure 3.10b). This shows a long range interaction of the proton peak at 0.73 ppm with a carbon at 33.5 ppm, which is shared by one of the aromatic proton peaks at 6.35 ppm. Likewise, the proton peak at 1.28 ppm and the aromatic proton peaks around 7.0 ppm share a mutual interaction with a carbon at 34.3 ppm. This indicates that the peaks at 0.73 and 1.28 ppm correspond to the aromatic *tert*-butyl peaks; by elimination, those of the TBDMS groups must give rise to the singlets at 0.93 and 0.85 ppm.

The reduction was next carried out by heating **158** with $SnCl_2$ in ethanol to reflux for 24 hours. Following removal of solvent and aqueous work-up with sodium hydroxide, **160** was obtained as light yellow solid in 80% yield. In contrast with the reduction of **145**, the product was isolated in good purity, suggesting that the impurities present in **155** were due to side-reactions of the unprotected alkynes. This is consistent with the findings in Chapter 2 that TBDMS protection of the alkyne improved the purity of the product of $SnCl_2$ mediated reduction.

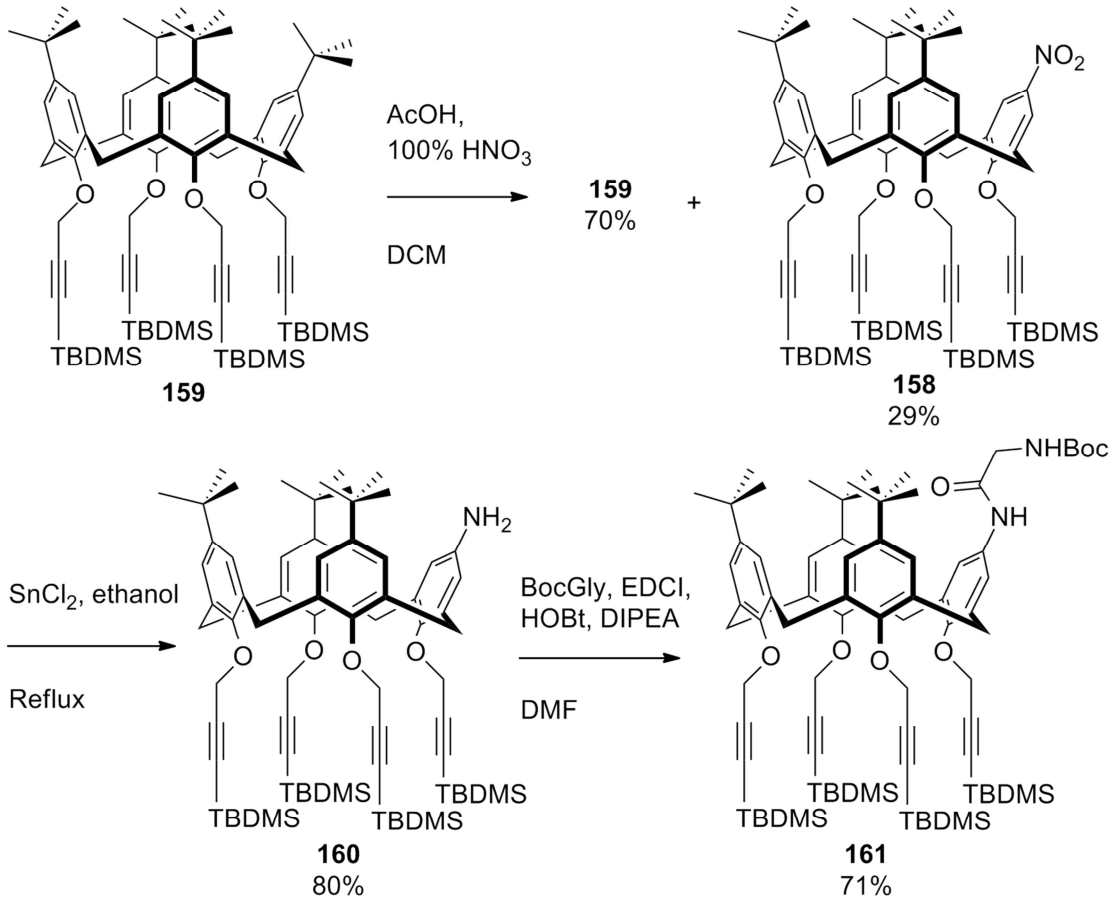

*Scheme 3.12: Synthesis of **161** via mono-nitration, reduction and amide coupling to Boc-glycine.*

The Boc-glycine residue could now be installed. A mixture of Boc-glycine, EDCI and HOBt were stirred together in dry DMF under argon, followed by addition of **160** in DMF and finally DIPEA, before stirring for 24 hours. Aqueous work-up followed by purification by column chromatography over silica gel (eluting with 14:1 DCM/ethyl acetate) gave **161** as yellow solid in 71% yield.

The stability of **161** to the conditions used for removal of the Boc group could now be tested, initially using the original method of gaseous HCl. Through a solution of **161** in DCM was bubbled HCl gas, monitoring the reaction by TLC until all starting material was consumed. This took 1.5 hours, which was an unexpectedly long period of time for the removal of a single Boc group. The product also remained soluble in the DCM. Following this, the compound was neutralised with saturated $NaHCO_3$ solution and extracted with DCM. The deprotected product **162** was isolated as colourless glass of satisfactory purity in 82% yield. It was decided to purify this compound at the next stage in the synthesis to avoid loss of the amine during purification.

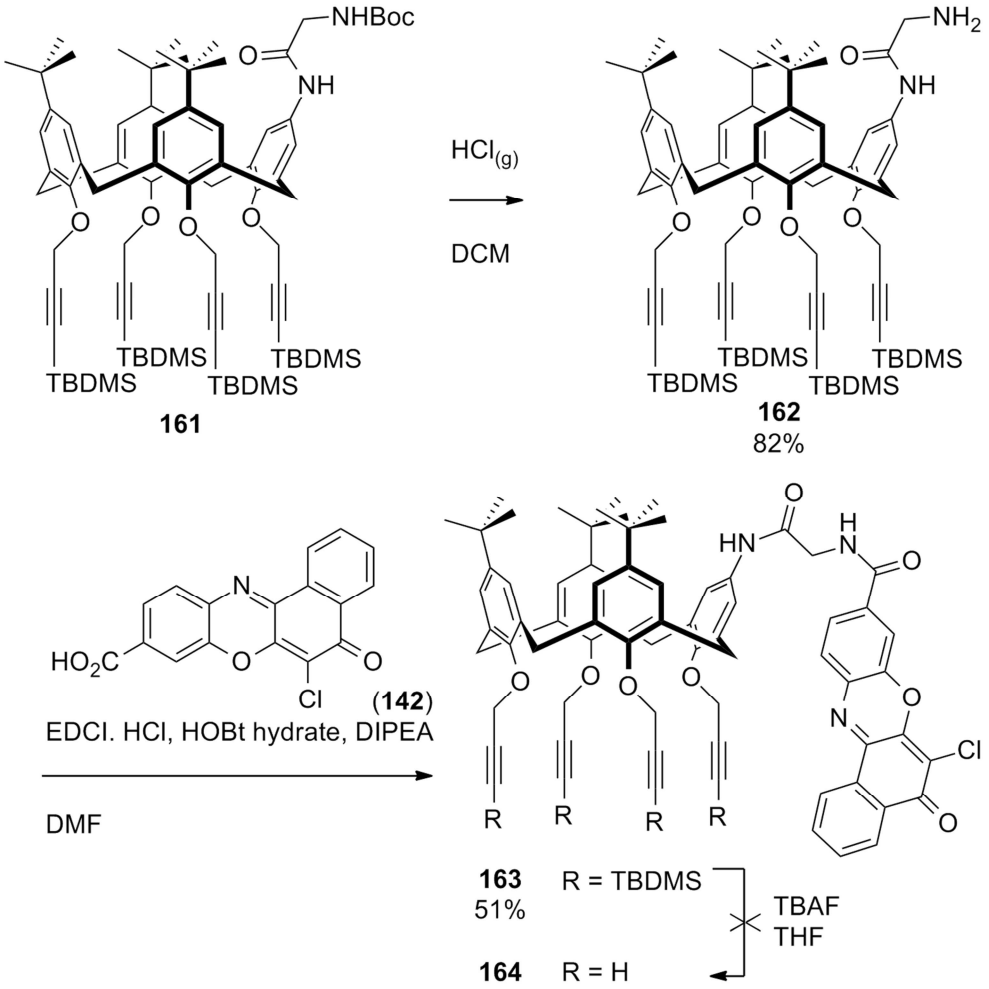

*Scheme 3.13: Synthesis of **163** via Boc-deprotection of **161** followed by conjugation with **142** and attempted synthesis of **164** by removal of TBDMS groups.*

The same deprotection with TFA was also tested. After 45 minutes, all starting material was consumed; however, the product that was isolated was of significantly lower purity than that obtained with gaseous HCl. The former therefore seems to be the better method in this case, with the TBDMS protecting groups preventing the degradation previously observed in the Boc deprotection.

The TBDMS groups could be removed either at this stage or after the conjugation reaction with the dye. It was decided to follow the latter route in the belief that the TBDMS groups would help to give a purer conjugation product.

A mixture of **162**, **142**, EDCI, HOBt and DIPEA were stirred in DMF under argon for 18 hours. Aqueous work-up followed by column chromatography over silica gel (eluting with 47:3 DCM/ethyl acetate) gave **163** as a red solid in 51% yield. In contrast with **151**, this product was fluorescent.

The correct product was confirmed from the ^{1}H-NMR spectrum (see Figure 3.11). The peaks arising from the aromatic protons on the dye can be found between 7.7 and 8.8 ppm. The two NH protons are both now linked to conjugated systems and so are both around 7.1 ppm. They can be distinguished by the coupling experienced by the NH adjacent to the methylene of the glycine linker; these give a broad triplet at 7.19 ppm and a doublet at 4.08 ppm, respectively. The methylenes of the alkynes are visible around 4.94 and 4.62 ppm; there seems to be little inequivalence between the protons on the alkyne adjacent to the functionalised ring in this case.

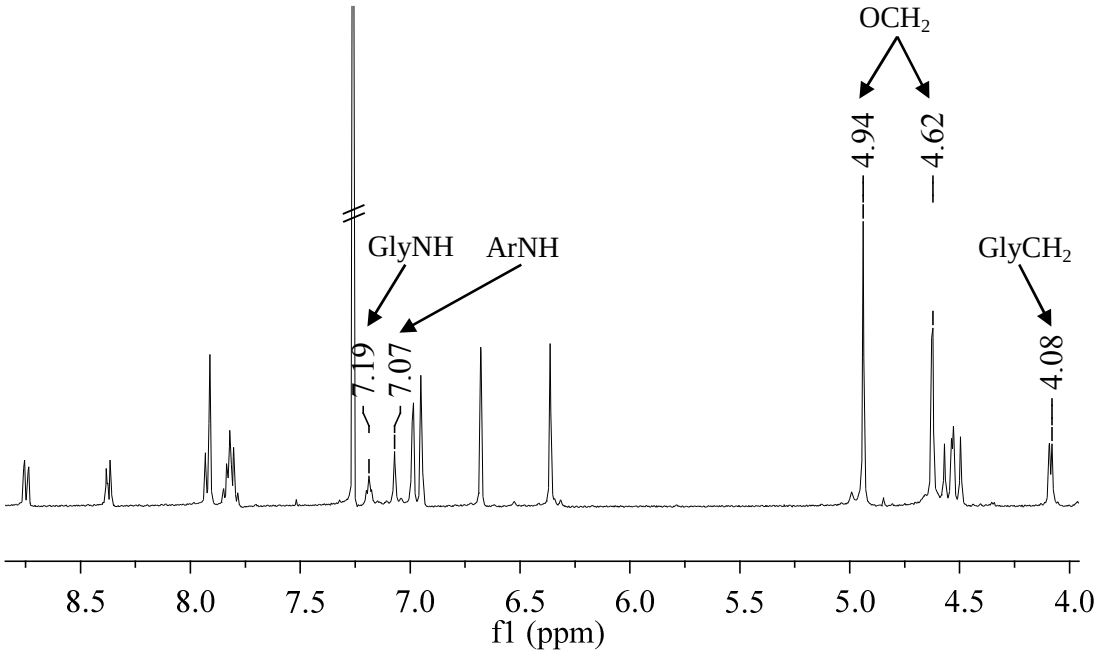

*Figure 3.11: ^{1}H-NMR spectrum of **163** ($CDCl_3$)*

The TBDMS groups could now be removed using TBAF as discussed in Chapter 2. However, when a solution of **163** was stirred with TBAF in THF, there was a colour change from red to darker red brown, and following aqueous work-up with saturated NH_4Cl the orange-brown powder that was isolated proved to be a complex mixture of products. Repeated reaction with a larger excess of TBAF gave a more complex mixture, indicating that the mixture was not due to partial deprotection, and was rather due to degradation of the product. This conclusion was supported by the concomitant loss of fluorescence in the product.

It was therefore concluded that the TBDMS protecting groups would need to be removed prior to conjugation of the dye. In this case, **162** was used directly as the hydrochloride salt and was isolated as off-white solid in 95% yield following reaction with gaseous HCl. This was stirred with TBAF in THF for 18 hours, followed by aqueous work-up with saturated NH_4Cl. Trituration of the residue with hexane removed the cleaved TBDMS groups, giving **157** as white powder in 78% yield.

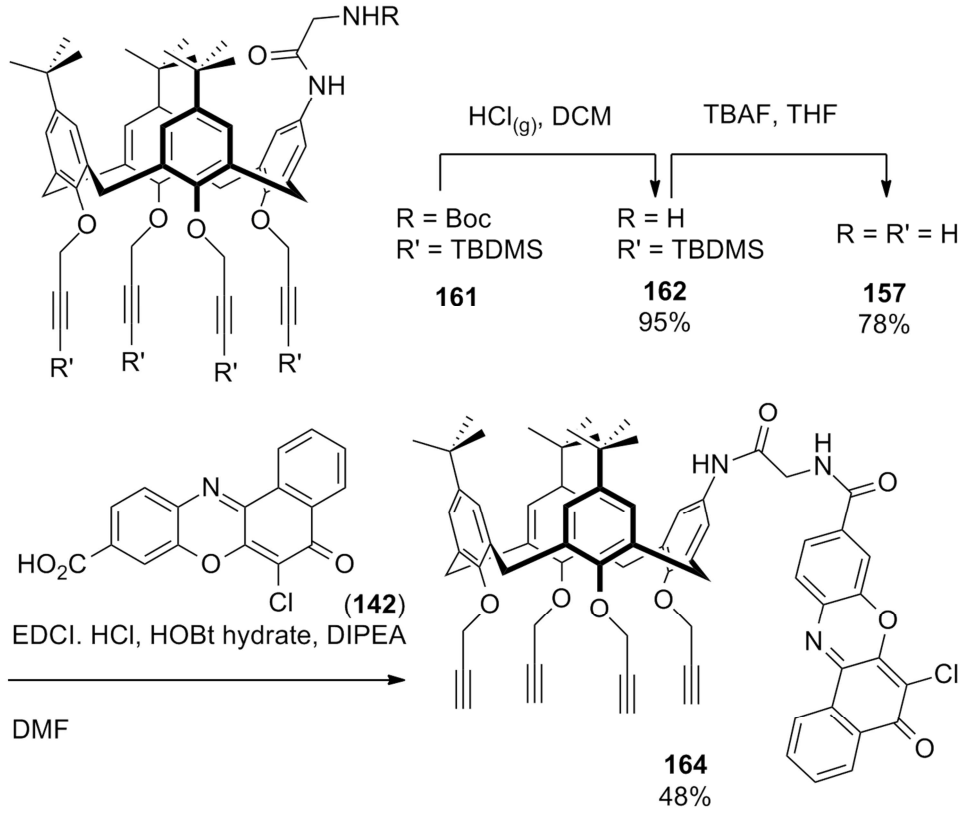

*Scheme 3.14: Synthesis of **164** from **161** via Boc-deprotection, removal of TBDMS groups and conjugation with **142**.*

The ^{1}H-NMR spectrum of **157** is shown in Figure 3.12. The terminal alkyne protons are present once again and the triplets corresponding to these can be seen around 2.5 ppm. Two of the associated doublets can be seen overlapping with the methylene bridge peaks of the calixarene at 4.63 ppm, whilst the two doublet of

doublets corresponding to the alkyne methylenes adjacent to the functionalised ring are overlapping at 4.88 ppm, giving rise to a pronounced 'rooftop' effect.

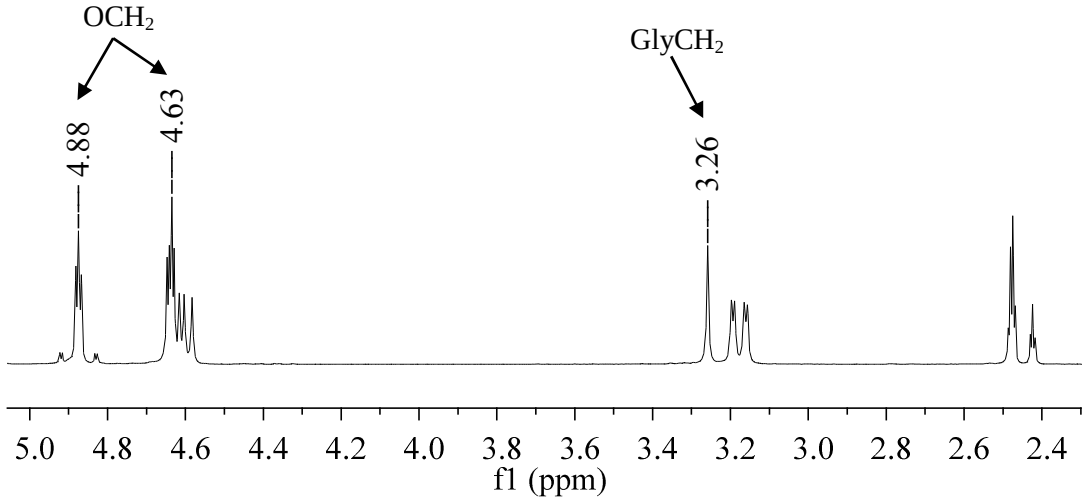

*Figure 3.12: ^{1}H-NMR spectrum of **157** ($CDCl_3$).*

The dye molecule could now be installed. A mixture of **142**, EDCI and HOBt were stirred in dry DMF under argon. To this was added **157** in DMF followed by DIPEA. After 18 hours, aqueous work-up was carried out using sodium hydroxide to remove the excess of **142**. After extracting the poorly soluble product with excess ethyl acetate, the isolated solid was subjected to column chromatography over silica gel (eluting with 3:2 hexane/ethyl acetate) to remove impurities of higher R_F than the product. Due to the poor solubility of the product causing significant smearing on the silica, it was then removed from the column using ethyl acetate. This partially purified product was finally triturated with DCM to remove the final impurity, giving **164** as bright-orange powder in 47% yield.

The ^{1}H-NMR spectrum of **164** (see Figure 3.13) confirms the correct product. The dye peaks can be seen between 8.8 and 7.8 ppm. The NH peaks are shifted further downfield than they were in **163** and lie beyond the dye peaks. This could be due to the use of DMSO instead of $CDCl_3$. Again, they can be distinguished from one another by the coupling of one of the NH protons to the methylene bridge of the glycine linker, giving a broad triplet at 9.08 ppm and a doublet at 3.97 ppm. The terminal alkyne peaks are visible as a set of 3 triplets at 3.43 ppm, with the methylene groups of the alkynes giving poorly resolved doublets around 4.7 ppm. In this case there appears to be no inequivalence between the protons on the alkynes adjacent to the functionalised ring.

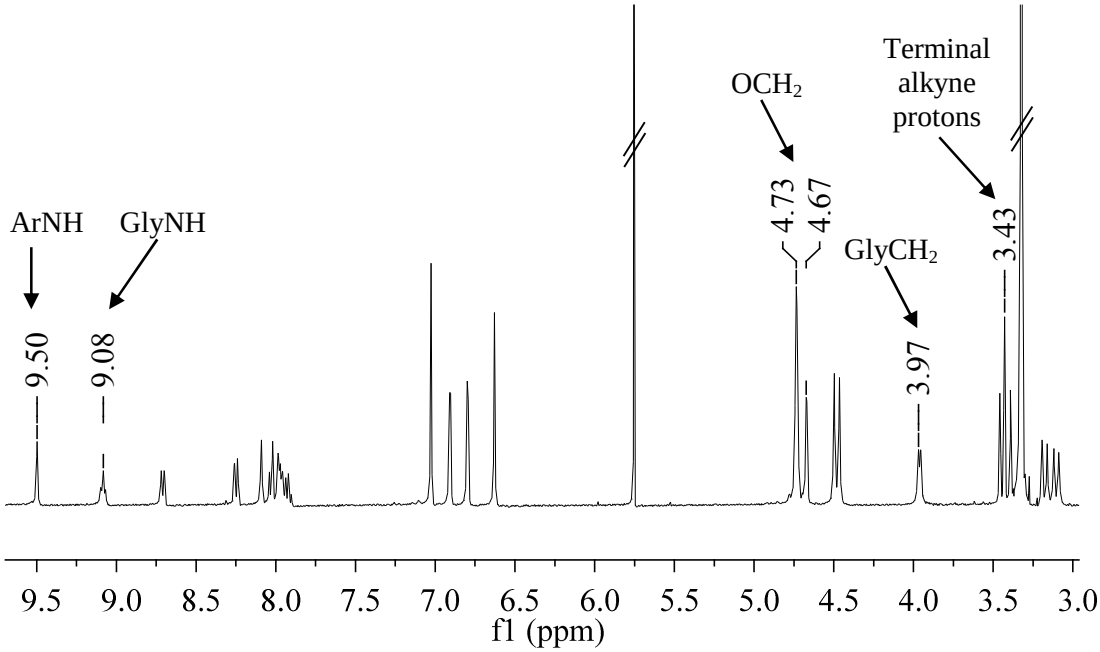

*Figure 3.13: ^{1}H-NMR spectrum of **164** (DMSO-d6).*

This final route therefore successfully gave a suitable fluorescent scaffold to synthesise a bi-functional glycoconjugate. Compound **164** was subsequently passed on to the research group of Sebastien Vidal to undergo the final conjugation reactions to the sugar (**149**) using CuAAC chemistry.

3.4 Conclusions and further work

In this chapter, a suitable synthetic route to a bifunctional calixarene, with a fluorescent dye on the upper rim and alkynes for sugar attachment on the lower rim, was developed. This synthesis allows for the diversification of the scaffold; different dyes could be conjugated to the upper rim of **157**, whilst different azide-functionalised sugars could be conjugated to the lower rim. A set of compounds could potentially be synthesised with different fluorescence wavelengths associated with different sugar conjugates to allow visualisation of multiple sugar-binding targets.

The utility of protecting the alkynes with TBDMS groups was demonstrated in their ability to improve the purity of products obtained in key transformations and, more importantly, to allow Boc-deprotection to be carried out on the upper rim without significantly degrading the product. This, along with the results obtained in Chapter 2, demonstrates that silylation of propargyl ethers has general utility in the synthesis of functionalised calixarenes.

An optimised procedure for the conjugation of the sugar moieties remains to be found. As discussed in section 3.3.3.5, this would require investigation of a method for deacetylation of the sugar-conjugate without compromising the dye-linked

scaffold, or alternatively the conjugation of deacetylated sugars. Whilst the latter method would circumvent the problem of degradation of the molecule under deacetylation conditions, the purification of the conjugate could prove to be challenging. It can be expected that such a reaction would not be completely efficient due to the aforementioned steric hindrance of the cone conformer; although **152** could be successfully purified, an analogous purification by reversed-phase chromatography would be more difficult to optimise.

Once the bifunctional scaffold has been successfully synthesised in its deacetylated state, the biological tests will be carried out by co-workers of Sebastien Vidal in Grenoble. This will allow confirmation of the binding to the conjugate to the free lectins, followed by investigation of the binding to *P. aeruginosa.*

3.5 Experimental

5,11,17,23-Tetra-*tert*-butyl-25,26,27-tripropargyloxy-28-hydroxy-calix[4]arene (143)[44]

p-tert-Butylcalix[4]arene **2** (20.10 g, 31.02 mmol) was dissolved in DMF (300 mL) and heated to 30 °C. BaO (7.15 g, 46.78 mmol) and $Ba(OH)_2.8H_2O$ (33.83 g, 107.39 mmol) were added and the mixture stirred for 30 mins. n-Propargyl bromide (94.29 g, 80% w/w in toluene, 660 mmol) was added and the mixture stirred for 18 hrs. Water (200 mL) and dilute HCl (200 mL) were added and the product extracted with DCM (3 x 100 mL), then washed with water (200 mL) and brine (200 mL). After drying over $MgSO_4$, the solvent was removed under reduced pressure. Purification by column chromatography over silica gel (eluent: 2:1 DCM/Hexane) gave **143** as light yellow crystals (6.7 g, 28%). **Mp** 155-157 °C; **IR** ν 1120, 1193, 1238, 1259, 1299, 1361, 1391, 1477, 1582, 1594, 2125, 2860, 2900, 2950, 3261, 3286, 3539 cm^{-1}; **^{1}H-NMR** (400 MHz, $CDCl_3$): δ 7.10 (s, 2 H, Ar*H*), 7.05 (s, 2 H, Ar*H*), 6.56 (s, 2 H, Ar*H*), 6.52 (s, 2 H, Ar*H*), 5.60 (d, *J* = 2 Hz, 2 H, OCH_2CCH), 6.62 (d, *J* = 2 Hz, 4 H, OCH_2CCH), 4.60 (d, *J* = 13 Hz, 2 H, $ArCH_2Ar$), 4.345 (d, *J* = 13 Hz, 2 H, $ArCH_2Ar$), 3.275 (d, *J* = 13 Hz, 2 H, $ArCH_2Ar$), 3.19 (d, *J* = 13 Hz, 2 H, $ArCH_2Ar$), 2.48 (t, *J* = 2 Hz, 2 H, OCH_2CCH), 2.42 (t, *J* = 2 Hz, 4 H, OCH_2CCH), 1.31 (s, 9 H, $C(CH_3)_3$), 1.30 (s, 9 H, $C(CH_3)_3$), 0.82 (s, 18 H, $C(CH_3)_3$).

5,11,17-Tri-*tert*-butyl-23-nitro-25,26,27-tripropargyloxy-28-hydroxy-calix[4]arene (144)

Compound **143** (1.00 g, 1.31 mmol) was dissolved in DCM (5 mL). Glacial acetic acid (3 mL) was added, followed by 65% nitric acid (0.5 mL), dropwise over 2 minutes. After stirring for 4 minutes, the reaction was quenched with H_2O (20 mL). The product was extracted into DCM (20 mL), washed with water (2 x 20 mL) and dried ($MgSO_4$). Removal of solvent under reduced pressure followed by purification by column chromatography over silica gel (eluent: 2:1 DCM/hexane) gave **144** as yellow crystals (0.43 g, 44%). **Mp** 195-197 °C; **IR** ν 1100, 1118, 1192, 1247, 1288, 1327, 1361, 1391, 1435, 1474, 1510, 1592, 2861, 2900, 2954, 2960, 3301, 3315 cm^{-1}; **^{1}H NMR** (400 MHz, $CDCl_3$): δ 8.07 (s, 2 H, Ar*H*), 7.14 (s, 2 H, Ar*H*), 6.62 (d, *J* = 2 Hz, 2 H, Ar*H*), 6.52 (d, *J* = 2 Hz, 2 H, Ar*H*), 5.00 (d, *J* = 2 Hz, 2 H, OC*H*$_2$CCH), 4.73 (dd, *J* = 16, 2 Hz, 2 H, OC*H*$_2$CCH), 4.59 (dd, *J* = 16, 2 Hz, 2 H, OC*H*$_2$CCH), 4.58 (d, *J* = 13 Hz, 2 H, ArC*H*$_2$Ar), 4.41 (d, *J* = 14 Hz, 2 H, ArC*H*$_2$Ar), 3.43 (d, *J* = 14 Hz, 2 H, ArC*H*$_2$Ar), 3.245 (d, *J* = 13 Hz, 2 H, ArC*H*$_2$Ar), 2.56 (t, *J* = 2 Hz, 2 H, OCH$_2$CC*H*), 2.49 (t, *J* = 2 Hz, 4 H, OCH$_2$CC*H*), 1.33 (s, 9 H, C(C*H*$_3$)$_3$), 0.84 (s, 18 H, C(C*H*$_3$)$_3$); **^{13}C NMR** (100 MHz, $CDCl_3$): δ 159.9, 152.2, 151.0 147.2, 147.0, 139.6, 136.1, 133.0, 130.6, 129.7, 126.2, 125.9, 124.8, 124.5, 81.7, 79.3, 76.2, 74.8, 63.1, 60.2, 53.7, 34.4, 34.0, 32.7, 31.9, 31.8, 31.2; **HRMS** (APCI) m/z: $[M+H]^+$ Calcd for $C_{49}H_{54}NO_6$ 752.3946; Found 752.3942.

5,11,17-Tri-*tert*-butyl-23-nitro-25,26,27,28-tetrapropargyloxy-calix[4]arene (145)

Method A: To a stirred solution of propargyl alcohol (157 μL, 2.66 mmol) in toluene (20 mL) was added TPP (0.70 g, 2.66 mmol). The solution was cooled in an ice bath and DIAD (0.53 mL, 2.66 mmol) was added dropwise. After stirring for 10 minutes, **144** (1.00 g, 1.33 mmol) dissolved in minimum toluene was added. The mixture was stirred for 16 hours at room temperature. The solvent was removed under reduced pressure and the product triturated with MeOH/H_2O, then filtered. ^{1}H-NMR showed no reaction.

Method B: To a stirred solution of propargyl alcohol (310 μl, 5.32 mmol) in toluene (20 mL) was added TPP (1.4 g, 5.32 mmol), followed by DEAD (0.84 mL, 5.32 mmol), dropwise. After stirring for 10 minutes, **144** (1.00 g, 1.33 mmol) dissolved in minimum toluene was added. The mixture was stirred for 72 hours at room temperature and then the solvent removed under reduced pressure. After

attempted trituration with MeOH/H_2O, the product was extracted into DCM and the solvent removed under reduced pressure. ^{1}H-NMR showed no reaction.

Calix[4]arene (146)[39]

To a mixture of *tert*-butyl calix[4]arene **2** (100 g, 154.08 mmol) and phenol (65 mL, 739 mmol) in 1 L of toluene was added $AlCl_3$ (112.72 g, 133.34 mmol) in small portions. After stirring for 4 hours the mixture was poured onto ice, mixed, then left to separate. The organic layer was decanted from the surface, washed with water, and the product extracted with DCM. Solvent was removed under reduced pressure and the product precipitated from the residue with methanol to give **146** as off-white powder (51.78 g, 79%). **Mp** 295-297 °C; **IR** ν 3150.5, 3093, 3058.5, 2931.5, 2867, 2769.5, 2706.5, 1608, 1594, 1466, 1463, 1448, 1446.5, 1410.5, 1376, 1299, 1267.5, 1259.5, 1245, 1236, 1213.5, 1202, 1194, 1145.5, 1094, 1077.5 cm^{-1}; **^{1}H NMR** (400 MHz, $CDCl_3$); 10.18 (s, 4H, ArO*H*), 7.04 (d, 8H, *J* = 7.5 Hz, Ar*H*), 6.72 (t, 4H, *J* = 7.5 Hz, Ar*H*), 4.25 (br s, 4H ArC*H*$_2$Ar), 3.53 (br s, 4H, ArC*H*$_2$Ar).

25,26,27,28- Tetra-propargyloxy-calix[4]arene (147)[45]

To a stirred solution of calix[4]arene (**146**) (10.00 g, 47.12 mmol) in DMF (400 mL) was added NaH (9.05 g, 376.96 mmol). The mixture stirred for 30 minutes before addition of propargyl bromide (56.05 g, 80% w/w in toluene, 376.96 mmol). After stirring for 72 hours, the solvent was removed under reduced pressure. Dilute HCl (200 mL) was added and the product extracted with DCM (3 x 100 mL), then washed with water (200 mL) and brine (200 mL). After drying over $MgSO_4$, the solvent was removed under reduced pressure. Purification by column chromatography over silica (eluent: 2:1 hexane/toluene) gave **147** as fine white powder (10.00 g, 37%). **Mp** 156-158 °C; **IR** ν 3298.5, 3278, 3058, 3010, 2982, 2972, 2950.5, 2911, 2847, 2117, 1585, 1455.5, 1428.5, 1364, 1295.5, 1278, 1268.5, 1248, 1241, 1198.5, 1184.5, 1178, 1156, 1088, 1076.5 cm^{-1}; **^{1}H NMR** (300 MHz, $CDCl_3$): δ 6.75-6.65 (m, 12H, Ar*H*), 4.78 (d, *J* = 2 Hz, 2H, OC*H*$_2$CCH), 4.63 (d, *J* = 14 Hz, 4H, ArC*H*$_2$Ar), 3.23 (d, *J* = 14 Hz, 4H, ArC*H*$_2$Ar), 2.47 (t, *J* = 2 Hz, 2H, OCH$_2$CC*H*).

5-Nitro-25,26,27,28-tetra-propargyloxy-calix[4]arene (148)

To a stirred solution of **147** (1.5 g, 2.60 mmol) in DCM (150 mL) was added 100% nitric acid (1.5 mL) and 95% sulphuric acid (6 drops). The solution was stirred for 1 hour before quenching with H_2O (100 mL). The product was extracted with DCM (3 x

50 mL) then washed with water (3 x 100 mL) and brine (100 mL). After drying over $MgSO_4$ the solvent was removed under reduced pressure and the product purified by column chromatography over silica gel (eluent: 1:1 DCM/hexane) to give **147** (0.93 g, 60%) and **148** (0.19 g, 12%). Impure fractions were recrystallized from DCM/methanol to give further **148** as off-white crystals (0.15 g, 9%). **Mp** 157-159 °C; **IR** ν 1159, 1197, 1208, 1258, 1264, 1303, 1344, 1436, 1455, 1521, 1588, 2125, 2862, 2930, 2987, 3036, 3071, 3274, 3303 cm^{-1}; **^{1}H NMR** (400 MHz, $CDCl_3$): δ 7.38 (s, 2H, Ar*H*), 6.94-6.82 (m, 6H, Ar*H*), 6.50-6.43 (m, 3H, Ar*H*), 4.85 (dd, *J* = 16, 2 Hz, 2H, OC*H*$_2$CCH), 4.81 (d, *J* = 2 Hz, 2H, OC*H*$_2$CCH), 4.75 (dd, *J* = 16, 2 Hz, 2H, OC*H*$_2$CCH), 4.71 (d, *J* = 14 Hz, 2H, ArC*H*$_2$Ar), 4.65 (d, *J* = 2 Hz, 2H, OC*H*$_2$CCH), 4.56 (d, *J* = 14 Hz, 2H, ArC*H*$_2$Ar), 3.28 (d, *J* = 14 Hz, 2H, ArC*H*$_2$Ar), 3.24 (d, *J* = 14 Hz, 2H, ArC*H*$_2$Ar), 2.50-2.49 (m, 4H, OCH_2CC*H*); **^{13}C NMR** (100 MHz, $CDCl_3$) δ 159.99, 155.34, 154.78, 143.42, 137.03, 136.34, 134.97, 134.56, 129.44, 128.56, 128.19, 123.97, 123.46, 123.30, 80.42, 80.10, 79.01, 76.07, 75.12, 75.07, 61.69, 61.25, 32.08, 31.76; **HRMS** (APCI) m/z: $[M+H]^+$ Calcd for $C_{40}H_{32}NO_6$ 622.2224; Found 622.2225.

6-Chloro-5-oxo-5H-benzo[a]phenoxazine-9-carboxylic acid (142)[29]

A mixture of 2,3-dichloro-1,4-napthoquinone (2.27 g, 10 mmol), 4-amino-3-hydroxybenzoic acid (1.53 g, 10 mmol) and potassium acetate (1.96 g, 20 mmol) were suspended in methanol (20 mL) and heated to reflux, with stirring, for 24 hours. The resulting orange-red suspension was cooled to room temperature, filtered and washed with water. The crude product was washed with hot methanol to give **142** as red powder (2.14 g, 66%). **Mp** >320 °C (decomp.); **IR** ν 3066, 1615.5, 1593, 1561, 1557, 1479, 1470.5, 1446.5, 1411, 1372.5, 1362, 1306.5, 1283, 1235, 1224.5, 1201.5, 1194, 1163, 1144, 1099, 1080, 1046, 1020.5 cm^{-1}; **^{1}H-NMR** (400 MHz, 7:1 Tol-d_8/DMSO-d_6) δ 8.53 – 8.51 (m, 1H, Ar*H*), 8.30 – 8.28 (m, 1H, Ar*H*), 8.10 (dd, *J* = 8.0, 1.5 Hz, 1H, Ar*H*), 8.08 (d, *J* = 1.5 Hz, 1H, Ar*H*), 7.65 (d, *J* = 8.0 Hz, 1H, Ar*H*), 7.45 – 7.38 (m, 2H, Ar*H*).

1-Azido-3,6-dioxaoct-8-yl-2',3',4',6'-tetra-O-acetyl-β-D-galactopyranoside (149)[41]

To a stirred solution of 2,3,4,6-tetra-O-acetyl-β-D-galactopyranoside (15 g, 38.43 mmol), $AgCO_2CF_3$ (12.72 g, 57.58 mmol) and 2-[2-(2-chloroethoxy)ethoxy]ethanol (8.40 mL, 57.79 mmol) in dry DCM (300 mL) under argon was added SnCl4 (1 M in

DCM, 115.2 mL, 115.2 mmol) dropwise over 30 minutes. After 90 minutes, saturated aq. $NaHCO_3$ was added to adjust pH to >8, and the solution was stirred for 12 hours. The biphasic solution was diluted with water (1000 mL) and product extracted with DCM (3 × 450 mL). The combined organic layers were washed with saturated aq. $NaHCO_3$ (450 mL), water (3 × 450 mL) and brine (2 × 450 mL). After drying over Na_2SO_4, the solvent was removed under reduced pressure. The yellow oil was dissolved in DMF (450 mL) before adding sodium azide (12.48 g, 192 mmol) and Bu_4NI (14.19 g, 38.42 mmol). The mixture was stirred at 70°C under argon for 18 h then cooled to RT, filtered, and the solid was washed with EtOAc (3 × 400 mL). The filtrate was diluted with EtOAc (800 mL) then washed with saturated aq. $NaHCO_3$ (3 × 900 mL), water (3 × 1000 mL), and brine (1000 mL). After drying over Na_2SO_4, the solvent was removed under reduced pressure and the residue was purified by flash column chromatography over silica gel (1:1 petroleum ether/ethyl acetate) to give **149** as viscous, light-yellow oil (10.01 g, 52% yield). **IR** ν 2937, 2871, 2102, 1743.5, 1436.5, 1367.5, 1214, 1174.5, 1132, 1122, 1073, 1055, 1043.5 cm^{-1}; **^{1}H-NMR** (300 MHz, $CDCl_3$) δ 5.38 (dd, *J* = 3.4, 1.0 Hz, 1H, C*H*), 5.21 (dd, *J* = 10.5, 7.9 Hz, 1H, C*H*), 5.01 (dd, *J* = 10.5, 3.4 Hz, 1H, C*H*), 4.57 (d, *J* = 7.9 Hz, 1H, C*H*), 4.20 – 4.08 (m, 2H, CH_2), 3.99 – 3.88 (m, 2H, C*H*, OCH_2), 3.79 – 3.64 (m, 9H, OCH_2), 3.39 (t, *J* = 5.0 Hz, 2H, CH_2N_3), 2.14 (s, 3H, CH_3), 2.06 (s, 3H, CH_3), 2.04 (s, 3H, CH_3), 1.98 (s, 3H, CH_3); **^{13}C-NMR** (100 MHz, $CDCl_3$) δ 169.80, 169.74, 169.52, 168.92, 100.77, 70.43, 70.20, 70.17, 70.14, 69.89, 69.54, 68.55, 68.40, 66.75, 60.92, 53.37, 50.18, 20.21, 20.11, 20.09, 20.02.

NRD appended tetra-propargyloxy-calix[4]arene (151)

A mixture of **148** (0.58 g, 0.93 mmol) and $SnCl_2{\cdot}2H_2O$ (1.37 g, 6.05 mmol) was heated to reflux in ethanol (60 mL) with stirring for 48 hours. Solvent was removed under reduced pressure and DCM (50 mL) added. After washing with 10% NaOH (100 mL), the product was extracted with DCM (3 x 50 mL) and washed with water (2 x 100 mL) then brine (100 mL). After drying over $MgSO_4$, the solvent was removed under reduced pressure to give a brown glass, which was verified by ^{1}H NMR as the intermediate amine **150** (0.35 g, 63%). **^{1}H-NMR** (400 MHz, $CDCl_3$) δ 6.82 – 6.67 (m, 9H, Ar*H*), 6.12 (s, 2H, Ar*H*), 4.84 (d, *J* = 2 Hz, 2H, OCH_2CCH), 4.81 (d, *J* = 2 Hz, 2H, OCH_2CCH), 4.81 (d, *J* = 2 Hz, 2H, OCH_2CCH), 4.75 (d, *J* = 2 Hz, 2H, OCH_2CCH), 4.69 (d, *J* = 13 Hz, 2H, ArCH_2Ar), 4.60 (d, *J* = 13 Hz, 2H, ArCH_2Ar), 3.28 (d, *J* = 13 Hz, 2H, ArCH_2Ar), 3.15 (d, *J* = 13 Hz, 2H, ArCH_2Ar), 2.50 – 2.49 (m,

4H, OCH_2CCH). The crude amine was stirred with **142** (0.19 g, 0.59 mmol), EDCI·HCl (0.25 g, 1.30 mmol), HOBt hydrate (0.17 g, 1.30 mmol) and NMM (0.26 mL, 2.42 mmol) in DMF (6 mL) for 18 hours. Water was added and the precipitate filtered. The solid was dissolved in ethyl acetate and washed with water (200 mL) and brine (200 mL). After drying over $MgSO_4$, the solvent was removed under reduced pressure and the solid purified by column chromatography over silica gel (eluent: DCM) to give **151** as a red solid (0.20 g, 37%). **Mp** 250 °C (decomp.); **IR** ν 3440, 3288.5, 3258, 3061, 3014, 2991, 2920.5, 2878.5, 2851, 2127, 2112, 1675.5, 1673, 1640.5, 1628.5, 1604, 1592.5, 1587, 1565, 1534, 1531.5, 1474, 1459.5, 1455, 1440, 1424, 1413, 1358.5, 1331.5, 1302.5, 1282.5, 1256.5, 1234.5, 1212.5, 1203.5, 1191, 1160, 1144.5, 1127.5, 1089, 1078, 1043.5, 1017.5, 1008.5 cm^{-1}; **^{1}H-NMR** (400 MHz, $CDCl_3$) δ 8.75 – 8.73 (m, 1H, ArH_{NRD}), 8.37 – 8.35 (m, 1H, ArH_{NRD}), 7.93 – 7.76 (m, 5H, ArH_{NRD}), 7.56 (br s, 1H, ArN*H*), 7.00 (br s, 2H, Ar*H*), 6.84 – 6.79 (m, 4H, Ar*H*), 6.74 – 6.71 (m, 4H, Ar*H*), 6.67 – 6.62 (m, 1H, Ar*H*), 4.82 (d, *J* = 2 Hz, 2H, OCH_2CCH), 4.82 (d, *J* = 2 Hz, 2H, OCH_2CCH), 4.78 (d, *J* = 2 Hz, 2H, OCH_2CCH), 4.77 (d, *J* = 2 Hz, 2H, OCH_2CCH), 4.68 (d, *J* = 13 Hz, 2H, ArCH_2Ar), 4.64 (d, *J* = 13 Hz, 2H, ArCH_2Ar), 3.27 (d, *J* = 13 Hz, 2H, ArCH_2Ar), 3.25 (d, *J* = 13 Hz, 2H, ArCH_2Ar), 2.50 – 2.48 (m, 4H, OCH_2CCH). **^{13}C-NMR** (100 MHz, $CDCl_3$) δ 177.35, 163.23, 155.08, 155.01, 152.35, 147.35, 146.40, 143.33, 137.96, 136.34, 135.48, 135.44, 135.02, 134.28, 132.73, 132.57, 131.15, 129.93, 129.76, 128.52, 128.38, 128.34, 126.71, 125.05, 124.43, 123.52, 123.22, 120.60, 115.24, 114.86, 80.44, 80.33, 75.10, 74.88, 74.84, 61.34, 61.27, 61.21, 32.10, 31.94; **HRMS** (APCI) m/z: $[M+H]^+$ Calcd for $C_{57}H_{40}ClN_2O_7$ 899.2519; Found 899.2533.

NRD appended 25,26,27,28-Tetra-{1'-[(2''',3''',4''',6'''-tetra-O-acetyl-β-D-galactopyranosyloxy)-3",6"-dioxaoct-8"-yl]-1',2',3'-triazol-4'-ylmethyleneoxy}-calix[4]arene (152)

A mixture of **149** (169 mg, 333.96 μmol), **151** (50 mg, 55.66 μmol), $CuSO_4$ (0.1 M in water, 278 μL, 27.83 μmol) and sodium ascorbate (17 mg, 83.49 μmol) in DMF (3 mL) was stirred at room temperature under argon for 24 hours. Further **149** (28.17 mg, 55.66 μmol), $CuSO_4$ (0.1 M in water, 278 μL, 27.83 μmol) and sodium ascorbate (17 mg, 83.49 μmol) was added and stirring continued for 24 hours. After removing solvent under reduced pressure, the product was purified by column chromatography over silica gel (eluent: 1:1 petroleum ether/ethyl acetate, ethyl acetate and 19:1 ethyl acetate/methanol) to give **152** as dark-orange solid (0.16 mg, 44%). **Mp** 68-70 °C; **IR**

ν 2920.5, 2871.5, 1790, 1651, 1595.5, 1565.5, 1540.5, 1460, 1435, 1367, 1301.5, 1218.5, 1176.5, 1134, 1045, 1018.5 cm^{-1}; **^{1}H-NMR** (300 MHz, $CDCl_3$) δ 8.75 – 8.72 (m, 1H, ArH_{NRD}), 8.37 – 8.34 (m, 1H, ArH_{NRD}), 8.14 (s, 1H, N*H*), 7.96 – 7.75 (m, 9H, ArH_{NRD} and Ar$H_{Triazole}$), 7.08 (s, 1H, Ar*H*), 7.04 (s, 1H, Ar*H*), 6.70 – 6.52 (m, 9H, Ar*H*), 5.38 – 5.36 (m, 4H, C*H*), 5.21 – 5.14 (m, 8H, C*H* and OCH_2C), 5.06 – 4.99 (m, 8H, C*H* and OCH_2C), 4.57 – 4.52 (m, 12H, C*H* and CH_2N), 4.22 – 4.07 (m, 12H, ArCH_2Ar and CH_2OAc), 3.96 – 3.84 (m, 16H, C*H* and OCH_2), 3.72 – 3.55 (m, 28H, OCH_2), 2.97 (d, *J* = 13 Hz, 4H, ArCH_2Ar), 2.12 – 1.96 (m, 48H, CH_3); **^{13}C-NMR** (75 MHz, $CDCl_3$) δ 177.44, 170.46, 170.43, 170.29, 170.18, 169.64, 169.52, 163.13, 155.12, 154.75, 152.13, 147.52, 146.70, 143.97, 143.53, 138.05, 136.51, 135.86, 135.02, 134.62, 134.47, 132.80, 132.47, 131.37, 130.01, 128.42, 128.29, 128.15, 126.79, 125.16, 124.66, 122.88, 120.54, 115.25, 115.19, 101.38, 70.92, 70.67, 70.52, 70.20, 69.58, 69.15, 68.84, 67.09, 66.84, 61.28, 50.13, 31.95, 31.44, 29.72, 29.39, 22.72, 20.85, 20.74, 20.72, 20.64; **ESI-MS** m\z: $[M+2H]^{2+}$ 1461.5, $[M+2Na]^{2+}$ 1483.5, $[M]^{+}$ 2921.8, $[M+Na]^{+}$ 2943.8.

NRD appended 25,26,27,28-Tetra-{1'-[(β-D-galactopyranosyloxy)-3",6"-dioxaoct-8"-yl]-1',2',3'-triazol-4'-ylmethyleneoxy}-calix[4]arene (153)

Compound **152** (62 mg, 21.22 μmol) was stirred in a mixture of 1:2:1 Et_3N/methanol/water (2.2 mL) under argon for 42 hours, then the solvent removed under reduced pressure. Attempted purification by reversed-phase column chromatography over C18 failed to give the desired product.

5,11,17,23-Tetra-*tert*-butyl-25,26,27,28-tetra-propargyloxy-calix[4]arene (154)[21]

To a stirred suspension of *tert*-butyl-calix[4]arene **2** (8 g, 12.33 mmol) in DMF (160 mL) was added NaH (2.35 g, 97.92 mmol) and the mixture stirred for 1 hour. Propargyl bromide (8.74 mL, 80% w/w in toluene, 81.12 mmol) was added and the reaction stirred for 48 hours. Water was added and the precipitate filtered, washed with water twice and air dried to give **154** as light brown powder (5.55 g, 53%). **Mp** 204-206 °C; **IR** ν 3309.5, 3283, 2965.5, 2951, 2921, 2906, 2861.5, 1602, 1583.5, 1478.5, 1474, 1438, 1434.5, 1414.5, 1392.5, 1363.5, 1299.5, 1273.5, 1261, 1237, 1192, 1121.5, 1107, 1019.5, 1009, 1003 cm^{-1}; **^{1}H-NMR** (400 MHz, $CDCl_3$) δ 6.79 (s, 8H, Ar*H*), 4.80 (d, *J* = 2 Hz, 8H, OCH_2CCH), 4.61 (d, *J* = 13 Hz, 4H, ArCH_2Ar), 3.17

(d, *J* = 13 Hz, 4H, ArC*H*$_2$Ar), 2.47 (t, *J* = 2 Hz, 4H, OCH$_2$CC*H*), 1.08 (s, 36H, C(CH$_3$)$_3$).

5,11,17-Tetra-*tert*-butyl-23-nitro-25,26,27,28-tetra-propargyloxy-calix[4]arene (145)

To a stirred solution of **154** (1.00 g, 1.125 mmol) in DCM (72 mL) was added glacial acetic acid (1.84 mL) and 100% HNO_3 (1.04 mL). After stirring for 30 minutes, the reaction was quenched with water (50 mL). The product was extracted with DCM (3 x 50 mL), washed with water (3 x 200 mL) and brine (200 mL). After drying over $MgSO_4$, the solvent was removed under reduced pressure and the residue purified by column chromatography over silica gel (eluent: 8-10% ethyl acetate in hexane) to give recovered **154** (0.4 g, 40%) as white powder and **145** (0.26 g, 26%) as a light yellow solid. **Mp** 87-89 °C; **IR** ν 3296, 3156, 2961, 2934, 2874, 1731, 1669.5, 1609.5, 1583.5, 1518.5, 1478, 1463, 1437.5, 1392.5, 1361.5, 1341.5, 1308.5, 1261, 1231.5, 1194.5, 1162, 1117.5, 1089, 1043, 1002 cm^{-1}; **^{1}H-NMR** (400 MHz, $CDCl_3$) δ 7.37 (s, 2H, Ar*H*), 7.12 (d, *J* = 2 Hz, 2H, Ar*H*), 7.08 (d, *J* = 2 Hz, 2H, Ar*H*), 6.31 (s, 2H, Ar*H*), 4.98 (dd, *J* = 16, 2 Hz, 2H, OC*H*$_2$CCH), 4.83 (dd, *J* = 16, 2 Hz, 2H, OC*H*$_2$CCH), 4.75 (d, *J* = 13 Hz, 2H, ArC*H*$_2$Ar), 4.73 (d, *J* = 2 Hz, 2H, OC*H*$_2$CCH), 4.56 (d, *J* = 2 Hz, 2H, OC*H*$_2$CCH), 4.51 (d, *J* = 13 Hz, 2H, ArC*H*$_2$Ar), 3.23 (d, *J* = 13 Hz, 2H, ArC*H*$_2$Ar), 3.20 (d, *J* = 13 Hz, 2H, ArC*H*$_2$Ar), 2.50 (t, *J* = 2 Hz, 2H, OCH$_2$CC*H*), 2.50 (t, *J* = 2 Hz, 1H, OCH$_2$CC*H*), 2.47 (t, *J* = 2 Hz, 1H, OCH$_2$CC*H*), 1.32 (s, 18H, C(CH$_3$)$_3$), 0.69 (s, 9H, C(CH$_3$)$_3$). **^{13}C-NMR** (100 MHz, $CDCl_3$) δ 159.46, 153.05, 152.11, 146.81, 145.86, 143.39, 136.32, 136.21, 134.74, 132.63, 126.68, 125.20, 124.80, 123.17, 81.28, 80.24, 79.02, 75.94, 74.87, 74.72, 62.09, 61.95, 60.73, 34.32, 33.44, 32.47, 32.12, 31.67, 30.75. **HRMS** (APCI) m/z: $[M+H]^+$ Clcd for $C_{52}H_{56}NO_6$ 790.4102; Found 790.4110.

5,11,17-Tetra-*tert*-butyl-23-BocGly-25,26,27,28-tetra-propargyloxy-calix[4]arene (156)

A mixture of **145** (1.02 g, 1.29 mmol) and $SnCl_2 \cdot 2H_2O$ (2.91 g, 12.9 mmol) in ethanol (70 mL) was heated to reflux for 18 hours. The solvent was removed under reduced pressure and the residue stirred with 10% NaOH (100 mL) for 5 minutes. The product was extracted with DCM (3 x 100 mL) then washed with water (200 mL) and brine (200 mL). After drying over $MgSO_4$, the solvent was removed under reduced pressure to give the crude intermediate amine **155** as a yellow solid (crude yield: 0.81

g, 83%). **^{1}H NMR** (400 MHz, $CDCl_3$) δ 7.02 (d, *J* = 2.5 Hz, 2H, Ar*H*), 6.94 (d, *J* = 2.5 Hz, 2H, Ar*H*), 6.42 (s, 2H, Ar*H*), 5.83 (s, 2H, Ar*H*), 4.88 (d, *J* = 2 Hz, 4H, OCH_2CCH), 4.63 (d, *J* = 2 Hz, 2H, OCH_2CCH), 4.62 (d, *J* = 12.9 Hz, 2H), 4.58 (d, *J* = 2 Hz, 2H, OCH_2CCH), 4.54 (d, *J* = 13 Hz, 2H, ArCH_2Ar), 3.18 (d, *J* = 13 Hz, 2H, ArCH_2Ar), 3.05 (d, *J* = 13 Hz, 2H, ArCH_2Ar), 2.47 (t, *J* = 2 Hz, 1H, OCH$_2$CC*H*), 2.46 (t, *J* = 2 Hz, 2H, OCH$_2$CC*H*), 2.42 (t, *J* = 2 Hz, 1H, OCH$_2$CC*H*), 1.26 (s, 18H, C(CH$_3$)$_3$), 0.86 (s, 9H, C(CH$_3$)$_3$). A mixture of BocGly (0.70 g, 4.01 mmol), EDCI·HCl (0.85 g, 4.42 mmol) and HOBt hydrate (0.60 g, 4.42 mmol) were stirred under argon in dry DMF (20 mL). To this was added **155** in dry DMF (1 mL) and DIPEA (1.44 mL, 8.24 mmol). The mixture was stirred for 24 hours and the solvent removed under reduced pressure. The residue was redissolved in DCM (100 mL) and washed with 10% NaOH (100 mL), water (100 mL) then brine (100 mL). After drying over $MgSO_4$, the solvent was removed under reduced pressure and the residue purified by column chromatography over silica gel (eluent: 5-7% ethyl acetate in DCM) to give **156** as a light yellow solid (1.18 g, 1.29 mmol). **Mp** 106-108 °C; **IR** ν 3405.5, 3290, 2954.5, 2931.5, 2906, 2866, 1685.5, 1603.5, 1539, 1505.5, 1476.5, 1437, 1417.5, 1392, 1363.5, 1285, 1274.5, 1251.5, 1241.5, 1193.5, 1166, 1132.5, 1116, 1054, 1014 cm^{-1}; **^{1}H-NMR** (400 MHz, $CDCl_3$) δ 7.23 (s, 1H, ArN*H*), 7.02 (s, 2H, Ar*H*), 6.97 (s, 2H, Ar*H*), 6.65 (s, 2H, Ar*H*), 6.39 (s, 2H, Ar*H*), 4.99 (s, 1H, CH$_2$N*H*), 4.90 (dd, *J* = 16, 2 Hz, 2H, OCH_2CCH), 4.84 (dd, *J* = 16, 2 Hz, 2H, OCH_2CCH), 4.63 – 4.57 (m, 8H, OCH_2CCH and ArCH_2Ar), 3.72 (d, *J* = 6 Hz, 2H, CH_2NH), 3.18 (d, *J* = 13 Hz, 2H, ArCH_2Ar), 3.15 (d, *J* = 13 Hz, 2H, ArCH_2Ar), 2.49 – 2.47 (m, 3H, OCH$_2$CC*H*), 2.43 (t, *J* = 2 Hz, 1H, OCH$_2$CC*H*), 1.45 (s, 9H, CO$_2$C(CH$_3$)$_3$), 1.26 (s, 18H, C(CH$_3$)$_3$), 0.81 (s, 9H, C(CH$_3$)$_3$); **^{13}C-NMR** (100 MHz, $CDCl_3$) δ 166.70, 156.29, 153.10, 152.44, 151.38, 146.08, 145.31, 135.74, 135.26, 135.07, 133.37, 132.33, 125.90, 125.27, 124.85, 119.40, 81.45, 80.63, 80.51, 80.38, 74.90, 74.66, 74.47, 61.79, 61.54, 60.84, 45.41, 34.18, 33.68, 32.44, 32.25, 31.67, 31.02, 28.41; **HRMS** (NSI) m/z: $[M+NH_4]^+$ Calcd for $C_{59}H_{72}N_3O_7$ 934.5365; Found 934.5352.

5,11,17-Tetra-*tert*-butyl-23-Gly-25,26,27,28-tetra-propargyloxy-calix[4]arene (157)

To a stirred solution of **156** (1.06 g, 1.16 mmol) in DCM (8 mL) was added TFA (4 mL). After stirring for 40 minutes, the solution was diluted with DCM (50 mL), then water (50 mL) was added followed by sufficient saturated $NaHCO_3$ to adjust to pH > 7. After mixing thoroughly the emulsion separated and the product was extracted with

DCM (3 x 50 mL) and washed with brine (100 mL). After drying over $MgSO_4$, the solvent was removed under reduced pressure to give an orange-brown solid that was revealed by ^{1}H NMR to be a complex mixture of products.

5,11,17-Tri-*tert*-butyl-23-nitro-25,26,27,28-tetra-[*tert*-butyl(dimethyl)silyl]-propargyloxy-calix[4]arene (158)

A solution of **145** (2.88 g, 3.65 mmol) in THF (25 mL) was cooled to -80 °C. To this was added 1 M LiHMDS in THF (21.9 mL, 21.9 mmol) followed by TBDMSCl (3.30 g, 21.9 mmol) in minimum THF. The mixture was allowed to warm to room temperature and stirred for 24 hours before quenching with saturated ammonium chloride (100 mL). Water (200 mL) was added to dilute and the product extracted with DCM (3 x 100 mL) then washed with brine (200 mL). After drying over $MgSO_4$, the solvent was removed under reduced pressure to give sticky dark-orange oil. ^{1}H-NMR showed loss of the terminal alkyne triplet but a complex mixture of products.

5,11,17,23-Tetra-*tert*-butyl-25,26,27,28-tetra-[*tert*-butyl(dimethyl)silyl]-propargyloxy-calix[4]arene (159)

A solution of **154** (10.00 g, 12.48 mmol) in THF (87 mL) was cooled to -80 °C. To this was added 1 M LiHMDS in THF (54.91 mL, 54.91 mmol) followed by TBDMSCl (11.29 g, 74.88 mmol) in minimum THF. The mixture was allowed to warm to room temperature and stirred for 18 hours before quenching with saturated ammonium chloride (150 mL). The product was extracted with ethyl acetate (3 x 150 mL), washed with dilute HCl (200 mL) and brine (200 mL). After drying over $MgSO_4$, the solvent was removed under reduced pressure and the product precipitated from the residue with methanol to give **159** as light brown powder (13.87 g, 88%). **Mp** 219-221 °C; **IR** ν 2953, 2928.5, 2902, 2856.5, 2855, 2176, 1603, 1586, 1480.5, 1471, 1462.5, 1411.5, 1391, 1361.5, 1314.5, 1301.5, 1280, 1247.5, 1197, 1121, 1106, 1097, 1040.5 cm^{-1}; **^{1}H-NMR** (400 MHz, $CDCl_3$) δ 6.75 (s, 8H, Ar*H*), 4.82 (s, 8H, OCH_2), 4.52 (d, *J* = 13 Hz, 4H, ArCH_2Ar), 3.11 (d, *J* = 13 Hz, 4H, ArCH_2Ar), 1.06 (s, 36H, C(CH_3)$_3$), 0.88 (s, 36H, SiC(CH_3)$_3$), 0.08 (s, 24H, SiCH_3); **^{13}C-NMR** (100 MHz, $CDCl_3$) δ 152.09, 145.28, 134.79, 124.87, 103.58, 89.53, 61.39, 33.99, 32.75, 31.57, 26.30, 16.61, -4.43; **MALDI-TOF** m/z: $[M+Na]^+$ 1281.40.

5,11,17-Tri-*tert*-butyl-23-nitro-25,26,27,28-tetra-[*tert*-butyl(dimethyl)silyl]-propargyloxy-calix[4]arene (158)

To a stirred solution of **159** (1.57 g, 1.25 mmol) in DCM (72 mL) was added glacial acetic acid (1.85 mL) and 100% nitric acid (1.04 mL). The solution was stirred for 1 hour before quenching with water (100 mL). The product was extracted with DCM (3 x 50 mL), washed with water (3 x 200 mL) and brine (200 mL). After drying over $MgSO_4$, the solvent was removed under reduced pressure and the product purified by column chromatography over silica gel (eluent: 4:1 then 2:1 hexane/DCM) to give recovered **159** (1.10 g, 70%) as white powder and **158** (0.45 g, 29%) as a light yellow solid. **Mp** 200-202 °C; **IR** ν 2953, 2928, 2898.5, 2885, 2856.5, 2181, 1585, 1521.5, 1481, 1470.5, 1462, 1411.5, 1390.5, 1361.5, 1341, 1312.5, 1278.5, 1256, 1249, 1205, 1195, 1158, 1116.5, 1085.5, 1035 cm^{-1}; **^{1}H-NMR** (400 MHz, $CDCl_3$) δ 7.37 (s, 2H, Ar*H*), 7.04 (d, *J* = 2 Hz, 2H, Ar*H*), 6.98 (d, *J* = 2 Hz, 2H, Ar*H*), 6.35 (s, 2H, Ar*H*), 4.94 (s, 2H, OCH_2), 4.92 (s, 2H, OCH_2), 4.78 (s, 2H, OCH_2), 4.66 (d, *J* = 13 Hz, 2H, ArCH_2Ar), 4.58 (s, 2H, OCH_2), 4.44 (d, *J* = 13 Hz, 2H, ArCH_2Ar), 3.18 (d, *J* = 13 Hz, 2H, ArCH_2Ar), 3.16 (d, *J* = 13.3 Hz, 2H, ArCH_2Ar), 1.28 (s, 18H, C(CH_3)$_3$), 0.92 (s, 9H, SiC(CH_3)$_3$), 0.86 (s, 9H, SiC(CH_3)$_3$), 0.85 (s, 18H, SiC(CH_3)$_3$), 0.73 (s, 9H, C(CH_3)$_3$), 0.12 (s, 6H, SiCH_3), 0.07 (s, 6H, SiCH_3), 0.06 (s, 12H, SiCH_3); **^{13}C-NMR** (100 MHz, $CDCl_3$) δ 159.61, 152.12, 152.02, 146.36, 145.71, 143.27, 136.68, 136.36, 135.02, 133.08, 126.30, 124.88, 124.73, 123.08, 103.17, 102.70, 101.14, 91.45, 90.07, 89.95, 62.62, 62.53, 60.67, 34.26, 33.52, 32.68, 32.33, 31.71, 30.87, 26.23, 26.21, 26.10, 16.58, 16.55, 16.49, -4.51, -4.61; **MALDI-TOF** m/z: $[M+Na]^+$ 1270.37, $[M+K]^+$ 1286.33.

5,11,17-Tri-*tert*-butyl-23-amino-25,26,27,28-tetra-[*tert*-butyl(dimethyl)silyl]-propargyloxy-calix[4]arene (160)

A mixture of **158** (7.81 g, 6.26 mmol) and $SnCl_2{\cdot}2H_2O$ (14.12 g, 62.60 mmol) in ethanol (330 mL) were heated to reflux for 24 hours. The solvent was removed under reduced pressure and the residue stirred with 10% NaOH for 5 minutes. The product was extracted with DCM (3 x 100 mL) then washed with water (2 x 200 mL) and brine (200 mL). After drying over $MgSO_4$, the solvent was removed under reduced pressure to give **160** as a light yellow solid (6.07 g, 80%). **Mp** 95-97 °C; **IR** ν 2952.5, 2927.5, 2899.5, 2885, 2855, 2176.5, 1741, 1615, 1605.5, 1589, 1479.5, 1471, 1463, 1411.5, 1390.5, 1361.5, 1317.5, 1303.5, 1281.5, 1248.5, 1194.5, 1137.5, 1116, 1028, 1005 cm^{-1}; **^{1}H-NMR** (400 MHz, $CDCl_3$) δ 6.96 (d, *J* = 2.5 Hz, 2H, Ar*H*), 6.88 (d, *J* =

2.5 Hz, 2H, Ar*H*), 6.41 (s, 2H, Ar*H*), 5.82 (s, 2H; Ar*H*), 4.93 (d, *J* = 1.5 Hz, 4H, OCH_2), 4.64 (s, 2H, OCH_2), 4.55 (s, 2H, OCH_2), 4.54 (d, *J* = 13 Hz, 2H, ArCH_2Ar), 4.45 (d, *J* = 13 Hz, 2H, ArCH_2Ar), 3.13 (d, *J* = 13 Hz, 2H, ArCH_2Ar), 3.00 (d, *J* = 13 Hz, 2H, ArCH_2Ar), 2.87 (s, 2H, NH_2), 1.24 (s, 18H, C(CH_3)$_3$), 0.93 (s, 9H, SiC(CH_3)$_3$), 0.92 (s, 9H, SiC(CH_3)$_3$), 0.85 (s, 9H, C(CH_3)$_3$), 0.85 (s, 18H, SiC(CH_3)$_3$), 0.11 (s, 6H, SiCH_3), 0.11 (s, 6H, SiCH_3), 0.04 (s, 12H, SiCH_3); **^{13}C-NMR** (100 MHz, $CDCl_3$) δ 152.27, 152.25, 147.90, 145.36, 144.92, 140.94, 136.44, 135.90, 135.05, 133.61, 125.34, 124.85, 124.72, 114.86, 103.66, 103.41, 103.14, 89.56, 89.52, 89.20, 62.47, 62.33, 60.51, 34.14, 33.75, 32.57, 32.54, 31.77, 31.71, 31.14, 26.27, 26.26, 26.24, 16.59, 16.58, 16.55, -4.45, -4.48, -4.50; **MALDI-TOF** m/z: $[M+Na]^+$ 1239.97, $[M+K]^+$ 1255.95.

5,11,17-Tri-*tert*-butyl-23-BocGly-25,26,27,28-tetra-[*tert*-butyl(dimethyl)silyl]-propargyloxy-calix[4]arene (161)

A mixture of Boc-glycine (1.71 g, 9.78 mmol), EDCI (1.87 g, 9.78 mmol) and HOBt (1.32 g, 9.78 mmol) was stirred in DMF (10 mL) under argon for 5 minutes. To this was added a solution of **160** (5.95 g, 4.89 mmol) in DMF (40 mL) and DIPEA (3.41 mL, 19.56 mmol). The mixture was stirred for 24 hours, the solvent removed under reduced pressure and water (200 mL) added. The product was extracted with DCM (3 x 100 mL), washed with water (2 x 200 mL) and brine (200 mL). After drying over $MgSO_4$, the solvent was removed under reduced pressure and the product purified by column chromatography over silica gel (eluent: 19:1 DCM/ethyl acetate) to give **161** as a yellow solid. **Mp** 114-116 °C; **IR** ν 2952.5, 2927, 2898.5, 2855.5, 2173, 2160.5, 1731, 1701, 1698, 1685.5, 1680, 1603.5, 1558, 1539, 1504, 1478, 1470, 1462.5, 1420, 1417.5, 1390.5, 1361.5, 1314.5, 1281, 1248.5, 1210, 1194, 1169, 1132.5, 1115.5, 1028 cm^{-1}; **^{1}H NMR** (400 MHz, $CDCl_3$) δ 7.17 (s, 1H, ArN*H*), 6.95 (s, 2H, Ar*H*), 6.91 (s, 2H, Ar*H*), 6.63 (s, 2H, Ar*H*), 6.39 (s, 2H, Ar*H*), 5.01 (s, 1H, CH_2N*H*), 4.91 (s, 4H, OCH_2), 4.65 (s, 2H, OCH_2), 4.62 (s, 2H, OCH_2), 4.52 (d, *J* = 13 Hz, 2H, ArCH_2Ar), 4.51 (d, *J* = 13 Hz, 2H, ArCH_2Ar), 3.73 (d, *J* = 6 Hz, 2H, CH_2NH), 3.13 (d, *J* = 13 Hz, 2H, ArCH_2Ar), 3.10 (d, *J* = 13 Hz, 2H, ArCH_2Ar), 1.45 (s, 9H, NHCO$_2$C(CH_3)$_3$), 1.23 (s, 18H, C(CH_3)$_3$), 0.91 (s, 18H, SiC(CH_3)$_3$), 0.85 (s, 18H, SiC(CH_3)$_3$), 0.82 (s, 9H, C(CH_3)$_3$), 0.11 (s, 6H, SiCH_3), 0.10 (s, 6H, SiCH_3), 0.05 (s, 12H, SiCH_3); **^{13}C NMR** (100 MHz, $CDCl_3$) δ 166.45, 156.08, 152.09, 152.07, 151.43, 145.51, 144.84, 136.10, 135.32, 133.56, 131.88, 125.42, 124.78, 124.55, 119.38, 103.32, 102.90, 102.67, 89.70, 89.56, 80.41, 62.16, 60.53, 60.40, 45.25,

34.01, 33.55, 32.44, 32.33, 31.60, 30.95, 28.30, 26.10, 26.09, 16.45, 16.41, -4.64; **MALDI-TOF** m/z: $[M+Na]^+$ 1397.63, $[M+K]^+$ 1413.49.

NRD appended tetra-[*tert*-butyl(dimethyl)silyl]propargyloxy-calix[4]arene (163)

Through a stirred solution of **161** (0.15 g, 0.11 mmol) in DCM (10 mL) was bubbled $HCl_{(g)}$ for 1.5 hours, at which point no more starting material could be seen by TLC (19:1 DCM/ethyl acetate). Water (10 mL) was added then the pH adjusted to above 7 with saturated $NaHCO_3$. The product was extracted with DCM (3 x 50 mL) and washed with brine (100 mL). After drying over $MgSO_4$, the solvent was removed under reduced pressure to give the intermediate amine **162** as a colourless glass (crude yield 0.11 g, 82%). To a solution of this in dry DMF (1 mL) was added **142** (0.085 g, 0.25 mmol), EDCI·HCl (0.10 g, 0.52 mmol), HOBt hydrate (0.11 g, 0.78 mmol) and DIPEA (0.059 mL, 0.34 mmol). The mixture was stirred under argon for 18 hours. Water (50 mL) was added and the product extracted with DCM (3 x 50 mL), washed with 10% NaOH (50 mL), dilute HCl (50 mL) and brine (100 mL). After drying over $MgSO_4$, the solvent was removed under reduced pressure and the product purified by column chromatography over silica gel (eluent: 95:6 DCM/ethyl acetate) to give **163** as a red solid (0.07 g, 51%). **Mp** 275-277 °C; **IR** ν 3347, 2953, 2927.5, 2898.5, 2855.5, 2176.5, 1694, 1658, 1650, 1633.5, 1596.5, 1565.5, 1537.5, 1510.5, 1478, 1470.5, 1462, 1435, 1418, 1390, 1361.5, 1301, 1279.5, 1248.5, 1222.5, 1206.5, 1193.5, 1159.5, 1135.5, 1128, 1115.5, 1028, 1020, 1004.5 cm^{-1}; **^{1}H-NMR** (400 MHz, $CDCl_3$) δ 8.76 – 8.74 (m, 1H, ArH_{NRD}), 8.38 – 8.36 (m, 1H, ArH_{NRD}), 7.93 – 7.91 (m, 2H, ArH_{NRD}), 7.85 – 7.78 (m, 3H, ArH_{NRD}), 7.19 (t, *J* = 4.5 Hz, 1H, CH_2NH), 7.07 (s, 1H, ArN*H*), 6.99 (d, *J* = 2 Hz, 2H, Ar*H*), 6.95 (d, *J* = 2 Hz, 2H, Ar*H*), 6.68 (s, 2H, Ar*H*), 6.36 (s, 2H, Ar*H*), 4.94 (s, 4H, OCH_2), 4.63 (s, 2H, OCH_2), 4.62 (s, 2H, OCH_2), 4.55 (d, *J* = 13 Hz, 2H, $ArCH_2Ar$), 4.51 (d, *J* = 13 Hz, 2H, $ArCH_2Ar$), 4.09 (d, *J* = 4.5 Hz, 2H, CH_2NH), 3.14 (d, *J* = 13 Hz, 2H, $ArCH_2Ar$), 3.12 (d, *J* = 13 Hz, 2H, $ArCH_2Ar$), 1.27 (s, 18H, $C(CH_3)_3$), 0.92 (s, 18H, $SiC(CH_3)_3$), 0.85 (s, 18H, $SiC(CH_3)_3$), 0.78 (s, 9H, $C(CH_3)_3$), 0.11 (s, 6H, $SiCH_3$), 0.11 (s, 6H, $SiCH_3$), 0.05 (s, 12H, $SiCH_3$); **^{13}C-NMR** (100 MHz, $CDCl_3$) δ 177.38, 165.87, 165.66, 152.22, 152.18, 151.69, 147.83, 146.62, 145.70, 144.84, 143.65, 136.42, 136.11, 135.52, 134.81, 133.58, 132.85, 132.17, 131.43, 130.09, 130.02, 126.89, 125.63, 125.31, 124.91, 124.66, 124.32, 119.21, 115.67, 115.51, 103.40, 102.95, 102.66, 89.92, 89.78, 89.74,

62.49, 62.38, 60.57, 44.80, 34.16, 33.63, 32.62, 32.45, 31.72, 31.06, 26.25, 26.21, 16.56, 16.54, -4.48, -4.51; **MALDI-TOF** m/z: $[M+Na]^+$ 1605.92, $[M+K]^+$ 1621.92.

NRD appended tetra-propargyloxy-calix[4]arene (164)

To a stirred solution of **163** (0.04 g, 0.025 mmol) in THF (0.25 mL) was added 1 M TBAF in THF (1 mL, 1 mmol). The solution was stirred for 18 hours then quenched with saturated ammonium chloride (10 mL). The product was extracted with DCM (3 x 20 mL), then washed with water (50 mL) and brine (50 mL). After drying over $MgSO_4$, the solvent was removed under reduced pressure and the residue triturated with hexane to precipitate the product. This was filtered, washed with hexane and air dried to give a dark red-brown powder. ^{1}H-NMR showed a complex mixture of products.

5,11,17-Tri-*tert*-butyl-23-Gly-25,26,27,28-tetra-propargyloxy-calix[4]arene (157)

Through a stirred solution of **162** (1.00 g, 0.73 mmol) in DCM (20 mL) was bubbled $HCl_{(g)}$ for 3 hours, at which point no more starting material could be seen by TLC (19:1 DCM/ethyl acetate). Solvent was removed under reduced pressure to give the hydrochloride salt of the intermediate amine **162** as an off-white solid (crude yield: 0.91 g, 95%). **^{1}H-NMR** (400 MHz, $CDCl_3$) δ 6.92 (s, 2H, Ar*H*), 6.89 (s, 2H, Ar*H*), 6.87 (s, 2H, Ar*H*), 6.49 (s, 2H, Ar*H*), 4.91 – 4.82 (m, 4H, OCH_2), 4.72 (s, 2H, OCH_2), 4.65 (s, 2H, OCH_2), 4.52 (d, *J* = 13 Hz, 2H, ArCH_2Ar), 4.50 (d, *J* = 13 Hz, 2H, ArCH_2Ar), 3.82 (s, 2H, CH_2NH), 3.13 (d, *J* = 13 Hz, 2H, ArCH_2Ar), 3.10 (d, *J* = 13 Hz, 2H, ArCH_2Ar), 1.18 (s, 18H, C(CH_3)$_3$), 0.92 (s, 9H, C(CH_3)$_3$), 0.90 (s, 9H, C(CH_3)$_3$), 0.86 (s, 27H, C(CH_3)$_3$), 0.10 (s, 6H, SiCH_3), 0.09 (s, 6H, SiCH_3), 0.06 (s, 12H, SiCH_3). To this was added 1 M TBAF in THF (27.6 mL, 27. 6 mmol) and the solution stirred for 18 hours. The reaction was quenched with saturated ammonium chloride solution (50 mL), diluted with water (100 mL) and the product extracted with DCM (3 x 50 mL) then washed with water (100 mL) and brine (100 mL). After drying over $MgSO_4$, the solvent was removed under reduced pressure and the residue triturated with hexane to precipitate the product. This was filtered and washed with hexane to give **157** as white powder (0.44 g, 78%). **Mp** 115-117 °C; **IR** ν 3293, 2953, 2926, 2906, 2862.5, 2113, 1682, 1604, 1526, 1477, 1435, 1415, 1392.5, 1361.5, 1300.5, 1273, 1260.5, 1238, 1194, 1135.5, 1116.5, 1075, 1014 cm^{-1}; **^{1}H-NMR** (400 MHz, $CDCl_3$) δ 8.70 (s, 1H, ArN*H*), 7.01 (d, *J* = 2 Hz, 2H, Ar*H*), 6.99 (d, *J* = 2 Hz,

2H, Ar*H*), 6.75 (s, 2H, Ar*H*), 6.41 (s, 2H, Ar*H*), 4.90 (dd, *J* = 16.5, 2.5 Hz, 2H, OC*H*$_2$CCH), 4.85 (dd, *J* = 16.5, 2.5 Hz, 2H, OC*H*$_2$CCH), 4.64 (d, *J* = 2.5 Hz, 2H, OC*H*$_2$CCH), 4.63 (d, *J* = 2.5 Hz, 2H, OC*H*$_2$CCH), 4.62 (d, *J* = 13 Hz, 2H, ArC*H*$_2$Ar), 4.60 (d, *J* = 13 Hz, 2H, ArC*H*$_2$Ar), 3.26 (s, 2H, C*H*$_2$NH$_2$), 3.18 (d, *J* = 13 Hz, 2H, ArC*H*$_2$Ar), 3.17 (d, *J* = 13 Hz, 2H, ArC*H*$_2$Ar), 2.48 (t, *J* = 2.5 Hz, 1H, OCH$_2$CC*H*), 2.47 (t, *J* = 2.5 Hz, 2H, OCH$_2$CC*H*), 2.42 (t, *J* = 2.5 Hz, 1H, OCH$_2$CC*H*), 1.26 (s, 18H, C(C*H*$_3$)$_3$), 0.82 (s, 9H, C(C*H*$_3$)$_3$); **^{13}C-NMR** (100 MHz, $CDCl_3$) δ 169.60, 153.04, 152.40, 150.99, 146.01, 145.18, 135.66, 135.15, 135.00, 133.32, 132.59, 125.77, 125.34, 124.81, 118.90, 81.44, 80.59, 80.41, 74.80, 74.65, 74.44, 61.75, 61.51, 60.75, 44.93, 34.15, 33.62, 32.37, 32.23, 31.64, 31.03; **HRMS** (NSI) m/z: $[M+H]^+$ Calcd for $C_{54}H_{61}N_2O_5$ 817.4575; Found 817.4565.

NRD appended tetra-propargyloxy-calix[4]arene (164)

A mixture of **142** (0.28 g, 0.86 mmol), EDCI·HCl (0.16 g, 0.86 mmol) and HOBT (0.12 g, 0.86 mmol) was stirred in DMF (1 mL) for 10 minutes before adding **157** (0.39 g, 0.43 mmol) in DMF (3.5 mL). DIPEA (0.30 mL, 1.72 mmol) was added and the mixture stirred for 18 hours. The suspension was mixed with 10% NaOH (200 mL) and the product extracted with ethyl acetate (3 x 200 mL), washed with water (300 mL) and brine (300 mL). After drying over $MgSO_4$, the solvent was removed under reduced pressure and the crude product subjected to column chromatography over silica gel (eluent: 3:2 hexane/ethyl acetate then ethyl acetate). The isolated product was triturated with DCM, filtered and air dried to give **164** as bright orange powder (0.23 g, 47%). **Mp** 223-225 °C; **IR** ν 3338, 3321, 3311, 3282.5, 3266, 3260.5, 2966, 2951.5, 2920.5, 2909, 2863, 2113, 1686.5, 1651.5, 1628.5, 1607.5, 1593, 1563, 1556, 1537.5, 1519.5, 1474.5, 1435.5, 1418, 1393, 1363.5, 1300, 1278, 1253.5, 1237.5, 1213, 1193, 1157.5, 1141.5, 1131.5, 1116.5, 1078, 1043.5, 1018.5 cm^{-1}; **^{1}H-NMR** (400 MHz, DMSO-d_6) δ 9.50 (s, 1H, ArN*H*), 9.08 (t, *J* = 6 Hz, 1H, CH_2N*H*), 8.71 (d, *J* = 7 Hz, 1H, Ar*H*$_{NRD}$), 8.25 (dd, *J* = 8, 1 Hz, 1H, Ar*H*$_{NRD}$), 8.09 (d, *J* = 1 Hz, 1H, Ar*H*$_{NRD}$), 8.04 – 7.90 (m, 4H, Ar*H*$_{NRD}$), 7.03 (s, 2H, Ar*H*), 6.91 (d, *J* = 2 Hz, 2H, Ar*H*), 6.80 (d, *J* = 2 Hz, 2H, Ar*H*), 6.63 (s, 2H, Ar*H*), 4.74 – 4.72 (m, 6H, OC*H*$_2$CCH), 4.67 (d, *J* = 2 Hz, 2H, OC*H*$_2$CCH), 4.48 (d, *J* = 13 Hz, 4H, ArC*H*$_2$Ar), 3.96 (d, *J* = 6 Hz, 2H, C*H*$_2$NH), 3.46 (t, *J* = 2 Hz, 1H, OCH$_2$CC*H*), 3.43 (t, *J* = 2 Hz, 2H, OCH$_2$CC*H*), 3.39 (t, *J* = 2 Hz, 1H, OCH$_2$CC*H*), 3.18 (d, *J* = 13 Hz, 2H, ArC*H*$_2$Ar), 3.10 (d, *J* = 13 Hz, 2H, ArC*H*$_2$Ar), 1.11 (s, 18H, C(C*H*$_3$)$_3$), 0.93 (s, 9H, C(C*H*$_3$)$_3$); **^{13}C-NMR** (100 MHz, DMSO) δ 176.54, 166.39, 164.61, 152.32, 152.18,

149.98, 147.36, 147.10, 144.86, 144.76, 143.03, 136.52, 134.79, 134.54, 133.99, 133.87, 133.63, 132.90, 132.63, 130.77, 129.84, 129.36, 125.91, 125.25, 124.92, 124.78, 124.64, 124.51, 118.51, 114.83, 112.93, 80.93, 80.71, 80.53, 77.54, 77.45, 77.30, 61.02, 60.55, 60.49, 54.89, 43.40, 33.62, 33.39, 32.04, 31.67, 31.22, 30.86; **HRMS** (NSI) m/z: $[M+Na]^+$ Calcd for $C_{71}H_{66}ClN_3O_8Na$ 1146.4431; Found 1146.4403.

3.6 References

(1) Collins, B. E.; Paulson, J. C. *Curr. Opin. Chem. Biol.* **2004**, *8*, 617–25.

(2) Lee, Y. C.; Lee, R. T. *Acc. Chem. Res.* **1995**, *28*, 321–327.

(3) Rendle, P. M.; Seger, A.; Rodrigues, J.; Oldham, N. J.; Bott, R. R.; Jones, J. B.; Cowan, M. M.; Davis, B. G. *J. Am. Chem. Soc.* **2004**, *126*, 4750–1.

(4) Ponader, D.; Wojcik, F.; Beceren-Braun, F.; Dernedde, J.; Hartmann, L. *Biomacromolecules* **2012**, *13*, 1845–52.

(5) André, S.; Pieters, R. J.; Vrasidas, I.; Kaltner, H.; Kuwabara, I.; Liu, F. T.; Liskamp, R. M.; Gabius, H. J. *Chembiochem* **2001**, *2*, 822–30.

(6) Cecioni, S.; Oerthel, V.; Iehl, J.; Holler, M.; Goyard, D.; Praly, J.-P.; Imberty, A.; Nierengarten, J.-F.; Vidal, S. *Chem.--Eur. J.* **2011**, *17*, 3252–61.

(7) Krenek, K.; Kuldova, M.; Hulikova, K.; Stibor, I.; Lhotak, P.; Dudic, M.; Budka, J.; Pelantova, H.; Bezouska, K.; Fiserova, A.; Kren, V.; Křenek, K.; Kuldová, M.; Hulíková, K.; Lhoták, P.; Dudič, M.; Pelantová, H.; Bezouška, K.; Fišerová, A.; Křen, V. *Carbohydr. Res.* **2007**, *342*, 1781–1792.

(8) Geraci, C.; Consoli, G. M. L.; Galante, E.; Bousquet, E.; Pappalardo, M.; Spadaro, A. *Bioconjug. Chem.* **2008**, *19*, 751–758.

(9) Marra, A.; Moni, L.; Pazzi, D.; Corallini, A.; Bridi, D.; Dondoni, A. *Org. Biomol. Chem.* **2008**, *6*, 1396–1409.

(10) Arosio, D.; Fontanella, M.; Baldini, L.; Mauri, L.; Bernardi, A.; Casnati, A.; Sansone, F.; Ungaro, R. *J. Am. Chem. Soc.* **2005**, *127*, 3660–3661.

(11) Viola, S.; Consoli, G. M. L.; Merlo, S.; Drago, F.; Sortino, M. A.; Geraci, C. *J. Neurochem.* **2008**, *107*, 1047–55.

(12) Lis, H.; Sharon, N. *Chem. Rev.* **1998**, *98*, 637–674.

(13) Mesaros, N.; Nordmann, P.; Plésiat, P.; Roussel-Delvallez, M.; Van Eldere, J.; Glupczynski, Y.; Van Laethem, Y.; Jacobs, F.; Lebecque, P.; Malfroot, A.; Tulkens, P. M.; Van Bambeke, F. *Clin. Microbiol. Infect.* **2007**, *13*, 560–78.

(14) Morrison, A.; Wenzel, R. *Rev. Infect. Dis.* **1984**, *6*, S627–S642.

(15) Ratjen, F. *Paediatr. Respir. Rev.* **2006**, *7*, S151–S153.

(16) Tielker, D.; Hacker, S.; Loris, R.; Strathmann, M.; Wingender, J.; Wilhelm, S.; Rosenau, F.; Jaeger, K.-E. *Microbiology* **2005**, *151*, 1313–23.

(17) Imberty, A.; Wimmerová, M.; Mitchell, E. P.; Gilboa-Garber, N. *Microbes Infect.* **2004**, *6*, 221–228.

(18) Chemani, C.; Imberty, A.; de Bentzmann, S.; Pierre, M.; Wimmerová, M.; Guery, B. P.; Faure, K. *Infect. Immun.* **2009**, *77*, 2065–75.

(19) Hauber, H.-P.; Schulz, M.; Pforte, A.; Mack, D.; Zabel, P.; Schumacher, U. *Int. J. Med. Sci.* **2008**, *5*, 371–6.

(20) Moni, L.; Pourceau, G.; Zhang, J.; Meyer, A.; Vidal, S.; Souteyrand, E.; Dondoni, A.; Morvan, F.; Chevolot, Y.; Vasseur, J.-J.; Marra, A. *Chembiochem* **2009**, *10*, 1369–1378.

(21) Cecioni, S.; Lalor, R.; Blanchard, B.; Praly, J.-P.; Imberty, A.; Matthews, S. E.; Vidal, S. *Chem.--Eur. J.* **2009**, *15*, 13232–13240.

(22) Consoli, G. M. L.; Granata, G.; Cafiso, V.; Stefani, S.; Geraci, C. *Tetrahedron Lett.* **2011**, *52*, 5831–5834.

(23) Cecioni, S.; Praly, J.-P.; Matthews, S. E.; Wimmerová, M.; Imberty, A.; Vidal, S. *Chem.--Eur. J.* **2012**, *18*, 6250–63.

(24) Cecioni, S.; Faure, S.; Darbost, U.; Bonnamour, I.; Parrot-Lopez, H.; Roy, O.; Taillefumier, C.; Wimmerová, M.; Praly, J.-P.; Imberty, A.; Vidal, S. *Chem.--Eur. J.* **2011**, *17*, 2146–2159.

(25) Sicard, D.; Cecioni, S.; Iazykov, M.; Chevolot, Y.; Matthews, S. E.; Praly, J.-P.; Souteyrand, E.; Imberty, A.; Vidal, S.; Phaner-Goutorbe, M. *Chem. Commun.* **2011**, *47*, 9483–9485.

(26) Imberty, A.; Vidal, S.; Matthews, S.; Faure, K.; Guery, B.; Cecioni, S. Glycomimetic compounds as anti-infectious against pathogens lectins. *WO 2012/076934A1* **2012**.

(27) Gerland, B.; Goudot, A.; Pourceau, G.; Meyer, A.; Vidal, S.; Souteyrand, E.; Vasseur, J.-J.; Chevolot, Y.; Morvan, F. *J. Org. Chem.* **2012**, *77*, 7620–6.

(28) Deguise, I.; Lagnoux, D.; Roy, R. *New J. Chem.* **2007**, *31*, 1321.

(29) Waller, Z. A. E. Targeting G-Quadruplex DNA with Triarylpyridines and Nile Red Derivatives. PhD Thesis, University of Cambridge, 2009.

(30) Lei, L.; Ping, L.; Chunying, X.; Limin, Z. *Indian J. Chem.* **2006**, *45B*, 2118–2122.

(31) Van Loon, J.-D.; Arduini, A.; Coppi, L.; Verboom, W.; Pochini, A.; Ungaro, R.; Harkema, S.; Reinhoudt, D. N. *J. Org. Chem.* **1990**, *55*, 5639–5646.

(32) Rashidi-Ranjbar, P.; Taghvaei-Ganjali, S.; Shaabani, B.; Akbari, K. *Molecules* **2000**, *5*, 941–944.

(33) Rudzevich, Y.; Rudzevich, V.; Bolte, M.; Böhmer, V. *Synthesis* **2008**, *5*, 754–762.

(34) Miao, R.; Zheng, Q.-Y.; Chen, C.-F.; Huang, Z.-T. *J. Org. Chem.* **2005**, *70*, 7662–2671.

(35) Dulcere, J. P.; Crandall, J.; Faure, R.; Santelli, M.; Agati, V.; Mihoubi, M. N. *J. Org. Chem.* **1993**, *58*, 5702–5708.

(36) Wang, J.; Gutsche, C. D. *Struct. Chem.* **2001**, *12*, 267–274.

(37) Zhang, D.; Cao, X.; Purkiss, D. W.; Bartsch, R. A. *Org. Biomol. Chem.* **2007**, *5*, 1251–1259.

(38) Li, Z.; Ma, J.; Chen, J.; Pan, Y.; Jiang, J.; Wang, L. *Chinese J. Chem.* **2009**, *27*, 2031–2036.

(39) Gutsche, C. D.; Lin, L.-G. *Tetrahedron* **1986**, *42*, 1633–1640.

(40) Schroeder, L. R.; Green, J. W. *J. Chem. Soc. C* **1966**, 530–531.

(41) Cecioni, S.; Almant, M.; Praly, J.-P.; Vidal, S. In *Carbohydrate Chemistry: Proven Synthetic Methods*; 2012; pp. 175–180.

(42) Wang, Z. In *Comprehensive Organic Name Reactions and Reagents*; John Wiley & Sons, Inc.: Hoboken, NJ, USA, 2010; pp. 3123–3128.

(43) Mogck, O.; Parzuchowski, P.; Nissinen, M.; Böhmer, V.; Rokicki, G.; Rissanen, K. *Tetrahedron* **1998**, *54*, 10053–10068.

(44) Lim, C.; Sandman, D.; Sukwattanasinitt, M. *Macromolecules* **2008**, *41*, 675–681.

(45) Xu, W.; Vittal, J. J.; Puddephatt, R. J. *Can. J. Chem.* **1996**, *74*, 766–774.

NATURE PUBLISHING GROUP LICENSE TERMS AND CONDITIONS

Jun 11, 2013

This is a License Agreement between Zoe Karthauser ("You") and Nature Publishing Group ("Nature Publishing Group") provided by Copyright Clearance Center ("CCC"). The license consists of your order details, the terms and conditions provided by Nature Publishing Group, and the payment terms and conditions.

All payments must be made in full to CCC. For payment instructions, please see information listed at the bottom of this form.

License Number	3165960002149
License date	Jun 11, 2013
Licensed content publisher	Nature Publishing Group
Licensed content publication	Nature Reviews Molecular Cell Biology
Licensed content title	Pathways of clathrin-independent endocytosis
Licensed content author	Satyajit Mayor, Richard E. Pagano
Licensed content date	Aug 1, 2007
Volume number	8
Issue number	8
Type of Use	reuse in a thesis/dissertation
Requestor type	academic/educational
Format	print and electronic
Portion	figures/tables/illustrations
Number of figures/tables/illustrations	1
High-res required	no
Figures	Figure 1
Author of this NPG article	no
Your reference number	
Title of your thesis / dissertation	A New Approach to Drug Delivery: Non-Peptidic, High Load Macrocyclic Alternatives to Cell Penetrating Peptides
Expected completion date	Aug 2013
Estimated size (number of pages)	220
Total	0.00 GBP
Terms and Conditions	

Terms and Conditions for Permissions

Nature Publishing Group hereby grants you a non-exclusive license to reproduce this material for this purpose, and for no other use,subject to the conditions below:

1. NPG warrants that it has, to the best of its knowledge, the rights to license reuse of this material. However, you should ensure that the material you are requesting is original to Nature Publishing Group and does not carry the copyright of another entity (as credited in the published version). If the credit line on any part of the material you have requested indicates that it was reprinted or adapted by NPG with permission from another source, then you should also seek permission from that source to reuse the material.

2. Permission granted free of charge for material in print is also usually granted for any electronic version of that work, provided that the material is incidental to the work as a whole and that the electronic version is essentially equivalent to, or substitutes for, the print version.Where print permission has been granted for a fee, separate permission must be obtained for any additional, electronic re-use (unless, as in the case of a full paper, this has already been accounted for during your initial request in the calculation of a print run).NB: In all cases, web-based use of full-text articles must be authorized separately through the 'Use on a Web Site' option when requesting permission.

3. Permission granted for a first edition does not apply to second and subsequent editions and for editions in other languages (except for signatories to the STM Permissions Guidelines, or where the first edition permission was granted for free).

4. Nature Publishing Group's permission must be acknowledged next to the figure, table or abstract in print. In electronic form, this acknowledgement must be visible at the same time as the figure/table/abstract, and must be hyperlinked to the journal's homepage.

5. The credit line should read:
   Reprinted by permission from Macmillan Publishers Ltd: [JOURNAL NAME] (reference citation), copyright (year of publication)
   For AOP papers, the credit line should read:
   Reprinted by permission from Macmillan Publishers Ltd: [JOURNAL NAME], advance online publication, day month year (doi: 10.1038/sj.[JOURNAL ACRONYM].XXXXX)

   Note: For republication from the *British Journal of Cancer*, the following credit lines apply.
   Reprinted by permission from Macmillan Publishers Ltd on behalf of Cancer Research UK: [JOURNAL NAME] (reference citation), copyright (year of publication)For AOP papers, the credit line should read:
   Reprinted by permission from Macmillan Publishers Ltd on behalf of Cancer Research UK: [JOURNAL NAME], advance online publication, day month year (doi: 10.1038/sj.[JOURNAL ACRONYM].XXXXX)

6. Adaptations of single figures do not require NPG approval. However, the adaptation should be credited as follows:

   Adapted by permission from Macmillan Publishers Ltd: [JOURNAL NAME] (reference citation), copyright (year of publication)

   Note: For adaptation from the *British Journal of Cancer*, the following credit line

applies.
Adapted by permission from Macmillan Publishers Ltd on behalf of Cancer Research UK: [JOURNAL NAME] (reference citation), copyright (year of publication)

7. Translations of 401 words up to a whole article require NPG approval. Please visit http://www.macmillanmedicalcommunications.com for more information.Translations of up to a 400 words do not require NPG approval. The translation should be credited as follows:

   Translated by permission from Macmillan Publishers Ltd: [JOURNAL NAME] (reference citation), copyright (year of publication).

   Note: For translation from the *British Journal of Cancer*, the following credit line applies.
   Translated by permission from Macmillan Publishers Ltd on behalf of Cancer Research UK: [JOURNAL NAME] (reference citation), copyright (year of publication)

We are certain that all parties will benefit from this agreement and wish you the best in the use of this material. Thank you.

Special Terms:

v1.1

If you would like to pay for this license now, please remit this license along with your payment made payable to "COPYRIGHT CLEARANCE CENTER" otherwise you will be invoiced within 48 hours of the license date. Payment should be in the form of a check or money order referencing your account number and this invoice number RLNK501040759. Once you receive your invoice for this order, you may pay your invoice by credit card. Please follow instructions provided at that time.

Make Payment To:
Copyright Clearance Center
Dept 001
P.O. Box 843006
Boston, MA 02284-3006

For suggestions or comments regarding this order, contact RightsLink Customer Support: customercare@copyright.com or +1-877-622-5543 (toll free in the US) or +1-978-646-2777.

Gratis licenses (referencing $0 in the Total field) are free. Please retain this printable license for your reference. No payment is required.

NATURE PUBLISHING GROUP LICENSE TERMS AND CONDITIONS

Jun 14, 2013

This is a License Agreement between Zoe Karthauser ("You") and Nature Publishing Group ("Nature Publishing Group") provided by Copyright Clearance Center ("CCC"). The license consists of your order details, the terms and conditions provided by Nature Publishing Group, and the payment terms and conditions.

All payments must be made in full to CCC. For payment instructions, please see information listed at the bottom of this form.

License Number	3167640600150
License date	Jun 14, 2013
Licensed content publisher	Nature Publishing Group
Licensed content publication	Nature
Licensed content title	Integrating molecular and network biology to decode endocytosis
Licensed content author	Eva M. Schmid and Harvey T. McMahon
Licensed content date	Aug 23, 2007
Volume number	448
Issue number	7156
Type of Use	reuse in a thesis/dissertation
Requestor type	academic/educational
Format	print and electronic
Portion	figures/tables/illustrations
Number of figures/tables/illustrations	1
High-res required	no
Figures	Figure1a
Author of this NPG article	no
Your reference number	
Title of your thesis / dissertation	A New Approach to Drug Delivery: Non-Peptidic, High Load Macrocyclic Alternatives to Cell Penetrating Peptides
Expected completion date	Aug 2013
Estimated size (number of pages)	220
Total	0.00 GBP
Terms and Conditions	

Terms and Conditions for Permissions

Nature Publishing Group hereby grants you a non-exclusive license to reproduce this material for this purpose, and for no other use,subject to the conditions below:

1. NPG warrants that it has, to the best of its knowledge, the rights to license reuse of this material. However, you should ensure that the material you are requesting is original to Nature Publishing Group and does not carry the copyright of another entity (as credited in the published version). If the credit line on any part of the material you have requested indicates that it was reprinted or adapted by NPG with permission from another source, then you should also seek permission from that source to reuse the material.

2. Permission granted free of charge for material in print is also usually granted for any electronic version of that work, provided that the material is incidental to the work as a whole and that the electronic version is essentially equivalent to, or substitutes for, the print version.Where print permission has been granted for a fee, separate permission must be obtained for any additional, electronic re-use (unless, as in the case of a full paper, this has already been accounted for during your initial request in the calculation of a print run).NB: In all cases, web-based use of full-text articles must be authorized separately through the 'Use on a Web Site' option when requesting permission.

3. Permission granted for a first edition does not apply to second and subsequent editions and for editions in other languages (except for signatories to the STM Permissions Guidelines, or where the first edition permission was granted for free).

4. Nature Publishing Group's permission must be acknowledged next to the figure, table or abstract in print. In electronic form, this acknowledgement must be visible at the same time as the figure/table/abstract, and must be hyperlinked to the journal's homepage.

5. The credit line should read:
   Reprinted by permission from Macmillan Publishers Ltd: [JOURNAL NAME] (reference citation), copyright (year of publication)
   For AOP papers, the credit line should read:
   Reprinted by permission from Macmillan Publishers Ltd: [JOURNAL NAME], advance online publication, day month year (doi: 10.1038/sj.[JOURNAL ACRONYM].XXXXX)

   Note: For republication from the *British Journal of Cancer*, the following credit lines apply.
   Reprinted by permission from Macmillan Publishers Ltd on behalf of Cancer Research UK: [JOURNAL NAME] (reference citation), copyright (year of publication)For AOP papers, the credit line should read:
   Reprinted by permission from Macmillan Publishers Ltd on behalf of Cancer Research UK: [JOURNAL NAME], advance online publication, day month year (doi: 10.1038/sj.[JOURNAL ACRONYM].XXXXX)

6. Adaptations of single figures do not require NPG approval. However, the adaptation should be credited as follows:

   Adapted by permission from Macmillan Publishers Ltd: [JOURNAL NAME] (reference citation), copyright (year of publication)

   Note: For adaptation from the *British Journal of Cancer*, the following credit line

applies.
Adapted by permission from Macmillan Publishers Ltd on behalf of Cancer Research UK: [JOURNAL NAME] (reference citation), copyright (year of publication)

7. Translations of 401 words up to a whole article require NPG approval. Please visit http://www.macmillanmedicalcommunications.com for more information.Translations of up to a 400 words do not require NPG approval. The translation should be credited as follows:

   Translated by permission from Macmillan Publishers Ltd: [JOURNAL NAME] (reference citation), copyright (year of publication).

   Note: For translation from the *British Journal of Cancer*, the following credit line applies.
   Translated by permission from Macmillan Publishers Ltd on behalf of Cancer Research UK: [JOURNAL NAME] (reference citation), copyright (year of publication)

We are certain that all parties will benefit from this agreement and wish you the best in the use of this material. Thank you.

Special Terms:

v1.1

If you would like to pay for this license now, please remit this license along with your payment made payable to "COPYRIGHT CLEARANCE CENTER" otherwise you will be invoiced within 48 hours of the license date. Payment should be in the form of a check or money order referencing your account number and this invoice number RLNK501043404. Once you receive your invoice for this order, you may pay your invoice by credit card. Please follow instructions provided at that time.

Make Payment To:
Copyright Clearance Center
Dept 001
P.O. Box 843006
Boston, MA 02284-3006

For suggestions or comments regarding this order, contact RightsLink Customer Support: customercare@copyright.com or +1-877-622-5543 (toll free in the US) or +1-978-646-2777.

Gratis licenses (referencing $0 in the Total field) are free. Please retain this printable license for your reference. No payment is required.